Panos Macheras *Editor*

Advances in Pharmacokinetics and Pharmacodynamics

aaps®

Springer

AAPS Introductions in the Pharmaceutical Sciences

Founding Editor

Robin Zavod, Chicago College of Pharmacy
Midwestern University, Downers
Grove, IL, USA

Volume 9

Series Editor

Claudio Salomon, National University of Rosario, Rosario, Argentina

The *AAPS Introductions in the Pharmaceutical Sciences* book series is designed to support pharmaceutical scientists at the point of knowledge transition. Springer and the American Association of Pharmaceutical Scientists (AAPS) have partnered again to produce a second series that juxtaposes the *AAPS Advances in the Pharmaceutical Sciences* series. Whether shifting between positions, business models, research project objectives, or at a crossroad in professional development, scientists need to retool to meet the needs of the new scientific challenges ahead of them. These educational pivot points require the learner to develop new vocabulary in order to effectively communicate across disciplines, appreciate historical evolution within the knowledge area with the aim of appreciating the current limitations and potential for growth, learn new skills and evaluation metrics so that project planning and subsequent evolution are evidence-based, as well as to simply "dust the rust off" content learned in previous educational or employment settings, or utilized during former scientific explorations. The *Introductions* book series will meet these needs and serve as a quick and easy-to-digest resource for contemporary science.

Panos Macheras

Editor

Advances in Pharmacokinetics and Pharmacodynamics

Springer

aaps®

Editor
Panos Macheras ⓘD
ATHENA Research Center,
PharmaInformatics Unit
National & Kapodistrian University
of Athens, Faculty of Pharmacy
Athens, Greece

Preface

This book is directed to all concerned with the applications of Pharmacokinetics (PK) and Pharmacodynamics (PD) to the development, evaluation and use of medicines. The book provides a concise overview of recent advances in PK and PD. I invited a number of scientists from academia, industry, and regulatory agencies to contribute to this book. My intention was to present informed opinions from those actively involved in addressing problems associated with the many recent aspects of PK, PD, and PK/PD studies.

The book consists of seven chapters and is divided in two sections. Part I addresses the state of the art in Physiologically Based Pharmacokinetic (PBPK) modeling (Chap. 1) as well as the assessment of food effect on drug absorption using PBPK modeling (Chap. 2). Chapters 3 and 4 describe the recent development of Physiologically Based Finite Time Pharmacokinetic (PBFTPK) models and their applications to pharmacokinetic data. Part II focuses on PK/PD modeling. Chap. 5 provides an overview of PK/PD modeling and simulation in clinical practice and studies. Chap. 6 deals with the subject/physiology variability issue encountered in PK/PD studies while Chap. 7 reviews the influence of clinical pharmacology in the modernization of drug development and regulation.

I would especially like to thank my co-author and colleague Dr. Athanasios A. Tsekouras for helping me bring this book project to fruition.

Athens, Greece   Panos Macheras

Contents

Part I
Pharmacokinetics

Chapter 1
Current Status in PBPK Modeling

Ryuta Asaumi and Kiyohiko Sugano

Abstract Physiologically based pharmacokinetic (PBPK) modeling is a mathematical approach that integrates the intrinsic pharmacokinetic properties of a drug and the physiological parameters of a target population. It has been utilized in a wide range of applications, from the early stages of drug discovery to the submission to regulatory authorities. In this chapter, we aimed to evaluate the accuracy of the PBPK models in predicting PK parameters related to drug absorption, distribution, metabolism, and excretion, as well as the plasma concentration–time profiles under various clinical scenarios including the effect of food, drug–drug interactions, hepatic or renal impairment, and pediatric growth processes. A survey of the recent literature revealed that, although the predicted values of area under the plasma concentration–time curve in each report were often claimed to be within twofold of the observed values, the following issues were found: (i) the method of model construction is not clearly described in the literature and (ii) the method of parameter optimization is not standardized among the literature. In order to increase the reliability of PK predictions by PBPK models, standardization of the model construction processes is desirable.

Keywords Physiologically based pharmacokinetic (PBPK) model · In vitro–in vivo extrapolation (IVIVE) · Middle-out approach · Optimization

R. Asaumi (✉)
Clinical Pharmacology and Exploratory Development, Astellas Pharma, Inc., Tokyo, Japan
e-mail: ryuta.asaumi@astellas.com

K. Sugano
Molecular Pharmaceutics Laboratories, College of Pharmaceutical Sciences, Ritsumeikan University, Kusatsu, Shiga, Japan
e-mail: suganok@fc.ritsumei.ac.jp

Abbreviations

AGP	α-1-glycoprotein
AUC	Area under the plasma concentration–time curve
AUCR	AUC ratio
CL_h	Hepatic clearance
CL_{int}	Intrinsic clearance
$CL_{int,esc}$	Intrinsic permeation clearance in intestinal basolateral membrane (intrinsic escaping clearance)
$CL_{int,met}$	Intrinsic clearance of hepatic or intestinal metabolism
$CL_{permeability}$	Intrinsic clearance by passive diffusion in intestine
CL_{total}	Total clearance
CP	Child-Pugh
CR_{CYP3A}	Ratio of the CYP3A contribution to oral clearance
CYP	Cytochrome P450
DDI	Drug–drug interaction
E_{act}	Active enzyme amount
$E_{act,ratio}$	Ratio of E_{act} with perpetrator to E_{act} without perpetrator
$EC_{50,u}$	Unbound concentration for the half-maximum induction effect
EM	Epithelial membrane
E_{max}	Maximum induction effect
F	Oral bioavailability
F_a	Fraction of dose absorbed from gut lumen
$F_a F_g$	Intestinal availability after an oral dose
f_B	Unbound fraction in blood
F_g	Fraction available after intestinal metabolism
F_h	Hepatic availability after an oral dose
f_m	Fractional metabolism
f_P	Unbound fraction in plasma
$f_{u,gut}$	Unbound fraction in enterocytes
GFR	Glomerular filtration rate
GMO	Global middle-out approach
HIP	Hepatic impairment patients
IC_{CYP3A}	Apparent increase in clearance of substrates produced by induction of CYP3A
IR_{CYP3A}	Time-averaged apparent inhibition ratio of CYP3A
IVIVE	In vitro–in vivo extrapolation
k_{deg}	Degradation rate constant
K_i	Inhibition constant
$K_{i,u}$	Unbound inhibition constant
K_{iapp}	Concentration of half-maximum inactivation
k_{inact}	Maximum rate constant of inactive enzyme formation
K_m	Michaelis–Menten constant
LMO	Local middle-out approach

M & S	Modeling & simulation
MDCK	Madin–Darby canine kidney
MID3	Model-informed drug discovery and development
MO	Middle-out approach
OA-PBPK	Oral absorption PBPK
PAMPA	Parallel artificial membrane permeability assay
PBPK	Physiologically based pharmacokinetic
PD	Pharmacodynamics
P_{eff}	Effective intestinal permeability
PK	Pharmacokinetics
Q_{tissue}	Blood flow rate in tissue
R_B	Blood-to-plasma concentration ratio
RIP	Renal impairment patients
SF	Scaling factor
UWL	Unstirred water layer
V_{max}	Maximum metabolism rate
v_{sys}	Synthesis rate

1.1 Introduction

Physiologically based pharmacokinetic (PBPK) models are widely used to predict the pharmacokinetics and pharmacodynamics of drugs in drug discovery, development, regulatory approval, and clinical practice. Advantages of the PBPK model would be mechanism-based and quantitative approaches using physiological and pharmacokinetic information. Quantitative analysis can enhance industry and regulatory decision-making. This chapter will cover the basics of a PBPK model, what it can do, and practical issues such as how to construct and verify a PBPK model. In addition, the predictive accuracy of PBPK models of small molecules was discussed as much as possible based on recent reports. We hope this chapter will help to understand the concepts and current status of PBPK modeling.

1.1.1 Background of Model-Informed Drug Discovery and Development

While the probability of successful drug development is declining, drug development costs are increasing in the pharmaceutical industry. To overcome the challenges, model-informed drug discovery and development (MID3) has been becoming active in various areas such as efficacy, safety, and pharmacokinetics [1, 2]. One of the most important benefits of these modeling and simulation (M & S) is the availability of quantitative predictions, which can facilitate decision-making in

drug discovery, development, and regulatory evaluation processes. A PBPK model is one of several PK models that can describe the pharmacokinetics of a drug in a variety of clinical situations (e.g., drug–drug interaction (DDI), food effect, hepatic or renal impairment patients, and children) [3]. The PBPK model consists of physiological parameters (population parameters), drug parameters, and model equations [4]. Regarding physiological parameters, many intrinsic and extrinsic factors can be incorporated into population models (e.g., age, body weight, gender, volume and blood flow rate of each tissue, the expression level of metabolizing enzymes and transporters, frequency of gene polymorphisms, smoking, and DDIs). This mechanism-based model can be replaced with the target population considering the differences in physiological and pathological conditions. In addition, by including inter- and intra-individual variability, virtual clinical trials can be conducted by generating virtual subjects matched to the actual study design. For drug parameters, a variety of pharmacokinetic parameters of an investigational drug can be input into the drug model, describing the absorption, distribution, metabolism, and excretion. This drug model is not limited to the unchanged form; it is also possible to construct its metabolite models. When multiple drug models are developed, DDIs can be predicted in co-administration conditions. Combining a population model with a drug model, the PBPK model analysis becomes highly versatile, potentially predicting the pharmacokinetics in various scenarios that may arise in clinical practice.

In recent years, predicted results of PBPK models have been included in new drug application documents [5]. Given the widespread use of the PBPK model, it is crucial to understand the concept of PBPK models and the construction and validation processes. However, modeling scientists must be aware that there are always limitations to the predicted results due to the assumptions and uncertainties in the model setting, even if a PBPK model is constructed by considering all data available at the time of the predictions. Therefore, this chapter is about the current status of the predictability of PBPK modeling.

1.1.2   Methods for PBPK Model Construction

The PBPK model of an investigational drug is constructed based on the purpose of the analysis, the amount of data available at the time, and the stage of development. There are two main approaches to construct a PBPK model: the bottom-up approach and the middle-out approach. The middle-out approach can be further divided into the local (drug-by-drug) middle-out approach (LMO) and the global middle-out approach (GMO). In this chapter, we will distinguish LMO from GMO and discuss the pros and cons later. The flow of PBPK model construction, verification, and refinement in drug development is generally as follows. In the preclinical stage, a PBPK model of an investigational drug is usually constructed by the bottom-up approach to predict pharmacokinetics in a phase I study using in vitro data. The constructed PBPK model can be verified by the human PK data. If necessary, the

PBPK model is refined by LMO, where some model parameters are back-calculated using the clinical PK data. Subsequently, the prediction, verification, and refinement cycle for the PBPK model is repeated as clinical pharmacology and phase II/III studies are conducted. The features and basic concepts of bottom-up and middle-out approaches are summarized in the next section.

1.1.2.1 Bottom-Up Approach

The bottom-up approach is a standard way to construct a PBPK model and a method that combines multiple in vitro data to predict in vivo PK. In this approach, some in vitro parameters are scaled up to in vivo parameters to account for physiological conditions. For example, intrinsic clearance of hepatic metabolism ($CL_{int,met}$) is scaled up from the in vitro data using human liver microsomes or hepatocytes in most cases. Given that $CL_{int,met}$ is proportional to the amount of metabolizing enzymes, the scaling factor (SF) considers the amount of metabolizing enzymes in the in vitro system and the human liver. Specifically, in vitro $CL_{int,met}$ (μL/min/mg microsomal protein) obtained from human liver microsomes is scaled up to in vivo $CL_{int,met}$ by multiplying (i) microsomal protein content per gram of liver and (ii) liver weight per person. On the other hand, some in vitro parameters do not need to be scaled up when in vitro experimental conditions can be considered to reflect in vivo environment, e.g., unbound fraction in plasma (f_P) obtained from in vitro protein binding study.

Since a bottom-up approach uses in vitro data (and in silico data if necessary), it is possible to predict clinical PK profiles prospectively even in the non-clinical phase. However, accurate prediction of this method is not guaranteed.

1.1.2.2 Local Middle-Out Approach (LMO)

The LMO is a combination of the bottom-up and top-down approaches [6–8]. In most cases, one or a few parameters (or scaling factors) are optimized to fit the clinical data in a *drug-by-drug manner*. This approach is used when the predictive accuracy of the bottom-up approach is poor. LMO may (or may not) be a realistic compromise for constructing a PBPK model. In this method, the selection of parameters to be optimized is most critical. In principle, the parameters accurately obtained from in vitro experiments are usually fixed in the model according to the bottom-up approach. In contrast, parameters that cannot be obtained from in vitro experiments should be optimized based on the top-down approach with specific clinical condition. The parameter must be identifiable from the PK data. Usually, a specific clinical study setting is required to determine the parameter accurately. For example, PK data with a specific cytochrome P450 (CYP) inhibitor should be used to back-calculate the fractional metabolism (f_m) of a victim drug (Fig. 1.1).

Despite these basic principles, the current reality is that the parameters to be optimized vary from literature to literature. In most cases, a common optimization
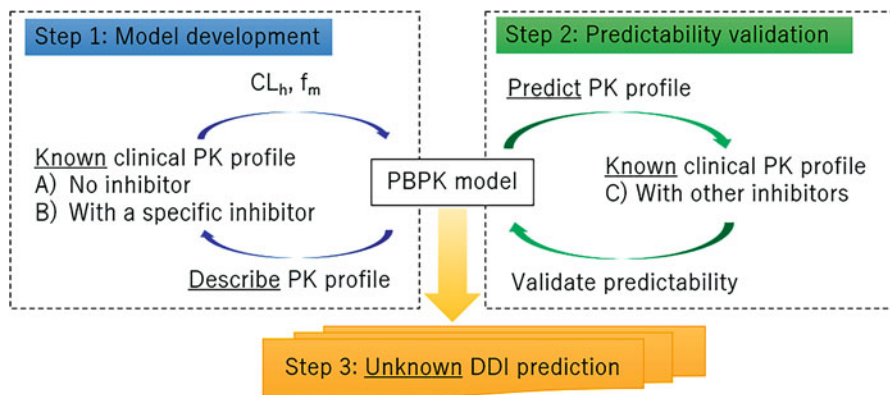
Fig. 1.1 Concept of local middle-out approach in the case of inhibition-mediated DDIs. The flow of constructing a PBPK model of an investigational drug (victim) with a specific inhibitor is as follows. Step 1: Model development. CL_h (or CL_{int}) of a victim is calculated using a victim PK profile after the intravenous dosing without a specific inhibitor, assuming negligible renal clearance (Step 1A). If the intravenous PK profile is not available, the assumption of victim bioavailability is required from preclinical data. Then, f_m of a victim is calculated using a victim PK profile with a specific inhibitor (e.g., itraconazole for CYP3A inhibition) (Step 1B). As the victim PBPK model is developed to fit to the victim PK profiles, this is just a description (not a prediction). Step 2: Predictability validation. The developed PBPK model can be used to predict DDIs with other inhibitors used in Step 1 and the predicted DDI data are compared to the observed data to validate the predictability. Step 3: Unknown DDI Prediction. The validated PBPK model can be used to predict untested DDIs within the range of steps 1 and 2 (interpolation). CL_h hepatic clearance, CL_{int} intrinsic clearance of hepatic metabolism, *DDI* drug–drug interaction, f_m fractional metabolism, *PK* plasma concentration–time

policy is applied within a report. It guarantees one specific approach for the compounds presented in that report, but it does not guarantee whether the same optimization approach can be applied to other compounds that were not included in the report. For instance, when a compound was metabolized by two enzymes (e.g., CYP3A4 and CYP2C9) and the predicted in vivo CL_{int} calculated from the in vitro data underestimated the observed in vivo CL_{int}, should one or the other, or both in vitro CL_{int} be optimized? As another example, when the uptake of a compound was evaluated using human hepatocytes, active uptake clearance via transporters and passive diffusion clearance were calculated. When the in vitro-derived uptake clearance underestimated the in vivo uptake, would one or both be optimized? These optimization policies are vital because they can significantly affect the predicted DDIs via the metabolizing enzymes or transporters. Thus, it is expected to establish a standardized middle-out approach in which the optimization policy in the model construction process is consistent among reports. The previous report by Yoshikado et al., which proposes a standard PBPK analysis procedure, should be consulted [9].

However, easy parameter optimization should be avoided because it may lead to a model that does not reflect in vivo situation. One should be keenly aware that, in

in vitro–in vivo extrapolation (IVIVE), an empirical scale-up factor must be used within the range where the optimized physiological factor makes sense. Therefore, great care should be taken in selecting parameters to be optimized, and one should always be aware of the validity of the optimized values.

1.1.2.3 Global Middle-Out Approach (GMO)

In the GMO, one or a few parameters (or scaling factors) are *back-calculated* from the clinical data of *many model drugs*. Once back-calculated, the parameter is commonly applied to all drugs for *forwarding prediction*. GMO is often used when a physiological parameter is difficult to measure directly. The model drugs are carefully selected so that their PK data reflect the physiological parameter of interest. The number of model drugs is set to have a sufficient degree of freedom (usually more than 4 drugs per one parameter (like $N = 3$ measurements)). In addition, structural identifiability is carefully considered.

1.1.3 Summary

This section presents the concepts of the PBPK model, the strategy of its use in drug research, and approaches to model construction. The idea of the PBPK model is based on the mechanisms of physiological and pharmacokinetic characteristics, focusing on IVIVE. It is challenging to accurately predict human PK profiles using only the bottom-up approach (Sects. 1.2 and 1.3). Therefore, the LMO approach has been employed in most cases. Since the purpose of PBPK analysis is different for each situation in drug research, the structures and parameters of PBPK models are also diverse. In addition, a standard method for selecting optimized parameters has not been established. To solve these issues, it is desirable to standardize the structure of PBPK models, the input parameters, and the analysis method, including the optimization policy, as much as possible. When using the LMO approach, it is necessary to explain why optimization was essential for the objective of PBPK modeling and why the parameters to be optimized were selected. Parameter optimization may adequately bridge the gap between in vitro and in vivo and deepen the understanding of the in vivo mechanism, but it may also lead to incorrect models that do not reflect the in vivo situation. Taken together, a PBPK model should be constructed in a mechanism-based manner, and if optimization is used, its validity must be objectively explained (also see Sect. 1.4).

1.2   Predictive Accuracy of IVIVE for Pharmacokinetic Parameters

1.2.1   Fraction of Dose Absorbed from Gut Lumen (F_a)

As for the bottom-up approach, the predictability of the oral absorption PBPK (OA-PBPK) model has been systematically evaluated and published in several reports [10–14]. All of them suggested that the dynamic and complex OA-PBPK models need further improvement, especially for drug development and clinical research use. A simple model, of which the predictability has been evaluated, may provide sufficient predictability for the uses in drug discovery [13, 15–19].

There are many case study reports regarding dynamic and complex OA-PBPK modeling in which the LMO (drug-by-drug parameter fitting) was utilized. However, as discussed in Sect. 1.4, it is difficult to judge the predictability of OA-PBPK models based on the case studies (or the compiles of the case studies) due to publication bias. In addition, the LMO process changes literature by literature. At least, drug-by-drug optimization of physiological parameters should be avoided.

1.2.2   Fraction Available after Intestinal Metabolism (F_g)

Intestinal metabolism could play an important role in the first-pass effect on the pharmacokinetics of CYP3A substrates [20]. Although it is difficult to evaluate in vivo F_g directly, the indirect methods for estimating F_g are reported. The values of hepatic availability (F_h) and oral bioavailability(F) are given by the PK profiles of a drug after an intravenous and an oral administration. Then, F_g can be calculated using the F_a value estimated by another method ($F_g = F/F_a/F_h$). There is a different method for estimating F_g using grapefruit juice–drug interaction data [21]. The F_g value can be calculated from the PK profiles of a drug before and after the concomitant use of grapefruit juice that inhibits CYP3A in the intestine.

From the viewpoint of IVIVE, the Q_{gut} model is reported as a useful method for easily predicting F_g [22]. This model calculates a Q_{gut} value as a hybrid parameter of the villous blood flow rate ($Q_{villous}$) and intrinsic clearance by passive diffusion in the intestine ($CL_{permeability}$) shown in Eq. 1.1.

$$Q_{gut} = \frac{Q_{villous} \times CL_{permeability}}{Q_{villous} + CL_{permeability}} \tag{1.1}$$

$CL_{permeability}$ is calculated through the following processes: (i) effective intestinal permeability in humans (P_{eff}) is first calculated from in vitro data on membrane permeability by Caco-2 cells, Madin–Darby canine kidney cells (MDCK cells), or parallel artificial membrane permeability assay (PAMPA), (ii) the calculated P_{eff} is then multiplied by the surface area of the intestinal lumen to obtain the $CL_{permeability}$.

Using the calculated Q_{gut} value, the F_g value can be determined in Eq. 1.2 where $f_{u,gut}$ and $CL_{int,met}$ are the unbound fraction in the enterocytes and the intrinsic clearance of intestinal metabolism, respectively.

$$F_g = \frac{Q_{gut}}{Q_{gut} + f_{u,gut} \times CL_{int,met}} \qquad (1.2)$$

In vivo $CL_{int,met}$ is scaled up from in vitro $CL_{int,met}$ evaluated with human intestinal microsomes considering physiological conditions. Because CYP3A is the most abundant CYP isoform in the intestine [23], the F_g values of structurally diverse CYP3A substrates were evaluated with the Q_{gut} model [20]. The predicted F_g values were within 1.5-fold of the observed values in 64% (16/25 cases. In this literature, the value of $f_{u,gut}$ was set to 1 to give higher predictive accuracy, even though this assumption is unrealistic. This point questions the correctness of the Q_{gut} model. Theoretically, F_g is determined by the ratio of $CL_{int,met}$ and intrinsic permeation clearance in basolateral membrane (intrinsic escaping clearance, $CL_{int,esc}$), but not the effective intestinal permeation (absorption) clearance (the rate-limiting process is different). In the latter case, the unstirred water layer (UWL) in the luminal side becomes the rate-limiting steps for most CYP3A4 substrates) (Eq. 1.3).

$$F_g = \frac{f_{u,gut}CL_{int,esc}}{f_{u,gut}CL_{int,esc} + f_{u,gut}CL_{int,met}} = \frac{CL_{int,esc}}{CL_{int,esc} + CL_{int,met}} \qquad (1.3)$$

The escaping clearance consists of three tandem processes (i) basolateral membrane permeation, (ii) diffusion through the sub-basolateral space to the blood flow, and (iii) removal by the blood flow (the efflux to the lumen was neglected) [24].

Based on this theory, a simplified model was proposed only using $CL_{int,met}$ and $CL_{int,esc}$ [25]. The $CL_{int,met}$ and $CL_{int,esc}$ values of 19 CYP3A substrates were evaluated with human intestinal microsomes and PAMPA, respectively. As a result, the predicted F_g values were within 1.5-fold of the observed values in 79% (15/19 cases). Kato et al. also proposed a simpler model [26]. Sugano proposed the anatomical F_g model, in which (i) to (iii) are all considered. The anatomical F_g model suggested that (ii) sub-basolateral diffusion can be the rate-limiting step of the escaping clearance for lipophilic drugs [24].

1.2.3 Hepatic Clearance (CL_h)

When predicting CL_h of metabolized drugs with the bottom-up approach, in vitro intrinsic clearance (CL_{int}) determined by human liver microsomes or hepatocytes is scaled up to in vivo CL_{int} using relevant amounts of metabolizing enzymes in the human liver (Sect. 1.1.2.1). This bottom-up approach tends to underestimate the in vivo CL_{int} in most cases [27]. When using human liver microsomes, the predicted

values of in vivo CL_{int} were within twofold of the observed values in 25% (21/83 drugs). In the case of human hepatocytes, the predicted in vivo CL_{int} were within twofold of the observed values in 24% (24/101 drugs). These data demonstrated that average fold underprediction was 2.8 for microsomes and 4.7 for hepatocytes. The reasons for the poor predictability are unknown, but the following factors may be involved: (i) large variability in the metabolic activity of hepatocytes, (ii) inaccuracy of drug unbound fraction (f_u) in microsomes or hepatocytes, (iii) involvement of metabolic enzymes and transporters not taken into account, (iv) erroneous in vitro CL_{int} due to the inhibitory effect of unsaturated fatty acids on the activity of metabolizing enzymes, and (v) potential limitation of drug entry into hepatocytes by plasma membrane and/or UWL [28–31]. To predict CL_h from in vivo CL_{int}, the well-stirred model or the other models considering hepatic blood flow are used. The hepatic blood flow rate can affect the predictability of the hepatic clearance [32].

In the preclinical phase, in vivo CL_{int} and CL_h of a drug candidate are routinely predicted by the bottom-up approach for estimating the plasma exposure and doses in a first-in-human study. Considering the low predictability for in vivo clearance, optimizing the clearance parameter in the PBPK analysis may be necessary to match the plasma exposure in clinical studies [29]. However, as mentioned in Sect. 1.1.2.2, the LMO process requires caution because optimization policy can change literature by literature.

1.2.4 Blood-to-Plasma Concentration Ratio (R_B)

To predict hepatic clearance, as described in Sect. 1.2.3, the unbound fraction in blood (f_B) of a drug, hepatic blood flow rate, and in vivo CL_{int} are required. The f_B value is calculated by dividing the unbound fraction in plasma (f_P) by the $R_B(f_B = f_P/R_B)$. Although f_P and R_B are often obtained in vitro, human R_B is sometimes assumed to be 1 when unavailable. However, since R_B is essential for the calculation of f_B, a prediction method for R_B values from in vitro data has been proposed [33]. Using rat R_B and f_P and human f_P, which are readily available for experimental data, 77.6% (45/58 compounds) of predicted human R_B were within 1.25-fold of the observed values. Therefore, this method may help predict a human R_B value.

1.3 PK Predictions for Clinical Situations by PBPK Models

1.3.1 Drug–Drug Interaction (DDI)

One of the areas where the PBPK model is most utilized is DDI predictions [5]. PBPK modeling can evaluate untested DDI scenarios and propose an optimized design for clinical DDI studies. Moreover, it can suggest appropriate dose

adjustment of drugs. The mechanism of DDI can be classified into three types: direct inhibition, mechanism-based inhibition, and induction. Direct inhibition means that a perpetrator (inhibitor) inhibits a metabolizing enzyme's activity without affecting the enzyme's amount. On the other hand, in the case of mechanism-based inhibition and induction, a perpetrator (inhibitor or inducer) fluctuates the amount of an active metabolizing enzyme by inactivation or induction.

In most cases, the magnitude of DDIs is evaluated with an index called the area under the plasma concentration–time curve ratio (AUCR) of a victim drug. The AUCR is the ratio of the AUC of a victim with perpetrator treatment (i.e., DDI condition) to the AUC without perpetrator treatment (i.e., control condition). After an oral administration of a victim in the control and DDI conditions, the AUC is given by $F_a \times F_g \times F_h \times \text{Dose}/CL_{\text{total}}$ and $F'_a \times F'_g \times F'_h \times \text{Dose}/CL'_{\text{total}}$, respectively, where CL_{total} is the total clearance. In addition, the AUCR can be approximated as $CL_{\text{int,met}}/CL'_{\text{int,met}}$ in Eq. 1.4 with the following assumptions: (i) the perpetrator causes hepatic-mediated DDIs and does not affect the intestinal-mediated DDIs ($F_a \times F_g = F'_a \times F'_g$), and (ii) the victim is metabolized and eliminated in the liver and is not excreted by the kidney ($CL_{\text{total}} = CL_h$).

$$AUCR = \frac{\frac{F'_a \cdot F'_g \cdot F'_h \cdot \text{Dose}}{CL'_{\text{total}}}}{\frac{F_a \cdot F_g \cdot F_h \cdot \text{Dose}}{CL_{\text{total}}}} = \frac{\frac{F'_h}{CL'_h}}{\frac{F_h}{CL_h}} = \frac{\frac{\frac{Q_h}{Q_h+f_B \cdot CL'_{\text{int,met}}}}{\frac{Q_h \cdot f_B \cdot CL'_{\text{int,met}}}{Q_h+f_B \cdot CL'_{\text{int,met}}}}}{\frac{\frac{Q_h}{Q_h+f_B \cdot CL_{\text{int,met}}}}{\frac{Q_h \cdot f_B \cdot CL_{\text{int,met}}}{Q_h+f_B \cdot CL_{\text{int,met}}}}} = \frac{CL_{\text{int,met}}}{CL'_{\text{int,met}}} \qquad (1.4)$$

For example, when the victim is a substrate of CYP3A and other CYP isoforms, the intrinsic clearance of hepatic metabolism ($CL_{\text{int,met}}$) is described by $CL_{\text{int,CYP3A}} + CL_{\text{int,others}}$. Using the fractional metabolism (f_m) mediated by CYP3A, $CL_{\text{int,others}}$ can be expressed with $CL_{\text{int,CYP3A}}$ and f_m. The ratio of $CL_{\text{int,met}}$ in the presence and absence of a perpetrator for CYP3A can be illustrated by Eq. 1.5. Therefore, the AUCR can be calculated simply using the values of f_m ranging from 0 to 1 and the $CL_{\text{int,CYP3A}}$ ratio.

$$\frac{CL_{\text{int,met}}}{CL'_{\text{int,met}}} = \frac{CL_{\text{int,CYP3A}} + CL_{\text{int,others}}}{CL'_{\text{int,CYP3A}} + CL_{\text{int,others}}}$$

$$= \frac{CL_{\text{int,CYP3A}} + CL_{\text{int,CYP3A}} \cdot \left(\frac{1}{f_m} - 1\right)}{CL'_{\text{int,CYP3A}} + CL_{\text{int,CYP3A}} \cdot \left(\frac{1}{f_m} - 1\right)} = \frac{1}{f_m \times \frac{CL'_{\text{int,CYP3A}}}{CL_{\text{int,CYP3A}}} + (1 - f_m)} \qquad (1.5)$$

To estimate the $CL'_{\text{int,met}}$ in DDI conditions, an inhibitory and inductive effect of a perpetrator should be considered in the next section.

1.3.1.1 Inhibition

Inhibition is a well-known and clinically significant DDI mechanism for metabolizing enzymes and transporters. Co-administration of an inhibitor can increase the plasma exposure and the risk of adverse events of a victim drug. During drug development, the CYP inhibitory effects of drug candidates and the effects they receive from inhibitors are routinely evaluated in vitro. Based on these preclinical data, the clinical impact of CYP inhibition can be predicted by PBPK models.

Modeling

Direct Inhibition

When a perpetrator (e.g., CYP3A inhibitor) shows competitive inhibition on the pharmacokinetics of a victim (e.g., CYP3A substrate), $CL'_{int,CYP3A}$ can be described based on the Michaelis–Menten equation (Eq. 1.6) where V_{max}, K_m, and $[C]_{tissue,victim}$ are the maximum metabolism rate, Michaelis–Menten constant, and concentration of the victim in the DDI sites such as hepatocytes, respectively.

$$CL'_{int,CYP3A} = \frac{V_{max}}{K_m \times \left(1 + \dfrac{f_{tissue,inhibitor} \cdot [I]_{tissue,inhibitor}}{K_{i,u,inhibitor}}\right) + [C]_{tissue,victim}} \quad (1.6)$$

$f_{tissue, inhibitor}$ and $[I]_{tissue, inhibitor}$ represent unbound fraction and concentration of the inhibitor in the DDI sites, respectively. The K_m value of the victim becomes $1 + f_{tissue} \times [I]_{tissue}/K_{i,u}$ times where $K_{i,u,inhibitor}$ is the unbound inhibition constant of the inhibitor. Assuming that the unbound concentration of the victim is much lower than the K_m value ($K_m \gg [C]_{tissue,victim}$), the $CL_{int,CYP3A}$ ratio of the victim in the absence and presence of the inhibitor can be described by Eq. 1.7.

$$CL_{int,CYP3A} \text{ ratio} = \frac{CL'_{int,CYP3A}}{CL_{int,CYP3A}} = \frac{1}{1 + \dfrac{f_{tissue,inhibitor} \cdot [I]_{tissue,inhibitor}}{K_{i,u,inhibitor}}} \quad (1.7)$$

Considering the Eqs. 1.4, 1.5, 1.6, and 1.7, the conditions for increasing the AUCR are as follows: (i) large f_m value of the victim and (ii) large $f_{tissue} \times [I]_{tissue}/K_{i,u}$ value of the inhibitor.

Mechanism-Based Inhibition

When an inhibitor exhibits a mechanism-based inhibition effect that inactivates the activity of a metabolizing enzyme (e.g., CYP3A), it is necessary to model the changes active enzyme amount, using the synthesis rate (v_{sys}) and degradation rate constant (k_{deg}), which are not considered in the case of competitive inhibition. A turnover model can represent the dynamics of the enzyme. Specifically, the changes

in the active enzyme amount (E_{act}) under DDI condition can be described as shown in Eq. 1.8 where $k_{inact,\,inhibitor}$ and $K_{iapp,\,inhibitor}$ are the maximum rate constant of inactive enzyme formation and concentration of half-maximum inactivation, respectively. Under the control condition, the v_{sys} equals the degradation rate ($v_{sys} = k_{deg} \times E_{act,control}$). Then, the E_{act} can be converted to the ratio of the E_{act} with the inhibitor to the E_{act} without the inhibitor ($E_{act,ratio}$) in Eq. 1.9.

$$\frac{dE_{act}}{dt} = v_{syn} - \left(k_{deg} + \frac{k_{inact,inhibitor} \times f_{tissue,inhibitor} \cdot [I]_{tissue,inhibitor}}{K_{iapp,u,inhibitor} + f_{tissue,inhibitor} \cdot [I]_{tissue,inhibitor}} \right) \times E_{act} \quad (1.8)$$

$$\frac{dE_{act,ratio}}{dt} = k_{deg} - \left(k_{deg} + \frac{k_{inact,inhibitor} \times f_{tissue,inhibitor} \cdot [I]_{tissue,inhibitor}}{K_{iapp,u,inhibitor} + f_{tissue,inhibitor} \cdot [I]_{tissue,inhibitor}} \right)$$
$$\times E_{act,ratio} \quad (1.9)$$

The conditions for decreasing the active enzyme amount are as follows: (i) large k_{inact} of the inhibitor and (ii) large $f_{tissue} \times [I]_{tissue}/(K_{iapp,u} + f_{tissue} \times [I]_{tissue})$ of the inhibitor.

Predictive Performance of PBPK Models

The predictive accuracy of PBPK models for mainly CYP3A-mediated inhibition was reported based on the submissions from pharmaceutical companies to the FDA between July 2008 and December 2013 [34]. In this literature, the inhibitory effects of 10 perpetrator drugs on the pharmacokinetics of 15 victim drugs were predicted for 26 clinical DDI trials. The victim models were developed by nine sponsors using a bottom-up approach (2 victims) or LMO (13 victims). While the detailed LMO procedure was not reported, the PK data of phase I studies were used. The major elimination pathway of the victims was considered hepatic CYP3A metabolism. For perpetrators, ketoconazole, ritonavir, and erythromycin were used mainly. The inhibitor models were used with the software default setting in half cases and developed by sponsors in the other cases. In 21 out of 26 cases (81%), the predicted AUCRs of the victims were within 1.25-fold of the observed AUCRs, suggesting the confidence in using PBPK models for the inhibition-mediated DDIs. Similarly, the predictive accuracy was summarized from the literature published from January 2001 to December 2016 [35]. The PBPK models of the investigational drugs, most of which were constructed by LMO (details were not shown), were used as victims in 80 cases and as perpetrators in 262 cases. The major DDI mechanism was CYP3A inhibition. When the investigational drugs were victims, the predicted AUCRs were within 1.25-fold of the observed AUCRs in 62% (49/80 cases) and twofold in all cases. Moreover, when investigational drugs were perpetrators, the predicted AUCRs of victims were within 1.25-fold of the observed AUCRs in 44%

(116/262 cases) and within twofold in 81% (213/262 cases). Taken together, the predictive accuracy of inhibitory DDIs is considered good with the twofold criteria, but sufficient model verification should be needed to improve the prediction accuracy such as 1.25-fold criteria.

While these reports could be valuable in understanding the predictive accuracy of the PBPK models at this moment, it should be recognized that these are the compiles of published case studies. Therefore, publication bias can compromise the assessment of predictability. Although the fold measure is generally used to evaluate the predictive accuracy, the criteria should be used with caution. This is because the acceptable prediction range becomes larger when the AUCR is closer to 1 than when the AUCR is higher. In the case of twofold criteria, if the AUC increases by 400% (AUCR: 5), the acceptable range is 150–900% (AUCR: 2.5–10), while if the AUC increases by only 10% (AUCR: 1.1), the acceptable range becomes relatively large from 45% to 120% (AUCR: 0.55–2.2). Therefore, the predictive accuracy tends to be higher when many DDI cases with AUCR close to 1 are collected. To avoid such potential bias, the Guest's criteria have been increasingly used [36]. With the criteria, the acceptable range can be set relatively narrow (0.8–1.25) when the observed AUCR is 1, and as the observed AUCR increases, the acceptable range approaches the twofold criteria. Therefore, the Guest's criteria, in which the acceptable range is set according to the observed AUCR, should be the first choice in the future.

Instead of using a PBPK model, a different framework for the quantitative prediction of CYP-mediated inhibition was proposed. In this method, AUCRs of victims after oral administration were predicted using only two parameters as shown in Eq. 1.10 [37]: CR_{CYP3A} is the ratio of the CYP3A contribution to oral clearance and IR_{CYP3A} is the time-averaged apparent inhibition ratio of CYP3A.

$$AUCR = \frac{1}{1 - CR_{\mathrm{CYP3A}} \times IR_{\mathrm{CYP3A}}} \tag{1.10}$$

Both values of IR_{CYP3A} of inhibitors and CR_{CYP3A} of victims were estimated from clinical DDI data. The predictive accuracy was verified using 60 clinical DDI studies between 14 substrates and 18 inhibitors including mechanism-based inhibitors for CYP3A. The predicted AUCRs were within 1.5-fold of the observed AUCRs in 80% (50/60 cases) and within twofold in 95% (57/60 cases). This is a simple and reliable DDI prediction method. The simplicity is in contrast to the PBPK models, which require many parameters.

1.3.1.2 Induction

Induction is as critical as inhibition in the DDI mechanism, which can decrease plasma exposure and efficacy of a victim drug. PBPK modeling of induction has evolved mainly for the predictions of CYP3A-mediated DDIs [38]. The predictive accuracy for the induction effect is controversial because sufficient information has not been accumulated. The reasons for the difficulty may include the following: (i) a

large degree of variability in the induced mRNA levels evaluated in vitro, (ii) uncertainty in the unbound fraction of an inducer and a victim at DDI sites, and (iii) involvement of multiple DDI mechanisms (e.g., inhibition and induction) for multiple metabolizing enzymes and transporters [39, 40].

Modeling

The induction mechanism of an inducer (e.g., rifampicin) for a metabolizing enzyme (e.g., CYP3A) can be described using a turnover model by Eq. 1.11, where $E_{max,inducer}$, $EC_{50,u,inducer}$, and $[I]_{tissue,inducer}$ are the maximum induction effect, unbound concentration for the half-maximum induction effect, and concentration of inducer in the DDI sites, respectively [41]. The change in $E_{act,ratio}$ is shown in Eq. 1.12, as is the case with the mechanism-based inhibition shown in Sect. 1.3.1.1. The $E_{act,ratio}$ indicates the increased levels of CYP3A under the inducer treatment, and $CL_{int,CYP3A}$ of a victim (e.g., midazolam) increase proportionally, resulting in a decrease in the AUC of the victim compared to the AUC in the control condition.

$$\frac{dE_{act}}{dt} = v_{syn} \times \left(1 + \frac{E_{max,inducer} \times f_{tissue,inducer} \cdot [I]_{tissue,inducer}}{EC_{50,u,inducer} + f_{tissue,inducer} \cdot [I]_{tissue,inducer}} \right) - k_{deg} \times E_{act} \quad (1.11)$$

$$\frac{dE_{act,ratio}}{dt} = k_{deg}$$
$$\times \left(1 + \frac{E_{max,inducer} \times f_{tissue,inducer} \cdot [I]_{tissue,inducer}}{EC_{50,u,inducer} + f_{tissue,inducer} \cdot [I]_{tissue,inducer}} - E_{act,ratio} \right) \quad (1.12)$$

Predictive Performance of PBPK Models

The predictive accuracy of PBPK models for CYP3A induction was reported based on the submissions from pharmaceutical companies to the FDA between July 2008 and December 2014 [42]. In this literature, PBPK models of 11 victim drugs and four CYP3A inducers were used for predicting 13 clinical DDI studies. The victim models were developed by six sponsors using a bottom-up approach (1 victim) or LMO (10 victims). While the detailed LMO procedure was not reported, the PK data of phase I studies were used. The major elimination pathway of the victims was considered hepatic CYP3A metabolism. For inducers, rifampicin, rifabutin, carbamazepine, and efavirenz were used in 9, 2, 1, and 1 studies, respectively. In 10 out of 13 cases (77%), the predicted AUCRs of the victims were within 1.25-fold of the observed AUCRs, suggesting that the validated PBPK models were submitted to the FDA. Another study also summarized the predictive accuracy for inductive DDIs by collecting PBPK analysis reports published from January 2001 to December 2016

[35]. Most cases analyzed CYP3A-mediated induction, but some cases analyzed induction for other CYP isoforms and transporters. The PBPK models of the investigational drugs were used as victims in 44 cases and as perpetrators in 98 cases. When the investigational drugs were victims, the predicted AUCRs were within 1.25-fold of the observed AUCRs in 50% (22/44 cases) and within two-fold in 80% (35/44 cases). Moreover, when the investigational drugs were inducers, the predicted AUCRs of victims were within 1.25-fold of the observed AUCRs in 43% (42/98 cases) and within two-fold in 86% (84/98 cases). Further improvements in predictive accuracy will be needed when the investigational drugs are inducers. Similar to the case of inhibitory predictions, it should be noted that these are the compiles of published case studies, most of which used the LMO approach.

Notably, there is a simpler method for predicting CYP3A induction than the PBPK models. The AUCRs of victims after oral administration can be predicted using an IC_{CYP3A} in addition to the CR_{CYP3A} shown in the previous section (Eq. 1.13) [43]. IC_{CYP3A} represents the apparent increase in clearance of substrates produced by induction of CYP3A.

$$AUCR = \frac{1}{1 + CR_{\mathrm{CYP3A}} \times IC_{\mathrm{CYP3A}}} \tag{1.13}$$

Both IC_{CYP3A} and CR_{CYP3A} were estimated from clinical DDI data. The predictive accuracy was verified using 42 clinical DDI studies between 22 substrates and seven inducers for CYP3A. In all 42 cases, the predicted AUCRs were within 1.2-fold of the observed AUCRs, indicating the robustness and usefulness of this model. If a clinical DDI study between an investigational drug and a typical CYP3A inducer (or substrate) is conducted, the CR_{CYP3A} (or IC_{CYP3A}) value of the investigational drug can be estimated and applied for the DDI predictions with untested CYP3A inducers (or substrates).

1.3.2 Food Effect

To predict the food effect on oral drug absorption, the effect of bile micelles on both solubility and intestinal membrane permeability should be considered in OA-PBPK modeling [44]. In general, bile micelles increase the solubility but decrease the permeability of a drug. This balance determines whether the food effect becomes positive or negative in many cases. The effect of bile micelles on the effective membrane permeability depends on the rate-limiting step of the permeation process. The drug molecules bound to bile micelles cannot permeate the epithelial membrane (EM) but can diffuse across the unstirred water layer (UWL) adjacent to the membrane. In the case of a low solubility/EM limited permeability drug, an increase in solubility is canceled out by a decrease in EM permeability, resulting in little food effect (e.g., pranlukast). In the case of a low solubility/UWL limited permeability drug, an increase in solubility is only slightly canceled out by a decrease in UWL

permeability, resulting in a positive food effect (e.g., danazol). In the case of a high solubility/EM limited permeability drug, if the drug can bind to bile micelles, the permeability is decreased, resulting in a negative food effect [45].

1.3.3 Hepatic Impairment

Hepatic impairment can be caused by chronic diseases such as hepatic and biliary cirrhosis. Liver cirrhosis is a progressive disease characterized by a decline in functional hepatocytes, hepatic blood flow, plasma protein (serum albumin, α-1-glycoprotein (AGP)), and expression levels of metabolizing enzymes and transporters in the liver as well as the intestine [46]. These changes can affect the pharmacokinetics of drugs. Then, PK predictions in hepatic impairment patients (HIP) are important for the optimization of clinical trial design as well as dose adjustments. Hepatic impairment is usually classified by the Child-Pugh (CP) grade: CP-A, CP-B, and CP-C represent mild, moderate, and severe hepatic impairment, respectively as shown below [47] (Table 1.1).

To construct each Child-Pugh population, the following factors varying with the degree of hepatic impairment have been incorporated: age distribution and sex ratio; liver size; expression levels of hepatic CYP isoforms; glomerular filtration rate (GFR); the plasma concentration of albumin and AGP; hematocrit; cardiac output; hepatic blood flow; and effect of portocaval shunting [48].

The population models of HIP were constructed by back calculating the expression levels of several CYP isoforms from the clinical data of each CYP probe substrate. The established population models of HIP (CP-A, CP-B, and CP-C) were verified using nine drugs (midazolam, caffeine, theophylline, metoprolol, nifedipine, quinidine, diclofenac, sildenafil, and omeprazole) which are mainly metabolism by CYP isoforms [48]. The predicted AUCRs (=AUC of HIP/AUC of healthy adults; the same hereafter in this section) of the drugs were within 0.8- to 1.25-fold of the observed AUCRs in 65% (13/20 cases). Another PBPK report extensively investigated the effect of hepatic impairment on the pharmacokinetics

Table 1.1 Classifications of hepatic impairment based on Child-Pugh Score

	Points scored for observed findings		
	1 point	2 points	3 points
Serum bilirubin (mg/dL)	<2	2–3	>3
Serum albumin (g/dL)	>3.5	2.8–3.5	<2.8
Prothrombin time (sec prolonged)	<4	4–6	>6
Encephalopathy grade	None	1–2	3 or 4
Ascites	Absent	Slight	Moderate

Child-Pugh A: 5–6 points (mild hepatic impairment)
Child-Pugh B: 7–9 points (moderate hepatic impairment)
Child-Pugh C: 10–15 points (severe hepatic impairment)

of 27 compounds, many of which are mainly metabolized in the liver [49]. As a result, 77% (43/56 cases, including 18 in mild, 25 in moderate, and 13 in severe hepatic impairment) of the predicted AUCRs were within two-fold of the observed AUCRs. Another article investigated the predictability of hepatic impairment on the pharmacokinetics of hepatic uptake and efflux transporter substrates [50]. Using bosentan, repaglinide, telmisartan, valsartan, and olmesartan, the uniform decreased level of several transporters in each HIP class to healthy adults was estimated by a top-down approach. Consequently, the described AUCRs were within 1.5-fold of the observed AUCRs in 5 out of 7 cases and within two-fold in all the cases. Considering the lack of supporting data for the predictions, such as the changes in protein levels of each transporter and the fractional contributions of each transporter to the overall uptake/efflux process of the substrates according to the Child-Pugh classification, the accumulation of such data in the future will enable more confident prediction from the IVIVE perspective.

To verify the population model of HIP, many efforts have been made to collect physiological data on HIP. However, we still rely on estimates based on a top-down approach for some parameters especially on the expression levels of metabolizing enzymes and transporters. Since quantifying their expression levels using biopsy samples is highly invasive and poses high implementation hurdles, the less invasive liquid biopsy method is expected to become a practical method in the future [51]. At this point, PK predictions in HIP might be used as reference data for optimizing the design of clinical studies, but the predictive accuracy would be on a case-by-case basis, as it depends on the accuracy of physiological data regarding the elimination route of an investigational drug. Of note, before PK prediction in HIP, it is necessary to confirm that a PBPK model of an investigational drug can appropriately describe pharmacokinetics in the control population (e.g., healthy adults).

1.3.4 Renal Impairment

Predicting the pharmacokinetics in renal impairment patients (RIP) is useful to inform dosing recommendations in the population. Glomerular filtration rate (GFR) is used as an index to classify the severity of renal function as shown below [52] (Table 1.2).

Table 1.2 Classifications of renal function

Classification	Range of values for renal function (mL/min/1.73 m^2)
Normal renal function	$\geq$90
Mild impairment	60–89
Moderate impairment	30–59
Severe impairment	15–29
Kidney failure	<15

It has been reported that renal impairment can affect the renal excretion of drugs, hepatic and intestinal metabolism, and serum albumin concentration [53–55]. The mechanisms of the decrease in hepatic and renal clearance seem to be the down-regulation of metabolizing enzymes and transporters and the inhibition effects on the enzymes by uremic toxins accumulated in the body [56]. Population models of RIP were constructed by including the various physiological parameters in renal impairment. Using PBPK models of 7 compounds eliminated mainly by renal excretion (fe > 0.79), the pharmacokinetics in mild, moderate, and severe RIP were predicted and compared with that in healthy adults [57]. The predicted AUCRs (=AUC of RIP/AUC of healthy adults; the same hereafter in this section) were within 1.5-fold of the observed AUCRs in 91% (20/22 cases) and within two-fold in 95% (21/22 cases). In contrast to this analysis by dynamic PBPK models, the authors also proposed a static model considering the differences in f_P, GFR, and hepatic intrinsic clearance between renal impairment patients and healthy adults. With the static model, the predicted AUCRs were within 1.5-fold of the observed AUCRs in 95% (21/22 cases) and within two-fold in all cases. Another PBPK report investigated the effect of renal impairment on the pharmacokinetics of 25 compounds, many of which are mainly metabolized in the liver [49]. As a result, 94% (47/50 cases including 8 in mild, 14 in moderate, 25 in severe renal impairment, and 3 in end-stage renal disease) of predicted AUCRs were within two-fold of the observed AUCRs.

Given that the observed AUCRs in the above literature were within three-fold in many cases, it may be difficult to evaluate the predictive accuracy appropriately. However, PBPK models that can describe PK profiles in healthy adults showed the potential to predict PK profiles in RIP, and these predictions could be helpful in considering the timing of a renal impairment PK study and optimizing the study design. It is also noteworthy that the prediction accuracy of the static model, which incorporates multiple factors in RIP, was at least as good as that of the dynamic PBPK model. Further understanding of physiological conditions according to the degree of renal impairment can improve the PK predictability.

1.3.5 Children

Although there is a growing demand for pediatric drug development, conducting frequent clinical trials on children is unrealistic. In addition, estimating the effective and safe doses is a significant challenge considering their rapid growth. While a PBPK model can be helpful in proposing pediatric doses in a first-in-pediatric study, the predictive accuracy has not been fully verified. After constructing a PBPK model in adults, pediatric PK profiles should be predicted by replacing population parameters in adults with pediatric subjects. In a previous report, the PBPK models of 10 drugs that are primarily metabolized by major CYP isoforms were constructed in adults (bottom-up or LMO not known) and used to predict pediatric pharmacokinetics in the following age groups: infants (1 month to <2 years), young children

(2 to <6 years), school-aged children (6 to <12 years), and adolescents (12 to <18 years) [58]. After the drugs were administered intravenously or orally, the predicted AUCs were within 1.5-fold of the observed AUCs in 64% (43/67 cases) and within two-fold in 87%(58/67 cases).

In this report, the PBPK model for CYP2C19 substrate (esomeprazole), which could predict PK profiles in adults appropriately, failed to predict PK profiles in infants. Moreover, the ontogeny profile of CYP2C8 significantly impacted the predictive accuracy of CYP2C8 substrates in infants. These findings suggest the need for validation of age-dependent physiological data and the possibility of estimating ontogeny profiles of metabolizing enzymes with GMO approach if sufficient PK data in children can be accumulated.

1.4 Summary and Opinion on PBPK Models

The PBPK model is utilized in a wide range of applications, from the early stages of drug discovery to the submission to regulatory authorities. This mechanism-based model could be highly versatile since it can predict various scenarios by changing the parameters related to a population when predicting the effects such as age and disease state, and by adding a perpetrator model when predicting DDI. The authors place a high expectation on PBPK models. But unfortunately, during the preparation of this manuscript, we recognized that the current practice of PBPK modeling has some issues as described below [59]. One possible way to overcome the issues would be to start with a simple PBPK model and progress step-by-step to more complex models (called Occam's razor principle). It is easier to report all details for a simple PBPK model. As discussed in the above sections, simple and/or static models for F_a, F_g, AUCR by DDI, and AUCR in RIP have been reported, and their predictability has been systemically evaluated using more than several dozens of drugs.

1.4.1 Transparency of Modeling Processes

For most of the studies using commercial software, we found that it was impossible to examine the model equations and physiological parameters, trace the calculation, and reproduce the results based on the disclosed information. The absence of transparency may shed a question on whether these articles could have had rigorous peer review before publication. This issue is not limited to complex PBPK models but is generally recognized in computational sciences. Recently, National Academies of Sciences, Engineering, and Medicine recommended the ways to improve transparency and rigor in research, saying, "All researchers should include a clear, specific, and complete description of how the reported results were reached." and "Journals should consider ways to ensure computational reproducibility for

publications that make claims based on computations, to the extent ethically and legally possible." [60]. It is critically important to disclose all model equations and physiological parameters for proper peer-review by referees and readers.

1.4.2 Literacy about Middle-out Approach

In many reports of the local middle-out approach (LMO), "description" and "prediction" has often been confused. LMO is conducted as (i) drug-by-drug back-calculation of one to several parameters from the existing clinical PK data (parameter fitting, optimization), and (ii) use those parameters for forwarding predictions for a different clinical situation. Unfortunately, (i) and (ii) have often been confused in the literature. Complex PBPK models are flexible and allow the users to perform parameter fitting as much as they want. In many cases, the users increase the number of parameters for fitting until obtaining a perfect match to the mean clinical data. When a parameter (s) of a complex PBPK model is fitted to the existing clinical PK data in such a way, a complex PBPK model can *describe* the existing data *always perfectly*. However, this does not mean that the model is correct and *predictive*. To make matters worse, parameter fitting hides any errors in the model. It should be noted that LMO using a scaling factor (SF) is mathematically the same as back calculating a physiological or a drug parameter (and vice versa) (SF is applied to these parameters, e.g., $SF \times CL_{int}$). The introduction of SF with no physiological meaning is regarded as instrumentalism rather than scientific realism. SF should be used following the rules of statistical empirical models.

1.4.3 Evidence Level of Local Middle-Out Approach

There is little or no systematic evaluation of LMO using complex PBPK models. Only case studies (or compiles of case studies) have been reported. Therefore, based on the concept of evidence-based medicine, the evidence level of LMO is low at this moment. In the future, it is highly desirable to systematically examine the predictability of the LMO approach using a wide variety of data as many as possible (at least several dozens) for each prediction purpose using a standardized procedure.

References

1. Wang Y, Zhu H, Madabushi R, Liu Q, Huang SM, Zineh I (2019) Model-informed drug development: current US regulatory practice and future considerations. Clin Pharmacol Ther 105:899–911

2. Krishnaswami S, Austin D, Pasqua OD, Gastonguay MR, Gobburu J, van der Graaf PH et al (2020) MID3: mission impossible or model-informed drug discovery and development? Point-counterpoint discussions on key challenges. Clin Pharmacol Ther 107:762–772

3. Zhao P, Zhang L, Grillo JA, Liu Q, Bullock JM, Moon YJ et al (2011) Applications of physiologically based pharmacokinetic (PBPK) modeling and simulation during regulatory review. Clin Pharmacol Ther 89:259–267

4. Jamei M, Dickinson GL, Rostami-Hodjegan A (2009) A framework for assessing inter-individual variability in pharmacokinetics using virtual human populations and integrating general knowledge of physical chemistry, biology, anatomy, physiology and genetics: a tale of 'bottom-up' vs 'top-down' recognition of covariates. Drug Metab Pharmacokinet 24:53–75

5. Zhang X, Yang Y, Grimstein M, Fan J, Grillo JA, Huang SM et al (2020) Application of PBPK modeling and simulation for regulatory decision making and its impact on US prescribing information: an update on the 2018–2019 submissions to the US FDA's office of clinical pharmacology. J Clin Pharmacol 60(Suppl 1):S160–S178

6. Li R, Barton HA, Yates PD, Ghosh A, Wolford AC, Riccardi KA et al (2014) A "middle-out" approach to human pharmacokinetic predictions for OATP substrates using physiologically-based pharmacokinetic modeling. J Pharmacokinet Pharmacodyn 41:197–209

7. Tsamandouras N, Rostami-Hodjegan A, Aarons L (2015) Combining the 'bottom up' and 'top down' approaches in pharmacokinetic modeling: fitting PBPK models to observed clinical data. Br J Clin Pharmacol 79:48–55

8. Pepin XJH, Huckle JE, Alluri RV, Basu S, Dodd S, Parrott N et al (2021) Understanding mechanisms of food effect and developing reliable PBPK models using a middle-out approach. AAPS J 23:12

9. Yoshikado T, Yoshida K, Kotani N, Nakada T, Asaumi R, Toshimoto K et al (2016) Quantitative analyses of hepatic OATP-mediated interactions between statins and inhibitors using PBPK modeling with a parameter optimization method. Clin Pharmacol Ther 100:513–523

10. Darwich AS, Margolskee A, Pepin X, Aarons L, Galetin A, Rostami-Hodjegan A et al (2017) IMI – Oral biopharmaceutics tools project – evaluation of bottom-up PBPK prediction success part 3: identifying gaps in system parameters by analysing in silico performance across different compound classes. Eur J Pharm Sci 96:626–642

11. Sjögren E, Thorn H, Tannergren C (2016) In silico modeling of gastrointestinal drug absorption: predictive performance of three physiologically based absorption models. Mol Pharm 13:1763–1778

12. Sjögren E, Thörn H, Tannergren C (2017) Reply to "Comment on 'In silico modeling of gastrointestinal drug absorption: predictive performance of three physiologically based absorption models'". Mol Pharm 14:340–343

13. Matsumura N, Hayashi S, Akiyama Y, Ono A, Funaki S, Tamura N et al (2020) Prediction characteristics of oral absorption simulation software evaluated using structurally diverse low-solubility drugs. J Pharm Sci 109:1403–1416

14. Ahmad A, Pepin X, Aarons L, Wang Y, Darwich AS, Wood JM et al (2020) IMI – Oral biopharmaceutics tools project – evaluation of bottom-up PBPK prediction success part 4: prediction accuracy and software comparisons with improved data and modelling strategies. Eur J Pharm Biopharm 156:50–63

15. Matsumura N, Ono A, Akiyama Y, Fujita T, Sugano K (2020) Bottom-up physiologically based oral absorption modeling of free weak base drugs. Pharmaceutics 12:844

16. Akiyama Y, Kimoto T, Mukumoto H, Miyake S, Ito S, Taniguchi T et al (2019) Prediction accuracy of mechanism-based oral absorption model for dogs. J Pharm Sci 108:2728–2736

17. Akiyama Y, Matsumura N, Ono A, Hayashi S, Funaki S, Tamura N et al (2022) Prediction of oral drug absorption in rats from in vitro data. Pharm Res; Online ahead of print

18. Sugano K, Nabuchi Y, Machida M, Aso Y (2003) Prediction of human intestinal permeability using artificial membrane permeability. Int J Pharm 257:245–251

19. Sugano K (2011) Fraction of a dose absorbed estimation for structurally diverse low solubility compounds. Int J Pharm 405:79–89

20. Gertz M, Harrison A, Houston JB, Galetin A (2010) Prediction of human intestinal first-pass metabolism of 25 CYP3A substrates from in vitro clearance and permeability data. Drug Metab Dispos 38:1147–1158
21. Gertz M, Davis JD, Harrison A, Houston JB, Galetin A (2008) Grapefruit juice-drug interaction studies as a method to assess the extent of intestinal availability: utility and limitations. Curr Drug Metab 9:785–795
22. Yang J, Jamei M, Yeo KR, Tucker GT, Rostami-Hodjegan A (2007) Prediction of intestinal first-pass drug metabolism. Curr Drug Metab 8:676–684
23. Paine MF, Hart HL, Ludington SS, Haining RL, Rettie AE, Zeldin DC (2006) The human intestinal cytochrome P450 "pie". Drug Metab Dispos 34:880–886
24. Sugano K (2012) Biopharmaceutics modeling and simulations: theory, practice, methods, and applications. Wiley
25. Nishimuta H, Sato K, Yabuki M, Komuro S (2011) Prediction of the intestinal first-pass metabolism of CYP3A and UGT substrates in humans from in vitro data. Drug Metab Pharmacokinet 26:592–601
26. Kato M, Chiba K, Hisaka A, Ishigami M, Kayama M, Mizuno N et al (2003) The intestinal first-pass metabolism of substrates of CYP3A4 and P-glycoprotein – quantitative analysis based on information from the literature. Drug Metab Pharmacokinet 18:365–372
27. Wood FL, Houston JB, Hallifax D (2017) Clearance prediction methodology needs fundamental improvement: trends common to rat and human hepatocytes/microsomes and implications for experimental methodology. Drug Metab Dispos 45:1178–1188
28. Hallifax D, Houston JB (2009) Methodological uncertainty in quantitative prediction of human hepatic clearance from in vitro experimental systems. Curr Drug Metab 10:307–321
29. Lee J, Yang Y, Zhang X, Fan J, Grimstein M, Zhu H et al (2021) Usage of in vitro metabolism data for drug-drug interaction in physiologically based pharmacokinetic analysis submissions to the US Food and Drug Administration. J Clin Pharmacol 61:782–788
30. Rowland A, Elliot DJ, Knights KM, Mackenzie PI, Miners JO (2008) The "albumin effect" and in vitro-in vivo extrapolation: sequestration of long-chain unsaturated fatty acids enhances phenytoin hydroxylation by human liver microsomal and recombinant cytochrome P450 2C9. Drug Metab Dispos 36:870–877
31. Wood FL, Houston JB, Hallifax D (2018) Importance of the unstirred water layer and hepatocyte membrane integrity in vitro for quantification of intrinsic metabolic clearance. Drug Metab Dispos 46:268–278
32. Hallifax D, Foster JA, Houston JB (2010) Prediction of human metabolic clearance from in vitro systems: retrospective analysis and prospective view. Pharm Res 27:2150–2161
33. Uchimura T, Kato M, Saito T, Kinoshita H (2010) Prediction of human blood-to-plasma drug concentration ratio. Biopharm Drug Dispos 31:286–297
34. Wagner C, Pan Y, Hsu V, Grillo JA, Zhang L, Reynolds KS et al (2015) Predicting the effect of cytochrome P450 inhibitors on substrate drugs: analysis of physiologically based pharmacokinetic modeling submissions to the US Food and Drug Administration. Clin Pharmacokinet 54:117–127
35. Hsueh C, Hsu V, Pan Y, Zhao P (2018) Predictive performance of physiologically-based pharmacokinetic models in predicting drug-drug interactions involving enzyme modulation. Clin Pharmacokinet 57:1337–1346
36. Guest EJ, Aarons L, Houston JB, Rostami-Hodjegan A, Galetin A (2011) Critique of the two-fold measure of prediction success for ratios: application for the assessment of drug-drug interactions. Drug Metab Dispos 39:170–173
37. Ohno Y, Hisaka A, Suzuki H (2007) General framework for the quantitative prediction of CYP3A4-mediated oral drug interactions based on the AUC increase by coadministration of standard drugs. Clin Pharmacokinet 46:681–696
38. Hariparsad N, Ramsden D, Taskar K, Badée J, Venkatakrishnan K, Reddy MB et al (2021. Online ahead of print) Current practices, gap analysis, and proposed workflows for PBPK modeling of cytochrome P450 induction: an industry perspective. Clin Pharmacol Ther 112:770

39. Kenny JR, Ramsden D, Buckley DB, Dallas S, Fung C, Mohutsky M et al (2018) Considerations from the innovation and quality induction working group in response to drug-drug interaction guidances from regulatory agencies: focus on CYP3A4 mRNA in vitro response thresholds, variability, and clinical relevance. Drug Metab Dispos 46:1285–1303

40. Zheng HX, Huang Y, Frassetto LA, Benet LZ (2009) Elucidating rifampin's inducing and inhibiting effects on glyburide pharmacokinetics and blood glucose in healthy volunteers: unmasking the differential effects of enzyme induction and transporter inhibition for a drug and its primary metabolite. Clin Pharmacol Ther 85:78–85

41. Asaumi R, Menzel K, Lee W, Nunoya K, Imawaka H, Kusuhara H et al (2019) Expanded physiologically-based pharmacokinetic model of rifampicin for predicting interactions with drugs and an endogenous biomarker via complex mechanisms including organic anion transporting polypeptide 1B induction. CPT Pharmacometrics Syst Pharmacol 8:845–857

42. Wagner C, Pan Y, Hsu V, Sinha V, Zhao P (2016) Predicting the effect of CYP3A inducers on the pharmacokinetics of substrate drugs using physiologically based pharmacokinetic (PBPK) modeling: an analysis of PBPK submissions to the US FDA. Clin Pharmacokinet 55:475–483

43. Ohno Y, Hisaka A, Ueno M, Suzuki H (2008) General framework for the prediction of oral drug interactions caused by CYP3A4 induction from in vivo information. Clin Pharmacokinet 47:669–680

44. Sugano K, Kataoka M, da Costa MC, Yamashita S (2010) Prediction of food effect by bile micelles on oral drug absorption considering free fraction in intestinal fluid. Eur J Pharm Sci 40:118–124

45. Akiyama Y, Ito S, Fujita T, Sugano K (2020) Prediction of negative food effect induced by bile micelle binding on oral absorption of hydrophilic cationic drugs. Eur J Pharm Sci 155:105543

46. Rodighiero V (1999) Effects of liver disease on pharmacokinetics. An update. Clin Pharmacokinet 37:399–431

47. Center for Drug Evaluation and Research (2003) Pharmacokinetics in patients with impaired hepatic function: study design, data analysis, and impact on dosing and labeling guidance for industry. Food and Drug Administration, Rockville. https://www.fda.gov/regulatory-information/search-fda-guidance-documents/pharmacokinetics-patients-impaired-hepatic-function-study-design-data-analysis-and-impact-dosing-and. Accessed May 2003

48. Johnson TN, Boussery K, Rowland-Yeo K, Tucker GT, Rostami-Hodjegan A (2010) A semi-mechanistic model to predict the effects of liver cirrhosis on drug clearance. Clin Pharmacokinet 49:189–206

49. Heimbach T, Chen Y, Chen J, Dixit V, Parrott N, Peters SA et al (2021) Physiologically-based pharmacokinetic modeling in renal and hepatic impairment populations: a pharmaceutical industry perspective. Clin Pharmacol Ther 110:297–310

50. Li R, Barton HA, Maurer TS (2015) A mechanistic pharmacokinetic model for liver transporter substrates under liver cirrhosis conditions. CPT Pharmacometrics Syst Pharmacol 4:338–349

51. Achour B, Al-Majdoub ZM, Grybos-Gajniak A, Lea K, Kilford P, Zhang M et al (2021) Liquid biopsy enables quantification of the abundance and interindividual variability of hepatic enzymes and transporters. Clin Pharmacol Ther 109:222–232

52. Center for Drug Evaluation and Research (2020) Pharmacokinetics in patients with impaired renal function – study design, data analysis, and impact on dosing guidance for industry: draft guidance. Food and Drug Administration, Silver Spring. https://www.fda.gov/regulatory-information/search-fda-guidance-documents/pharmacokinetics-patients-impaired-renal-function-study-design-data-analysis-and-impact-dosing-and. Accessed September 2020

53. Yeo KR, Aarabi M, Jamei M, Rostami-Hodjegan A (2011) Modeling and predicting drug pharmacokinetics in patients with renal impairment. Expert Rev Clin Pharmacol 4:261–274

54. Nolin TD, Naud J, Leblond FA, Pichette V (2008) Emerging evidence of the impact of kidney disease on drug metabolism and transport. Clin Pharmacol Ther 83:898–903

55. Dreisbach AW, Lertora JJL (2008) The effect of chronic renal failure on drug metabolism and transport. Expert Opin Drug Metab Toxicol 4:1065–1074

56. Yeung CK, Shen DD, Thummel KE, Himmelfarb J (2014) Effects of chronic kidney disease and uremia on hepatic drug metabolism and transport. Kidney Int 85:522–528
57. Yee KL, Li M, Cabalu T, Sahasrabudhe V, Lin J, Zhao P et al (2018) Evaluation of model-based prediction of pharmacokinetics in the renal impairment population. J Clin Pharmacol 58:364–376
58. Zhou W, Johnson TN, Bui KH, Cheung SYA, Li J, Xu H et al (2018) Predictive performance of physiologically based pharmacokinetic (PBPK) modeling of drugs extensively metabolized by major cytochrome P450s in children. Clin Pharmacol Ther 104:188–200
59. Sugano K (2021) Lost in modelling and simulation? ADMET DMPK 9:75–109
60. The National Academies of Sciences, Engineering, and Medicine (2019) Reproducibility and replicability in science. The National Academies Press, Washington, DC

Chapter 2
Physiologically Based Pharmacokinetic (PBPK) Modeling Application on Food Effect Assessment

Di Wu, John P. Gleeson, and Filippos Kesisoglou

Abstract Food–drug interaction is one of the major factors that impact clinical pharmacokinetics in drug development. Unfortunately, the available in vitro and preclinical models do not appropriately predict food effects due to the complex mechanisms. It is recognized by the FDA that a food effect study should be conducted in the early clinical stage to inform the dosing paradigm and establish food effects risks in patients. Physiologically based biopharmaceutics modeling (PBBM) is a powerful tool to predict clinical PK by incorporating physiology-related and drug product-related factors in the mechanistic absorption model. PBBM has been utilized in various applications in drug development, such as biopharmaceutics risk assessment, bioequivalence safe space setup, and pH-mediated drug–drug interaction evaluation. The application of utilizing PBBM for food effect assessment has been tested and validated through many published case studies. In this chapter, an overview of food effects including current assessment practice, various food–drug interaction mechanisms, and clinical considerations is included. Thorough instruction on using PBBM to evaluate food effects is provided, followed by two detailed case studies. Though PBBM has shown potential in food effect prediction, it is still an evolving area, and current gaps and future directions are discussed.

2.1 Introduction

In the past decades, physiologically based pharmacokinetic (PBPK) modeling or physiology-based biopharmaceutics modeling (PBBM) has been an evolving area in drug development to support clinical pharmacology assessment such as drug–drug

D. Wu · J. P. Gleeson · F. Kesisoglou (✉)
Pharmaceutical Sciences and Clinical Supply, Merck & Co., Inc., Rahway, NJ, USA
e-mail: filippos_kesisoglou@merck.com

interaction (DDI) prediction, pH-mediated DDI, food effect, and biopharmaceutics applications including formulation development, bioequivalence prediction, in vitro specification settings, application for study waivers, and internal decision making [1, 2]. PBBM is considered a powerful tool in drug development, that can describe or predict a drug product's exposure in human by incorporating physiological conditions, physicochemical properties of the compound, and additional relevant factors into the model parameters [3]. Advanced compartmental absorption transit (ACAT) or advanced dissolution, absorption, and metabolism (ADAM) models are the most commonly used mechanistic models to mimic in vivo absorption processes in PBBM [4]. Health authorities have released guidance on PBPK and PBBM to encourage their applications in drug development for both innovators and generic companies in the past years [3].

The interaction between drug and food is a significant factor that may impact the drug product's bioavailability, safety, and efficacy. About 40% of on-market drug products have a significant food effect [5]. In the early stage of drug development, in vitro testing and preclinical studies are two major approaches for assessing potential food effects. However, the food effect mechanism can be complicated, so there are no mature or biopredictive in vitro tools for food effect assessment. Moreover, the translation from preclinical to clinical is hard to manage due to species barrier. Hence, the overall prediction accuracy using in vitro or preclinical strategies still requires refinement. In the clinical stage, the most effective approach to evaluate food effect is through clinical study, which is recognized by the agency [6]. PBBM is advantageous over other in vitro approaches for food effect assessment by taking into account the changes in physiology, compound characterizations, elimination parameters, etc., which may be altered in the presence of food. In addition, the regulatory agency usually encourages an early assessment of food effects in the clinic to inform later clinical studies [6]. To avoid unnecessary clinical studies in the late stage, PBBM is an alternative tool to evaluate food effects with formulation changes.

Food–drug interaction can potentially alter the exposure of drug products in the clinic, which further impacts the safety and efficacy profiles [6]. As stated, the FDA has recommended assessing the food effect in the early stage of drug development and conducting a food effect study in the early clinical phases. In practice, a food effect study is a routine study in a Phase I clinical trial in drug development. To define a food effect, if the 90% confidence interval (CI) for the ratio of the population geometric means between fed and fasted conditions for AUC_{0-INF} (AUC_{0-t} when appropriate) and C_{max} fall in the equivalence limits (80–125%), then it is considered to have no food effect for the tested drug product, otherwise, it would be either positive or negative food effect [6], as shown in Fig. 2.1.

Food effect assessment is critical to inform the overall drug development program, further dosing instructions with food, and the final labeling. Hence, a food effect study is highly recommended by FDA for all orally administered new chemical entities (NCE). The only study waiver included in the current food effect guidance for the investigation of a new drug (IND) and new drug application (NDAs) is for biopharmaceutics classification system (BCS) I drug (high
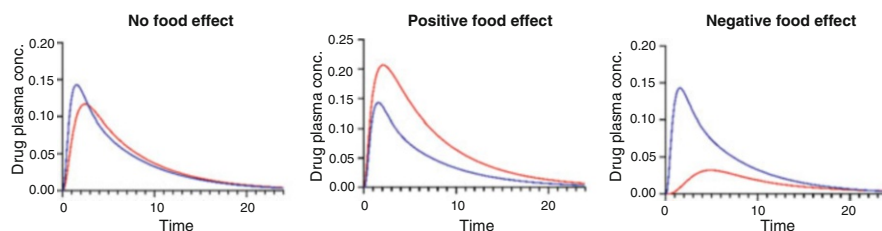
Fig. 2.1 Schematic figure on food-drug interactions

permeability, high solubility) that are formulated as immediate-release (IR) and show high bioavailability ($F \geq 0.85$) and low first-pass extraction [6].

The effect of food on drug dissolution, solubility, absorption, and clearance is very complex as it pertains to the drug, the formulation, and the GI fluids. Commonly studied mechanisms can be classified into direct interaction between drug products and food and indirect interaction [7, 8]. Specific mechanistic food effects will be discussed in detail in the following sections. In this chapter, a detailed description of the food effect mechanism, modeling instruction, and case studies to show how to use PBBM to assess food effect, and current gaps and future directions are included.

2.2 Food–Drug Interactions

2.2.1 Specific Food–Drug Interactions

2.2.1.1 Milk

Bovine milk is a commonly consumed beverage in Western diets; however, it poses a pharmacokinetic risk due to its complex composition and can result in positive or negative food effects depending on the physicochemical characteristics of the active pharmaceutical ingredient (API; drug). Whole-fat cow's milk has a calorie content of 65 kcal/100 mL, and per 100 g contains 3.4 g of protein, 4.6 g of carbohydrates, and 3.7 g of fats (predominantly medium- and long-chain fatty acids). The fats and proteins in milk form an oil-in-water emulsion which can have positive food effects on the absorption of lipophilic drug API. Lumefantrine, an anti-malarial drug, had improved absorption when co-administered with 200 ml of whole milk containing 6.8 g of fat [9]. However, an increase in oral bioavailability was not observed with the co-administration of the lipophilic erlotinib, a chemotherapeutic, and 250 ml of cow's milk containing 3.9% fat [10].

Negative food effects are more commonly found when a drug is co-administered in the presence of milk. The high protein content in milk is metabolized by gastric and pancreatic enzymes to release free amino acids and small peptides which compete with drugs for absorption via the intestinal di- and tripeptide transporter

PEPT1 (SLC15A1) [11]. The oral absorption of oseltamivir, an anti-viral prodrug substrate for PEPT1, had a reduced C_{max} and delayed T_{max} when co-administered with 400 ml of milk compared to water likely due to competition for PEPT1-mediated uptake [12]. Chelation also poses a negative food effect on certain classes of drugs such as bisphosphonates and tetracyclines. The Ca^{2+} ions present in milk form insoluble chelates of tetracycline reducing the drug's ability to be absorbed [13]. The oral bioavailability of demeclocycline, a tetracycline antibiotic, was reduced by 80% when co-administered with milk [14]. The major protein in milk, casein, can also contribute to both physical and chemical drug binding reducing the amount of free drug in the intestinal lumen available for absorption [15].

2.2.1.2 Grapefruit Juice

Some prescription and over-the-counter (OTC) drugs have label claims warning against co-administration with grapefruit juice. Citrus fruits including grapefruits, Seville oranges, limes, and pomelos contain large amounts of the flavonoid naringin, and the furanocoumarins bergamottin and $6'$, $7'$-dihydroxy-bergamottin. These polyphenols impact the pharmacokinetic profile of a drug in two ways: (1) inhibition of cytochrome P450 (CYP) enzymes leading to decreased drug clearance and (2) inhibition of uptake and efflux transporters leading to decreased or increased absorption, respectively.

Bailey and colleagues discovered the interaction between grapefruit and the calcium channel blockers, felodipine, and nifedipine [16, 17]. The oral bioavailability of felodipine increased from 15% to 270% when co-administered with 250 ml of grapefruit juice [18]. This was due to the inhibition of CYP3A4 in both the intestinal enterocytes and liver hepatocytes that under normal conditions metabolize the drug thus reducing the oral bioavailability. These polyphenols have also been reported to inhibit the intestinal efflux transporter P-glycoprotein (P-gp) in cell models which altered the absorption of talinolol (a beta-blocker) and vinblastine (a chemotherapeutic) [19]. It is unclear how much this contributes to altered pharmacokinetic profile in vivo as these cell models are often directly exposed to high concentrations of drugs and inhibitors. However, metabolizing enzymes and P-gp substrates can be factored into models in systems such as a GastroPlus® and Simcyp™.

2.2.1.3 Alcohol (Ethanol)

Ethanol consumption can lead to both specific and unspecific interactions when co-administered with a drug. BCS Class II and IV drugs typically have a higher solubility in the presence of ethanol as a solvent/solubilizing agent. In one such study, non-ionizable and weak acid drugs had increased solubility in the presence of 20% ethanol in dissolution media (either NaCl at pH 2.5 or FaSSGF), whereas weak base drugs' solubility was unaffected by the presence of ethanol [20]. In a rat study,

with co-administration of 20% ethanol and either felodipine or indomethacin, the oral absorption of the drugs was not impacted by the presence of ethanol [21]. However, when healthy volunteers were co-administered 0.8 g/kg ethanol with diazepam, there was an increase in plasma drug levels, particularly for whiskey, beer, and white wine [22]. Although diazepam is a BCS Class I drug, it has increased solubility in the presence of alcohol that increases the AUC. Non-specifically, alcohol-dependent patients have intestinal barrier inflammation and dysfunction leading to increase intestinal permeability and oral bioavailability that would not be accounted for in simulations or models [23, 24].

2.2.2 Non-specific Food–Drug Interactions

2.2.2.1 Description of Fasted and Fed Conditions in Clinical Studies by the Agency

The FDA guides the planning and specifics of food effects studies for orally administered drugs. Under these guidelines, the FDA defines "*Fasted Conditions*" as an overnight fast of at least 10 h and the drug should be administered with 240 ml of water with additional water permitted ad-lib an hour after administration. The FDA defines "*Fed Conditions*" as an overnight fast of at least 10 h and consumption of a meal (Table 2.1) 30 min before drug administration and the meal should be consumed within 30 min. Like the fasted state, the drug is administered with 240 ml of water, and water is permitted ad-lib an hour after administration. If there are data to suggest positive or negative food effects and a potential label restriction is being sought, e.g., "no food should be consumed *X hours before* or *Y hours after* drug administration," then this would fall under "*Modified Fasted Conditions*" and the study should be designed with appropriate separation times between drug administration and food consumption [6].

Similar recommended diets are not prescribed for pediatric studies; however, the FDA suggests comparing the age-appropriate formulation in adults and subsequently

Table 2.1 Test meal definitions and composition [6]

Meal type		High fat	Low-fat
Total Kcal		800–1000	400–500
Fat	Kcal	500–600	100–125
	Grams	55–65	11–14
	Percent	50	25
Example of meal		Two eggs fried in butter. Two strips of bacon. Two slices of toast with butter. Four ounces of hash brown potatoes. Eight ounces of while milk.	One boiled egg. One packet flavored instant oatmeal made with water. Eight ounces of milk (1% fat).

testing appropriate food interactions, e.g., apple sauce and pudding [25]. Mini-tablet and sprinkle/granule formulations are increasingly developed for pediatric patients, and these are often delivered in a food vehicle. The pH range of typically delivered foods needs to be anticipated with on the impact of these formulations, e.g., fruit juices pH is 3–4.5 white milk pH is ~6.5 [26].

2.2.2.2 Gastrointestinal Transit Time

The gastric emptying half-life is estimated to be 11–15 min with 85% of the initial gastric volume being emptied after 30 min under fasting conditions [27]. The disintegration of immediate-release (IR) dosage forms is estimated to be 10–20 min in the fasted stomach and ~ 40 min in the fed stomach [28]. In simulations, the transit time in the fasted is 15 mins such as the fasted human ACAT™ (Advanced Compartmental and Transit) in GastroPlus®, whereas, in the fed-state human ACAT™ is 1 hour. The small intestinal transit time has been measured and found that age and sex do not impact transit time of 3–4 h [29]. Similarly, food effects do not impact the transit time in the small intestine and the regional transit times are consistent in ACAT™ models in GastroPlus®.

2.2.2.3 Physicochemical Properties of Luminal Fluid

The luminal fluids in the gastrointestinal tract undergo physicochemical changes when a meal is consumed. The gastric fluid volume under the fasting state is ~35 ml, and drug formulations in the clinic are typically administered with 240 ml which is cleared within 30 minutes [30]. In healthy volunteers after the intake of a high-calorie high-fat standard meal (as per FDA guidelines), the gastric fluid increases to 500–600 ml directly after ingestion and over the course of 3–4 h decreases toward basal conditions [31]. Though the gastric fluid volume increases rapidly, the fasted state of small intestinal fluid increases more slowly from ~40 ml to ~90 ml at 12 min after dosing of 240 ml water and the volume remains >60 ml for 2 h [30, 32]. Data are sparse on the small intestinal fluid volume under fed conditions as the MRI method used for quantifying volume cannot accurately measure chyme or mixed fluid content. It is assumed that the fluid volume is at least equivalent to fasted state although the viscosity of the chyme is likely much higher than that of water [33]. Luminal contents from healthy adults after eating a solid meal of 645 ml indicate that the volume of chyme that passed the mid-duodenum and proximal jejunum was 1.5 and 0.75 L, respectively, over 2 h [34].

The stomach has a resting fasted state pH between 1 and 2 (Table 2.2); however, after ingesting a meal, the pH rapidly increases >4, and the osmolality increases from 50–180 to 300–500 mOsm/kg [35]. The altered gastric pH and osmolality will impact the dissolution of a drug formulation and it may be necessary to carry out dissolution testing in fed-state simulated gastric fluid (FeSSGF) [36]. Additionally, the consistency of the meal impacts the gastric fluid pH, a homogenous liquid meal

Table 2.2 Composition and characteristics of simulated and human gastrointestinal fluids [39, 42, 79, 80]

	SGF	Stomach (fasted)	Stomach (fed)	FaSSIF	Fasted HIF	FeSSIF	Fed HIF
pH	1.6	1.4–2-5	4.3–5.4	6.5	6.83	5	5.96
Buffer capacity (mmol/L/pH)	–	7–18	14–28	10–12	5.4 ± 0.1	72–76	18.0 ± 0.8
Osmolarity (mmol/kg)	120	171–276	217	270	189	635–670	372
Total bile salt content (mM)	0.08	0.08 ± 0.03	0.06	3	3.52	15	8.91

leads to higher postprandial gastric pH in the first hour compared to a solid–liquid meal. The resting pH of the upper small intestine under fasting conditions is slightly acidic (pH 6.1–7.0) and decreases to pH 6.4 (1 h postprandial) and pH 5.3–6.1 (2–3 h postprandial) [37]. The buffer capacity increases significantly from 6.9–9.0 to >20 mmol/L/ΔpH after ingestion of 240 ml of water or a meal [38]. Similarly, the osmolality increases from ~100–200 to ~300–400 mOsm/kg after ingestion of water or a meal.

Beyond these compositional changes, the bile salt, phospholipid, cholesterol, and free fatty acid concentrations increase postprandial which impact the solubility and absorption of drugs across the intestinal epithelium. For example, danazol (a neutral compound steroid) and phenytoin (a weak acid antiepileptic) have significantly high solubility and faster dissolution in fed-state simulated intestinal fluid (FeSSIF) than fasted-state SIF (FaSSIF) or blank buffers due to bile salt solubilization [39]. The duodenal bile salt composition profile has minor changes between prandial states, e.g., taurocholic acid increases from 14% to 19% of total bile salt composition [40]. However, the concentration of bile salt in human intestinal fluids increases dramatically: glycocholic acid (1–2.7 mM), taurocholic acid (0.5–1.7 mM), glycochenodeoxycholic acid (0.8–2 mM), and taurochenodeoxycholic acid (0.4–1.2 mM) changes in fasted to fed states respectively. The regional concentration of bile salts in the duodenum and jejunum in fasted conditions fall within the same range of 570–5137 μM and 829–5470 μM respectively [40]. Simulated intestinal fluids (SIF) used for dissolution and solubility assessment in vitro only contain one bile salt (taurocholate) with a concentration of 3 mM (fasted) and 10–15 mM (fed) [39]. However, FeSSIF has been shown to underestimate the solubility and dissolution of drugs such as cyclosporine, valsartan, and ketoconazole when compared to human intestinal fluid (HIF) likely due to the lower bile salt concentration and differing composition [41, 42].

2.2.2.4 Intestinal Barrier: Transporters and Blood Flow

Although there is a myriad of influx transporters on the apical surface of the intestinal enterocytes in regards to food effects studies, much focus is given to the

intestinal di- and tripeptide transporter PEPT1 (SLC15A1) and the organic anion transporting polypeptide 2B1 (OATP2B1), and the efflux transporter P-glycoprotein 1 (Pgp; MDR1). OATP2B1 has broad substrate specificity and is involved in the absorption of steroid hormone conjugates (estrone sulfate), statins (HMG-coenzyme A inhibitors), and small molecules (fexofenadine) [43]. An in vitro study of HEK293 (human embryonic kidney cells) transiently overexpressing OATP2B1 indicated that food additives such as colorants were inhibitors of OATP2B1 at dietary concentrations at both pH 5.5 and 7.4 [44]. PEPT1 is a similarly broad specificity transporter and therefore suffers from the competition of substrates for absorption. In a mouse study looking at food effects of PEPT1, researchers found that the absorption of dipeptide substrate (Gly-Sar) was reduced by 30% in the presence of food [45]. These transporters typically result in negative food effects, e.g., a decrease in the amount of drug that is absorbed resulting in a reduced C_{max} and AUC. The efflux transporter P-gp is known to limit the bioavailability of several drugs belonging to different chemical classes including cyclosporin A, talinolol, digoxin, and vinblastine [46]. Cell-based in vitro assays have allowed for the assessment of food-derived Pgp substrates including inhibitors that will decrease drug efflux (green tea, rosemary extract, and mint extract), and stimulators that will increase drug efflux (olive oil secoiridoid oleocanthal and palm oil γ-tocotrienol) [46, 47]. Many BCS Class III drugs have negative food effects (decreased drug absorption) due to inhibition of uptake transporters.

In addition to the physiological food effects topics discussed, the increased blood flow and increase in clearance of biliary compounds can impact the absolute oral bioavailability of a drug formulation. The exact mechanism that leads to increased splanchnic blood flow remains unknown; however, it is clear that the increase in hepatic blood flow accelerates the uptake of drugs from the portal vein into systemic circulation but also increases first-pass metabolism [48]. Estimated hepatic blood flow increased by 34% an hour after a high protein meal was delivered to patients [49]. Using available data sets, Xiao and colleagues showed that a high-fat meal increased the biliary clearance of BCS I/II drugs by 39% and BCS III/IV drugs by 125% based on the equation:

$$CL_{B,fasted/fed} = CL_{fed/fasted} - (CL_M + CL_R)$$

where $CL_{B,fasted/fed}$ is the biliary clearance; $CL_{fed/fasted}$, CL_M, and CL_R are the total clearance, metabolic clearance, and renal clearance, respectively [8].

2.2.2.5   In Vitro, In Vivo Testing of Food Effects

Based on the food-drug DDI mechanism, to assess food effect, in vitro testing on drug substance and drug products and animal PK models are commonly used [50–54]. As previously mentioned, bile salts contribute to the solubility and dissolution of orally administered drugs. Unfortunately, there is no perfect in vitro model to

determine food effects as it is such a complicated process; however, a combination of in vitro solubility testing combined with in silico calculations can help predict food effects. Henze et al. used the in vitro solubility of venetoclax (a BCS IV drug) in pig-specific FaSSIF and a fasted min-pig ACAT™ (Advanced Compartmental and Transit) in GastroPlus® to predict food effects accurately (T_{max}: 6 h [observed] vs 6.4 h [predicted], AUC: 12.5 ± 3.2 [observed; µg.h/ml] vs 9.53 [predicted] [55]. This example indicates the necessity of species-specific in vitro buffers due to the difference in bile salt concentration can lead to an underprediction of the bile salt solubilization ratio (SR). The bile salt SR is a parameter in GastroPlus® that can be derived from the solubility difference in buffer that contain bile salts (FaSSIF and FeSSIF) and buffers that a free of bile salts (PBS). The solubilization ratio determines the bile salts' contribution to the solubility of the drug using the following equation:

$$C_{sx} = C_{so} + (SC_{bs})(MW)([NaTC])$$

where C_{sx} is the solubility in the presence of taurocholate, C_{so} is the solubility in the absence of bile salts, SC_{bs} is the solubilization capacity of the bile salt for the drug predicted from the partition coefficient, MW is the molecular weight of the drug, and [NaTC] is the concentration of sodium taurocholate [56].

2.3 Tutorial of PBPK Modeling for Food Effect Assessment

PBPK models consider the body to have various compartments due to the physiological differences of tissues/organs. The incorporated mechanistic absorption models such as ACAT and ADAM models represent the absorption process. PBPK modeling integrates physiological conditions with compound-specific parameters to describe or predict drug concentration in tissue or plasma. In practice, three aspects are considered in PBPK modeling, including physicochemical properties of test compound (compound tab), physiology conditions (physiology tab), and disposition parameters (pharmacokinetics tab). Detailed information on each tab is described below.

2.3.1 Compound Tab: Physiochemical Property

The input in the compound tab is compound-specific, and it is the determining factor in the absorption of the drug product. Information such as pH solubility/biorelevant solubility, pKa, permeability, particle size, and precipitation time is the key parameters for model simulation. The high quality of parameter input is critical to model confidence. For example, for poorly soluble drugs or weak basic compounds, the input of pH-solubility profile should cover the whole physiology pH range

(pH 1.3–6.8), and it is preferred to cover intrinsic solubility for a better pKa estimation. For food effect assessment, it is preferred to input solubility in biorelevant media including FaSSIF and FeSSIF for a biopredictive prediction. The apparent permeability (P_{app}) value can be obtained from in vitro transport assays in cell lines such as Caco-2, MDCK, and LLC-PK1. The measured P_{app} can be calculated into human effective permeability (P_{eff}) based on default software build-in calculation or company internal correlation. In silico approach such as quantitative structure–property relationship (QSPR) allows an estimation of some essential parameters including lipophilicity, acidity/basicity, clearance, solubility, permeability, binding to red blood cells, and plasma protein especially when the experimental value is hard to measure or drug development is still in the early stage. ADMETPredictor® is a build-in tool in Gastroplus. By importing the structure (mol. file) from software such as ChemDraw into Gastroplus allows the software to predict parameter values based on structure. Combining QSPR and ADMETPredictor® enables the estimation of the compounds' properties allowing for an initial evaluation of the drug characterization and behavior.

2.3.2 Physiology Tab: Meal Type and Physiological Changes

The physiology tab has incorporated the mechanistic absorption model (ACAT for Gastroplus and ADAM for Simcyp) to account for physiological changes of each compartment in the GI tract such as composition, volume, and transit time. As discussed in the previous section on the food effect mechanism, the major impact of food–drug interaction on the gastrointestinal (GI) tract is gastric transit time, lumen fluid, and transporters. In Gastroplus, the default value of GI parameters is used for human under fasted status, with 0.25-h gastric transit time. The ASF model accounts for the permeability of each sub-compartment in the GI tract. The optimized logD Model SA/V 6.1 is considered more suitable for human prediction (Fig. 2.2).

When modeling food ingestion, the gastric transit time is changed to 1 h by default for high-calorie high fat (HCHF) meals, and there are slight changes in the ASF values in the gastric and upper small intestine. In the commercial software, the fed option under physiology can be selected to account for the fed status, and selections for different meal types are available such as FDA high-fat breakfast, user-defined meal, and the HCHF meal. The gastric emptying time depends on the calorie content of a meal. Zero-order gastric emptying will be applied for all new meal selections based on the preponderance of literature gastric emptying studies. The gastric transit time can be further optimized to fit each clinical subject for weak acid drugs since the transit time will be highly dependent on the phases of interdigestive migrating myoelectric complex (IMMC), which brings more viability to the transit time [57]. In the study of Xavier et al., the individual gastric transit time was fit to the clinical pharmacokinetic profile and used for further simulation, also
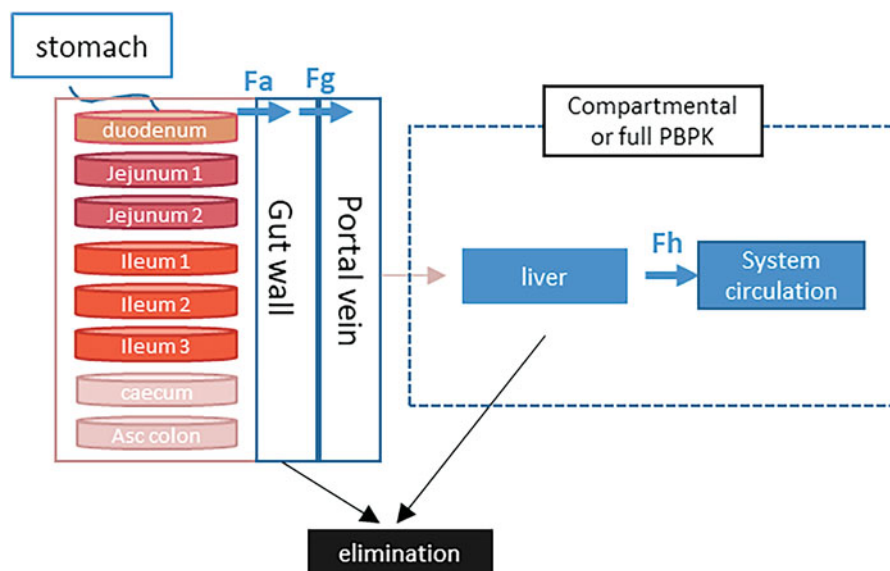
Fig. 2.2 Mechanistic absorption model and an overview of PBBM, modified from [1, 78]

the longer transit time is used to account for the double peak observed in the clinic [58].

Another critical influencing parameter on the absorption of food is luminal fluid, especially for poorly solubility compounds. Lumen bile salt concentration in the modeling depends on the fat percentage in the meal. The higher the fat%, the higher the bile salt concentration, which contributes to higher potential drug solubilization in the lumen. The water percentage in the intestine is another determining factor. The input of water content in the small intestine and colon under the physiology tab allows the user to adjust the water fraction of the intestine total volume. The default setting for small intestine and colon water volume is 40 and 10%, respectively; however, several studies have reported much lower values, such as 10% and 2% or 7.5% and 2.5% by fitting the observed PK data [58].

2.3.3 PK Tab: Compartmental or Whole-Body Models

Normally in PBBM, two models (compartmental model and whole-body PBPK model) are available to describe drug distribution and disposition. The compartmental model derives PK parameters using compartmental PK analysis. For most drug compounds, the compartmental PK model is preferred, as PBBM is more focused on the absorption process. Two major independent PK parameters, clearance (CL) and volume of distribution (Vd), account for drug disposition and distribution, respectively. By definition, clearance describes the efficiency of the irreversible elimination

of a drug from the body. Vd is not a real volume; it is the parameter relating the concentration of a drug in the plasma to the total amount of the drug in the body.

The PK parameters can be determined from preclinical, in vitro assays, and clinical PK profiles. When clinical PK is not available or in the early stage of drug development, multiple approaches can be used to extrapolate CL and Vd from in vitro experiments and preclinical PK studies using allometric scaling approaches, such as in vitro in vivo extrapolation (IVIVE), single species scaling approach, Wajima method or estimated from QSPR. A detailed comparison of the different extrapolation approaches is discussed in other reviews [59]. If clinical PK is available, IV dosing or oral solution formulation with a lower dose assuming a full absorption is preferred use to determine CL and Vd. Usually, the clearance and volume of distribution used for fasted conditions stay the same for fed status unless there is a specific reason. For example, food may impact the blood flow rate, for compounds with high hepatic clearance, the consideration of biliary flow rate is critical for food effect simulation.

2.3.4 Model Optimization and Strategy

A well-summarized article by Li M. et al. has assessed case studies in the filing from FDA NDAs of using PBPK models to evaluate food effects [60]. That study showed simulation for fed conditions using prospective predictions taken up to 49% of the tested compounds, and among these cases, 60% has predicted food effect within twofold by comparing the ratio of PK parameters (AUC and C_{max}) with and without food taken. For the optimized cases, optimization on dissolution rate and precipitation time are the most commonly optimized parameters when PBPK modeling cannot predict fed conditions by changing the physiology status from fasted to fed. The pH-dependent solubility (including biorelevant solubility), disposition parameters (Vd and CL), in vitro release rate, and apparent permeability were also adjusted in 22% (2/9), 22% (2/9), 11% (1/9), and 11% (1/9) of the cases, respectively [60].

Another summary by Kesisoglou F. compiled case studies from peer-reviewed publications up to Feb 2020 on the same topic [61]. In this book chapter, an extended table was generated to include published case studies using PBBM to assess food effects at the time of publishing (May 2022) as shown in Table 2.3. It is worth noticing that the published or submitted case studies using modeling strategy to assess food effects are mostly changes in solubility or gastric emptying time by the fed state. From the observation of Table 2.3, the commonly optimized parameters for such cases include precipitation time, permeability, solubility, gastric emptying time, and disposition parameters. These optimized parameters are particularly difficult to evaluate in vitro due to limitations in methodology.

The ideal situation would be to fit the clinical PK data using a "bottom-up" approach, where the simulation greatly depends on the in vitro or in silico experimental data. However, the in vitro characterization is not always biopredictive. The "middle-out" approach incorporates in vitro testing and in vivo observation to

Table 2.3 Summary of case studies of using PBBM/PBPK to evaluate food effect, modified from [61]

Compound	BCS	Food effect	Food effect mechanism	prospective or middle-out approach to modeling	Publication
Nefazodone-HCl	I	Negative	Slow gastric emptying, lower first-pass gut extraction	Prospective	[81]
Theophylline (CR)	I	None	Slower absorption due to slower gastric emptying	Prospective	[82]
Proprietary compound (NVS732)	I	None	Slower absorption due to slower gastric emptying	Prospective	[83]
Zolpidem MR	I	Negative	Viscosity and meal components affecting release rate	Modeled using in vitro data mechanistic investigation to identify best in vitro conditions to describe the data	[84]
Proprietary compound	I	None	Slower absorption due to slower gastric emptying	Prospective	[85]
Aprepitant	II	Positive (micronized tablet), no (nanosuspension)	Micronized tablet: pH and bile salt concentration changes affecting solubilization	Prospective	[81]
Pazopanib-HCl	II	Positive	Bile salt concentration changes affecting solubility using bicarbonate media	Prospective (low confidence)	[70]
Ziprasidone-HCl	II	Positive	Bile salt concentration changes increase solubility	Prospective, optimized precipitation time, ion effect was considered (low confidence)	[70]
Alpelisib	II	Positive	Bile salt concentration changes increase solubility	Prospective	[64]

(continued)

Table 2.3 (continued)

Compound	BCS	Food effect	Food effect mechanism	prospective or middle-out approach to modeling	Publication
Rivaroxaban	II	Positive	pH and bile salt concentration changes affecting solubility	Prospective	[86]
Aprepitant	II	Positive/none	Bile salt concentration changes increase solubility. Slower absorption due to slower gastric emptying for nanosized.	Model parameters optimized based on fasted data (permeability and regional solubility)	[82]
Aprepitant	II	(micron/nano-sized)	Bile salt concentration changes increase solubility. Slower absorption due to slower gastric emptying for nanosized.	Fed GET adjusted based on dog data	[82]
Celecoxib	II	Positive	Bile salt concentration changes increase solubility	PK disposition parameters fitted to both fed and fasted data	[87]
Aprepitant	II	Positive/none	Bile salt concentration changes increase solubility	Dissolution rate modeled via in vitro dissolution data. Middle-out approach for dissolution/solubility	[88]
Aprepitant	II	(micron/nano-sized)	Bile salt concentration changes increase solubility	Dissolution rate modeled via in vitro dissolution data. PK disposition parameters fitted to both fed and fasted data	[88]
Proprietary compound (NVS406)	II	Positive	Bile salt concentration changes increase solubility	Prospective	[83]
Proprietary compound (NVS701)	II	Positive	pH changes and bile salt concentration changes	Prospective—Precipitation optimized based	

(continued)

Table 2.3 (continued)

Compound	BCS	Food effect	Food effect mechanism	prospective or middle-out approach to modeling	Publication
			affecting solubilization and precipitation	on preclinical fed/fasted PK data	
Proprietary compound (NVS113)	II	Negative	Solubility changes	Solubility for formulations optimized based on preclinical PK data—But failed to capture negative food effect	
Proprietary compound (NVS123)	II	Positive	pH changes affecting solubilization/ precipitation;	Middle out—In vitro dissolution data used for model; dissolution input optimized	[89]
Ketoconazole	II	Positive	pH changes and bile salt concentration changes affecting solubilization and precipitation	GET adjusted to reflect calorie content, precipitation adjusted based on available intraluminal data	[90]
Posaconazole	II	Positive	pH changes and bile salt concentration changes affecting solubilization and precipitation	GET adjusted to reflect calorie content, precipitation adjusted based on available intraluminal data	
Alectinib	II	Positive	Bile salt concentration changes increase solubility	Optimized solubility to account for regional bile salt differences	[91]
Ziprasidone	II	Positive	Bile salt concentration changes increase solubility	Permeability/ precipitation fit to duodenal infusion data. Adjustments to GET and bile salts for different meals.	[68]
Propranolol	II	Positive	Changes in liver blood flow	Prospective but model did not	[92]

Table 2.3 (continued)

Compound	BCS	Food effect	Food effect mechanism	prospective or middle-out approach to modeling	Publication
			affecting first-pass metabolism	fully capture food effect	
Ibrutinib	II	Positive	Changes in liver blood flow affecting first-pass metabolism	Prospective but model did not fully explain the observed effect	[92]
Mebendazole	II	Positive	pH changes and bile salt concentration changes affecting solubilization	Prospective—in vitro dissolution data used to model precipitation	[85]
Bitopertin	II	Positive	Bile salt concentration changes increase solubility	Prospective	
Proprietary compound	II	None	Bile salt concentration changes increase solubility	Prospective—Intestinal volume adjusted based on fasted data	
Clarithromycin	II	None	Gastric emptying time affecting absorption rate	Prospective	[93]
Trospium-cl	III	Negative	Slower dissolution rate in fed state, reduced jejunum Peff	Top-down optimized permeability (low confidence)	[70]
Proprietary compound (NVS001)	III	Negative	Food competitive inhibiting uptake transporter	Middle-out—Transporter parameters fitted against observed data	[89]
Furosemide	IV	Negative	Limited absorption window in small intestine?	Prolonged stomach transit time (2 h instead of default 1 h), reduce fluid volume, middle-out approach with measured Peff in duodenum and jejunum	[81]
Danirixin HBr	IV	Negative		Prospective	[94]

(continued)

Table 2.3 (continued)

Compound	BCS	Food effect	Food effect mechanism	prospective or middle-out approach to modeling	Publication
			Interactions with food components		
Ritonavir	IV	Negative	Luminal fluid viscosity and permeability difference	Prospective	[95]
Proprietary compound (NVS169)	IV	None	Solubility for microemulsion formulation optimized based on preclinical PK data slower absorption due to slower gastric emptying	Prospective—Solubility optimized based on preclinical PK data	[89]
Venetoclax	IV	Positive	Bile salt concentration changes increase solubility	Prospective—Low-fat meal predicted correctly but high-fat meal underpredicted	[96]
Proprietary compound (NVS562)	II or IV	Positive	pH changes and bile salt concentration changes impacting solubilization/precipitation slower absorption due to slower gastric emptying for SEDDS formulation.	Prospective; precipitation estimated from in vitro data	[89]
Proprietary compound	II or IV	Positive	pH and bile salt concentration changes affecting solubilization/precipitation	Precipitation fit to fasted/fed data. Stomach pH changes over time taken into account	[97]
Ribociclib	II or IV	None	Gastric emptying time affecting absorption rate	Prospective	[85]

optimize the parameters. To be noted, any optimization should provide mechanistic justification, as recognized in FDA 2020 PBPK guidance [3].

2.3.5 PBBM/PBPK Model Validation and Acceptance Criteria

A workflow for PBBM/PBPK development, validation, and application is shown in Fig. 2.3. Upon the model development, the model should be validated against available independent clinical studies. The FDA 2020 PBPK Guidance recommends
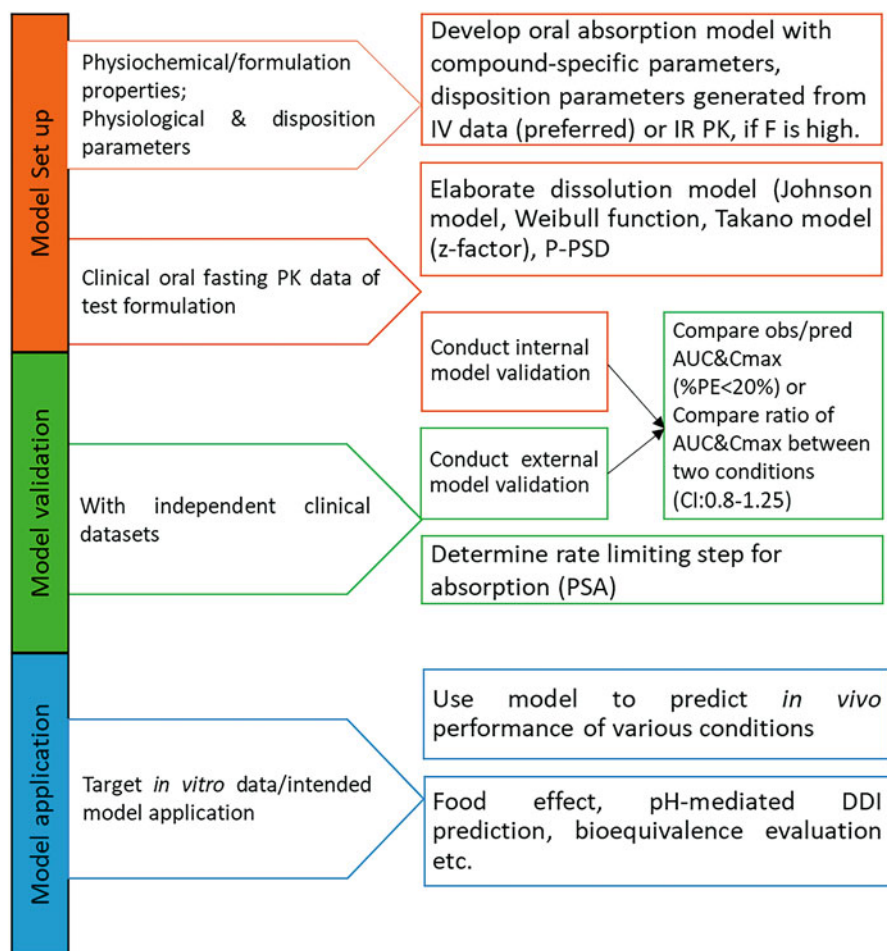
Fig. 2.3 Example of workflow of PBBM development, validation, and application, modified from [78]

model validation should consider the clinical risk and the intended purpose [3]. In general, independent clinical datasets not used for model development should be used for validation for regulatory uses of the model. There were extensive discussions on the use of clinical PK data of "non-bioequivalence batch" to evaluate model predictive performance. Although it is ideal, in many cases, these PK data from non-BE batches are not readily available. Collaboration across regulatory agencies and the industry for a robust model validation approach is desired.

Model verification is to test if the model is robust and can be applied for model applications. Unfortunately, there are no formal acceptance criteria proposed by the agency on PBBM. The current practice is to align with IVIVC acceptance criteria, in which the % prediction error (%PE) should be smaller than 10% [62]. It should be noted, that the recommended acceptance criteria for IVIVC are for a carefully designed cross-over study, while it is not the case for most of the studies used for PBBM, especially when it is preferred to set up the model with independent clinical studies. In addition, the acceptance criteria should be drug product, model application, and drug development stage-dependent. In early-stage drug development, the criteria can be less strict for internal decision-making, and in the later stages or for filling purposes, the acceptance criteria should be more strict.

Some common practices for model verification observed in published studies are as follows. Besides to reach a desirable agreement between observed and predicted PK profiles, the commonly applied verification method is to calculate the difference between the PK parameters (AUC and C_{max}) of predicted and observed data as a comparison. In some studies, the average fold error (AFE)/absolute average fold error (AAFE), or coefficient of determination (R^2) was calculated. The value of AFE and R^2 is desired to be close to 1. For AAFE, it is usually set below 2 [58]. This approach shares the same principle of comparing the PK parameters. For DDI studies such as pH-mediated DDI and food effect, the ratio of PK parameters (AUC and C_{max}) with or without food or acid-reducing agents (ARA) is compared between predicted and observed data [63]. It is well accepted that if the simulated ratios of AUC and C_{max} with or without food or ARAs are comparable with clinical observation (CI = 0.8–1.25), the model is considered biopredictive and can be used to aid drug development or further applications.

2.4   Case Studies of PBPK Models to Assess Food Effects

In this section, we will provide examples from the literature of models that identify potential food effect risks: positive and negative. This will enable the reader to utilize the previous sections' tutorial information in conjunction with these case studies to navigate food effects assessment in their work.

2.4.1 Positive Food Effect: A PBPK Model of the BCS Class II Drug Alpelisib

Alpelisib (a PI3K inhibitor prescribed for breast cancer treatment) is a weak base drug with both pH-dependent and bile acid concentration-dependent solubility [64]. An increase in the stomach pH due to acid-reducing agents such as antacids, proton pump inhibitors (omeprazole), or H2 receptor antagonists (ranitidine) would lead to a decrease in the solubility and reduction of the drug in bioavailability. While an increase in bile acid secretion under the fed state would increase the solubility of the drug and likely lead to a positive food effect. Due to these characteristics of alpelisib, Gajewska and colleagues established a GastroPlus® PBPK and validated it with clinical data to assess food effects and pH-mediate drug interactions. We will highlight the key input criteria and optimizations employed by the authors to validate their model.

Parameter Input and Model Establishment Beyond standard input parameters (described in Sect. 3.1.1), the pH solubility for alpelisib in FeSSIF was measured across a pH range as it was known that the drug had increased solubility in fed state. The authors note that assessment of the Johnson vs Takano or Z-factor model was necessary as they account for particle size on dissolution or in vitro dissolution data, respectively, and cannot be used at the same time. Based on simulations, a constant Z-factor was fitted to experimental in vitro dissolution data per formulation condition. Preclinical PK studies in rats and dogs showed a low plasma clearance, moderate volume of distribution, and an elimination half-life ~3–4 h. Data from two clinical studies were also available to the researchers: (1) a five-period cross-over study of two formulations to investigate the impact of elevated stomach pH (ranitidine), different prandial conditions (high-fat high-calorie [HFHC], and low-fat low-calorie meal [LFLC]), and their combined effects on alpelisib absorption where n = 20 and 2) a bioequivalence study of two formulations in healthy volunteers in fasted or fed (HFHC) state where n = 95 [65]. The authors used two approaches to estimate the drug CL and Vd using either clinical data (population pharmacokinetic [popPK] modeling) or preclinical data (Dedrick Plot and Wajima method) [66, 67] The ACAT model was coupled with a compartmental PK model that represented the plasma and the rest of the body. The available parameters within GastroPlus® were used for fasted state and the HFHC state; however, for the LFLC state, the stomach transit time and volume were modified to reflect a smaller meal, and for ranitidine, the stomach pH was set to 6.5 [68, 69]. The Johnson dissolution model was used to simulate the conditions of the first clinical trial, and the Takano/Z-factor dissolution model for the second clinical trial. The authors note that this strategy was used to train the model toward its validation and application based on clinical data in healthy subjects.

Model Results The pharmacokinetic parameters from popPK, Dedrick Plot, and Wajima method predicted a CL of 20 L/h and Vd of 100 L for 70 kg body weight (Dedrick Plot overestimated the Vd parameter). The simulations aligned with the

observed clinical data that (1) HFHC and LFLC meals had a positive food effect on the C_{max} and AUC_{0-inf}, (2) co-administration of ranitidine resulted in a decrease in C_{max} and AUC_{0-inf}, and (3) co-administration of ranitidine with LFLC meal had an increase in C_{max} and AUC_{0-inf} compared to fasted but lower than LFLC alone. However, although the simulations trended similar to clinical observations, the T_{max} in simulations was delayed by 0.5–1 h in all simulations except the fasted state. The simulations for the second clinical study were again in agreement with clinical observations, although this time, the simulations were even more accurate and the C_{max} and AUC_{0-inf} were within the predefined bioequivalence boundaries of 0.80 and 1.25 (0.932 and 0.961, respectively). Though the authors used different dissolution models in the simulations, they concluded that the dissolution models were similar with a slightly higher fraction absorbed predicted using the Takano/Z-factor model. In conclusion, Gajewska et al. demonstrate that PBPK models can be used to predict a positive food effect, drug–drug interaction, and bioequivalence of a BCS Class II drug.

2.4.2 Negative Food Effect: A PBPK Model of the BCS Class III Drug Trospium-Cl

Trospium-Cl is an antispasmodic and antimuscarinic agent prescribed for overactive bladder and is a quaternary ammonium cation drug that is ionized upon dissolution. From a physicochemical perspective, it has low lipophilicity (log P $= -1.22$), low permeability, and a high solubility and therefore is classified as a BCS class III drug [70, 71]. Both immediate-release (IR) and modified-release (MR) formulations of trospium-Cl have been shown to have negative food effects in healthy volunteers [72, 73]. Due to the clinical observation of a negative food effect, Wagner and co-authors used trospium-Cl along with pazopanib-HCl and ziprasidone-HCl (positive food effects) as model compounds in their study to improve PBPK predictions of food–drug interactions with typically poor predictive confidence [70]. We will highlight the key input criteria and optimizations employed by the authors to validate their model.

Parameter Input and Model Establishment The authors provide input parameters for both GastroPlus® and Simcyp™ but as the alpelisib case study provided parameters for GastroPlus® we will focus on these for comparison. The CL and renal CL (CL_R) were calculated in the software based on published data on the IV bolus administration of 0.5 mg of trospium-Cl to a single healthy volunteer [74]. Using PKPlus™, a 2-compartment PK model was fitted to the IV data and used for simulations. The authors fitted effective permeability data (P_{eff}) to PK data from a gastric infusion over 6 h in fed and fasted states to account for variations in permeability under different prandial scenarios (fed: 0.008 and fasted: 0.018×10^{-4} cm/s). The authors note that a low log P and high solubility drug do not typically predict an impact of bile salts on solubilization; therefore, this was not a factor in the

model. The Johnson dissolution model was used to simulate drug dissolution for IR formulations while a Weibull function was used for the dissolution of the MR formulation. The Weibull function allowed for the model to factor in the decreased dissolution rate due to the higher viscosity of postprandial luminal fluid [75]. Simulations were run using a standard high-fat high-calorie breakfast in healthy volunteers to allow comparison to clinical study data.

Model Results To validate the basal conditions of the model (fasted-state with IR formulation), the authors ran simulations of 20, 30, and 40 mg doses based on clinical data. The model predictions for 20 and 40 mg were on trend with the clinical observed data for AUC (ratio predictive/observed: 1.41 [20 mg] and 0.82 [40 mg]) and C_{max} (ratio predictive/observed: 0.83 [20 mg] and 0.92 [40 mg]). However, the 30 mg simulation significantly underpredicted both C_{max} and AUC (ratio predictive/observed: 0.45 and 0.56, respectively). The authors stated that the 20 and 40 mg data conformed to pre-established criteria for model verification [76] and thus applied this model to the food effects data. The simulation of a 30 mg IR formulation in a fed state using the Johnson dissolution model resulted in an overprediction of the C_{max}, delay in the T_{max}, and underprediction of the AUC. When the Weibull function based on increased viscosity causing decreased dissolution has applied to the simulation, it resolved the C_{max} prediction (ratio predictive/observed: 0.85) and the authors concluded that the model captured the negative food effect. Although the Weibull function improved the C_{max} prediction, the AUC and T_{max} were still under and overpredicted respectively and it is likely to further optimization of the dissolution model and permeability may be necessary to resolve the T_{max} and AUC, respectively. The authors conclude that the higher permeability of trospium-Cl in the fasted state is due to the ion-pair formation with bile salts whereas the increased viscosity of chyme in the fed-state impacts the dissolution of IR and MR formulations. A better understanding of the impact of hydrodynamics on the in vivo dissolution of drug formulations in a fed state will enable better calculation of this in such models and simulations. In conclusion, the use of the Weibull function combined with in vitro dissolution data in a higher viscosity buffer enabled this model to predict a negative food effect of a BCS Class III drug.

2.5   Utilization of PBPK to Streamline Food Effect Assessment in Clinical Development

The BCS classifies drugs based on their permeability and solubility as follows: BCS I (high permeability, high solubility), BCS II (high permeability, low solubility), BCS III (low permeability, high solubility), and BCS IV (low permeability, low solubility). To better utilize PBBM to streamline food effect assessment, Kesisoglou F. has proposed a decision tree on the PBBM application scenario based on BCS classification [61]. It is well accepted that most of the BCS I compounds formulated as IR exhibit a low probability of food effect due to high solubility and high

permeability, which is acknowledged by the FDA, as this class is the only one approachable for a food effect study waiver. PBBM can be utilized to study the impact of gastric emptying time on PK exposure if necessary. BCS III compounds are likely to have negative food effects due to the inhibition of update transporters in the intestine, and the increase of biliary excretion. Those potential mechanisms are hard to evaluate with the current modeling approach or in vitro testing [8]. If the observed food effect is related to changes in dissolution rate due to the presence of bile salts, PBBM can be used to assess the food effect, which will require clinical PK to confirm. BCS II/IV compounds are mostly studied in food effect assessment using PBBM. As shown in Table 2.3, 39 case studies were included and 32 of them (82%) are BCS II/IV compounds. For those compounds, the absorption is usually solubility limited, and if the food effect mechanism is related to the solubility increase caused by food intake, a PBBM can be considered with sufficient confidence.

2.6 Current Gaps and Future Directions

Despite the progress made in recent years in PBPK modeling of food effects, it is fair to state that the field is still evolving. In our opinion, future efforts in the field should concentrate on three areas (a) expansion of food effect mechanisms that can be addressed by PBPK modeling; (b) increase regulatory acceptance for clinical decision-making; c) expansion to pediatric populations.

As discussed in this book chapter, food can interact with drug absorption in multiple ways. A recent manuscript by the IQ Consortium Food Effect PBPK Working Group highlighted that current PBPK models show significantly greater predictability for positive food effects related to changes in the intestinal lumen environment (i.e., solubilization by bile salts) and gastrointestinal transit (i.e., delayed gastric emptying) compared to all other plausible sources of food–drug interactions or negative food effects [76]. In fact, the authors a priori excluded from the analysis mechanisms related to interactions with transporters as too difficult to attempt the model. As shown in Table 2.3, the majority of studied food effect mechanisms are due to pH and bile salt changes. However, the issue with the application of the models to only a subset of food effects is not solely a computational one. While opportunities exist to improve PBPK models to, e.g., better account for dissolution of salts, PBPK models rely on relevant in vitro data inputs; in the case of food effect modeling, this differential input will need to come from distinct in vitro data sets for these two prandial states. While biorelevant media are available, those primarily focus on capturing the solubility difference in fed and fasted stomach/intestine; accounting for direct interactions with food components or differential behavior of dosage forms due to, e.g., disintegration differences is currently only achievable retrospectively. Thus, a parallel investment in in vitro methodologies along with the PBPK models appears needed.

Based on manuscripts and presentations by regulators, it is fair to state that currently there is healthy skepticism on the application of models to replace clinical

food effect studies [6, 60, 77]. A lot of the concern comes from the diversity of food effect mechanisms and the non-standardized workflows for model development. Several authors have more recently proposed a more standardized approach to food effect modeling with appropriate model validation against clinical data to increase confidence [61, 76]. We also believe that more consistency in the model development will facilitate adoption. Furthermore, focusing on more narrow food effect scenarios as a starting point may make more sense rather than looking for broad food effect study waivers via PBPK. One such example may be the application of the models to repeat food effect studies for new formulations/potencies. Under that scenario the baseline model, and thus the mechanism of food effect, will have been confirmed against clinical data, thus increasing confidence for model application.

Finally, while the focus of PBPK modeling has been on adult food effect studies, many pediatric formulations are currently dosed with soft foods [6]. PBBM modeling for pediatrics is still in its early stages and largely relies on the extrapolation of models from adults. In vitro methodologies to simulate dissolution in the gastrointestinal tract of younger children are far from being standardized and their use is quite inconsistent. Thus, similar to the situation with expanding food effect mechanisms discussed above, a parallel investment in the advancement of in vitro and PBPK tools specific to pediatric populations is needed.

References

1. Wu F et al (2021) Biopharmaceutics applications of physiologically based pharmacokinetic absorption modeling and simulation in regulatory submissions to the US food and drug administration for new drugs. AAPS J 23(2):1–14
2. K, Y., et al., Applications of PBPK/PBBM modeling in generic product development: An industry perspective. J Drug Deliv Sci Technol, 2022. 69: p. 103152.
3. U.S. FDA (2020) The use of physiologically based pharmacokinetic analyses—biopharmaceutics applications for oral drug product development, manufacturing changes, and controls. https://www.fda.gov/media/142500/download
4. Huang W, Lee SL, Yu LX (2009) Mechanistic approaches to predicting oral drug absorption. AAPS J 11(2):217–224
5. O'Shea JP et al (2019) Food for thought: formulating away the food effect—a PEARRL review. J Pharm Pharmacol 71(4):510–535
6. U.S. FDA (2020) Assessing the effects of food on drugs in INDs and NDAs. https://www.fda.gov/media/121313/download
7. Goncalves P et al (2012) Inhibition of butyrate uptake by the primary bile salt chenodeoxycholic acid in intestinal epithelial cells. J Cell Biochem 113(9):2937–2947
8. Xiao J et al (2020) Biliary excretion–mediated food effects and prediction. AAPS J 22(6):124
9. Mwebaza N et al (2013) Comparable lumefantrine oral bioavailability when co-administered with oil-fortified maize porridge or milk in healthy volunteers. Basic Clin Pharmacol Toxicol 113(1):66–72
10. Veerman GDM et al (2021) Influence of cow's milk and esomeprazole on the absorption of erlotinib: a randomized, crossover pharmacokinetic study in lung cancer patients. Clin Pharmacokinet 60(1):69–77

11. Gleeson JP et al (2018) Sodium caprate enables the blood pressure-lowering effect of Ile-pro-pro and Leu-Lys-pro in spontaneously hypertensive rats by indirectly overcoming PepT1 inhibition. Eur J Pharm Biopharm 128:179–187

12. Morimoto K et al (2011) Effect of milk on the pharmacokinetics of oseltamivir in healthy volunteers. J Pharm Sci 100(9):3854–3861

13. Singh BN (1999) Effects of food on clinical pharmacokinetics. Clin Pharmacokinet 37(3): 213–255

14. Neuvonen PJ (1976) Interactions with the absorption of Tetracyclines. Drugs 11(1):45–54

15. Stebler T, Guentert TW (1990) Binding of drugs in milk: the role of casein in milk protein binding. Pharm Res 7(6):633–637

16. Bailey DG et al (1991) Interaction of citrus juices with felodipine and nifedipine. Lancet 337(8736):268–269

17. Bailey DG et al (1989) Ethanol enhances the hemodynamic effects of felodipine. Clin Invest Med 12(6):357–362

18. Lown KS et al (1997) Grapefruit juice increases felodipine oral availability in humans by decreasing intestinal CYP3A protein expression. J Clin Invest 99(10):2545–2553

19. de Castro WV et al (2007) Grapefruit juice—drug interactions: grapefruit juice and its components inhibit P-glycoprotein (ABCB1) mediated transport of talinolol in Caco-2 cells. J Pharm Sci 96(10):2808–2817

20. Fagerberg JH, Sjögren E, Bergström CAS (2015) Concomitant intake of alcohol may increase the absorption of poorly soluble drugs. Eur J Pharm Sci 67:12–20

21. Keemink J et al (2019) Does the intake of ethanol affect oral absorption of poorly soluble drugs? J Pharm Sci 108(5):1765–1771

22. Laisi U et al (1979) Pharmacokinetic and pharmacodynamic interactions of diazepam with different alcoholic beverages. Eur J Clin Pharmacol 16(4):263–270

23. Parlesak A et al (2000) Increased intestinal permeability to macromolecules and endotoxemia in patients with chronic alcohol abuse in different stages of alcohol-induced liver disease∗∗dedicated to Dr. Dr. Herbert Falk, director of the Falk Foundation, on the occasion of his 75th birthday. J Hepatol 32(5):742–747

24. Leclercq S et al (2012) Role of intestinal permeability and inflammation in the biological and behavioral control of alcohol-dependent subjects. Brain Behav Immun 26(6):911–918

25. Abdel-Rahman SM et al (2007) Considerations in the rational design and conduct of phase I/II pediatric clinical trials: avoiding the problems and pitfalls. Clin Pharmacol Ther 81(4):483–494

26. Lee HS et al (2020) Sprinkle formulations—a review of commercially available products. Asian J Pharm Sci 15(3):292–310

27. Grimm M et al (2018) Interindividual and intraindividual variability of fasted state gastric fluid volume and gastric emptying of water. Eur J Pharm Biopharm 127:309–317

28. Pentafragka C et al (2020) Disposition of two highly permeable drugs in the upper gastrointestinal lumen of healthy adults after a standard high-calorie, high-fat meal. Eur J Pharm Sci 149: 105351

29. Davis SS, Hardy JG, Fara JW (1986) Transit of pharmaceutical dosage forms through the small intestine. Gut 27(8):886–892

30. Mudie DM et al (2014) Quantification of gastrointestinal liquid volumes and distribution following a 240 mL dose of water in the fasted state. Mol Pharm 11(9):3039–3047

31. Koziolek M et al (2014) Intragastric volume changes after intake of a high-caloric, high-fat standard breakfast in healthy human subjects investigated by MRI. Mol Pharm 11(5): 1632–1639

32. Grimm M et al (2018) Gastric emptying and small bowel water content after administration of grapefruit juice compared to water and Isocaloric solutions of glucose and fructose: a four-way crossover MRI pilot study in healthy subjects. Mol Pharm 15(2):548–559

33. SCHILLER C et al (2005) Intestinal fluid volumes and transit of dosage forms as assessed by magnetic resonance imaging. Aliment Pharmacol Ther 22(10):971–979

34. Fordtran JS, Locklear TW (1966) Ionic constituents and osmolality of gastric and small-intestinal fluids after eating. Am J Dig Dis 11(7):503–521
35. Pentafragka C et al (2018) The impact of food intake on the luminal environment and performance of oral drug products with a view to in vitro and in silico simulations: a PEARRL review. J Pharm Pharmacol 71(4):557–580
36. Baxevanis F, Kuiper J, Fotaki N (2016) Fed-state gastric media and drug analysis techniques: current status and points to consider. Eur J Pharm Biopharm 107:234–248
37. Vertzoni M et al (2012) Luminal lipid phases after administration of a triglyceride solution of danazol in the fed state and their contribution to the flux of danazol across Caco-2 cell monolayers. Mol Pharm 9(5):1189–1198
38. Kalantzi L et al (2006) Characterization of the human upper gastrointestinal contents under conditions simulating bioavailability/bioequivalence studies. Pharm Res 23(1):165–176
39. Klein S (2010) The use of biorelevant dissolution media to forecast the in vivo performance of a drug. AAPS J 12(3):397–406
40. Moreno MPDLC et al (2010) Characterization of fasted-state human intestinal fluids collected from duodenum and jejunum. J Pharm Pharmacol 58(8):1079–1089
41. Persson EM et al (2005) The effects of food on the dissolution of poorly soluble drugs in human and in model small intestinal fluids. Pharm Res 22(12):2141–2151
42. Dahlgren D et al (2021) Fasted and fed state human duodenal fluids: characterization, drug solubility, and comparison to simulated fluids and with human bioavailability. Eur J Pharm Biopharm 163:240–251
43. Medwid S et al (2021) Organic anion transporting polypeptide 2B1 (OATP2B1) genetic variants: in vitro functional characterization and association with circulating concentrations of endogenous substrates. Front Pharmacol 12
44. Tikkanen A et al (2020) Food additives as inhibitors of intestinal drug transporter OATP2B1. Mol Pharm 17(10):3748–3758
45. Ma K, Hu Y, Smith DE (2012) Influence of fed-fasted state on intestinal PEPT1 expression and in vivo pharmacokinetics of glycylsarcosine in wild-type and Pept1 knockout mice. Pharm Res 29(2):535–545
46. Deferme S, Augustijns P (2003) The effect of food components on the absorption of P-gp substrates: a review. J Pharm Pharmacol 55(2):153–162
47. Abuznait AH et al (2011) Induction of expression and functional activity of P-glycoprotein efflux transporter by bioactive plant natural products. Food Chem Toxicol 49(11):2765–2772
48. Yan J-H (2017) Food effect on oral bioavailability: old and new questions. Clin Pharmacol Drug Dev 6(4):323–330
49. Olanoff LS et al (1986) Food effects on propranolol systemic and oral clearance: support for a blood flow hypothesis. Clin Pharmacol Ther 40(4):408–414
50. Gu C-H et al (2007) Predicting effect of food on extent of drug absorption based on physico-chemical properties. Pharm Res 24(6):1118–1130
51. Fleisher D et al (1999) Drug, meal and formulation interactions influencing drug absorption after oral administration. Clin Pharmacokinet 36(3):233–254
52. Wu C-Y, Benet LZ (2005) Predicting drug disposition via application of BCS: transport/absorption/elimination interplay and development of a biopharmaceutics drug disposition classification system. Pharm Res 22(1):11–23
53. Zhang T, Wells E (2020) A review of current methods for food effect prediction during drug development. Curr Pharmacol Rep 6(5):267–279
54. Lentz KA (2008) Current methods for predicting human food effect. AAPS J 10(2):282–288
55. Henze LJ et al (2021) Combining species specific in vitro & in silico models to predict in vivo food effect in a preclinical stage—case study of Venetoclax. Eur J Pharm Sci 162:105840
56. Mithani SD et al (1996) Estimation of the increase in solubility of drugs as a function of bile salt concentration. Pharm Res 13(1):163–167
57. Li M et al (2021) Understanding in vivo dissolution of immediate release (IR) solid ORAL drug products containing weak acid BCS class 2 (BCS class 2a) drugs. AAPS J 23(6):1–13

58. Pepin XJH et al (2016) Justification of drug product dissolution rate and drug substance particle size specifications based on absorption PBPK modeling for lesinurad immediate release tablets. Mol Pharm 13(9):3256–3269

59. Lin W et al (2022) Applications, challenges, and outlook for PBPK modeling and simulation: a regulatory, vol 39. Ind Acad Perspect, Pharm Res, p 1701

60. Li M et al (2018) Predictive performance of physiologically based pharmacokinetic models for the effect of food on oral drug absorption: current status. CPT Pharmacometrics Syst Pharmacol 7(2):82–89

61. Kesisoglou F (2020) Can PBPK modeling streamline food effect assessments? J Clin Pharmacol 60(S1):S98–S104

62. U.S. FDA (1997) Extended release oral dosage forms: development, evaluation, and application of in vitro/in vivo correlations

63. Dong Z et al (2020) Application of physiologically-based pharmacokinetic modeling to predict gastric pH-dependent drug–drug interactions for weak base drugs. CPT Pharmacometrics Syst Pharmacol 9(8):456–465

64. Gajewska M et al (2020) Physiologically based pharmacokinetic modeling of oral absorption, pH, and food effect in healthy volunteers to drive Alpelisib formulation selection. AAPS J 22(6):134

65. Pharmaceuticals N (2015) Study assessing the efficacy and safety of alpelisib plus fulvestrant in men and postmenopausal women with advanced breast cancer which progressed on or after aromatase inhibitor treatment (SOLAR-1). https://clinicaltrials.gov/ct2/show/NCT02437318

66. Boxenbaum H, Ronfeld R (1983) Interspecies pharmacokinetic scaling and the dedrick plots. Am J Phys Regul Integr Comp Phys 245(6):R768–R775

67. Vuppugalla R et al (2011) PhRMA CPCDC initiative on predictive models of human pharmacokinetics, part 4: prediction of plasma concentration–time profiles in human from in vivo preclinical data by using the Wajima approach. J Pharm Sci 100(10):4111–4126

68. Sutton SC, Nause R, Gandelman K (2017) The impact of gastric pH, volume, and emptying on the food effect of ziprasidone oral absorption. AAPS J 19(4):1084–1090

69. Kakuda TN, Falcon RW (2006) Effect of food and ranitidine on saquinavir pharmacokinetics and gastric pH in healthy volunteers. Pharmacotherapy 26(8):1060–1068

70. Wagner C et al (2021) Use of physiologically based pharmacokinetic modeling for predicting drug–food interactions: recommendations for improving predictive performance of low confidence food effect models. AAPS J 23(4):85

71. Tadken T et al (2016) Trospium chloride is absorbed from two intestinal "absorption windows" with different permeability in healthy subjects. Int J Pharm 515(1):367–373

72. U.S. FDA (2003) Clinical pharmacology and biopharmaceutics review—trospium chloride. https://www.accessdata.fda.gov/drugsatfda_docs/nda/2004/21-595_Sanctura_BioPharmr_P1.pdf

73. U.S. FDA (2007) Clinical pharmacology and biopharmaceutics review—trospium chloride modified release. https://www.accessdata.fda.gov/drugsatfda_docs/nda/2007/022103s000_ClinPharmR.pdf

74. Schladitz-Keil G, Spahn H, Mutschler E (1986) Determination of the bioavailability of the quaternary compound trospium chloride in man from urinary excretion data. Arzneimittelforschung 36(6):984–987

75. Radwan A, Amidon GL, Langguth P (2012) Mechanistic investigation of food effect on disintegration and dissolution of BCS class III compound solid formulations: the importance of viscosity. Biopharm Drug Dispos 33(7):403–416

76. Riedmaier AE et al (2020) Use of physiologically based pharmacokinetic (PBPK) modeling for predicting drug-food interactions: an industry perspective. AAPS J 22(6):123

77. Zhang X et al (2020) Application of PBPK modeling and simulation for regulatory decision making and its impact on US prescribing information: an update on the 2018-2019 submissions to the US FDA's Office of Clinical Pharmacology. J Clin Pharmacol 60(S1):S160–S178

78. Di Wu MS, Kollipara S, Ahmed T, Saini AK, Heimbach T (2022) Physiologically based pharmacokinetics modeling in biopharmaceutics: case studies for establishing the bioequivalence safe space for generic and innovator drugs (submitted). Pharm Res 40:337

79. Mudie DM, Amidon GL, Amidon GE (2010) Physiological parameters for oral delivery and in vitro testing. Mol Pharm 7(5):1388–1405

80. Mudie DM et al (2020) Selection of in vivo predictive dissolution media using drug substance and physiological properties. AAPS J 22(2):34–34

81. Pepin XJ et al (2021) Understanding mechanisms of food effect and developing reliable pbpk models using a middle-out approach. AAPS J 23(1):1–14

82. Parrott N et al (2009) Predicting pharmacokinetics of drugs using physiologically based modeling—application to food effects. AAPS J 11(1):45–53

83. Heimbach T et al (2013) Case studies for practical food effect assessments across BCS/BDDCS class compounds using in silico, in vitro, and preclinical in vivo data. AAPS J 15(1):143–158

84. Andreas CJ et al (2017) Mechanistic investigation of the negative food effect of modified release zolpidem. Eur J Pharm Sci 102:284–298

85. Tistaert C et al (2019) Food effect projections via physiologically based pharmacokinetic modeling: predictive case studies. J Pharm Sci 108(1):592–602

86. Kushwah V et al (2021) On absorption modeling and food effect prediction of rivaroxaban, a BCS II drug orally administered as an immediate-release tablet. Pharmaceutics 13(2):283

87. Shono Y et al (2009) Prediction of food effects on the absorption of celecoxib based on biorelevant dissolution testing coupled with physiologically based pharmacokinetic modeling. Eur J Pharm Biopharm 73(1):107–114

88. Shono Y et al (2010) Forecasting in vivo oral absorption and food effect of micronized and nanosized aprepitant formulations in humans. Eur J Pharm Biopharm 76(1):95–104

89. Xia B et al (2013) Utility of physiologically based modeling and preclinical in vitro/in vivo data to mitigate positive food effect in a BCS class 2 compound. AAPS PharmSciTech 14(3):1255–1266

90. Cristofoletti R, Patel N, Dressman JB (2016) Differences in food effects for 2 weak bases with similar BCS drug-related properties: what is happening in the intestinal lumen? J Pharm Sci 105(9):2712–2722

91. Parrott NJ et al (2016) Physiologically based absorption modeling to explore the impact of food and gastric pH changes on the pharmacokinetics of alectinib. AAPS J 18(6):1464–1474

92. Rose RH et al (2017) Incorporation of the time-varying postprandial increase in splanchnic blood flow into a PBPK model to predict the effect of food on the pharmacokinetics of orally administered high-extraction drugs. AAPS J 19(4):1205–1217

93. Radwan A et al (2019) Evaluation of food effect on the oral absorption of clarithromycin from immediate release tablet using physiological modelling. Biopharm Drug Dispos 40(3–4):121–134

94. Lloyd RS et al (2020) Negative food effect of Danirixin: use of PBPK modelling to explore the effect of formulation and meal type on clinical PK. Pharm Res 37(12):233

95. Arora S et al (2020) Biopharmaceutic in vitro in vivo extrapolation (IVIV_E) informed physiologically-based pharmacokinetic model of ritonavir Norvir tablet absorption in humans under fasted and fed state conditions. Mol Pharm 17(7):2329–2344

96. Emami Riedmaier A et al (2018) Mechanistic physiologically based pharmacokinetic modeling of the dissolution and food effect of a biopharmaceutics classification system IV compound—the Venetoclax story. J Pharm Sci 107(1):495–502

97. Zhang H et al (2014) Application of physiologically based absorption modeling to formulation development of a low solubility, low permeability weak base: mechanistic investigation of food effect. AAPS PharmSciTech 15(2):400–406

Chapter 3
Physiologically Based Finite Time Pharmacokinetic (PBFTPK) Models: Inception and Development

Athanasios A. Tsekouras and Panos Macheras

Abstract Oral drug absorption has always been modeled as a first-order process that lasts indefinitely. Since common knowledge takes for granted that this is not so, the concept of Finite Absorption Time (FAT) was introduced recently and relevant models were generated for one- and two-compartment disposition in conjunction with zero-order absorption kinetics. This chapter justifies these choices by considering all possible classes of drugs based on the BCS classification system. It also presents simulations to show accessible variability as well as successful fits to the pharmacokinetic data of several orally administered drugs.

3.1 Introduction

Most drugs are administered orally owing to the convenience provided by this route. In the simplest case, the pharmacokinetic analysis of oral drug absorption data relies on the classical Bateman equation (Eq. 3.1), which assumes a one-compartment model disposition with the first-order absorption and elimination rates [1]:

A. A. Tsekouras
Department of Chemistry, National and Kapodistrian University of Athens, Athens, Greece

PharmaInformatics Unit, ATHENA Research Center, Athens, Greece

P. Macheras (✉)
PharmaInformatics Unit, ATHENA Research Center, Athens, Greece

Faculty of Pharmacy, National and Kapodistrian University of Athens, Athens, Greece
e-mail: macheras@pharm.uoa.gr

$$C(t) = \frac{FDk_a}{V_d(k_a - k_{el})} \left(e^{-k_{el}\,t} - e^{-k_a\,t}\right) \tag{3.1}$$

Where C is the drug concentration in the body (compartment) at time t, F is the bioavailable fraction of dose D, V_d is the volume of distribution, and k_a and k_{el} are the absorption and elimination rate constants, respectively. Depending on the relative magnitude of the rate constants, classical ($k_a > k_{el}$) and flip-flop ($k_a < k_{el}$) cases are encountered. In the special case of equality of rate constants ($k_a = k_{el} = k$), the time dependence of drug concentration becomes (Eq. 3.2):

$$C(t) = \frac{FDkt}{V_d} e^{-kt} \tag{3.2}$$

If we assume a two-compartment disposition model, the drug concentration can be expressed with (Eq. 3.3):

$$C(t) = \frac{FDk_a}{V_c} \left(\frac{(k_{21} - \alpha)e^{-\alpha t}}{(k_a - \alpha)(\beta - \alpha)} + \frac{(k_{21} - \beta)e^{-\beta t}}{(k_a - \beta)(\alpha - \beta)} + \frac{(k_{21} - k_a)e^{-k_a t}}{(\alpha - k_a)(\beta - k_a)}\right) \tag{3.3}$$

$$\text{Where } \alpha + \beta = k_{12} + k_{21} + k_{10} \text{ and } \alpha\beta = k_{21}k_{10} \tag{3.4}$$

and k_{12}, k_{21}, and k_{10} are the rate microconstants for the first-order kinetics of transfer from the central (blood) to the peripheral compartment, the reverse process, and the removal process, respectively.

The history of Eq. 3.1 goes back to 1910 when the British mathematician Henry Bateman [2] solved the problem of the conversion of successive radioactive isotopes. As long as there are radioactive isotopes, they will undergo transformation to different elements. 43 years later, this solution was adopted by H. F. Dost [1] to describe the concentration of a drug in the blood as a function of time (see Fig. 3.1). The common underlying principle was that both the absorption and the elimination processes follow the first-order kinetics just the same as the conversion of radioactive isotopes. However, the infinite time of drug absorption is not physiologically
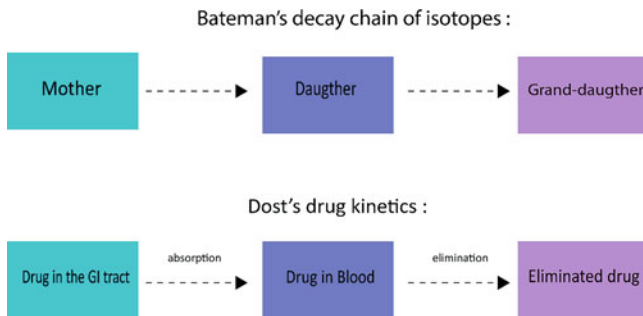
Fig. 3.1 Henry Bateman's vis-a-vis Friedrich Harmut Dost's kinetic considerations

sound since drugs are not absorbed beyond their absorptive sites in the gastrointestinal (GI) tract. In fact, oral drug absorption takes place in a certain period of time in accordance with the biopharmaceutical properties of the drug as well as the physiological, gastric, intestinal, and colon transit times reported in the literature [3]. For sufficiently fast processes, the similarities allow adequate implementation of the radioactivity equations in the pharmacokinetics problem. But this condition is not met if absorption in the GI tract is not fast enough and the drug is removed from the GI tract before it has the chance to be absorbed in the blood. This situation leads to obvious shortcomings of the model equation (Eq. 3.1). Nonetheless, this fact had not been appreciated for many decades and Eq. 3.1 as well as its extension Eq. 3.3 have been used without reservations to describe pharmacokinetic data.

3.1.1   Background

The oral route is the most common pathway for drug administration. Extensive work in this research field revealed that two basic drug properties, namely, solubility and permeability of gastrointestinal membrane dictate the extent of oral drug absorption. These scientific advances lead to the development of the biopharmaceutic classification system (BCS), the biopharmaceutic drug disposition classification system (BDDCS), and the publication of relevant regulatory guidelines, by the Food and Drug Administration (FDA) and the European Medicines Agency (EMA) [4–7]. These guidelines formulate the scientific requirements for the performance or not of bioequivalence studies towards the approval of generics/drugs classified into four drug classes (I, II, III, and IV). For example, a highly soluble, highly permeable drug (Class I) can get a biowaiver status for bioequivalence studies. This does not apply to Class II (low solubility and high permeability) and Class IV (low solubility and low permeability) drugs. For Class III (high solubility and low permeability) a biowaiver status can be assigned under certain conditions [6, 7]. Class I drugs exhibit extensive absorption (the fraction of dose absorbed >0.90), while for Class II, III, and IV drugs, the fraction of dose absorbed is certainly lower than 0.90. However, it is very well known that the absorption of orally administered drugs is complex and depends not only on drug properties but also on physiological aspects of the GI tract such as (a) drug/formulation-dependent factors—drug physicochemical properties [e.g., aqueous solubility, permeability, molecular size, aggregation, complexation, charge, pK_a, H-bonding potential, hydrophobicity, and crystal lattice energy] and formulation composition (e.g., dosage form, absorption enhancers, and drug release) and (b) system dependent factors— physiological parameters (e.g., gastric emptying, intestinal motility, intestinal pH, site-dependent permeability, intestinal content composition, and disease state) and biochemical parameters (e.g., metabolism, efflux transporters, and active uptake transporters). Due to this complexity, during the last 15 years or so different modeling approaches have been proposed and software packages (GastroPlus®

Software, n.d.; Simcyp® Simulator, n.d.; PK-Sim® Software, n.d.) have been developed for the analysis of oral drug absorption. These advances have resulted in the development of physiologically based pharmacokinetic (PBPK) modeling field [8–11].

One characteristic of paramount importance for all modeling approaches is the duration of the absorption process, the so-called mean intestinal transit time. In the most of the cases, the user/modeler can fix the value to a finite time period e.g. 199 min [12–15]. The selection of finite time is crucial for the predictive purposes of the model/software. However, in hundreds and hundreds of pharmaco-kinetic pharmacokinetic-pharmacodynamic, and pharmacometric studies dealing with oral drug absorption, the rate of drug input is routinely estimated with the absorption rate constant [16, 17]. This parameter is the hallmark of the first-order rate of drug absorption, which is associated with an infinite absorption time. Its use started in 1953 when Dost introduced the term pharmacokinetics [1] by adopting the relevant Bateman equation [2] quoted in all pharmacokinetic textbooks. The current chapter focuses on the duration of oral drug absorption.

3.2 Coupling Biopharmaceutic Classification System (BCS) with Pharmacokinetics Using the Finite Absorption Time (FAT) Concept

Basically, drugs pass through the gastrointestinal membranes by passive diffusion. Fick's laws of diffusion describe the flux of solutes (drugs) undergoing classical diffusion. The simplest system to consider is a solution of a drug with two regions of different concentrations, C_{GI} at the absorption site of the gastrointestinal lumen and blood concentration, C of a boundary (GI membrane) separating the two regions. The driving force for drug transfer is the concentration gradient between the con-centrations of the drug molecules in the two regions.

Thus, the rate of penetration can be written as follows:

$$\textbf{Rate of Penetration} = P \cdot SA \cdot (C_{GI} - C) \tag{3.5}$$

Where P is the permeability of drug expressed in velocity units (length/time) and SA is the surface area of the membrane in (length)^2 units. The sheer size of the body, by diluting absorbed drug, tends to maintain sink conditions in which C is much smaller than C_{GI}, therefore,

$$\textbf{Rate of Penetration} = P \cdot SA \cdot C_{GI} \tag{3.6}$$

Equation 3.6 can be written in terms of drug amount, A_{GI} assuming that the volume of fluid at the absorption site V_{GI} remains relatively constant,

$$\textbf{Rate of Penetration} = P \cdot SA \cdot \frac{A_{\text{GI}}}{V_{\text{GI}}} = k_a \cdot A_{\text{GI}} \tag{3.7}$$

where k_a is the absorption rate constant expressed in $(\text{time})^{-1}$ units, which is equal to $P \cdot (SA)/V_{\text{GI}}$. In all pharmacokinetic text books, the classical analysis of the one-compartment model starts from Eq. 3.7 assuming a first-order decrease in the amount of drug, A_{GI}:

$$\frac{dA_{\text{GI}}}{dt} = -k_A \cdot A_{\text{GI}} \tag{3.8}$$

which upon integration from $t = 0$, $A_{\text{GI}} = FD$ to $t = t$, $A_{\text{GI}} = A_{\text{GI}}$ one obtains:

$$A_{\text{GI}} = F \cdot D \cdot e^{-k_a t} \tag{3.9}$$

Equation 3.9 is further coupled with the differential equation describing the change of drug concentration in blood, C, which eventually leads to Eq. 3.1. Thus, the infinite absorption time implied from Eq. 3.1 results from the first-order change (Eq. 3.8) of the amount of drug in the gastrointestinal lumen, A_{GI}.

One of the most important steps in oral drug absorption is the dissolution of drug in the GI fluids [18]. In this context, we reconsider below the rate of drug permeation for the various drug classes (I–IV) [4] using the fundamental Eq. 3.6 taking into account the dissolution process. For the moment, the pharmacokinetic considerations rely on the one-compartment model disposition assuming for simplicity no first-pass effect, i.e., the fraction of dose absorbed equals bioavailable fraction. As the FAT notion unravels, one will have the chance to get acquainted with finer equations describing the kinetics of more than one-compartment models along with multiple input steps. Extensive materialized fittings and simulations will satisfy the most demanding reader.

Class I Drugs For highly soluble, highly permeable drugs (Class I), the rate of permeation is high, Eq. 3.6, Fig. 3.2. Regardless of the formulation administered (drug solution or solid formulation), these drugs do not exhibit either dissolution or permeability-limited absorption. Therefore, the high value of P coupled with the high surface area, $(SA)_i$, of the small intestine leads to rapid and extensive absorption, Fig. 3.2. Therefore, this rapid absorption can be approximated with a constant rate of drug penetration:

$$(\textbf{Rate of Penetration})_{\text{I}} = P \cdot (SA)_i \cdot C_{\text{GI}} = k_{\text{I}} = \frac{F_i D}{\tau_i} \tag{3.10}$$

where k_{I} denotes the constant penetration rate (mass/time units) for Class I drugs, F_i is the fraction of dose absorbed in the stomach and small intestine and τ_i is the duration of this initial absorption phase. Since Class I drugs are absorbed fully,
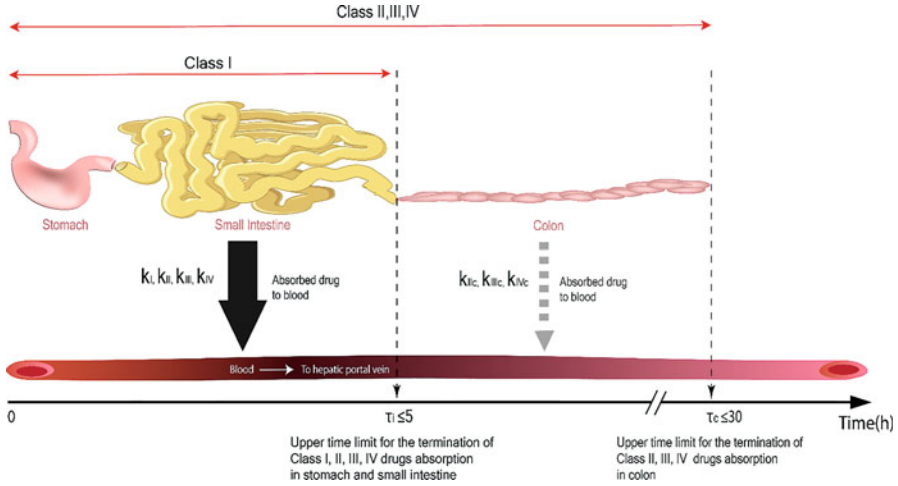
Fig. 3.2 A schematic of the biopharmaceutical/physiological drug absorption model, which relies on the transit times of the drug along the gastrointestinal tract. For Class I drugs, the completion of absorption (F > 0.90) ceases in a shorter time than the duration of the stomach and the small intestine transit 4.86 h [3]. For Class II, III, and IV drugs, the limited overall absorption (F < 0.90) can be continued beyond the ileocecal valve and lasts not more than the whole gut transit time e.g. 29.81 h [3]. The absorbed drug reaches the hepatic portal vein; the blood flow (20–40 cm/s) [19] imposes sink conditions on drug transfer. The thick black arrow denotes the major site of drug absorption, namely, the small intestine. The dashed arrow indicates the potentially limited drug absorption from the colon

$F_i = 1$ is being used in Eq. 3.10. Accordingly, the change of drug blood concentration C as a function of time for Class I drugs is:

$$\frac{V_d dC}{dt} = k_I - k_{el}(CV_d) = \frac{D}{\tau_i} - k_{el}(CV_d) \tag{3.11}$$

Plausibly, the small intestine is the major site of absorption for Class I drugs while absorption always ceases in much shorter time than 4.86 h, which is the sum of the gastric and small intestine transit time, Fig. 3.2. Equation 3.8 gives upon integration for $t = 0$, $C = 0$ and $t = t$, $C = C$:

$$C(t) = \frac{Dk_a}{\tau_i(V_d \, k_{el})} \left(1 - e^{-k_{el} \, t}\right) \tag{3.12}$$

Upon completion of the absorption phase at time $t = \tau_i$, the drug concentration will be $C(\tau_i)$ in accordance with Eq. 3.12. The change of drug concentration beyond time τ_i is described by the following equation:

$$\frac{dC}{dt} = -k_{el} \cdot C \tag{3.13}$$

Equation 3.13 upon integration for $t = \tau_i$, $C = C(\tau_i)$ and $t \rightarrow \infty$, $C = 0$, leads to Eq. 3.14 which describes the monotonic elimination phase

$$C(t) = C(\tau_i) \cdot e^{-k_{el}\,(t-\tau_i)} \tag{3.14}$$

Class II Drugs For low soluble, highly permeable drugs (Class II), the rate of drug permeation is low, Eq. 3.6. This is so, since the maximum value of the term C_{GI}, of Eq. 3.6 cannot be higher than the low saturation solubility, C_S, of the drug in the gastrointestinal fluids. This solubility value can be also considered constant. Therefore, the rate of gastric and small intestine penetration for a Class II drug can be approximated:

$$(\textbf{Rate of Penetration})_{\mathbf{II}} = P \cdot (SA)_i \cdot C_S = k_{II} = \frac{F_i D}{\tau_i} \tag{3.15}$$

where k_{II} denotes the constant penetration rate (mass/time units) for Class II drugs, Fig. 3.2. Accordingly, the change of drug blood concentration C as a function of time assuming the one-compartment model disposition for Class II drugs is

$$\frac{V_d dC}{dt} = k_{II} - k_{el}(CV_d) = \frac{F_i D}{\tau_t} - k_{el}(CV_d) \tag{3.16}$$

Equations 3.15 and 3.16 roughly operate for not more than 4.86 h, which is the sum of gastric and small intestine transit time [3]. The passage of Class II drugs to the colon via the ileocecal valve, which separates the small intestine and the large intestine, can either result in the termination of drug absorption or the significant reduction of the rate of drug penetration since the effective surface area $(SA)_c$ is much smaller in the colon and the amount of unabsorbed drug at the ileocecal valve is equal to $(1-F_i)D$:

$$(\textbf{Rate of Penetration})_{\mathbf{II,c}} = P \cdot (SA)_c \cdot C_S = k_{II,c} = \frac{(1-F_i)D}{\tau_c - \tau_i} \tag{3.17}$$

where τ_c denotes the termination time of drug absorption from the colon and $k_{II,c}$ denotes the constant penetration rate (mass/time units) for Class II drugs in the colon, Fig. 3.2. Accordingly, the change of drug blood concentration C as a function of time assuming one-compartment model disposition for Class II drugs during the drug passage through the colon is

$$\frac{V_d dC}{dt} = k_{II,c} - k_{el}(CV_d) \tag{3.18}$$

This equation roughly holds from 4.86 h to the time needed for the drug to reach the non-absorptive sites of the colon, τ_c, but certainly shorter than 20.28 or 31.95 h, i.e., the colon transit time for a single-unit or multi-unit formulation, respectively [3], Fig. 3.2. At time τ_c absorption ceases; beyond this time point, the drug is only eliminated from the body. Hence, the drug concentration decreases according to Eq. 3.19, which is similar to Eq. 3.14:

$$C(t) = C(\tau_c) \cdot e^{-k_{el}\,(t-\tau_i)} \tag{3.19}$$

where $C(\tau_c)$ is the drug concentration at time τ_c.

Class III Drugs For highly soluble, low permeable drugs (Class III), the rate of drug permeation is low, Eq. 3.6. This is so, since the low permeability value, P_l, is rate limiting for absorption; therefore, the rate of penetration for a Class III drug, throughout the passage of drug from the stomach and small intestine, can be approximated

$$(\textbf{Rate of Penetration})_{\text{III}} = P_l \cdot (SA)_i \cdot (C_{GI}) = k_{\text{III}} = \frac{F_i D}{\tau_i} \tag{3.20}$$

where k_{III} denotes the constant penetration rate (mass/time units) for Class III drugs, Fig. 3.2. Accordingly, the change of drug blood concentration C as a function of time for Class III drugs is

$$\frac{V_d dC}{dt} = k_{\text{III}} - k_{el}(CV_d) \tag{3.21}$$

Equations 3.20 and 3.21 roughly operate for not more than 4.86 h, which is the sum of gastric and small intestine transit time [3]. The passage of Class III drugs to the colon via the ileocecal valve can either result in the termination of drug absorption or the significant reduction of the rate of drug penetration since the effective surface area $(SA)_c$ is much smaller in the colon and the amount of unabsorbed drug at the ileocecal valve is equal to $(1 - F_i)D$:

$$(\text{Rate of Penetration})\text{III}, c = P_l \cdot (SA)_c \cdot C_{GI} = k_{\text{III},c} = \frac{(1 - F_i)D}{\tau_c - \tau_i} \tag{3.22}$$

where $k_{\text{III},c}$, denotes the zero-order penetration rate (mass/time units) for Class III drugs in the colon. Accordingly, the change of drug blood concentration C as a function of time assuming the one-compartment model disposition for Class III drugs in the colon is

$$\frac{V_d dC}{dt} = k_{\text{III},c} - k_{el}(CV_d) \tag{3.23}$$

This equation roughly holds from 4.86 h to the time needed for the drug to reach the non-absorptive sites of the colon, τ_c, but certainly shorter than 20.28 or 31.95 h, i.e., the colon transit time for a single-unit or multi-unit formulation, respectively [3]. At time τ_c absorption ceases; beyond this time point, the drug is only eliminated from the body. Hence, the drug concentration decreases according to Eq. 3.19 for $t \geq \tau_c$.

Class IV Drugs For low soluble, low permeable (Class IV) drugs, the rate of permeation is low, Eq. 3.6. Both solubility and permeability are limiting absorption. The low values of the terms P and C_{GI} in Eq. 3.6 allow their replacement, as explained above, with P_l and C_S, respectively. This leads to slow and limited absorption ($F < <0.90$). Therefore, this slow absorption can be approximated with a constant rate of penetration:

$$(\textbf{Rate of Penetration})_{\textbf{IV}} = P_l \cdot (SA)_i \cdot (C_S) = k_{\text{IV}} = \frac{F_i D}{\tau_i} \qquad (3.24)$$

where k_{IV} denotes the constant penetration rate (mass/time units) for Class IV drugs, Fig. 3.2. Using the same syllogism delineated above, the differential equation describing the change of drug blood concentration C during the passage of drug from the stomach and small intestine (roughly, 4.86 h) [3] is as follows:

$$\frac{V_d dC}{dt} = k_{\text{IV}} - k_{\text{el}}(CV_d) \qquad (3.25)$$

The passage of Class IV drugs to the colon via the ileocecal valve can either result in the termination of drug absorption or the significant reduction of the rate of drug penetration since the effective surface area is much smaller in the colon $(SA)_c$ and the amount of unabsorbed drug at the ileocecal valve is equal to $(1 - F_i)D$:

$$(\textbf{Rate of Penetration})_{\textbf{IV,c}} = P \cdot (SA)_c \cdot C_{\text{GI}} = k_{\text{IV},c} = \frac{(1 - F_i)D}{\tau_c - \tau_i} \qquad (3.26)$$

where $k_{\text{IV},c}$ denotes the constant penetration rate (mass/time units) for Class IV drugs in the colon. Accordingly, the change of drug blood concentration C as a function of time assuming one-compartment model disposition for Class IV drugs in the colon is

$$\frac{V_d dC}{dt} = k_{\text{IV},c} - k_{\text{el}}(CV_d) \qquad (3.27)$$

As explained above, this equation roughly holds from 4.86 h to the time needed for the drug to reach the non-absorptive sites of the colon, τ_c, (< 20.28 or < 31.95 h), i.e., the colon transit time for a single-unit or multi-unit formulation, respectively [3]. Beyond, this time point, τ_c, the drug is only eliminated from the body. Hence, the drug concentration decreases according to Eq. 3.19 for $t \geq \tau_c$.

The theoretical section of oral drug absorption was established on (i) the FAT concept, (ii) the physiologically based transit times reported in the literature [3], and (iii) the basic drug properties, namely, solubility and permeability, which have been adopted by the regulatory authorities as the key factors controlling oral drug absorption (6.7). However, the reader should be aware of the qualitative character of biopharmaceutics classification system, which implies large differences in the drug properties among the drugs of the same class. Accordingly, the theoretical aspects developed here can be considered a general framework of drug absorption while the in vivo drug behavior can vary remarkably even for drugs of the same Class (6.7). Moreover, deviations from the general modeling framework may be applied in accordance with the experimental observations. For example, a drug may exhibit the regional rate of absorption differences in the various segments of the small intestines, e.g., jejunum and ileum. In such a case, two successive constant input rates can be considered. Although the development of models up to this point was based on the one-compartment model disposition, similar equations can be written assuming a two-compartment model disposition. The reader will have the chance to become familiar with the relevant equations later on. Due to the physiological relevance of the finite time absorption models developed, we coin the term physiologically based finite time pharmacokinetic (PBFTPK) models [20].

The physiological aspects of the PBFTPK models rely on the physiological/ anatomical differences between the two regions, the small intestine and the large intestine. It is widely known today that because of its permeability, large surface area and high blood flow, the small intestine is the primary site for drug absorption, Fig. 3.2. In fact, a monolayer of enterocytes that is characterized by protrusions that extend into the gut lumen, called villi, results in a potential absorptive surface area of 60 m^2 in both the jejunum and ileum [21]. On the contrary, the colon surface area totals around 0.25 m^2 as there are no villi [22]; this huge anatomical difference causes a very large difference in the rate of drug absorption, Fig. 3.2. Besides, drug's transport from the GI lumen to the portal vein relies on the sink conditions' principle of the universally accepted passive drug absorption notion. This is substantiated by the fact that the blood in the portal vein has a velocity of 20–40 cm/s [19], which does not allow Fick's reversibility considerations for the drug transfer. In parallel, the small intestine was presented (Fig. 3.2) as a homogeneous compartment in terms of drug's uptake. However, drug absorption takes place mainly from the lower part of the small intestine. For example, drug absorption can be higher from the jejunum than the ileum.

The unique features of the PBFTPK models [20] are the finite termination times for the absorption phases, τ_i and τ_c, respectively. The upper limit for τ_i is 5 h, Fig. 3.2, with the most frequently observed values in the literature in the range 1–3 h depending on the drug's biopharmaceutical properties. The upper limit for τ_c is 30 h, Fig. 3.2, while the most usual values for τ_c are unknown since estimates for τ_c have not been explored so far. However, a large number of in vivo studies based on imaging techniques like gamma scintigraphy or magnetic resonance imaging coupled with drug blood measurements have shown that the completion of the absorption phase is terminated during the drug's passage from the small intestine,

e.g., erythromycin study [23]. Needless to say that according to the current theory (Eq. 3.1), the termination of either the elimination or the absorption phase is irreconcilable.

3.3   Mathematical Modeling

All of the above considerations lead to the development of model equations [24] that have the following properties:

(a) Absorption in the GI tract is described as a zero-order kinetics process that lasts for a limited time and then ceases altogether. The absorption rate constant can have a single value throughout the absorption stage or it may have different values for specific time intervals. The number of intervals may vary from one to half a dozen.

(b) Disposition may involve just the blood circulation (one, central compartment) or it may happen in more than one compartment. In what follows, we will consider two compartments. Furthermore, we will expect the elimination of the drug to take place only through the central compartment. In short, this means that the elimination phase follows a simple exponential decay (one-compartment models) or a double exponential decay (two-compartment models).

According to the fundamental model developed in [20], drugs are absorbed passively under sink conditions for physiological reasons [3, 19], Fig. 3.3a. Drug absorption under sink conditions has been used and is still used extensively and successfully in physiologically based pharmacokinetic (PBPK) modeling [8–11]. Due to the anatomical-physiological characteristics of the GI tract, drugs with different biopharmaceutical properties, e.g., solubility, permeability, and ionization, can exhibit one or two or three successive constant input rates, Fig. 3.3b [24].

For drugs following linear disposition kinetics, we coin the term p-PBFTPK-m, where p is the number of the successive input rates 1, 2, 3, and m takes the values 1 or 2 denoting the disposition characteristics of the drug, namely, one- or two-compartment model, respectively. For the metabolized drugs following non-linear Michaelis–Menten disposition kinetics, we coin the term p-PBFTPK-m(MM). A schematic representation of models exhibiting linear or non-linear disposition kinetics is shown in Fig. 3.4.

The differential equations for the linear models, p-PBFTPK-m, are listed in Table 3.1 [24]. For the sake of brevity, we present only the simplest and the most complicated case, since the intermediate ones can be easily inferred. The corresponding equations for drug's concentration change as a function of time in the central compartment, $C(t)$, and in the peripheral compartment, $C_P(t)$, for these models are listed in Tables 3.2 and 3.3. It should be noted that the ratio of the distribution volumes of the central and the peripheral compartment is not included explicitly in the following expressions. This does not affect any calculations or conclusions because there are no data on the actual drug concentration in the peripheral compartment.
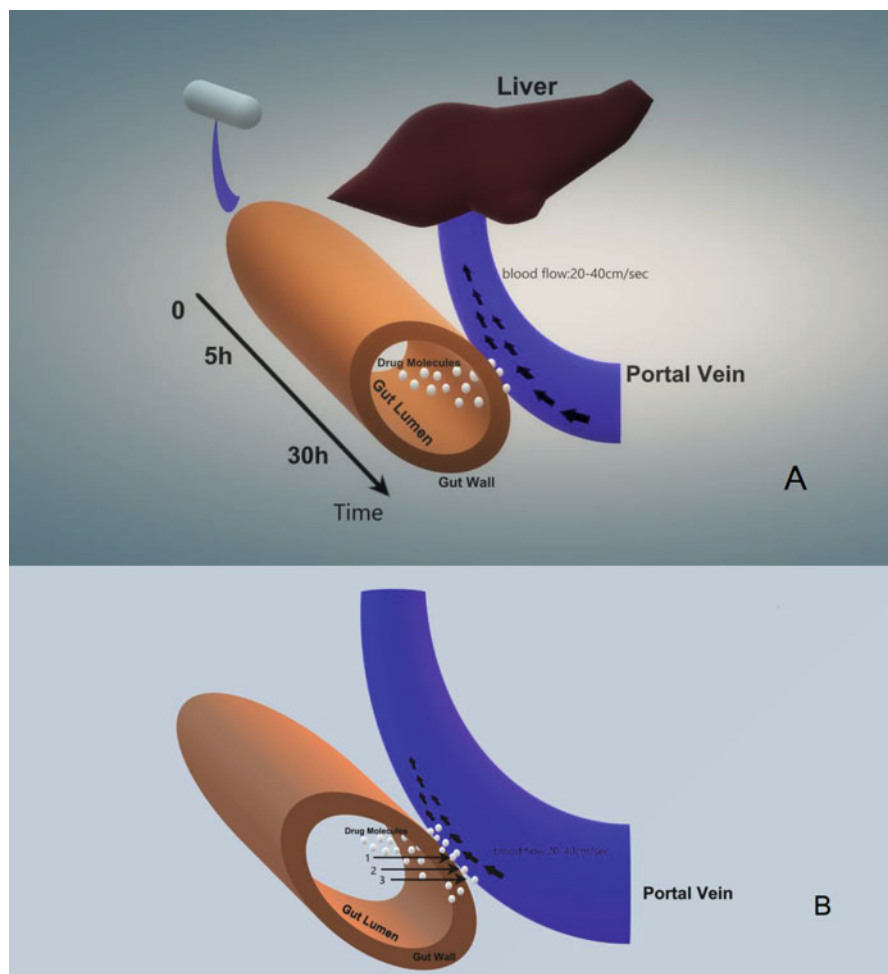
Fig. 3.3 (**a**) Schematic of the passive transfer of dissolved drug molecules (white spheres) from the gut lumen to the portal vein. The blood flow in the portal vein, 20–40 cm/s [19] ensures sink conditions for the passive drug transfer due to its continuous removal from the portal vein to the liver. The physiological time limits 5 and 30 h for drug absorption from the small intestines and colon [3], respectively are shown on the time axis. (**b**) Enlargement of the region gut wall-portal vein for the drug transfer; the arrows indicate up to three successive constant input rates for the dissolved drug molecules (white spheres) passive transfer under sink conditions

3.4 Simulations

Figures 3.5 and 3.6 show the simulated concentration-time curves generated from the model equations for one- and two-compartment model drugs, respectively. Both Figures demonstrate the resemblance of the simulated curves with real life data reported in the literature. When a single input rate is applied (Figs. 3.5a and 3.6a), the
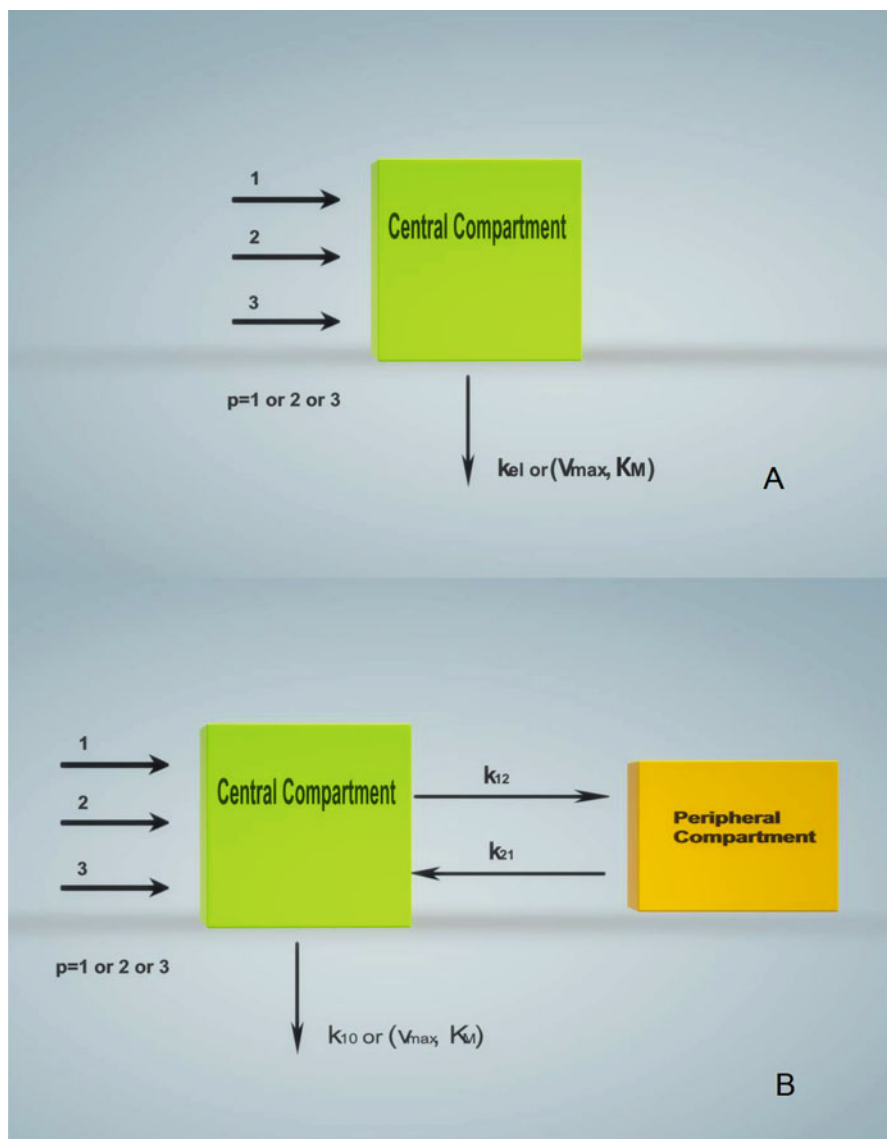
Fig. 3.4 Schematic representation of one-compartment (**a**) and two-compartment (**b**) p-PBFTPK-m models. In all cases, the horizontal arrows at the left-hand side of the central compartment denote the number of successive constant drug input rates, not necessarily of the same drug amount or duration; k_{el} is the elimination rate constant, k_{10} is the elimination rate constant of the central compartment of the two-compartment model drugs; k_{12} and k_{21} are the disposition micro-constants for the transfer of drug from the central to the peripheral compartment and vice versa, respectively; V_{max} and K_M correspond to the maximum biotransformation rate and the constant of the Michaelis–Menten kinetics

Table 3.1 Differential equations for linear models p-PBFTPK-m^{a}

p	m	i	Kinetic (differential) equations	t_{i-1}	t_i	Equations
1	1	1	$\frac{dC}{dt}=\frac{FD}{\tau V_d}-k_{\mathrm{el}}C$	0	τ	3.28
		2	$\frac{dC}{dt}=-k_{\mathrm{el}}C$	τ	∞	3.29
4	1	1	$\frac{dC}{dt}=\frac{F_iD}{\tau_i V_d}-k_{\mathrm{el}}C$	0	τ_1	3.30
		2	Same as above	τ_1	$\tau_1+\tau_2$	
		3	Same as above	$\tau_1+\tau_2$	$\tau_1+\tau_2+\tau_3$	
		4	Same as above	$\tau_1+\tau_2+\tau_3$	$\tau_1+\tau_2+\tau_3+\tau_4$	
		5	$\frac{dC}{dt}=-k_{\mathrm{el}}C$	$\tau_1+\tau_2+\tau_3+\tau_4$	∞	3.31
1	2		$\frac{dC}{dt}=\frac{FD}{\tau V_d}-k_{12}C-k_{10}C+k_{21}C_P$	0	τ	3.32
			$\frac{dP}{dt}=k_{12}C-k_{21}C_P$			3.33
			$\frac{dC}{dt}=-k_{12}C-k_{10}C+k_{21}C_P$	τ	∞	3.34
			$\frac{dP}{dt}=k_{12}C-k_{21}C_P$			3.35
4	2	1	$\frac{dC}{dt}=\frac{F_iD}{\tau_i V_d}-k_{12}C-k_{10}C+k_{21}C_P$	0	τ_1	3.36
			$\frac{dP}{dt}=k_{12}C-k_{21}C_P$			3.37
		2	Same as above	τ_1	$\tau_1+\tau_2$	
		3	Same as above	$\tau_1+\tau_2$	$\tau_1+\tau_2+\tau_3$	
		4	Same as above	$\tau_1+\tau_2+\tau_3$	$\tau_1+\tau_2+\tau_3+\tau_4$	
		5	$\frac{dC}{dt}=-k_{12}C-k_{10}C+k_{21}C_P$	$\tau_1+\tau_2+\tau_3+\tau_4$	∞	3.38
			$\frac{dP}{dt}=k_{12}C-k_{21}C_P$			3.39

[a]Each equation is defined for t in the range $t_{i-1}<t<t_i$

Table 3.2 Solutions to linear models p-PBFTPK-1$^{\mathrm{a}}$

p	m	i	$C(t)$	t_{i-1}	t_i	Equations
1	1	1	$\frac{FD}{\tau V_d k_{\mathrm{el}}}\left(1-e^{-k_{\mathrm{el}}t}\right)$	0	$T\alpha$	3.40
		2	$C(\tau)e^{-k_{\mathrm{el}}(t-\tau)}$	τ	∞	3.41
4	1	1	$\frac{F_iD}{\tau_i V_d k_{\mathrm{el}}}\left(1-e^{-k_{\mathrm{el}}t}\right)$	0	τ_1	3.42
		2	$C(t_{i-1})e^{-k_{\mathrm{el}}(t-t_{i-1})}+\frac{F_iD}{\tau_i V_d k_{\mathrm{el}}}\left(1-e^{-k_{\mathrm{el}}(t-t_{i-1})}\right)$	τ_1	$\tau_1+\tau_2$	3.43
		3	Same as above	$\tau_1+\tau_2$	$\tau_1+\tau_2+\tau_3$	
		4	Same as above	$\tau_1+\tau_2+\tau_3$	$\tau_1+\tau_2+\tau_3+\tau_4$	
		5	$C(t_{i-1})e^{-k_{\mathrm{el}}(t-t_{i-1})}$	$\tau_1+\tau_2+\tau_3+\tau_4$	∞	3.44

[a]Each equation is defined for t in the range $t_{i-1}<t<t_i$

simulated data exhibit a patent change of drug concentration $C(\tau)$ at the end of the duration of the absorption process at time τ, (marked with the symbol ▲), which also corresponds to the maximum drug concentration, $C_{\max}$, observed in plasma. For the simulated data with multiple input rates, the values of $C(\tau)$ can be either equal to $C_{\max}$ (Figs. 3.5b, d and 3.6d) or smaller (Figs. 3.5c and 3.6b, c), i.e., the termination of the absorption phase is observed at the descending limb of the curve. The simulated results for the $C_P(t)$ curves show the shape similarity of the generated

Table 3.3 Solutions to linear models p-PBFTPK-2[a]

p	m	l	$C(t),\ C_P(t)$	t_{i-1}	t_i	Equations
1	2	1	$C(t) = \dfrac{FD}{\tau V_d}\left(\dfrac{(k_{21}-\alpha)(1-e^{-\alpha t})}{\alpha(\beta-\alpha)} + \dfrac{(k_{21}-\beta)(1-e^{-\beta t})}{\beta(\alpha-\beta)} \right)$	0	$T\alpha$	3.45
			$C_P(t) = \dfrac{FDk_{12}}{(\beta-\alpha)\tau V_d}\left[\dfrac{1}{\alpha}(1-e^{-\alpha t}) - \dfrac{1}{\beta}(1-e^{-\beta t}) \right]$			3.46
		2	$C(t) = \dfrac{FD}{\tau V_d}\dfrac{(k_{21}-\alpha)(1-e^{-\alpha \tau})}{\alpha(\beta-\alpha)}e^{-\alpha(t-\tau)} + \dfrac{FD}{\tau V_d}\dfrac{(k_{21}-\beta)(1-e^{-\beta \tau})}{\beta(\alpha-\beta)}e^{-\beta(t-\tau)}$	τ	∞	3.47
			$C_P(t) = \dfrac{k_{12}}{\beta-\alpha}\left(\left(C(\tau)+\dfrac{k_{21}}{k_{21}-\alpha}C_P(\tau)\right)e^{-\alpha(t-\tau)} - \left(C(\tau)+\dfrac{k_{21}}{k_{21}-\beta}C_P(\tau)\right)e^{-\beta(t-\tau)} \right)$			3.48
4	2	1	$C(t) = \dfrac{FD}{\tau V_d}\left[\dfrac{k_{21}-\alpha}{\alpha(\beta-\alpha)}(1-e^{-\alpha t}) + \dfrac{k_{21}-\beta}{\beta(\alpha-\beta)}(1-e^{-\beta t}) \right]$	0	τ_1	3.49
			$C_P(t) = \dfrac{F_\tau Dk_{12}}{(\beta-\alpha)\tau_\tau V_d}\left[\dfrac{1}{\alpha}(1-e^{-\alpha t}) - \dfrac{1}{\beta}(1-e^{-\beta t}) \right]$			3.50
		2	$C(t) = \dfrac{1}{\beta-\alpha}\Big(C(t_{i-1})\left[\beta e^{-\beta(t-t_{i-1})} - \alpha e^{-\alpha(t-t_{i-1})}\right] + (k_{21}[C(t_{i-1})+C_P(t_{i-1})]) \times$ $(e^{-\alpha(t-t_{i-1})} - e^{-\beta(t-t_{i-1})})\Big) + \dfrac{F_\tau D}{(\beta-\alpha)\tau_\tau V_d}\left(\dfrac{k_{21}-\alpha}{\alpha}(1-e^{-\alpha(t-t_{i-1})}) - \dfrac{k_{21}-\beta}{\beta}(1-e^{-\beta(t-t_{i-1})}) \right)$	τ_1	$\tau_1+\tau_2$	3.51
			$C_P(t) = \dfrac{k_{12}}{\beta-\alpha}\left(\left(C(t_{i-1})+\dfrac{k_{21}}{k_{21}-\alpha}C_P(t_{i-1})\right)e^{-\alpha(t-t_{i-1})} - \left(C(t_{i-1})+\dfrac{k_{21}}{k_{21}-\beta}C_P(t_{i-1})\right)e^{-\beta(t-t_{i-1})} \right)$ $+ \dfrac{k_{12}F_\tau D}{(\beta-\alpha)\tau_\tau V_d}\left[\dfrac{1}{\alpha}(1-e^{-\alpha(t-t_{i-1})}) - \dfrac{1}{\beta}(1-e^{-\beta(t-t_{i-1})}) \right]$			3.52
		3	Same as above	$\tau_1+\tau_2$	$\tau_1+\tau_2+\tau_3$	
		4	Save as above	$\tau_1+\tau_2+\tau_3$	$\tau_1+\tau_2+\tau_3+\tau_4$	
		5	$C(t) = \dfrac{[C(t_{i-1})(k_{21}-\alpha)+C_P(t_{i-1})k_{21}]e^{-\alpha(t-t_{i-1})}}{\beta-\alpha} + \dfrac{[C(t_{i-1})(k_{21}-\beta)+C_P(t_{i-1})k_{21}]e^{-\beta(t-t_{i-1})}}{\alpha-\beta}$	$\tau_1+\tau_2+\tau_3+\tau_4$	∞	3.53
			$C_P(t) = \dfrac{k_{12}}{\beta-\alpha}\left(\left(C(t_{i-1})+\dfrac{k_{21}}{k_{21}-\alpha}C_P(t_{i-1})\right)e^{-\alpha(t-t_{i-1})} - \left(C(t_{i-1})+\dfrac{k_{21}}{k_{21}-\beta}C_P(t_{i-1})\right)e^{-\beta(t-t_{i-1})} \right)$			3.54

[a]Each equation is defined for t in the range $t_{i-1} < t < t_i$
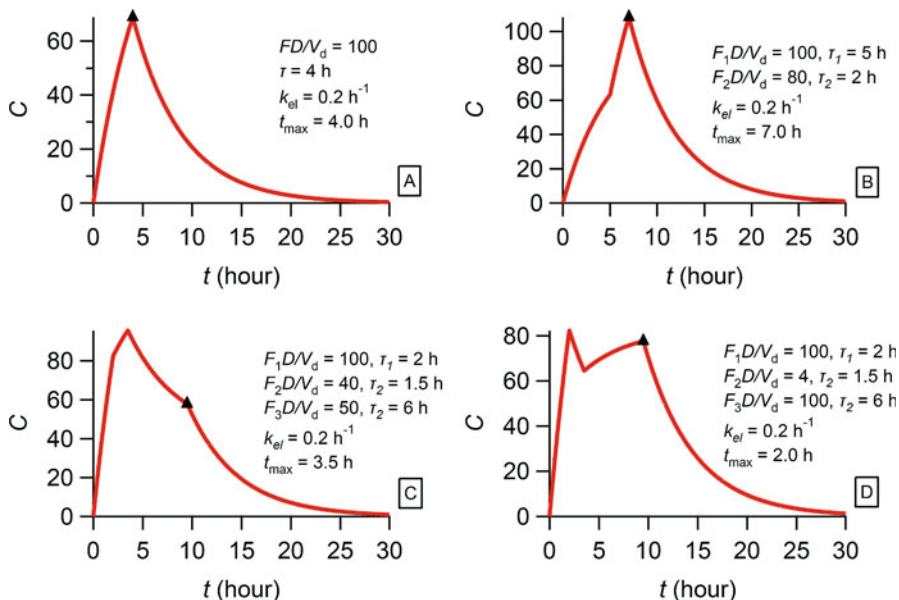
Fig. 3.5 Simulated curves for one-compartment model drugs ($m = 1$) following linear disposition kinetics with $p = 1$ (Eqs. 3.40 and 3.41, panel **a**), $p = 2$ (Eqs. 3.42, 3.43, and 3.44, panel **b**), $p = 3$ (Eqs. 3.42, 3.43, and 3.44, panels **c** and **d**). Model parameter values are shown in each panel. The symbol ▲ denotes the termination of all absorption stages
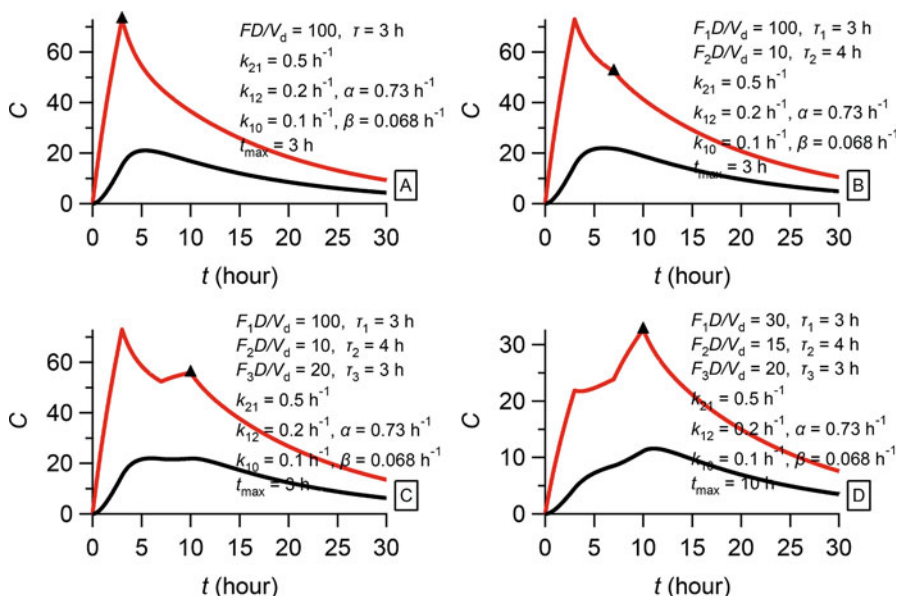
Fig. 3.6 Simulated curves for two-compartment model drugs ($m = 2$) following linear-linear disposition kinetics showing the central (red) and peripheral (black) compartment concentrations for $p = 1$ (Eqs. 3.45, 3.46, 3.47 and 3.48, panel **a**), $p = 2$ (Eqs. 3.49, 3.50, 3.51, 3.52, 3.53 and 3.54, panel **b**), $p = 3$ (Eqs. 3.49, 3.50, 3.51, 3.52, 3.53 and 3.54, panels **c** and **d**). Model parameters are shown in each panel. The symbol ▲ denotes the termination of all absorption stages
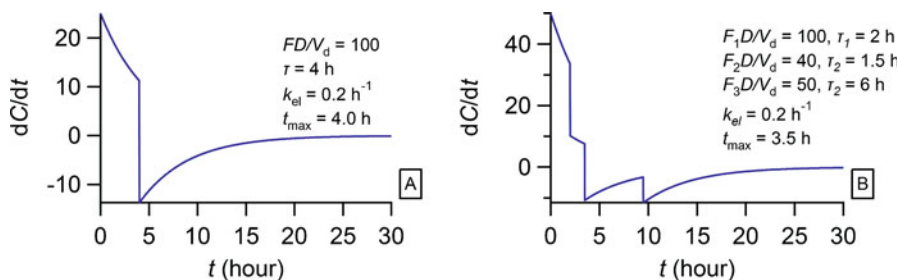
Fig. 3.7 Plots of the derivative dC/dt as a function of time. A. $t_{max} = \tau = 4.0$ h and the derivative was calculated from Eqs. 3.40 and 3.41. B. $t_{max} = 3.5$ h $< \tau = 9.5$ h and the derivative was calculated from Eqs. 3.42, 3.43, and 3.44

curves, which poorly reflect the changes of the drug concentration in the central compartment $C(t)$, Fig. 3.6 [24].

In all above plots, the $(C(\tau), \tau)$ pair is a discontinuity datum point. When $t_{max} = \tau$, there is a more patent change of the concentration-time curve in the neighborhood of the discontinuity time point, Figs. 3.5a, b, 3.6a, and d. On the contrary, when $t_{max} < \tau$, the discontinuity datum point lies in the descending part of the concentration–time curve, Figs. 3.5c, d, 3.6b, and c and therefore, this change is less abrupt. In Fig. 3.7, one can see the change of the derivative dC/dt for two examples with $t_{max} = \tau$ and $t_{max} < \tau$. In the former case, the derivative changes from positive to negative values at $t_{max} = \tau$; in the latter case, the sign of the derivative is maintained negative close to τ and throughout the descending portion of the curve. These plots demonstrate that under experimental conditions, the estimation of τ will be easier when $t_{max} = \tau$. When $t_{max} < \tau$, the presence of experimental error and the sparse sampling close to τ can make the estimation of τ impossible.

3.5 Sample Data Fitting

We present an example exhibiting a single zero-order input (paracetamol) and then extend our applications to drugs belonging to various biopharmaceutical classes exhibiting more complex absorption and following one-or two-compartment model disposition. In all cases, modified-release formulations were not examined. The term "best-fit results" quoted in the legend of the figures below corresponds to the best model found among the PBFTPK and the classical first-order models tested.

(i) Paracetamol. We analyzed the experimental data of a pharmacokinetic study [24]. The best fit results using Eqs. (3.40 and 41), which adhere to the simplest model with a constant input rate and first-order elimination are shown in Fig. 3.8. According to the results presented in Fig. 3.8, paracetamol absorption is very fast and terminates at 0.51 ± 0.03 h.

$FD/V_d = 10.5 \pm 0.5$ µg/mL
$k_{el} = 0.30 \pm 0.03$ h^{-1}
$\tau = 0.51 \pm 0.03$ h
$\chi^2 = 4.9641e+06$, $R^2 = 0.986$
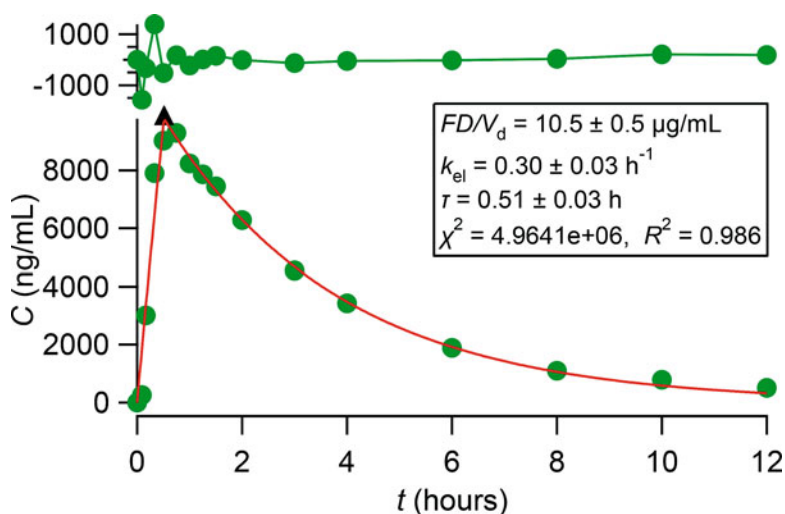
Fig. 3.8 Best fit results of Eqs. 3.40 and 3.41 to paracetamol experimental data [25]. The symbol ▲ denotes the end of the absorption process. The top panel depicts the fit residuals

(ii) Ibuprofen. This is a classical BCS class II drug with low solubility at pH 1.2 and 4.5 and high solubility at pH 6.8 since it is a carboxylic acid. We analyzed the experimental data of a pharmacokinetic study [25]. The best-fit results using Eqs. (3.42, 3.43 and 3.44), which adhere to a model with two constant input rates and first-order elimination are shown in Fig. 3.9. These data reveal that absorption terminates at 2.3 h, namely, ibuprofen is absorbed in the small intestine.

(iii) Almotriptan malate. This is a selective serotonin receptor agonist with hydrophilic properties. We analyzed the experimental data of a pharmacokinetic study [26]. The best-fit results using Eqs. (3.42, 3.43, and 3.44), which adhere to a model with two constant input rates and first-order elimination are shown in Fig. 3.10. These data reveal that absorption terminates at 2.8 h, namely, almotriptan is absorbed in the small intestine.

(iv) Cyclosporine. This is a Class II drug with very low solubility [27]. We analyzed the experimental data of the fundamental bioequivalence study under fasted and fed conditions, which led to the replacement of the reference formulation (Sandimmune) with the test formulation (Sandimmune Neoral) [28]. The best-fit results for the test (administered as a single oral dose of 180 mg) and reference (administered as a single oral dose of 300 mg) formulations under fasted and fed conditions are shown in Fig. 3.11.

The plots of Fig. 3.11a, b, and c reveal that the absorption of cyclosporine for the test formulation (Sandimmune Neoral) under both fasted and fed conditions as well as for the reference formulation (Sandimmune) under fasted conditions is described by the zero-order input process, which terminates at 1.6, 1.7, and 2.9 h, respectively.
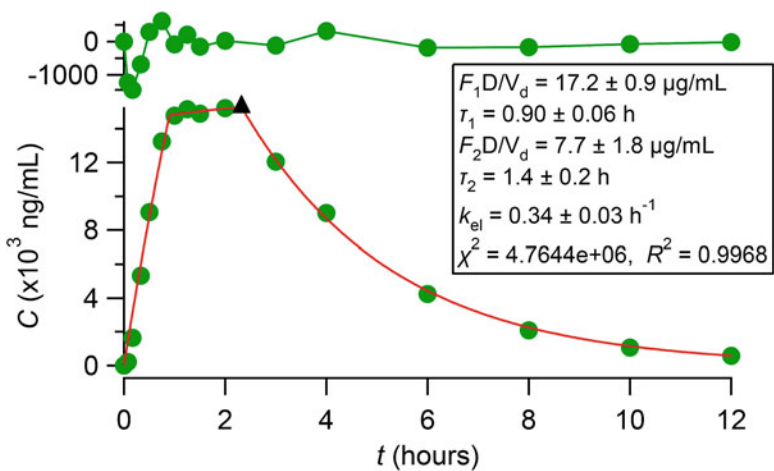
Fig. 3.9 Best fit results of Eqs. 3.42, 3.43, and 3.44 to ibuprofen experimental data [25]. The symbol ▲ denotes the end of the absorption processes

Box in figure 3.9:
$F_1 D/V_d = 17.2 \pm 0.9$ µg/mL
$T_1 = 0.90 \pm 0.06$ h
$F_2 D/V_d = 7.7 \pm 1.8$ µg/mL
$T_2 = 1.4 \pm 0.2$ h
$k_{el} = 0.34 \pm 0.03$ h^{-1}
$\chi^2 = 4.7644e+06$, $R^2 = 0.9968$
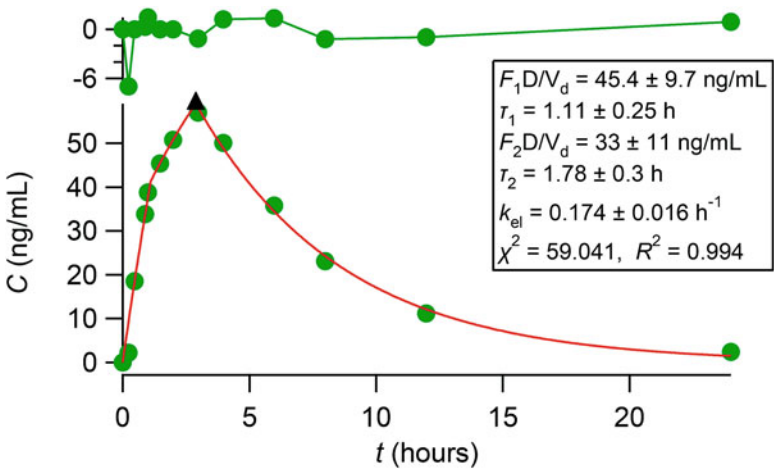
Fig. 3.10 Best fit results of Eqs. 3.42, 3.43, and 3.44 to almotriptan experimental data [26]. The symbol ▲ denotes the end of the absorption processes

Box in figure 3.10:
$F_1 D/V_d = 45.4 \pm 9.7$ ng/mL
$T_1 = 1.11 \pm 0.25$ h
$F_2 D/V_d = 33 \pm 11$ ng/mL
$T_2 = 1.78 \pm 0.3$ h
$k_{el} = 0.174 \pm 0.016$ h^{-1}
$\chi^2 = 59.041$, $R^2 = 0.994$

This shows that cyclosporine absorption terminates sooner with the test formulation than with the reference formulation. The graph in Fig. 3.11d shows the complex absorption of cyclosporine from the test formulation under fed conditions; in fact, the best fit corresponds to a model with three successive fluctuating input rates of the total duration of 4.6 h. All these results are indicative of the erratic absorption of cyclosporine from the reference formulation in the presence of food. These findings are related to the hydrophobic nature of cyclosporine and the pharmaceutical
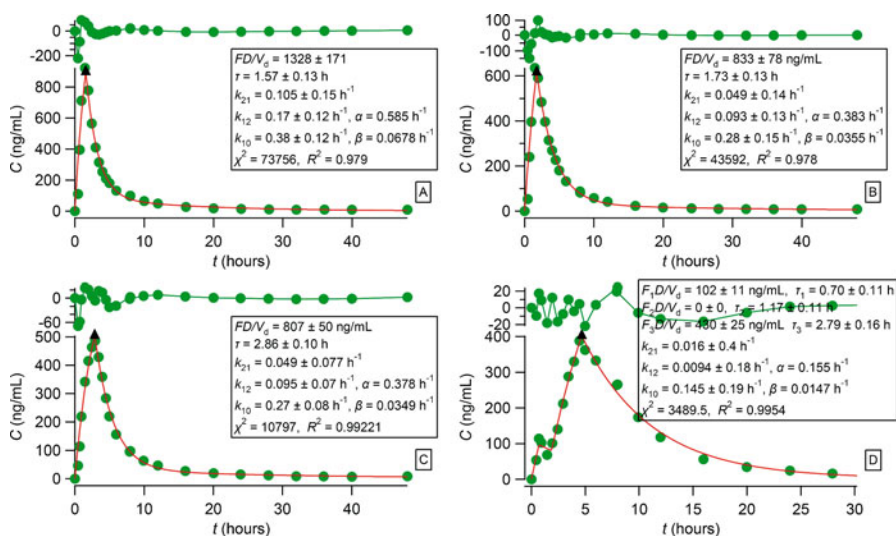
Fig. 3.11 Best fit results of Eqs. 3.45 and 3.47 to test formulation under fasted (**a**), fed (**b**) conditions, and reference formulation under fasted (**c**) conditions [28]. Best fit results of Eqs. 3.49, 3.51, 3.53 to reference formulation under fed (**d**) conditions. The symbol ▲ denotes the end of the absorption processes

differences of the two formulations, namely, the test formulation is a micro-emulsion while the reference formulation is a solution of cyclosporine in olive oil. The reader should also notice the high uncertainty (SDs) of the disposition parameters of cyclosporine in the panel of Fig. 3.11d in contrast to the corresponding values in panels of Fig. 3.11a, b, and c. In all cases, the fits presented in Fig. 3.11 were superior (data not shown) to the fits of Eqs. 3.1 or 3.3 to the experimental data.

(v) Niraparib. This is an orally bioavailable anticancer agent. Here, we analyze the pharmacokinetics of an absolute bioavailability study of niraparib [29] using the PBFTPK models. The best-fit results using Eqs. (3.51 and 3.53), which adhere to a model with two constant input rates and two-compartment disposition are shown in Fig. 3.12. These data reveal that absorption terminates at 3.4 h, namely, niraparib is absorbed in the small intestine; the long stay of the drug in the body is due to the slow disposition characteristics.

3.6 Towards a Biophamraceutic-Pharmacokinetic Classification System

The analysis of data, Figs. 3.8, 3.9, 3.10, 3.11 and 3.12, underlines the fact that the duration, τ, of the absorption process is a fundamental biopharmaceutical parameter of drugs when administered as an immediate-release formulation. The type of
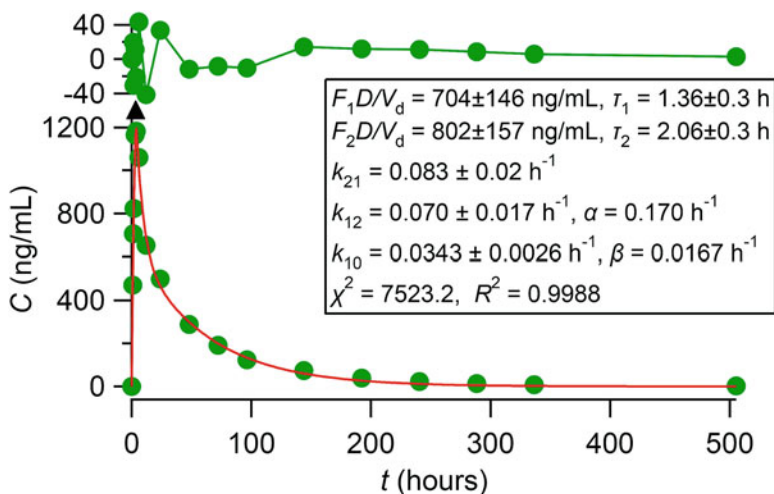
Fig. 3.12 Best-fit results of Eqs. 3.51, 3.53 to the experimental data of niraparib [29]. The symbol ▲ denotes the end of the absorption processes

immediate-release formulation can also have an impact on the τ estimate (see cyclosporine results, Fig. 3.11).

For years and years, the absorption rate constant became the sole parameter for expressing quantitatively the rate of drug absorption in classical and population pharmacokinetic studies. However, it was found to be the most variable parameter with non-meaningful physiological units (time^{-1}), not allowing a valid interspecies or pediatric scaling and relying on the unphysical assumption of infinite time of absorption [16, 17]. The results presented in Figs. 3.8, 3.9, 3.10, 3.11 and 3.12, if contrasted with the results derived from the fitting of Eqs. 3.1 and 3.3 to the same data, clearly demonstrate the superiority of the PBFTPK models for the description of absorption characteristics of drugs/formulations. Roughly, the more complex the absorption is the better is the performance of the PBFTPK models compared to the Bateman equation (Eq. 3.1).

The assessment of permeation in the physiologically based pharmacokinetic (PBPK) models [8–11] is based on permeability estimates; thus, the use of the absorption rate constant for the assessment of the drug's input rate has been abandoned in the PBPK modeling work. The current work relies on the FAT concept [20, 24] and allows the estimation of τ, which can characterize each drug/formulation given as an immediate-release formulation, Figs. 3.8, 3.9, 3.10, 3.11 and 3.12. This is so since τ is conceptually associated with the fundamental biopharmaceutical properties of solubility and permeability as shown in Sect. 3.2. Intuitively, drugs/immediate release formulations can be classified into: (i) rapidly absorbing $\tau < 1.5$ h like paracetamol and borderline cyclosporine (Sandimmune Neoral) administered under fasted conditions in the present study; (ii) medium absorbing $1.5 \leq \tau < 5$ h like ibuprofen, almotriptan, and cyclosporine (Sandimmune Neoral) administered under
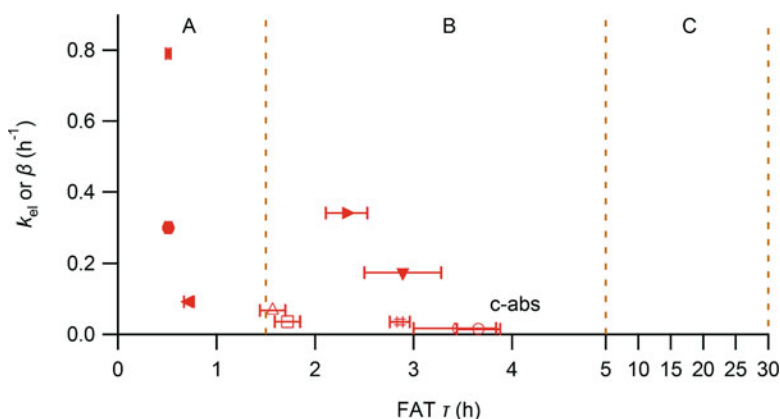
Fig. 3.13 Plot of elimination rate constant, k_{el} or β, estimates vs. finite absorption time (FAT), τ, estimates (±SD) Key: paracetamol (●), cyclosporine (Sandimmune Neoral, fasted) (Δ), ibuprofen (▶), almotriptan (▼), cyclosporine (Sandimmune Neoral fed) (□), cyclosporine (Sandimmune, fasted) (#), niraparib (◇), theophylline [30] (◀), BMS-626529 drug [30] (◆). Filled symbols correspond to k_{el} estimates (one-compartment model drugs), while empty symbols correspond to β estimates (two-compartment model drugs). The term c-abs next to cyclosporine (Sandimmune, fed) (o) administered under fed conditions, denotes complex absorption

fed conditions as well as cyclosporine (Sandimmune) administered under fasted conditions in the present study and niraparib; (iii) slow absorbing $5 \leq \tau < 30$ h not observed in the present study. For the first two categories, drug absorption takes place only in the small intestine, while for the third category, colon absorption is also operating. Several drugs/formulations exhibiting either selective regional permeability or solubility/ionization characteristics which lead to precipitation/re-dissolution comprise a fourth category characterized by a complex absorption profile like cyclosporine (Sandimmune) administered under fed conditions in the present study (see Fig. 3.11d). Figure 3.13 shows the proposed three categories (A, B, and C) of a biophamraceutic-pharmacokinetic classification system where a drug exhibiting complex absorption, denoted with c-abs, can also be classified in accordance with its τ estimate. All estimates for τ are coupled with the corresponding estimate for drug's elimination rate constant k_{el} or β for drugs obeying one-or two-compartment model kinetics, respectively, Fig. 3.13.

Visual inspection of Fig. 3.13 reveals that the one-compartment model drugs paracetamol (Fig. 3.8) and theophylline [30], which are biowaivers, are located in Class A close to the ordinate. This is in accordance with their extensive absorption calculated from oral data, if one applies the one-compartment model methodology described for theophylline in Ref. [30]. This also applies for the BMS-626529 drug [30, 31]. All cyclosporine formulations, ibuprofen and almotriptan are classified in Class B.

In all examples analyzed, the estimate for τ was found to be equal to t_{max}. Reliable estimates were derived for τ using our PBFTPK software, Figs. 3.8, 3.9, 3.10, 3.11 and 3.12, since an adequate number of samples were available throughout the time

course of drug in the body. For the one-compartment model drugs exhibiting one input rate like paracetamol, this finding, $\tau = t_{max}$, is a logical consequence of the FAT concept. On the contrary, estimates for τ were not found in the descending leg of the curves ($\tau > t_{max}$), which could be observed in other drugs. Although this is theoretically possible (Fig. 3.7b), the fitting results and the statistical measures are presented in Figs. 3.7, 3.8, 3.9, 3.10, 3.11 and 3.12 provide conclusive evidence that $\tau = t_{max}$. However, the sampling design in the neighborhood of τ and the magnitude of the experimental error of the data can make the estimation of τ not possible using the PBFTPK software developed. Interested readers can contact the authors in case they wish to use it.

Overall, the application of finite absorption time (FAT) concepts can open new avenues in the oral drug absorption research. Thus, the FAT concepts can be also applied to interspecies and pediatric scaling using the τ estimates for each one of the species or children/adults as a core parameter in the scaling exercise. Additionally, the application of PBFTPK software for the re-analysis of oral data can provide input rate estimate(s) ($FD/\tau V_d$), which will be certainly associated with the rate-controlling parameter(s) of absorption, solubility and/or permeability as explained in Sect. 3.2. The analysis of big oral data using machine learning techniques coupled with molecular descriptors can also elucidate critical factors of oral drug absorption phenomena. Besides, further applications of PBFTPK models to the following topics can be envisaged too: (i) the development of models based on multiple oral drug administration; (ii) the construction of percent absorbed versus time plots and use in in vitro-in vivo correlations (IVIVC) under the prism of the FAT concept; (iii) the extension/application of the modeling work to population studies; and (iv) coupling the PBFTPK modes with pharmacodynamic models. These applications (i–iv) can be also considered in the light of non-linear (Michaelis–Menten) kinetics. All above, if coupled with the implications of finite absorption time models on bioavailability/ bioequivalence issues [5, 25], point to a new era in the scientific and regulatory aspects of oral drug absorption. To this end, a Finite Absorption Time-Group (FAT-G) has been established for all those interested in the experimental and theoretical analysis of oral drug absorption phenomena using the FTA concepts, which can be contacted via the website http://www.athenarc.gr/.

References

1. Dost FH (1953) Der Blutspiegel. Kinetik der Konzentrationsabläufe in der Kreislaufflüssigkeit. Thieme, Leipzig
2. Bateman H (1910) Solution of a system of differential equations occurring in the theory of radioactive transformations. Proc Camb Philos Soc Math Phys Sci 15:423–427
3. Abuhelwa A, Foster D, Upton R (2016) A quantitative review and meta-models of the variability and factors affecting oral drug absorption-part II: gastrointestinal transit time. AAPS J 18:1322–1333. https://doi.org/10.1208/s12248-016-9953-7

4. Amidon GL, Lennernäs H, Shah VP, Crison JR (1995) A theoretical basis for a biopharmaceutic drug classification: the correlation of in vitro drug product dissolution and in vivo bioavailability. Pharm Res 12:413–420. https://doi.org/10.1023/a:1016212804288

5. Wu C, Benet L (2005) Predicting drug disposition via application of BCS: transport/absorption/ elimination interplay and development of a biopharmaceutics drug disposition classification system. Pharm Res 22:11–23. https://doi.org/10.1007/s11095-004-9004-4

6. Food and Drug Administration. Center for Drug Evaluation and Research (CDER) (2017) Waiver of in vivo bioavailability and bioequivalence studies for immediate-release solid oral dosage forms based on a biopharmaceutics classification system. Guidance for Industry U.-S. Department of Health and Human Services

7. European Medicines Agency (2017) Committee for medicinal products for human use (CHMP). Guideline on the investigation of bioequivalence. London

8. Charalabidis A, Sfouni M, Bergström C, Macheras P (2019) BCS and BDDCS: beyond guidelines. Int J Pharm 566:264–281. https://doi.org/10.1016/j.ijpharm.2019.05.041

9. Lin L, Wong H (2017) Predicting oral drug absorption: mini review on physiologically-based pharmacokinetic models. Pharmaceutics 9:41. https://doi.org/10.3390/pharmaceutics9040041

10. Chung J, Kesisoglou F (2018) Physiologically based oral absorption modelling to study gut-level drug interactions. J Pharm Sci 107:18–23. https://doi.org/10.1016/j.xphs.2017.08.015

11. Stillhart C, Pepin X, Tistaert C et al (2019) PBPK absorption modeling: establishing the in vitro-in vivo link-industry perspective. AAPS J 21:19. https://doi.org/10.1208/s12248-019-0292-3

12. Yu LX, Amidon GL (1999) A compartmental absorption and transit model for estimating oral drug absorption. Int J Pharm 186:119–125. https://doi.org/10.1016/s0378-5173(99)00147-7

13. Macheras P, Karalis V, Valsami G (2013) Keeping a critical eye on the science and the regulation of oral drug absorption: a review. J Pharm Sci 102:3018–3036. https://doi.org/10.1002/jps.23534

14. Rinaki E, Dokoumetzidis A, Valsami G, Macheras P (2004) Identification of biowaivers among class II drugs: theoretical justification and practical examples. Pharm Res 21:1567–1572. https://doi.org/10.1023/B:PHAM.0000041450.25106.c8

15. Macheras P, Karalis V (2014) A non-binary biopharmaceutical classification of drugs: the ΑΒΓ system. Int J Pharm 464:85–90. https://doi.org/10.1016/j.ijpharm.2014.01.022

16. Macheras P (2019) On an unphysical hypothesis of Bateman equation and its implications for pharmacokinetics. Pharm Res 36:94. https://doi.org/10.1007/s11095-019-2633-4

17. Macheras P, Tsekouras AA (2022) The Finite Absorption Time (FAT) concept en route to PBPK modeling and pharmacometrics. J Pharmacokinet Pharmacodyn 50:5. https://doi.org/10.1007/s10928-022-09832-w

18. Dokoumetzidis A, Macheras P (2006) A century of dissolution research: from Noyes and Whitney to the biopharmaceutics classification system. Int J Pharm 321:1–11. https://doi.org/10.1016/j.ijpharm.2006.07.011

19. Iranpour P, Lall C, Houshyar R, Helmy M, Yang A, Choi JI, Ward G, Goodwin SC (2016) Altered Doppler flow patterns in cirrhosis patients: an overview. Ultrasonography 35:3–12. https://doi.org/10.14366/usg.15020

20. Macheras P, Chryssafidis P (2020) Revising pharmacokinetics of oral drug absorption: I models based on biopharmaceutical/physiological and finite absorption time concepts. Pharm Res 37:187. https://doi.org/10.1007/s11095-020-02894-w. Erratum Pharm Res 37:206. https://doi.org/10.1007/s11095-020-02935-4

21. Vertzoni M, Augustijns P, Grimm M, Koziolek M, Lemmens G, Parrott N, Pentafragka C, Reppas C, Rubbens J, Van Den Abeele J, Vanuytsel T, Weitschies W, Wilson CG (2019) Impact of regional differences along the gastrointestinal tract of healthy adults on oral drug absorption: an UNGAP review. Eur J Pharm Sci 134:153–175. https://doi.org/10.1016/j.ejps.2019.04.013

22. Kararli T, Searle GD (1995) Comparison of the gastrointestinal anatomy, physiology, and biochemistry of humans and commonly used laboratory animals. Biopharm Drug Disp 16: 351–380. https://doi.org/10.1002/bdd.2510160502

23. Digenis GA, Sandefer EP, Parr AF, Beihn R, McClain C, Scheinthal BM, Ghebre-Sellassie I, Iyer U, Nesbitt RU, Randinitis E (1990) Gastrointestinal behavior of orally administered radiolabeled erythromycin pellets in man as determined by gamma scintigraphy. J Clin Pharmacol 30:621–631. https://doi.org/10.1002/j.1552-4604.1990.tb01865.x

24. Chryssafidis P, Tsekouras AA, Macheras P (2022) Re-writing oral pharmacokinetics using physiologically based finite time pharmacokinetic (PBFTPK) models. Pharm Res 39:691–701. https://doi.org/10.1007/s11095-022-03230-0

25. Atkinson HC, Stanescu I, Frampton C, Salem II, Beasleyr CPH, Robson R (2015) Pharmacokinetics and bioavailability of a fixed-dose combination of ibuprofen and paracetamol after intravenous and oral administration. Clin Drug Investig 35:625–632. https://doi.org/10.1007/s40261-015-0320-8

26. Jansat JM, Costa J, Salva P, Fernandez FJ, Martinez-Tobed A (2002) Absolute bioavailability, pharmacokinetics, and urinary excretion of the novel antimigraine agent almotriptan in healthy male volunteers. J Pharmacokinet Pharmacodyn 42:1303–1310. https://doi.org/10.1177/0091270002239359

27. Ismailos G, Reppas C, Dressman J, Macheras P (1991) Unusual solubility behaviour of cyclosporine A in aqueous media. J Pharm Pharmacol 43:287–289. https://doi.org/10.1111/j.2042-7158.1991.tb06688.x

28. Mueller EA, Kovarik JM, van Bree JB, Grevel J, Lucker PW, Kutz K (1994) Influence of a fat-rich meal on the pharmacokinetics of a new oral formulation of cyclosporine in a crossover comparison with the market formulation. Pharm Res 11:151–155. https://doi.org/10.1023/a:1018922517162

29. Van Andel L, Rosing H, Zhang Z, Hughes L, Kansra V, Sanghvi M, Tibben MM, Gebretensae A, Schellens JHM, Beijnen JH (2018) Determination of the absolute oral bioavailability of niraparib by simultaneous administration of a 14C-microtracer and therapeutic dose in cancer patients. Cancer Chemother Pharmacol 81:39–46. https://doi.org/10.1007/s00280-017-3455-x

30. Chryssafidis P, Tsekouras AA, Macheras P (2021) Revising pharmacokinetics of oral drug absorption: II bioavailability-bioequivalence considerations. Pharm Res 38:1345–1356. https://doi.org/10.1007/s11095-021-03078-w

31. Brown J, Chien C, Timmins P, Dennis A, Doll W, Sandefer E, Page R, Nettles RE, Zhu L, Grasela D (2013) Compartmental absorption modeling and site of absorption studies to determine feasibility of an extended-release formulation of an hiv-1 attachment inhibitor phosphate ester prodrug. J Pharm Sci 102:1742–1751. https://doi.org/10.1002/jps.23476

Chapter 4
Physiologically Based Finite Time Pharmacokinetic (PBFTPK) Models: Applications

Check for updates

Athanasios A. Tsekouras, Nikolaos Alimpertis, and Panos Macheras

Abstract The concept of finite absorption time is applied to a detailed discussion of generated models in bioavailability and bioequivalence. Considering detailed expressions for full and partial areas under the curve (AUCs), interesting conclusions are arrived at. Old digoxin pharmacokinetic data are reanalyzed under this prism. Physiologically based pharmacokinetic modeling and pharmacometrics are contrasted with the models derived from the Finite Absorption Time (FAT) concept and complicated concentration profiles successfully fit with these models.

Keywords Oral drug absorption · Finite absorption time · Pharmacokinetics · Bioavailability · Bioequivalence

4.1 The Finite Absorption Time (FAT) Concept as Columbus' Egg

The introduction of the finite absorption time (FAT) concept [1–5] has led to the development of the relevant physiologically based finite time (PBFTPK) models, which were successfully fitted to experimental data; reliable estimates for FAT and the other model parameters were derived. The FAT concept causes a paradigm shift in oral drug absorption. This is shown diagrammatically in a schematic for the underlying processes in the gastrointestinal (GI) membrane/vena cava (V.C.) region, which are supportive of the FAT concept (Fig. 4.1a). Furthermore, panels b, c, and d of Fig. 4.1 show the resulting variations of drug concentration in the blood.

A. A. Tsekouras
Department of Chemistry, National and Kapodistrian University of Athens, Athens, Greece

PharmaInformatics Unit, ATHENA Research Center, Athens, Greece

N. Alimpertis · P. Macheras (✉)
PharmaInformatics Unit, ATHENA Research Center, Athens, Greece

Faculty of Pharmacy, National and Kapodistrian University of Athens, Athens, Greece
e-mail: macheras@pharm.uoa.gr
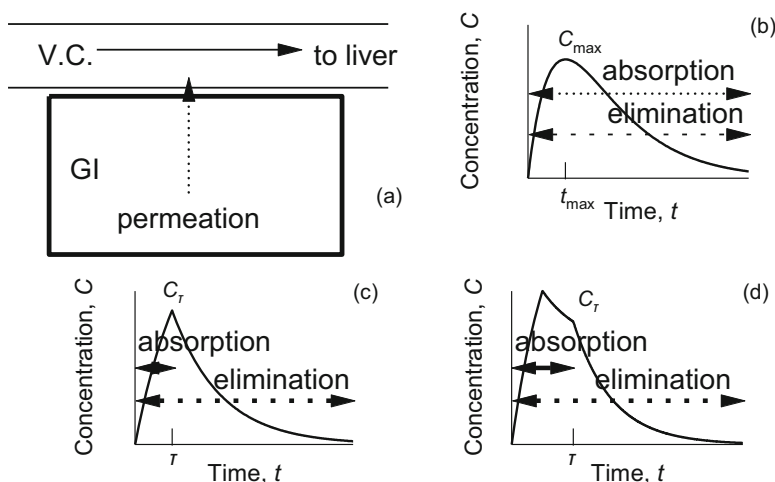
Fig. 4.1 A paradigm shift in oral drug absorption [6, 7]. (**a**) The passive transport of drug molecules (vertical arrow) from the GI tract to the blood in the vena cava (V.C.) always takes place under sink conditions, since the blood flow rate is very high, 20–40 cm/s [8] (horizontal arrow), resulting in the constant drug input rate to the liver. (**b**) According to the established view, drug absorption and elimination operate concurrently from zero time to infinity [9]. (**c, d**) According to the F.A.T. concept [1–5], drug absorption and elimination operate concurrently from zero to τ, while only elimination continues to operate until infinity. Two different profiles can be observed with (**c**) $t_{\max} = \tau$ and (**d**) $t_{\max} < \tau$. Such behavior has been observed in a number of drugs [5] including paracetamol, cyclosporine, and axitinib [10] formulations, respectively

We consider Fig. 4.1a as a "Columbus egg" since the underlying microscopic processes were not known at the beginning of pharmacokinetics [8], but they have been very well known for several decades now. However, it was only recently realized that the high blood flow (20–40 cm/s) in the vena cava ensures sink conditions for the drug transfer [5–7]. In fact, this blood flow rate is five orders of magnitude higher than the usual drug-effective permeability estimates $\sim 10^{-4}$ cm/s. Hence, the rate of presentation of drug to the liver is the product of this blood flow and the drug's concentration in blood, which changes linearly in accordance with its permeability expressed in velocity units (cm/s), Fig. 4.1a. Plausibly, this constant drug input entry to the liver terminates, when either the drug has been completely absorbed prior to its passage from the absorptive sites in the intestines or the dissolved and undissolved drug species pass beyond the absorptive sites; the latter, in the great majority of cases, are located in the small intestines. Accordingly, beyond time τ only drug elimination is operating, Fig. 4.1c, d.

All the work published so far on the FAT concept and PBFTPK models have focused on passively absorbed drugs. Here, we consider briefly the application of the FAT concept to drugs following the carrier-mediated transport assuming one-compartment model disposition, first-order elimination kinetics, and a single

input rate following Michaelis–Menten saturation kinetics operating for time τ. In such a case, it is not possible to arrive at an analytic expression for the drug concentration in the blood as a function of time, but the situation can be remedied with a numerical approach whose main disadvantage is that it is not as elegant, but equally valid. As expected, the general form of the resulting curve has the familiar form of a rising and a falling part, with the details depending on the duration of the input stage and the values of the model parameters, namely, the maximum transport velocity, the Michaelis constant for the drug transport, and the elimination rate constant.

4.2 Bioavailability/Bioequivalence Implications

The results of a recent study [5] provide conclusive evidence that in all experimental sets examined, drug absorption from the gastrointestinal tract takes place in finite time, τ. Accordingly, the corresponding area $[AUC]_0^\tau$ and not $[AUC]_0^\infty$ is the appropriate metric for a drug's extent of absorption. This has been theoretically explained on the basis of FAT. concept [3] and it was verified [4] using digoxin data from a bioavailability study carried out in 1973 [11] and a bioequivalence study analyzed by FDA [12], Fig. 4.2.

The termination of digoxin absorption in the former study was estimated to be at 1 and 3 h under fasting and fed conditions, respectively utilizing the PBFTPK models. Using the pertinent AUC ratios, i.e., $\frac{[AUC]_0^1 \text{fasted}}{[AUC]_0^3 \text{fed}}$ we found the same result (equal bioavailability) with the results derived from the cumulative five-day urinary excretion of digoxin [11]. Similarly, the duration of drug absorption in the 1992 bioequivalence study [12] under fasting and fed conditions was found to be 1 and 1.5 h, respectively; the corresponding ratios $\frac{[AUC]_0^1 \text{fasted, test}}{[AUC]_0^1 \text{fasted, reference}}$, $\frac{[AUC]_0^{1.5} \text{fed, test}}{[AUC]_0^{1.5} \text{fed, reference}}$ were quite similar to the classical comparison of AUCs calculated up to the very end of the sampling scheme (144 h) and infinity, namely, $[AUC]_0^{144}$ and $[AUC]_0^\infty$, reported in the FDA document [12].

The take-home message from these findings is that $[AUC]_0^\tau$ can replace $[AUC]_0^\infty$ in bioequivalence studies, as a more proper indicator of the extent of absorption, while $[AUC]_0^\infty$ can be maintained as an exposure metric. Several aspects of the current FDA [13] and EMA [14] guidelines concerning the sampling period of the study for a reliable estimation of $[AUC]_0^\infty$ are not in accord with the FAT concept; e.g., the sampling schedule required to be long enough to achieve $[AUC]_0^t$ covers at least 80% of $[AUC]_0^\infty$. Moreover, the recommended time limit of 72 h for the truncated AUC, namely, $[AUC]_0^{72}$, to be used as an alternative to $[AUC]_0^t$, is much longer than the physiological FAT limit of ~30 h [2, 15] for immediate release formulations.

A long time ago, an experimental study [16] and more recent simulation studies [17–19] focused on the use of truncated concentration-time curves for bioequivalence assessment; albeit the first-order character of gastrointestinal absorption was maintained, in all cases [17–19], the experimental and simulation results validated
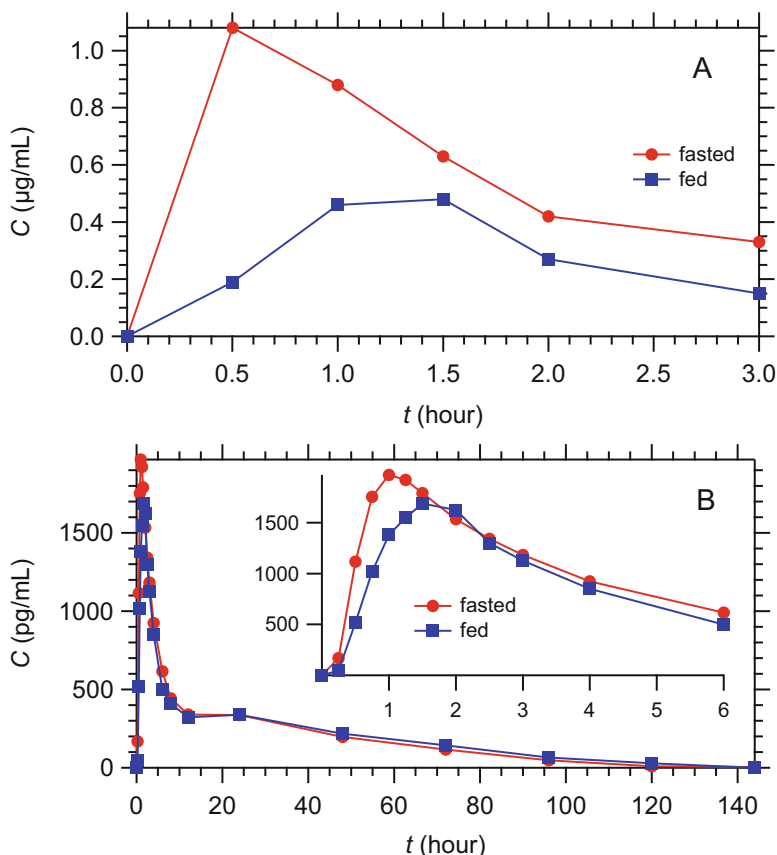
Fig. 4.2 Concentration-time data from a bioavailability study (**a**) [11] and a bioequivalence study (**b**) [12]. Inset in (**b**) shows an expanded view of the first 6 h of the data

the use of the truncated areas for bioequivalence assessment. In the same vein, our recent work [2–5] not only provides conclusive evidence that truncated concentration-time curves can be used reliably for bioequivalence assessment, but also the ideal metric is $[AUC]_0^\tau$ since time τ denotes the termination of drug's absorption.

4.3 Theoretical Background for Bioavailability and Bioequivalence

The development of bioavailability concepts and metrics both for the extent and rate of absorption was based on the parameters $[AUC]_0^\infty$, C_{max} and t_{max}, which are derived from Eq. 4.1 [3].

$$C(t) = \frac{FD k_a}{V_d(k_a - k_{el})} \left(e^{-k_{el} t} - e^{-k_a t} \right) \tag{4.1}$$

$$[AUC]_0^\infty = \frac{FD}{V_d k_{el}} = \frac{FD}{CL} \tag{4.2}$$

$$t_{max} = \frac{1}{k_a - k_{el}} \ln\left(\frac{k_a}{k_{el}} \right) \tag{4.3}$$

$$C_{max} = \frac{FD}{V_d} \left(\frac{k_a}{k_{el}} \right)^{-\left(\frac{k_{el}}{k_a - k_{el}} \right)} \tag{4.4}$$

where CL is the drug clearance. $[AUC]_0^\infty$ is the infinite integral of Eq. 4.1, t_{max} is calculated by equating the first derivative of Eq. 4.1 with zero, and C_{max} is evaluated from Eq. 4.1 by setting $t = t_{max}$.

(PBFTPK)$_0$ Models We utilize the index "zero" to indicate PBFTPK models [5] with the zero-order input lasting for time τ. For the one-compartment model, the following equation was used to describe the drug blood concentration for $t \leq \tau$ assuming the termination of absorption at time τ [7]:

$$C(t) = \frac{FD}{\tau} \frac{1}{V_d k_{el}} \left(1 - e^{-k_{el} t} \right) \quad t \leq \tau \tag{4.5}$$

while for $t > \tau$, Eq. 4.6 applies.

$$C(t) = C(\tau) e^{-k_{el}(t - \tau)} \quad t \leq \tau \tag{4.6}$$

The drug blood concentration $C_b(\tau)$ corresponding to time τ, for the one-compartment (PBFTPK)$_0$ model is derived from Eq. 4.5 using $t = \tau$:

$$C(\tau) = \frac{FD}{\tau} \frac{1}{V_d k_{el}} \left(1 - e^{-k_{el} \tau} \right) = \frac{FD}{\tau} \frac{1}{CL} \left(1 - e^{-k_{el} \tau} \right) \tag{4.7}$$

while the areas $[AUC]_0^\tau$ and $[AUC]_\tau^\infty$ are derived by integrating Eqs. 4.5 and 4.6, respectively:

$$[AUC]_0^\tau = \frac{FD}{\tau} \frac{1}{V_d k_{el}} \left(\tau - \frac{1 - e^{-k_{el}\tau}}{k_{el}} \right) = \frac{FD}{V_d k_{el}} \left(1 - \frac{1 - e^{-mln2}}{mln2} \right) =$$
$$= [AUC]_0^\infty \left(1 - \frac{1 - e^{-mln2}}{mln2} \right) \tag{4.8}$$

where m is the ratio ($m = \tau/t_{1/2}$) of τ over the half-life $t_{1/2}$ while $k_{el} = (\ln2)/t_{1/2}$.

$$[AUC]_\tau^\infty = \frac{C(\tau)}{k_{el}} = \frac{FD}{V_d k_{el}} \frac{1}{k_{el}\tau} \left(1 - e^{-k_{el}\tau} \right) = [AUC]_0^\infty \frac{1}{mln2} \left(1 - e^{-mln2} \right) \tag{4.9}$$

The sum of the two last integrals, Eqs. 4.8 and 4.9, gives $[AUC]_0^\infty$, Eq. 4.3.

A hypothetical curve corresponding to the same dose given as an intravenous bolus dose would follow the same track for $t \geq \tau$. Having the general form of

$$C_{iv}(t) = Ge^{-k_{el}t} \tag{4.10}$$

Requiring

$$C_{iv}(t) = C(t) \text{ for } t \geq \tau, \tag{4.11}$$

we get:

$$Ge^{-k_{el}t} = C(\tau)e^{-k_{el}(t-\tau)} = \frac{FD}{\tau} \frac{1}{V_d k_{el}} \left(1 - e^{-k_{el}\tau} \right) e^{-k_{el}(t-\tau)} \tag{4.12}$$

giving

$$G = \frac{FD}{\tau} \frac{1}{V_d k_{el}} \left(1 - e^{-k_{el}\tau} \right) e^{k_{el}\tau} = \frac{FD}{\tau} \frac{1}{V_d k_{el}} \left(e^{k_{el}\tau} - 1 \right) \tag{4.13}$$

Then, the hypothetical curve would give:

$$[AUC_{iv}]_0^\infty = \frac{G}{k_{el}} = \frac{FD}{V_d k_{el}} \frac{1}{k_{el}\tau} \left(e^{k_{el}\tau} - 1 \right) = [AUC]_0^\infty \frac{1}{k_{el}\tau} \left(e^{k_{el}\tau} - 1 \right) \tag{4.14}$$

Re-arranging the last equation, we get

$$F = \frac{[AUC]_0^\infty}{[AUC_{iv}]_0^\infty} = \frac{k_{el}\tau}{e^{k_{el}\tau} - 1} \tag{4.15}$$

where F is the fraction of dose absorbed since both oral and intravenous data rely on a single oral administration of dose to an individual. However, if the first-pass effect is not encountered then F in Eq. 4.9 denotes the bioavailable fraction.

Although more than one constant input rate may operate successively under in vivo conditions, this section focuses on the simplest case, i.e., the one-compartment model with constant input rate and first-order elimination. However, the concepts developed herein can be adapted to models with more than one input rate.

(PBFTPK)$_1$ Models We utilize the index "one" to indicate PBFTPK models [5] with the first-order input lasting for time τ. These models rely on Eqs. 4.1 and 4.6. Using

$$C(\tau) = \frac{FDk_a}{V_d(k_a - k_{el})} \left(e^{-k_{el}\tau} - e^{-k_a\tau} \right) \tag{4.16}$$

the areas $[AUC]_0^\tau$ and $[AUC]_\tau^\infty$ are derived by integrating Eqs. 4.1 and 4.7, respectively:

$$[AUC]_0^\tau = \frac{FD}{V_d k_{el}} - \frac{FDk_a}{V_d(k_a - k_{el})} \left(\frac{e^{-k_{el}\tau}}{k_{el}} - \frac{e^{-k_a\tau}}{k_a} \right) \tag{4.17}$$

$$[AUC]_\tau^\infty = \frac{C_b(\tau)}{k_{el}} = \frac{FDk_a}{V_d k_{el}(k_a - k_{el})} \left(e^{-k_{el}\tau} - e^{-k_a\tau} \right) \tag{4.18}$$

The sum of Eqs. 4.24 and 4.25 gives

$$[AUC]_0^\infty = \frac{FD}{V_d k_{el}} \left(1 - e^{-k_a\tau} \right) \tag{4.19}$$

The deviation of the latter quantity from the required value of $\frac{FD}{V_d k_{el}}$ is associated with the discrepancy between the physical assumption that the drug is not absorbed any more beyond time τ, and the mathematics of the first-order absorption process, which lasts until infinity. In fact, the term in parentheses of Eq. 4.19 is linked with the absorption characteristics, i.e., the absorption rate constant k_a and the duration of absorption τ. The impact of this term becomes smaller for high values of k_a and τ, Fig. 4.3; the term used in the ordinate of Fig. 4.3 allows a dimensionless plot.

A hypothetical curve corresponding to the same dose given as an intravenous bolus dose would follow the same track for $t \geq \tau$. Having the general form of

$$C_{iv}(t) = Ge^{-k_{el}t} \tag{4.20}$$

Requiring

$$C_{iv}(t) = C(t) \text{ for } t \geq \tau, \tag{4.21}$$

we get:
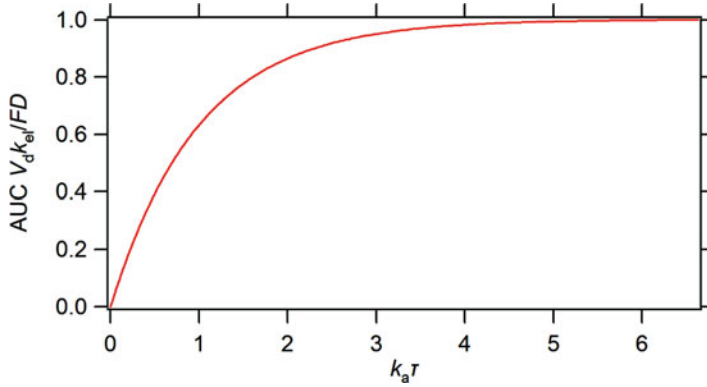
Fig. 4.3 Plot of $[AUC]_0^\infty k_{el} V_d / FD$ as a function of k_a and τ. (see Eq. 4.19)

$$\text{G}e^{-k_{el}t} = C(\tau)e^{-k_{el}(t-\tau)} = \frac{FDk_a}{V_d(k_a - k_{el})}\left(e^{-k_{el}\tau} - e^{-k_a\tau}\right)e^{-k_{el}(t-\tau)} \qquad (4.22)$$

giving

$$G = \frac{FDk_a}{V_d(k_a - k_{el})}\left(e^{-k_{el}\tau} - e^{-k_a\tau}\right)e^{k_{el}\tau} = \frac{FDk_a}{V_d(k_a - k_{el})}\left(1 - e^{-(k_a - k_{el})\tau}\right) \qquad (4.23)$$

Then, the curve for the hypothetical intravenous bolus administration of an equal dose would give:

$$[AUC_{iv}]_0^\infty = \frac{G}{k_{el}} = \frac{FDk_a}{V_d k_{el}(k_a - k_{el})}\left(1 - e^{-(k_a - k_{el})\tau}\right) \qquad (4.24)$$

Using Eqs. 4.19 and 4.24 one can find

$$F = \frac{[AUC]_0^\infty}{[AUC_{iv}]_0^\infty} = \left(1 - \frac{k_{el}}{k_a}\right)\frac{1 - e^{-k_a\tau}}{1 - e^{-(k_a - k_{el})\tau}} \qquad (4.25)$$

where F is the fraction of dose absorbed since both oral and intravenous data rely on a single oral dose administration to an individual. However, if the first-pass effect is not encountered, then F in Eq. 4.25 denotes the bioavailable fraction. The limit of Eq. 4.25 for $\tau = 0$ (intravenous bolus dose) correctly predicts F tends to 1 as k_a tends to a very large number. The visual inspection of Eq. 4.25, reveals that F is fully dependent on the values of the rate constants k_a, k_{el} and τ. Hence, an estimate for F can be obtained, based on the estimates of these parameters derived from the oral experimental data of oral administration.

4.4 Model Implementations

In the last 20 years or so, biopharmaceutical scientists gradually unveiled the complex nature of gastrointestinal drug absorption phenomena, e.g., drug solubilization, supersaturation, drug dissolution, drug precipitation, the interplay of food with the various processes, (selective) permeability, and drug ionization changes along the gastrointestinal lumen affecting all above processes. In our days, all these phenomena are interpreted (modeled) with the use of the PBPK (physiologically based pharmacokinetic) models [19–21]. Undoubtedly, a single value of the absorption rate constant cannot capture the complex dynamics of the absorption phase phenomena taking place concurrently. It is worthy to mention that drug absorption is assessed in the PBPK studies using the permeability estimate expressed in the constant velocity units (length/time), i.e., "a zero-order type parameter". Likewise, drug absorption in the $(PBFTPK)_0$ models [5] is also expressed in constant mass/time units. For both $(PBFTPK)_0$ and $(PBFTPK)_1$ models, the duration of the absorption process, τ is a pivotal element. Similarly, the user/modeler of the software packages (GastroPlus® Software, n.d.; Simcyp® Simulator, n.d.; PK-Sim® Software, n.d.) of the PBPK [19–21] models fix a finite-time absorption period, e.g., 199 min [22, 23] or transit times for each anatomical segment are specified [19–21]. In some cases, when PBPK models are coupled with a pharmacokinetic model, the fraction of dose absorbed is related proportionally to drug concentration in the gastrointestinal lumen since "the blood on the basolateral side of the membrane is regarded as an ideal sink". Overall, the fixed time duration of the absorption processes and the deviations from the classical first-order absorption have been adopted in the PBPK models [19–21].

(PBFTPK)₀ and (PBFTPK)₁ Models: A Pictorial Comparison Using Simulations Figures in the previous chapter show $(PBFTPK)_0$ model simulations; $(PBFTPK)_1$ models simulations as well as curves generated from the classical Bateman equation (Eq. 4.1) without time restrictions for comparative purposes are shown in Fig. 4.4.

Three examples with various finite time absorption durations deviating from the classical first-order absorption (top curve in all graphs of Fig. 4.4) are shown using three different values of the absorption rate constant k_a, namely, 0.1 h^{-1} (Fig. 4.4a), 0.25 h^{-1} (Fig. 4.4b), and 0.5 h^{-1} (Fig. 4.4c). The curves corresponding to the lower value of the absorption rate constant 0.1 h^{-1} depicted in Fig. 4.4a clearly indicate that the smaller is the duration of the absorption time, the larger is the difference in the concentration-time profiles compared to the classical top curve. The examples shown in Fig. 4.4b, c using higher values for the absorption rate constant, 0.25 and 0.5 h^{-1}, respectively, demonstrate that the concentration-time profiles become progressively indistinguishable from the classical case (top curve) as the values of the duration of drug absorption, τ and the absorption rate constant k_a are increasing. These observations are in full agreement with Eq. 4.18 and the relevant plot of Fig. 4.3. It is worthy to mention that the classical top curve of Fig. 4.4a exhibits appreciable drug absorption of drug beyond the physiological limit of 30 h [2, 15]
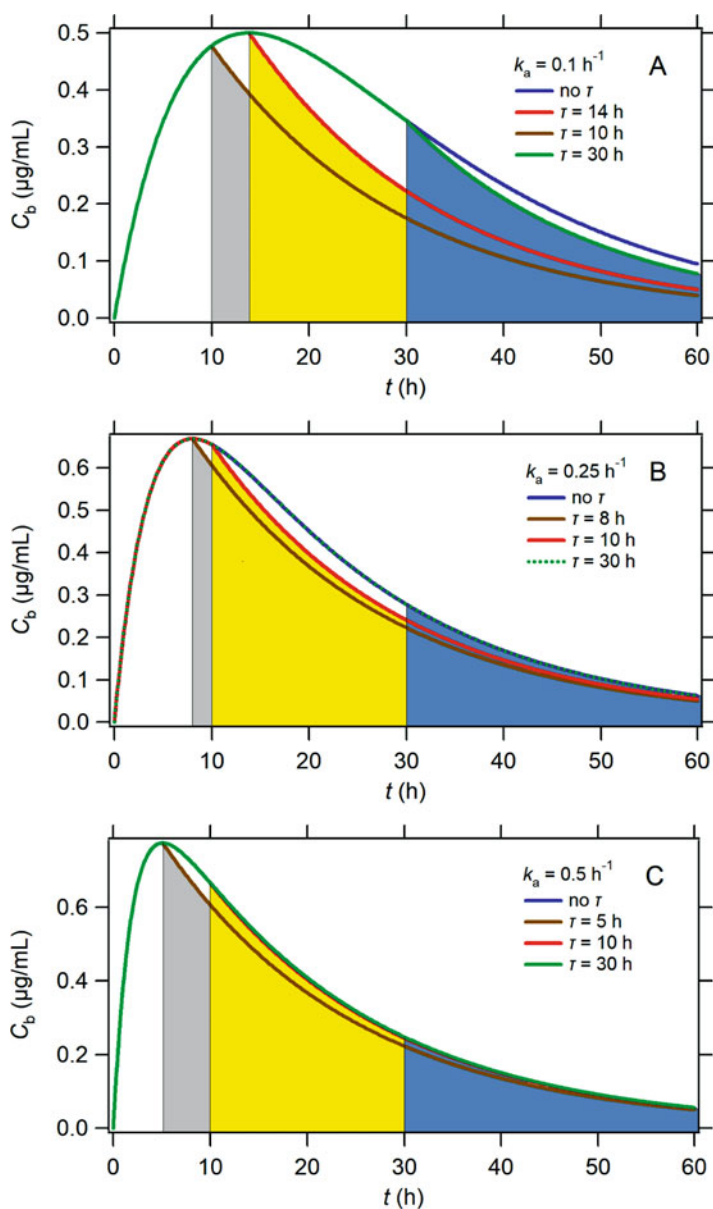
Fig. 4.4 Truncated Bateman drug concentration profiles with (**a**) $k_a = 0.1 \text{ h}^{-1}$, $k_{el} = 0.05 \text{ h}^{-1}$ and termination times 10 h (gray), 14 h (yellow), and 30 h (blue); (**b**) $k_a = 0.25 \text{ h}^{-1}$, $k_{el} = 0.05 \text{ h}^{-1}$ and termination times 8 h (gray), 10 h (yellow), and 30 h (blue); (**c**): $k_a = 0.5 \text{ h}^{-1}$, $k_{el} = 0.05 \text{ h}^{-1}$ and termination times 5 h (gray), 10 h (yellow), and 30 h (blue)

using the frequently encountered values for absorption and elimination rate constants, 0.1 and 0.05 h^{-1}, respectively. Accordingly, the concern is rising for significant drug absorption beyond the absorptive sites [4]. According to Eq. 4.19, the ratio of the area under the curve for τ values 14 and 30 h compared to the area of the top curve in Fig. 4.4a is 75 and 95%, respectively, indicating that a misinterpretation for an infinite absorption is quite possible.

The simulated examples of Fig. 4.4 demonstrate the rich dynamic behaviors associated with the $(PBFTPK)_1$ models. Most importantly, Fig. 4.4 shows that the relative magnitude of the parameters C_{max}, t_{max} *vis-a-vis* $C(\tau)$, and τ can vary remarkably according to the specific case examined. In all cases, however, the concentration of drugs starts to decline monotonically beyond the datum point $(C(\tau), \tau)$, i.e., drug absorption is not taking place beyond time τ.

Intuitively, one can conclude that the shorter the absorption time duration τ is, the higher is the resemblance of the concentration-time profiles generated from the $(PBFTPK)_0$, $(PBFTPK)_1$ models and the classical Bateman function (Eq. 4.1). This is so since all curves approximate the limiting case, i.e., the intravenous bolus administration in the one-compartment model.

Rate Metrics: (C_{max}, t_{max}) vis a vis $(C(\tau), \tau)$ The use of C_{max} as a measure of the rate of absorption is historically associated with its derivation from Eq. 4.1 as a steady-state value. Although it is used as a bioavailability rate parameter, Eq. 4.4 reveals that C_{max} is also dependent on the extent of absorption. During the previous decades, concerns on this problem were raised and several alternative metrics and methodologies have been suggested [24–28]. However, C_{max} is always being used as a rate parameter in all bioequivalence guidelines, but mainly its numerical value provides the maximum concentration of the drug in the blood.

According to Eq. 4.7 of $(PBFTPK)_0$ models, $C(\tau)$ is proportional to the rate of input FD/τ. This is an ideal property for the rate of input parameter; besides, time τ underlines the termination of the absorption process, which is the fundamental characteristic of the $(PBFTPK)_0$ models. Although C_{max} and $C(\tau)$ differ conceptually, in actual practice, the two quantities may or may not be identical since $C_{max} \geq C(\tau)$. When $C_{max} = C(\tau)$, one can easily derive from the $(PBFTPK)_0$ models [2]

$$\text{Rate in} = \frac{V_d C}{dt} = \frac{FD}{\tau} - k_{el}CV_d = 0 \tag{4.26}$$

$$C(\tau) = C_{max} = \frac{FD}{\tau k_{el} V_d} = \frac{FD}{\tau CL} \tag{4.27}$$

This equality means that the absorption of drugs has been terminated or completed at time τ while C_{max} or $C(\tau)$ are proportional to the input rate (FD/τ) as well as to the extent of absorption (FD), Eq. 4.27. However, C_{max} or $C(\tau)$ is not the asymptotic limit of a zero-order absorption process with first-order elimination usually found as a steady-state solution in continuous intravenous infusion. In other words, the $(C(\tau),\tau)$ datum point is a discontinuity point associated with

(i) the completion of the input process (no more drug is available for absorption) or (ii) a sudden change in drug's solubility, e.g., precipitation or (iii) drug's permeability change, e.g., reduced regional permeability because of pH changes or (iv) drug's transit beyond the absorptive sites.

The termination of absorption at time τ in the (PBFTPK)$_1$ models may result from the completion of drug absorption or the passage of drug beyond the absorptive sites. The corresponding value of $C(\tau)$ (Eq. 4.7), is always equal to or smaller than the experimental C_{max}, Fig. 4.4. However, the experimental values for $C(\tau)$ and τ of (PBFTPK)$_1$ models are not steady-state values, namely, C_{max} (Eq. 4.4) and t_{max} (Eq. 4.3), respectively; the pair $(C(\tau), \tau)$ represents a discontinuity time point.

Exposure Metrics: $[AUC]_0^\infty$ ***Versus*** $[AUC]_0^\tau$ ***and*** $[AUC]_\tau^\infty$ The golden standard for the extent of absorption, without any doubt, in bioavailability-bioequivalence studies is $[AUC]_0^\infty$, Eq. 4.2. This is also justified here for the (PBFTPK)$_0$ models since the sum of Eqs. 4.8 and 4.9, adhering to the (PBFTPK)$_0$ model principles, is equal to $[AUC]_0^\infty$, Eq. 4.2. Although Eq. 4.8 reveals that $[AUC]_0^\tau$ is a fraction of $[AUC]_0^\infty$, its magnitude is solely determined from the quantity m, namely, the ratio of duration of the absorption process τ over the elimination half-life, $(m = \tau/t_{1/2})$. Therefore, the meaning of $[AUC]_0^\tau$ for the (PBFTPK)$_0$ models is not in accord with the usual concept of partial areas used as indicators for the initial rate of exposure [25–27]. Besides, $[AUC]_0^\tau$ for the (PBFTPK)$_1$ models is dependent on τ (Eq. 4.17), while $[AUC]_0^\infty$ (Eq. 4.19) is also dependent on τ. Hence, for both (PBFTPK)$_0$ and (PBFTPK)$_1$ models, the usual role of partial areas (portions of $[AUC]_0^\tau$) is not applicable due to the involvement of τ in the calculations.

According to Eq. 4.9, $[AUC]_\tau^\infty$ is proportional to the fraction of dose absorbed, which is in the general circulation at time τ [12]. This proportionality is valuable for bioequivalence studies when the duration of the absorption process is short or very short and the absorption phase data exhibit high variability; this is the case with inhalers [29–31] and nasal products [32]. For these formulations, the test-reference comparison can be based on the area $[AUC]_\tau^\infty$ which is proportional to the fraction of dose absorbed being in the general circulation at time τ. Table 4.1 shows the results based on the analysis of $[AUC]_\tau^\infty$ for the test and reference formulations of three bioequivalence studies [29–31]. All ratios for the five drugs studied $\left([AUC]_\tau^{72}\right)_{test}$ / $\left([AUC]_\tau^{72}\right)_{reference}$ lie in the range 0.828–1.104. Although the 90% confidence intervals for the means were not constructed, these values lie in the range of 80–125% used in bioequivalence testing. Besides, the ratios $[AUC]_\tau^{72}/[AUC]_0^{72}$ for all drugs and formulations studied are in the range 0.858–0.999, Table 4.1, which indicates that the area $[AUC]_\tau^{72}$ represents a very large portion (>80%) of the total area $[AUC]_0^\infty$. Since the variability of the experimental data in the ascending limb of the curve of the inhaled products is very high [29–31], while a dense sampling strategy is usually applied, the use of $[AUC]_\tau^{72}$ as an extent of absorption metric can lead to a smaller number of volunteers and a less dense sampling protocol in

Table 4.1 The ratio of $[AUC]_T^{72}$ of the test over the reference formulation of five pulmonary drugs and one oral drug in bioequivalence studies

PK parameters	Salmeterol [31]	Fluticasone [29]	Budesonide [30]	Formoterol [30]	Salmeterol [29]	Digoxin [12]
$\dfrac{\left([AUC]_T^{72}\right)_{test}}{\left([AUC]_T^{72}\right)_{reference}}$	1.012	1.104	0.828	0.935	1.074	1.006
$\dfrac{\left([AUC]_T^{72}\right)_{reference}}{\left([AUC]_0^{72}\right)_{reference}}$	0.987	0.858	0.977	0.994	0.935	0.958
$\dfrac{\left([AUC]_T^{72}\right)_{test}}{\left([AUC]_0^{72}\right)_{test}}$	0.986	0.920	0.946	0.985	0.999	0.957

Table 4.2 The ratio of $[AUC]_\tau^{14}$ of the test over the reference formulation in a nasal absorption bioequivalence study of budesonide [33] and $[AUC]_\tau^3$ or $[AUC]_\tau^4$ ratios (powder vs. solution) in a comparative systemic bioavailability study [34] of three nasal remimazolam (RMZ) formulations

PK parameters	Budesonide	PK parameters	RMZ (10 mg)	PK parameters	RMZ (20 mg)	RMZ (40 mg)
$\dfrac{\left([AUC]_\tau^{14}\right)_{test}}{\left([AUC]_\tau^{14}\right)_{reference}}$	1.024	$\dfrac{\left([AUC]_\tau^{3}\right)_{powder}}{\left([AUC]_\tau^{3}\right)_{solution}}$	1.226	$\dfrac{\left([AUC]_\tau^{4}\right)_{powder}}{\left([AUC]_\tau^{4}\right)_{solution}}$	1.422	2.118
$\dfrac{\left([AUC]_\tau^{14}\right)_{reference}}{\left([AUC]_0^{14}\right)_{reference}}$	0.942	$\dfrac{\left([AUC]_\tau^{3}\right)_{solution}}{\left([AUC]_0^{3}\right)_{solution}}$	0.831	$\dfrac{\left([AUC]_\tau^{4}\right)_{solution}}{\left([AUC]_0^{4}\right)_{solution}}$	0.854	0.858
$\dfrac{\left([AUC]_\tau^{14}\right)_{test}}{\left([AUC]_0^{14}\right)_{test}}$	0.944	$\dfrac{\left([AUC]_\tau^{3}\right)_{powder}}{\left([AUC]_0^{3}\right)_{powder}}$	0.893	$\dfrac{\left([AUC]_\tau^{4}\right)_{powder}}{\left([AUC]_0^{4}\right)_{powder}}$	0.858	0.904

Table 4.3 The meaning of the classical and novel bioequivalence parameters in the light of $(PBFTPK)_0$ and $(PBFTPK)_1$ models

Parameters	Remarks
$C_{max}, C(\tau)$	When $t_{max} = \tau$, C_{max} is equal to $C(\tau)$; it corresponds to the blood concentration at the termination or completion of drug absorption at time τ. When $t_{max} < \tau$, then $C_{max} > C(\tau)$; C_{max} does not correspond to the termination or completion of drug absorption at time τ.
$t_{max}, \tau\alpha$	When $t_{max} = \tau$, the recorded t_{max} corresponds to the termination or completion of drug absorption at time τ. When $t_{max} < \tau$, the numerical value of τ is the physiologically meaningful parameter, since it denotes the duration of the absorption process.
Partial areas (portions of $[AUC]_0^\tau$)	For the $(PBFTPK)_0$ models, the magnitude of the areas (portions of $[AUC]_0^\tau$) depends exclusively on m, ($m = \tau/t_{1/2}$); therefore, these portions cannot be used as early absorption rate indicators. For the $(PBFTPK)_1$ models, the magnitude of the areas (portions of $[AUC]_0^\tau$) and the total area ($[AUC]_0^\infty$) are both dependent on τ; therefore these portions are not typical indicators of the early absorption rate.
$[AUC]_\tau^\infty$	Proportional to the fraction of the dose absorbed and remaining in the body at time τ. It could be used instead of $[AUC]_0^\infty$ when very fast absorption is encountered.

bioequivalence studies. Data on oral absorption of digoxin [12], which also exhibit fast absorption assuming $t_{max} = \tau$, were analyzed in the same way and included in Table 4.1. Additional relevant data from two nasal absorption studies were analyzed assuming $t_{max} = \tau$ and are presented in Table 4.2.

Scientific-Regulatory Implications In the light of $(PBFTPK)_0$ and $(PBFTPK)_1$ models, a re-consideration of the meaning and use of the typical bioequivalence parameters were analyzed and presented (C_{max}, t_{max} and partial areas), which is required. This is summarized in Table 4.3 along with the meaning and potential use of the novel parameters $C(\tau)$, τ, $[AUC]_\tau^\infty$. Undoubtedly, the duration of absorption τ plays a pivotal role in all novel parameters of both $(PBFTPK)_0$ and $(PBFTPK)_1$ models. Its use should follow the physiological time constraints for intestinal and colon absorption [7].
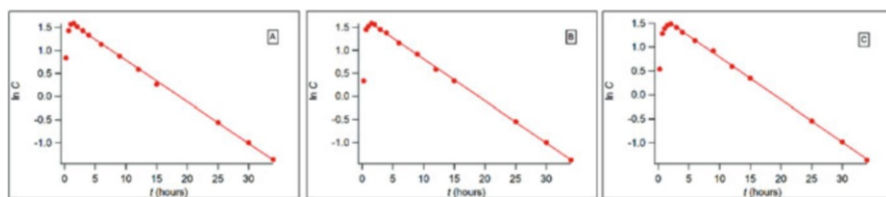
Fig. 4.5 Semi-logarithmic concentration-time plots of theophylline formulations A, B, and C [35]

The remarks quoted in Table 4.3 can guide regulatory agencies for potential changes in the assessment of bioequivalence studies. The utilization of the parameters τ and $[AUC]_\tau^\infty$ as well as the re-consideration of the partial area utility as a rate of exposure metric are the most challenging questions. In addition, the two recommendations of the current bioequivalence guidelines [9, 10], namely, (i) "The sampling schedule should also cover the plasma concentration-time curve long enough to provide a reliable estimate of the extent of exposure, which is achieved if $[AUC]_0^t$ covers at least 80% of $[AUC]_0^\infty$" and (ii) the specific time limit of 72 h, for the calculation of total AUC, i.e., "AUC truncated at 72 h ($[AUC]_0^{72}$) may be used as an alternative to $[AUC]_0^t$ for the comparison of extent of exposure as the absorption phase has been covered by 72 h for immediate release formulations", should be re-considered in view of the results of the present study. This is so since drug absorption beyond 30 hours is not physiologically sound [7, 31]. However, long half-life drugs may require extensive sampling design because of the very slow disposition characteristics. Overall, this first analysis and the above-mentioned remarks will certainly need further investigation and may eventually lead to regulatory implications.

Towards the Unthinkable: Application of Eqs. 4.15 and 4.25 for the Estimation of Absolute Bioavailability from Oral Data Exclusively In this section, we analyzed published data from a bioequivalence study with three formulations of theophylline [35]. We first analyzed the entire set of elimination phase data using a semi-logarithmic plot, Fig. 4.5. All plots are linear and the regression coefficients, R^2 found were 0.9995, 0.9997, and 0.9998 for formulations A, B, and C, respectively. This verifies that the entire set of elimination phase data follows one-compartment model disposition. Then, an unrestricted non-linear least squares fit of the $(PBFTPK)_0$ model (Eqs. 4.5 and 4.6), $(PBFTPK)_1$ model (Eqs. 4.1 and 4.6), and Bateman equation (Eq. 4.1 without time restriction) was applied, Fig. 4.6. The parameter estimates are listed in Table 4.4 along with the calculated F values derived from Eqs. 4.15 and 4.25 adhering to the $(PBFTPK)_0$ and $(PBFTPK)_1$ models, respectively.

Excellent fits were observed for all data sets, Table 4.4. There is a minor superiority of the Bateman function and the $(PBFTPK)_1$ model over the $(PBFTPK)_0$ model, which is associated with the usually more erratic absorption phase whereas one or two data points deviate slightly from the $(PBFTPK)_0$ model fitting. However, Eq. 4.15 provides for F a single estimate, 0.97 for all formulations studied, while the
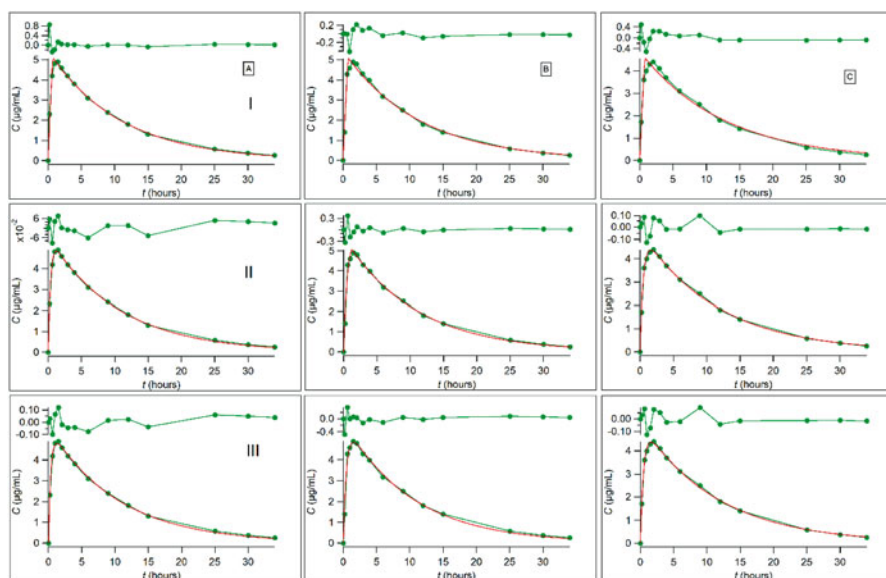
Fig. 4.6 Analysis of concentration-time data of theophylline formulations A, B, and C using the (PBFTPK)$_0$ model (Eqs. 4.5 and 4.6) (I), (PBFTPK)$_1$ model (Eqs. 4.1 and 4.6) (II), and Bateman equation (III). Shown are the experimental data [35], model fit curves and residuals

estimates for F based on Eq. 4.27 are 1.04 for formulations A and B and 1.45 for formulation C. The latter numerical value originates from the poor estimate for τ, 2.93 (3.04) h derived from the (PBFTPK)$_1$ model fitting. It is very well known that estimates for F cannot be derived from the fitting of the Bateman function to oral data. Nevertheless, all three approaches demonstrate that theophylline absorption has terminated in the small intestine; however, the (PBFTPK)$_0$ and (PBFTPK)$_1$ model fittings clearly show *the complete absorption of theophylline in the small intestines from the three formulations studied.* Needless to say that no clear advantage of the (PBFTPK)$_0$ and (PBFTPK)$_1$ models over the classical Bateman equation in terms of the modeling exercise could be concluded. This is so since the infinite time implied in the use of the first-order input, everyone knows, never happens in the real world. The absorption process is almost completed after ca. 3 absorption half-lives. The remaining ca. 10% left to be absorbed is either not detectable or confounded by the experimental error. In practice, however, the use of the finite absorption time limit in the (PBFTPK)$_0$ and (PBFTPK)$_1$ models allowed the estimation of F. This cannot be accomplished using the classical approach. The estimates for F derived in Table 4.4 are in full agreement with the reported value for F, 0.96 ± 0.03 for the immediate release of theophylline tablets [36].

Table 4.4 Parameter estimates (1 σ) derived from the fittings of (PBFTPK)$_0$ model (Eqs. 4.5 and 4.6), (PBFTPK)$_1$ model (Eqs. 4.1 and 4.6), and Bateman equation (Eq. 4.1 without time restriction) to experimental data [35], correlation coefficients for the fits and calculated bioavailable fraction F; the estimates for F designated F_{areas} are derived from Eq. 4.29

Model	Formulation	FD/V_d (μg/mL)	k_a (h^{-1})	k_{el} (h^{-1})	τ (h)	R^2	F	F_{areas}
(PBFTPK)$_0$	A	5.29 (0.17)	–	0.092 (0.008)	0.72 (0.05)	0.990	0.967	0.960
	B	5.28 (0.09)	–	0.088 (0.004)	0.75 (0.03)	0.997	0.967	0.962
	C	4.73 (0.14)	–	0.079 (0.006)	0.76 (0.05)	0.989	0.970	0.959
(PBFTPK)$_1$	A	5.47 (0.09)	2.703 (0.122)	0.094 (0.002)	1.49 (0.30)	0.9997	1.043	–
	B	6.35 (0.66)	1.626 (0.329)	0.093 (0.005)	1.21 (0.18)	0.997	1.036	–
	C	5.03 (0.05)	2.062 (0.085)	0.087 (0.002)	2.93 (3.04)	0.9993	1.451	–
Bateman	A	5.42 (0.05)	2.776 (0.089)	0.096 (0.002)	–	0.9995	–	–
	B	5.63 (0.15)	2.072 (0.180)	0.098 (0.006)	–	0.996	–	–
	C	5.04 (0.05)	2.060 (0.069)	0.087 (0.002)	–	0.9993	–	–

Estimation of **F** ***From Oral Data Exclusively Using a Ratio of Areas Under***
The Curve For drugs obeying one-compartment model disposition following any
type of input kinetics lasting τ time units, an estimate for F can be also derived from
the areas proportionality corrected in terms of dose:

$$F = \frac{[(AUC)]^{\infty}_{0\ \text{oral}}Dose}{[(AUC)^{\infty}_0]_{hy.i.v}\text{FDose}} \tag{4.28}$$

where $[(AUC)^{\infty}_0]_{hy.i.v}$, (Fig. 4.8), corresponds to the area of the hypothetical intra-
venous bolus administration of the same dose derived from the back extrapolation of
the elimination phase experimental data beyond time τ of the oral dose. Its numerical
value is calculated from the ratio $e^{(y\ -\ \text{intercept})}/k_{\text{el}}$, where the y-intercept on the *lnC*
axis corresponds to the back extrapolated regression line with slope $-k_{\text{el}}$ of *lnC, t*
elimination phase data beyond time τ. The integral $[(AUC)]^{\infty}_{0\ \text{oral}}$ is calculated using
the trapezoidal rule from the experimental data, Fig. 4.8. Solving Eq. 4.29 in terms of
F,

$$F^2 = \frac{[(AUC)]^{\infty}_{0\ \text{oral}}}{[(AUC)^{\infty}_0]_{hy.i.v}} \tag{4.29}$$

The positive root of Eq. 4.29 provides the estimate for F. Eq. 4.29 was used for
the estimation of F of theophylline formulations, Table 4.4. The results show that
very similar estimates were derived using the two methodologies, i.e., Eq. 4.15 or
4.25 and Eq. 4.29. Figure 4.7a shows the graphical analysis of a theophylline
formulation. Besides, very similar results (not shown) were obtained using the
experimental t_{max} values of theophylline formulations instead of τ estimates. In
this context, we analyzed the concentration plasma data of BMS-626529 drug [37]
assuming $\tau = t_{\text{max}}$ and found $F = 0.904$, Fig 4.7b.
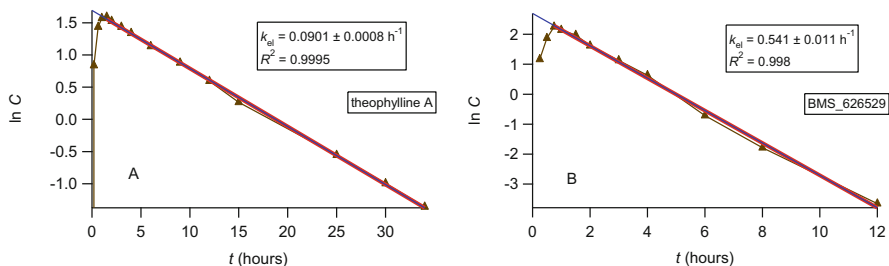
Fig. 4.7 Semi-logarithmic plot of theophylline (**a**) from formulation A and BMS-626529 (**b**)
plasma data. For both drugs, the "triangle" represents the $[(AUC)^{\infty}_0]_{hy.i.v}$ semi-logarithmically
while the $[(AUC)]^{\infty}_{0\ \text{oral}}$ corresponds to the area under the curve of the experimental data points,
depicted semi-logarithmically too

4.5 PBPK Modeling and Pharmacometrics with Finite-Absorption Time

PBPK Versus PBFTPK models Since the PBFTPK models are "top-down", while the currently used Physiologically-Based Pharmacokinetics (PBPK) models are "bottom-up" models, their application to the same dataset will enhance our understanding of drug absorption phenomena. The first such application [38] using six Merck drugs revealed correlations between the simulated luminal drug concentrations from the PBPK model with the absorption rate estimates derived from the PBFTPK models using the same datasets. This finding is fundamental and in accord with the basic biopharmaceutical-physiological principles of PBFTPK models. In addition, both models resulted in absorption time estimates within the small intestinal transit time, with PBFTPK models generally providing shorter time estimates. This should be attributed to the Gastro Plus software used for the estimation of drug absorbed over time curve, i.e., the simulation of absorption with differential equations based on indefinite integral and not finite integral with a time limit was used. It should be noted here that this "first-order approach" contradicts the quantification of the uptake rate in the PBPK models on the basis of permeability estimates.

The combinatory applications of PBPK/PBFTPK modes for studies involving modified release formulations are anticipated. The PBFTPK models can provide an estimate for the "prolonged" duration of drug absorption as well as drug's input rate (s), i.e., the two principal components of drug absorption from modified release formulations. Other potential applications of PBFTPK models can be envisaged in interspecies or pediatric pharmacokinetic scaling studies, which focus on bioavailability.

Pharmacometrics Since the early days of NONMEM (Non-Linear Mixed Effect Modeling) software, population approaches have been applied extensively in numerous oral, pulmonary, and intranasal PK, PD, and PK-PD studies, all of which involve absorption step(s). These studies have interpreted drugs' kinetics-dynamics as well as the variability associated with the parameters on the basis of what we call "a valid population model". However, this vast literature relies on structural models, which are invariably mostly using either one- or two-compartment disposition model "*with a first-order absorption rate constant, k_a*" governing the absorption process. In fact, citations for "the absorption rate constant" as a function of time in PUBMED from the beginning of its use circa 1964, both in the pre-NONMEM and the meta-NONMEM era, are over 7000. The increase after 2005 is most likely associated with the explosion of pharmacometric studies and the development of PBPK, pharmacometric software packages close to the turn of the century. It is widely understood that these commonly utilized models of drug absorption in population pharmacokinetics, with and without lag time or with transit compartments, often estimate large variabilities associated with the absorption rate constant, k_a, which are unrealistic. In this context, it is not uncommon to see "impossible" k_a estimates

submitted to and accepted by Drug Agencies since physically/physiologically sound alternatives do not exist.

However, one can also see pharmacometricians replacing the models with the first-order rate constant assuming complex absorption kinetics [39]. Common examples are mixed first-order and zero-order absorptions, either sequentially or simultaneously, and fast and slow parallel first-order absorptions, e.g., [40, 41]. Although these models provide better fits in comparison with their single first-order absorption counterparts, the physical/physiological meaning of the first-order parameters does not comply with the passive or active drug transport operating for time τ in accord with the finite absorption time concept.

In this vein, we analyzed [42], using PBFTPK models, nine sets of PK data from a mavoglurant population study [43] whose complex absorption processes have been modeled with a sum of two or three inverse Gaussian functions. PBFTPK models with one, two, three, or four constant successive input rates and two-compartment model disposition were used. Figure 4.8 presents the successful fitting results of the PBFTPK models to four out of nine sets of data in three subjects.

Figure 4.8 shows that mavoglurant absorption from the immediate release formulation exhibits one, three, and four absorption phases for subjects S16, S18, and S38 respectively. The absorption of mavoglurant from the modified-release
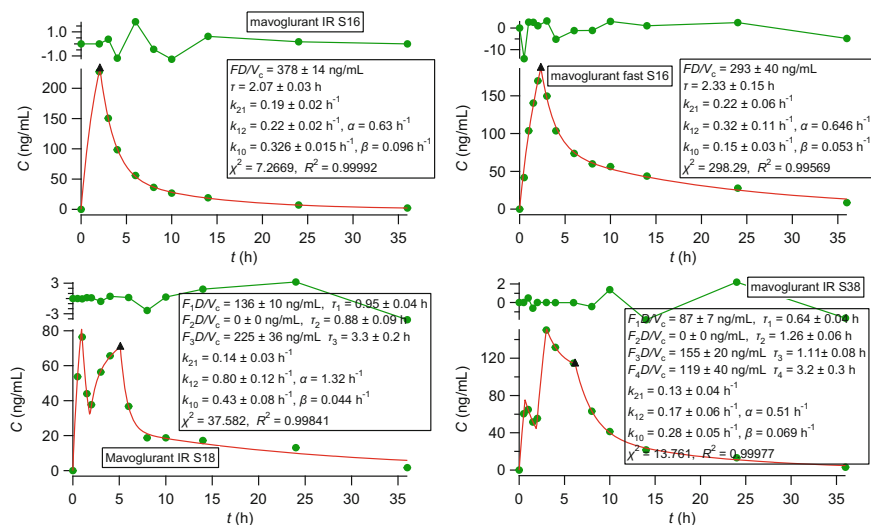
Fig. 4.8 Fitting results of a PBFTPK model with one (top panels) or three (bottom left panel) or four (bottom right panel) constant input rates of a specific time total duration, τ and two-compartment model disposition to four sets of mavoglurant data [43]. Parameter estimates for τ, the concentration factor FD/V_c and the compartmental constants are shown in each inset. Upper left and bottom panels: Immediate-release (IR) formulation administered to subjects S16, S18, and S38 [43]. Top right panel: oral administration of modified release formulation to fasted subject S16. The solid triangles denote the end of the absorption process. The upper portion of each graph shows the fit residuals

formulation administered to the fasted subject S16 has one single phase of absorption, i.e., it is quite similar to the absorption profile with the immediate release formulation in the same subject. Based on the total time of drug duration quoted in Fig. 4.3, mavoglurant absorption from the immediate release formulation terminates at the upper part of the small intestine ($\tau = 2.07$ h) for subject S16, close to the ileocecal valve that separates the small intestine from the large intestine ($\tau = 5.13$ h) for subject S18 and the beginning of the ascending colon for subject S38 ($\tau = 6.21$ h). For fitting purposes and in order to avoid negative values for the input rate, the mavoglurant input rate was set equal to zero during the declining portion of the absorption phase, Fig. 4.8. The unsuccessful fittings of the PBFTPK models to the rest of the five sets of data provide unreliable parameter estimates. However, it was found again that mavoglurant is absorbed in successive input stages; the large variability of data coupled with the small number of data points compared to the large number of estimated parameters results in large uncertainties for the parameter estimates.

The development of the FAT concept has led to a paradigm shift in oral pharmacokinetics. It is hoped that the application of FAT in PBPK modeling and pharmacometrics will place an end to the perpetuation of infinite oral drug absorption fallacy. Overall, the envisioned new technology based on the PBFTPK models would ultimately lead to better population approaches in the dosage regimen design adjustment in various therapeutic areas and speed up the development of generic medicines. Most of the advances made in the FAT concept have been included in a relevant book published recently [44].

References

1. Macheras P (2019) On an unphysical hypothesis of Bateman equation and its implications for pharmacokinetics. Pharm Res 36:94. https://doi.org/10.1007/s11095-019-2633-4
2. Macheras P, Chryssafidis P (2020) Revising pharmacokinetics of oral drug absorption: I models based on biopharmaceutical/physiological and finite absorption time concepts. Pharm Res 37: 187. https://doi.org/10.1007/s11095-020-02894-w
3. Chryssafidis P, Tsekouras AA, Macheras P (2021) Revising pharmacokinetics of oral drug absorption: II bioavailability-bioequivalence considerations. Pharm Res 38:1345–1356. https://doi.org/10.1007/s11095-021-03078-w
4. Tsekouras AA, Macheras P (2021) Re-examining digoxin bioavailability after half a century: time for changes in the bioavailability concepts. Pharm Res 38:1635–1638. https://doi.org/10.1007/s11095-021-03121-w
5. Chryssafidis P, Tsekouras AA, Macheras P (2022) Re-writing oral pharmacokinetics using physiologically based finite time pharmacokinetic (PBFTPK) models. Pharm Res 39. https://doi.org/10.1007/s11095-022-03230-0
6. Tsekouras AA, Macheras P (2022) Columbus' egg: oral drugs are absorbed in finite time. Eur J Pharm Sci 176:106265. https://doi.org/10.1016/j.ejps.2022.106265
7. Macheras P, Tsekouras AA (2023) Revising oral pharmacokinetics, bioavailability and bioequivalence based on the finite absorption time concept. Springer, Berlin

8. Iranpour P, Lall C, Houshyar R, Helmy M, Yang A, Choi JI, Ward G, Goodwin SC (2016) Altered Doppler flow patterns in cirrhosis patients: an overview. Ultrasonography 35:3–12. https://doi.org/10.14366/usg.15020

9. Dost FH (1953) Der Blutspiegel. Kinetik der Konzentrationsverläufe in der Kreislaufflüssigkeit, Thieme, Leipzi

10. Alimpertis N, Tsekouras AA, Macheras P (2022) Revising the assessment of bioequivalence in the light of finite absorption time concept: the axitinib case. Poster submitted to 30th PAGE meeting, Ljubljana, Slovenia, 28 June–1 July, 2022

11. Sanchez N, Sheiner LB, Halkin H, Melmon KL (1973) Pharmacokinetics of digoxin: interpreting bioavailability. Br Med J 4:132. https://doi.org/10.1136/bmj.4.5885.132

12. Center for Drug Evaluation and Research (2002) Digoxin Bioequivalency Review 76268. https://www.accessdata.fda.gov/drugsatfda_docs/anda/2002/76268_Digoxin_Bioeqr.pdf

13. Food and Drug Administration (2017) Center for Drug Evaluation and Research (CDER) waiver of in vivo bioavailability and bioequivalence studies for immediate-release solid Oral dosage forms based on a biopharmaceutics classification system. Guidance for Industry 82 FR 61011. https://www.federalregister.gov/d/2017-27786

14. European Medicines Agency (2010) Committee for medicinal products for human use (CHMP) guideline on the investigation of bioequivalence, London

15. Abuhelwa A, Foster DJR, Upton RN (2016) A quantitative review and meta-models of the variability and factors affecting oral drug absorption-part II: gastrointestinal transit time. AAPS J 18:1322–1333. https://doi.org/10.1208/s12248-016-9953-7

16. Lovering EG, McGilveray IJ, McMillan I, Tostowaryk W (1975) Comparative bioavailabilities from truncated blood level curves. J Pharm Sci 64:1521–1524. https://doi.org/10.1002/jps.2600640921

17. Sugano K (2012) Biopharmaceutics modeling and simulations: theory, practice, methods, and applications

18. Sugano K (2021) Lost in modelling and simulation? ADMET DMPK 9:75–109

19. Endrenyi L, Tothfalusi L (1997) Truncated AUC evaluates effectively the bioequivalence of drugs with long half-lives. Int J Clin Pharmacol Ther 35:142–150

20. Charalabidis A, Sfouni M, Bergstrom C, Macheras P (2019) BCS and BDDCS: beyond guidelines (invited review). Int J Pharm 566:264–281. https://doi.org/10.1016/j.ijpharm.2019.05.041

21. Sager JE, Yu J, Ragueneau-Majlessi I, Isoherranen N (2015) Physiologically Based pharmacokinetic (PBPK) Modeling and simulation approaches: a systematic review of published models, applications, and model verification. Drug Metab Dispos 43:1823–1837. https://doi.org/10.1124/dmd.115.065920

22. Sjögren E, Westergren J, Grant I, Hanisch G, Lindfors L, Lennernäs H, Abrahamsson B, Tannergren C (2013) In silico predictions of gastrointestinal drug absorption in pharmaceutical product development: application of the mechanistic absorption model GI-Sim. Eur J Pharm Sci 49:679–698. https://doi.org/10.1016/j.ejps.2013.05.019

23. Rinaki E, Dokoumetzidis A, Valsami G, Macheras P (2004) Identification of biowaivers among class II drugs: theoretical justification and practical examples. Pharm Res 21:1567–1572. https://doi.org/10.1023/B:PHAM.0000041450.25106.c8

24. Macheras P, Karalis V (2014) A non-binary biopharmaceutical classification of drugs: the ABΓ system. Int J Pharm 464:85–90. https://doi.org/10.1016/j.ijpharm.2014.01.022

25. Endrenyi L, Fritsch S, Yan W (1991) Cmax/AUC is a clearer measure than Cmax for absorption rates in investigations of bioequivalence. Int J Clin Pharmacol Ther Toxicol 29:394–399

26. Chen ML (1992) An alternative approach for assessment of rate of absorption in bioequivalence studies. Pharm Res 9:1380–1385. https://doi.org/10.1023/A:1015842425553

27. Chen ML, Davit B, Lionberger R, Wahba Z, Ahn HY, Yu LX (2011) Using partial area for evaluation of bioavailability and bioequivalence. Pharm Res 28:1939–1947. https://doi.org/10.1007/s11095-011-0421-x

28. Macheras P, Symillides M, Reppas C (1996) An improved intercept method for the assessment of absorption rate in bioequivalence studies. Pharm Res 13:1755–1758. https://doi.org/10.1023/A:1016421630290

29. Macheras P, Symillides M, Reppas C (1994) The cutoff time point of the partial area method for assessment of rate of absorption in bioequivalence studies. Pharm Res 11:831–834. https://doi.org/10.1023/A:1018921622981

30. Soulele K, Macheras P, Silvestro L, Rizea Savu S, Karalis V (2015) Population pharmacokinetics of fluticasone propionate/salmeterol using two different dry powder inhalers. Eur J Pharm Sci 80:33–42. https://doi.org/10.1016/j.ejps.2015.08.009

31. Soulele K, Macheras P, Karalis V (2018) On the pharmacokinetics of two inhaled budesonide/formoterol combinations in asthma patients using modeling approaches. Pulm Pharmacol Ther 48:168–178. https://doi.org/10.1016/j.pupt.2017.12.002

32. Soulele K, Macheras P, Karalis V (2017) Pharmacokinetic analysis of inhaled salmeterol in asthma patients: evidence from two dry powder inhalers. Biopharm Drug Dispos 38:407–419. https://doi.org/10.1002/bdd.2077

33. FDA Guidance (2003) Bioavailability and bioequivalence studies for nasal aerosols and nasal sprays for loca action

34. Borges NCDC, Astigarraga RB, Sverdloff CE, Borges BC, Paiva TR, Galvinas PR, Moreno RA (2011) Budesonide quantification by HPLC coupled to atmospheric pressure photoionization (APPI) tandem mass spectrometry. Application to a comparative systemic bioavailability of two budesonide formulations in healthy volunteers. J Chromatogr B 879:236–242. https://doi.org/10.1016/j.jchromb.2010.12.003

35. Pesic M, Schippers F, Saunders R, Webster L, Donsbach M, Stoehr T (2020) Pharmacokinetics and pharmacodynamics of intranasal remimazolam-a randomized controlled clinical trial. Eur J Clin Pharmacol 76:1505–1516. https://doi.org/10.1007/s00228-020-02984-z

36. Meyer MC, Jarvi EJ, Straughn AB, Pelsor FR, Williams RL, Shah VP (1999) Bioequivalence of immediate-release theophylline capsules. Biopharm Drug Dispos 20:417–419. https://doi.org/10.1002/1099-081x(199912)20:9<417::aid-bdd205>3.0.co;2-w

37. Hendeles L, Weinberger M, Bighley L (1977) Absolute bioavailability of oral theophylline. Am J Hosp Pharm 34:525–527. https://doi.org/10.1093/ajhp/34.5.525

38. Brown J, Chien C, Timmins P, Dennis A, Doll W, Sandefer E, Page R, Nettles RE, Zhu L, Grasela D (2013) Compartmental absorption modeling and site of absorption studies to determine feasibility of an extended-release formulation of an hiv-1 attachment inhibitor phosphate ester prodrug. J Pharm Sci 102:1742–1751. https://doi.org/10.1002/jps.23476

39. Wu D, Tsekouras AA, Macheras P, Kesisoglou F (2022) Physiologically based pharmacokinetic models under the prism of the finite absorption time concept. Pharm Res 39:1–11. https://doi.org/10.1007/s11095-022-03357-0

40. Zhou H (2003) Pharmacokinetic strategies in deciphering atypical drug absorption profiles. J Clin Pharmacol 43:211–227. https://doi.org/10.1177/0091270002250613

41. Cosson VF, Fuseau E (1999) Mixed effect modeling of Sumatriptan pharmacokinetics during drug development: II. From healthy subjects to phase 2 dose ranging in patients. J Pharmacokinet Pharmacodyn 27:149–171. https://doi.org/10.1023/A:1020601906027

42. Garrigues TM, Martin U, Peris-Ribera JE et al (1991) Dose-dependent absorption and elimination of cefadroxil in man. Eur J Clin Pharmacol 41:179–183. https://doi.org/10.1007/BF00265914

43. Macheras P, Tsekouras AA (2022) The finite absorption time (FAT) concept en route to PBPK modeling and pharmacometrics. J Pharmacokinet Pharmacodyn

44. Wendling T, Ogungbenro K, Pigeolet E, Dumitras S, Woessner R, Aarons L (2015) Model-based evaluation of the impact of formulation and food intake on the complex oral absorption of mavoglurant in healthy subjects. Pharm Res 32:1764–1778. https://doi.org/10.1007/s11095-014-1574-1

Part II
Pharmacodynamics

Chapter 5
Pharmacokinetic–Pharmacodynamic Modeling and Simulation in Clinical Practice and Studies

Thomas P. C. Dorlo and Elin M. Svensson

Abstract The past decade has seen a revival of the use of modeling and simulation of pharmacokinetics and pharmacodynamics in clinical practice. This resulted in a concept that is called model-informed precision dosing (MIPD), for which a wide range of software tools has been developed to be implemented in the clinical routine. These tools use modeling and model-based predictions to optimize the first or subsequent dosing for a patient based on what is already known about pharmacokinetic–pharmacodynamic relationships in combination with collected concentration-time data and patient characteristics. Newer applications have attempted to use also pharmacodynamic outcomes to inform dosing regimens using model-based approaches. This chapter discusses the use of modeling and simulation of both pharmacokinetics and pharmacodynamics in clinical practice and how it can be implemented in clinical routine. A particularly important clinical field where modeling and simulation of pharmacokinetics and pharmacodynamics have made a disproportionally large impact is drug dosing in children. Examples are provided of model-based pediatric dose regimens that have been implemented in clinical practice, as well as pharmacometric simulation approaches that can aid design of clinical pharmacokinetic–pharmacodynamic studies.

Keywords Pharmacometrics · Model-informed precision dosing (MIPD) ·
Therapeutic drug monitoring (TDM) · Pharmacokinetics-pharmacodynamics ·
Pediatric dosing

T. P. C. Dorlo (✉)
Department of Pharmacy, Uppsala University, Uppsala, Sweden

Department of Pharmacy & Pharmacology, Netherlands Cancer Institute, Amsterdam,
The Netherlands
e-mail: thomas.dorlo@farmaci.uu.se

E. M. Svensson
Department of Pharmacy, Uppsala University, Uppsala, Sweden

Department of Pharmacy, Radboud University Medical Centre, Nijmegen, The Netherlands
e-mail: elin.svensson@farmaci.uu.se

5.1   Introduction

While the science of quantitative modeling and simulation of pharmacokinetics and pharmacodynamics is currently particularly associated with informing decisions in the contemporary drug development process as part of modern model-informed drug development (MIDD), its advent and introduction actually find its roots in the clinic. Methods were sought to deal with the highly heterogeneous data collected in clinical practice and how these could be used to find the optimal dose for the individual patient [1]. When Lewis Sheiner, Stuart Beal, and colleagues introduced nonlinear mixed-effects modeling in the field of pharmacokinetics and pharmacodynamics through the development of the software package NONMEM in the late 1970s and early 1980s, their evaluations focused on how this new methodology was better capable at dealing with the sparse and heterogeneous data collected in routine clinical settings and how this could inform individualized dose regimens based on patient-specific covariates [1–4]. In the past decade, there has been a revival of the use of modeling and simulation of pharmacokinetics and pharmacodynamics in clinical practice. This renewed interest has resulted in a concept that is called model-informed precision dosing (MIPD), for which a wide range of software tools have been developed to be implemented in the clinical routine. These tools use modeling and model-based predictions to optimize the first or subsequent dosing of a patient based on either patient characteristics plus what is already known about the pharmacokinetics and pharmacokinetic–pharmacodynamic relationships of a drug in this particular patient population, and/or previously collected drug concentration–time data of this patient, to further optimize the future dosing of this particular patient. Newer applications have attempted to use pharmacodynamic outcomes on top or instead of drug concentrations to inform dosing regimens using model-based approaches. This chapter will focus on the use of modeling and simulation of both pharmacokinetics and pharmacodynamics in clinical practice and how it can be implemented in clinical routine. A particularly important clinical field where modeling and simulation of pharmacokinetics and pharmacodynamics have made a disproportionally large impact is drug dosing in children. Pediatric dose finding and optimization are often neglected during drug development, leading to long delays before novel therapies become available also to young patients. Model-based approaches incorporating physiological and other changes in this patient population affecting drug disposition and drug effects can be a very powerful way to derive pediatric regimens faster and more accurately. We will provide a few examples of model-based pediatric dose regimens that have been implemented in clinical practice, as well as pharmacometric simulation approaches that can aid pharmacokinetic–pharmacodynamic studies in clinical practice.

5.2 Use of Pharmacokinetic–Pharmacodynamic Models in Clinical Practice

5.2.1 Personalized Medicine

Driven by an increased interest and capacity in pharmacogenetics in the past two decades, the current perception and interpretation of "personalized medicine" is often only limited to pharmacogenetics-based treatment adjustment, where, e.g., the identification of a single nucleotide polymorphism could indicate a required dose adjustment or expression of a particular drug target in cancer determines the choice of pharmacotherapy. This can be related to individual treatment response, e.g., drug target expression such as BRAF V600E expression indicating the use of BRAF inhibitor vemurafenib [5]; or both individual treatment exposure and subsequently treatment response, e.g., in the case of metabolic enzyme expression such as dihydropyrimidine dehydrogenase (DPYD) variant expression determining 5-fluorouracil and capecitabine metabolism and severe toxicity [6]. This is, however, a too narrow interpretation of the term, given that metabolomic and genetic predisposition is only one of the many covariates influencing individual pharmacodynamic response. The impact and overall effect size of pharmacogenetics on individual drug exposure and drug response is arguably rather limited, with a few exceptions, particularly when compared to other influential covariates, such as body weight and renal function.

A more holistic view on "personalized medicine" would thus incorporate all individual factors, covariates, or biomarkers affecting or defining drug exposure and treatment response, with the aim to distill the most influential ones that eventually can and should be used to determine the dose or the requirement for a dose adjustment or even the type of treatment or drug, ultimately resulting in an optimal therapy for the individual patient. Population pharmacokinetic and pharmacodynamic models are of course quintessentially suitable to identify these (changes in) clinical factors, patient characteristics and biomarkers, including pharmacogenetic markers, eventually determining treatment response. In addition, population pharmacokinetic and pharmacodynamic models can estimate the effect size and quantify the impact of the factors on drug exposure and/or treatment response, where model-based simulations can assess the impact of dose or treatment adjustments on an individual and population level. Population pharmacokinetic and pharmacodynamic modeling and simulation is thus an essential tool in enabling personalizing medicine and providing evidence for treatment guideline development, certainly in those instances where "one dose does *not* fit all."

5.2.2 Model-Informed Precision Dosing

5.2.2.1 From Therapeutic Drug Monitoring to Model-Informed Precision Dosing

The approach and interpretation of personalized medicine as discussed in the previous paragraph could be considered as a priori individualization or stratification of therapy based on clinical and patient characteristics. Treatment and particularly drug dose can also be adjusted during the course of treatment, based on initial or continued treatment response, resulting in an optimized and personalized treatment. This is commonly done by means of therapeutic drug monitoring. Given the overall assumption of a dose–exposure–response relationship for any type of treatment and a common delay in actual measurement of treatment response, often drug concentration instead of clinical response or disease biomarker is measured. This is then compared to a reference concentration or concentration window, also referred to as therapeutic window.

Traditionally, such a therapeutic drug monitoring approach to adjust the dose has been highly empirical, titrating the dose in increments followed by subsequent repeated measurements of the drug plasma concentration until the drug concentration, often a trough concentration (C_{min}) right before the next dose, is within the specified or aimed target concentration window. There are various apparent issues for this traditional therapeutic drug monitoring approach, complicating a fast optimization of individual dose and treatment, without exposing the patient to non-optimal or non-toxic levels of drug exposure.

Firstly, conventional therapeutic drug monitoring is often based on sample collection around the time of C_{min}, which is not only difficult to collect and time, particularly in an outpatient context, but is also yielding only limited pharmacological information. For dose adjustment, the individual drug clearance will be of key importance, while a C_{min} is typically not very informative for this pharmacokinetic parameter. Moreover, in clinical practice, samples are typically taken on an ad hoc basis, instead of the targeted time right before the next dose.

Secondly, the actual algorithms for dose adjustment based on the concentration target attainment are often ill-defined and either based on, e.g., standard increments or the decision is entirely left to the treating clinician's own experience or conviction. This can be particularly dangerous if there is a large inter-individual variability in any of the parameters defining the dose–exposure–response relationship. Such an empirical approach will also increase the duration of under- or over-exposure, given that in most individual cases it will take multiple cycles of dose adjust-measure concentration until the desired target is achieved. Despite wide adoption of therapeutic drug monitoring, particularly in the field of antibiotics, this empirical approach and the passive nature underlying therapeutic drug monitoring have also received criticism. Amongst others, a concept called *target concentration intervention* was introduced, which emphasized on the more active approach to *intervene* rather than to *monitor* [7]. Rather than specifying a therapeutic window

or range, a single target drug concentration or biomarker response is being considered and based on existing pharmacokinetic and pharmacodynamic knowledge the corresponding dose is calculated to derive an individualized intervention to be implemented by the clinician.

These aforementioned issues related to therapeutic drug monitoring have led to the adoption of Bayesian forecasting approaches, where Bayesian priors based on population pharmacokinetic or pharmacokinetic–pharmacodynamic models are being used in combination with the observed patient concentration or biomarker and individual covariate information for covariates included in the previously developed models, to derive a posterior set of predicted individual model parameters that can then be used to adjust the individual dosing regimen. The first so-called "computer-aided dosing" algorithms arose more than 50 years ago [8–10], which actually initiated and formed the impetus for the field of population pharmacokinetic modeling or pharmacometrics. More recently, this model-based approach to optimize individual therapy has been referred to as model-informed precision dosing.

5.2.2.2 Model-Informed Precision Dosing Software Tools

Uptake and implementation of model-informed precision dosing in clinical practice and routines have been relatively limited, even though it is emergingly popular among clinical pharmacologists and pharmacometricians. Model-informed precision dosing generally requires custom-made software tools and the use and implementation of these tools have historically been limited to academic centers of excellence. The main reasons for the lack of implementation have been suggested to include a lack of published evidence of large-scale utility and clinical impact of software implementing model-informed precision dosing, a lack of technical and computational expertise at the clinical site of implementation, a lack of standardized validation requirements of these software tools, and a lack of user-friendliness of the software tools themselves [11]. Particularly, the lack of prospective evidence for improved patient outcomes or a decrease in overall healthcare costs, generated through randomized controlled clinical trials has been identified as a major limitation and barrier for implementation [11, 12]. An example of such a prospective trial focused on the prediction of individual vancomycin dosing using model-informed precision dosing compared to the conventional use of $C_{\min}$, which showed indeed better clinical outcomes for the model-based tool approach [13].

There is a large range of software tools for model-informed precision dosing available, either developed as a spin-off from academic or clinical activities or by for-profit companies (Table 5.1) [14]. A recent evaluation of their performance, assessed by an expert-based evaluation, evaluated these tools on user-friendliness, user support, computational aspects, population models, quality and validation, output generation, privacy & data security, and cost [15]. Overall, all tools showed an adequate performance, but with large differences in terms of number of drug modules and populations, quality control and user interface design [15], where the choice of the optimal software tool is probably highly dependent on the specific local requirements and personal preference and existing know-how.

Table 5.1 Overview of available model-informed precision dosing software tools. (Adapted from Kantasiripitak et al. Front Pharmacol. 2020;11:620 [15])

	AutoKinetics	BestDose	DoseMeRx	ID-ODS	InsightRX Nova	MwPharm++	NextDose	PrecisePK	TDMx	Tucuxi
Institution/Company	Amsterdam UMC, and OLVG Hospital	Children's Hospital Los Angeles	DoseMe	Optimum Dosing Strategies	Insight Rx Inc.	Mediware a.s.	University of Auckland	Healthware Inc.	University of Hamburg	School of Engineering and Management Vaud
Computer language source code	Asp.net and vb.net	Fortran, R	Perl, R, python	Ionic, R	R, JavaScript	C#	Javascript, PHP, MySQL, NM-TRAN	C++, PHP Web App: JSX, C++	R/C++	C++
Purpose of use	Research and Clinical	Research	Research and Clinical	Clinical	Research and Clinical	Research and Clinical	Research and Clinical	Research and Clinical	Research and Clinical	Clinical
Website	autokinetics.eu	lapk.org/bestdose.php	doseme-rx.com	optimum-dosing-strategies.org/id-ods/	insight-rx.com	mediware.cz	nextdose.org	precisepk.com	tdmx.eu	tucuxi.ch

5.2.2.3 Issues in Model-Informed Precision Dosing

A first issue for any type of model-informed precision dosing tool and its implementation in the clinic is model selection and model qualification. Model selection can be a daunting task given that for many drugs, a multitude of published models is available, most of which developed in different populations, in different clinical contexts and, perhaps most importantly, developed for different reasons and with different aims. Ideally, the population pharmacokinetic or pharmacokinetic–pharmacodynamic model to be used to optimize dosing in a certain patient should be relevant for the intended population. Therefore, practically, a model should be developed in a matching age group (pediatric, adolescent, adult, etc.), clinical indication, disease severity (intensive care unit, outpatient, etc.), body composition (normal weight, obese, etc.), genetic background, studied dose ranges/levels, etc. [16]. Most models have been developed in rather limited population, for instance only in adults or only in pediatrics, based on a focused clinical trial, which poses threats to extrapolations from those models, particularly outside original covariate ranges.

Therefore, it is pivotal to evaluate whether the chosen model or models are fit-for-purpose and for this the predictive performance should be evaluated in the particular context and setting where the model-informed precision dosing is intended to be used, e.g., based on historical (therapeutic drug monitoring) data from the institution or context where the tool will be implemented [16]. The different aspects of the model to evaluate depend on the purpose of implementation and can include a priori predictive value to assess the optimal starting dose for an individual, or rather the performance of the a posteriori Bayesian forecasting when the aim is to adjust dosing based on measured drug concentrations or other biomarker quantifications in an individual. The importance of evaluating the predictive value for extrapolation in a therapeutic drug monitoring setting was recently highlighted by a large systematic review on the extrapolation of population pharmacokinetic models to enable model-informed precision dosing of antibiotics [17]. Only 25% of the identified external evaluation studies actually assessed predictive performance by Bayesian forecasting. That population models for the same drug exhibit large variability in their predictive performance was shown recently for vancomycin and the predicted pharmacokinetic–pharmacodynamic target attainment, which varied by more than 300%, directly having a large impact on associated decisions on dose optimization bases on these predictions. This systematic evaluation of Bayesian forecasting indicated some model properties associated with a predictive performance: (1) the larger the population the model is based on, the better the predictive performance, (2) misspecifications in the population models can lead to biased predictions, often based on biased sampling designs, such as exclusive use of C_{min} [18].

One of the solutions that has been proposed for this issue of model selection and evaluating whether its fit-for-purpose or fit-for-context and ultimately to create more standardization in the implementation and adoption of model-informed precision dosing is a process introduced as a "continuous learning approach" [19]. This approach entails the adaptation of a population model to a local context, by

re-estimating population parameters based on locally available, good-quality, well-registered, historic data, e.g., based on historic therapeutic drug monitoring. The overall aim of this approach is to reduce the prediction error and optimize the model to a local population and context. Another proposed solution to the model selection issue is an algorithm known as "model averaging." Here, a set of available (candidate) models from literature is used, which may not all be optimal or adapted to the local context or individual patient targeted. The model averaging algorithm can either select a population model or average a combination of population models for an individual patient on an a posteriori basis once biomarker concentration data of this individual become available. Such a model averaging approach has been evaluated as well for vancomycin, where both available models and data sets are highly heterogeneous, leading to an improved predictive performance [20].

A second issue is the predictive ability for extreme patients, i.e., patients that exhibit characteristics at the edges or even outside the covariate range for the population the model was originally build for. While the model-informed precision dosing is probably of high clinical relevance for these types of extreme patients, these patients are typically poorly fitted and poorly predicted based on a population model. A solution for this is to flatten the model priors or by downweighing them in the likelihood function. This makes the predictions to be relying more on the (extreme) observed data and thus allows more extreme individual parameter estimates. The balance between overfitting of extreme observed data by downweighing priors and on the other hand relying on these prior estimates to enable robust model-based predictions is highly delicate and further emphasizes the need to collect more data in extreme patients for confirmation [16].

A third issue for model-informed precision dosing might be time-variable changes in pharmacokinetics and pharmacodynamics, e.g., as a result of changes in patient (patho)physiology. Such variability in pharmacokinetics and pharmacodynamics over time might also be random between dosing occasions, which can be considered in models as between-occasion variability. This poses difficulties as it might reduce, in various ways, the importance of historical data in an individual for the predictive value of future treatment course [16]. In the case of random between-occasion variability, this should be properly implemented, as its omission has been shown to lead to imprecisions in Bayesian forecasting [21]. Drugs that are to a large extent affected by between-occasion variability, most often oral drugs with a day-to-day variable absorption rate and extent of absorption, might require repeated sampling and observations over multiple occasions to enable disentangling of between-subject and between-occasion variability and improve individual predictions.

A more practical issue, particularly in low- and middle-income countries, limiting the widespread global implementation of model-informed precision dosing, is the non-availability of easily accessible bioanalytical facilities that can provide drug quantifications at a low cost with a short turnaround after sample collection. Additional problems can arise in terms of patient data protection and other privacy-related issues, where model-informed precision dosing requires implementation and integration in hospital IT systems and infrastructure where patient record files are maintained. More recent data protection regulations, such as the General Data Protection Regulation implemented in the European Union in 2018, complicate this integration and potentially the use of cloud-based solutions.

5.2.2.4 Pharmacodynamic Model-Informed Precision Dosing

While model-informed precision dosing is most often based on drug concentrations as a biomarker, in the form of therapeutic drug monitoring, the biomarker of choice can of course be a pharmacodynamic endpoint instead of a pharmacokinetic endpoint, which is likely more closely related to the desired clinical outcome. In this paragraph, a few examples of applications of dose individualization based on Bayesian tools for pharmacodynamic endpoints will be discussed: dose individualization of (I) warfarin based on international normalized ratio (INR), (II) chemotherapy based on neutrophils, and (III) tyrosine kinase inhibitors based on soluble vascular-endothelial growth factor receptor-3 (sVEGFR-3).

International Normalized Ratio for Warfarin Dose Individualization

Despite being in use for more than 50 years now, the clinical application of warfarin for the management of thromboembolic events is, while highly effective, rather limited by a narrow therapeutic range and particular variability in response to a given dose. The variability in response is not only due to pharmacokinetic variation in the patient population as a result of genetic polymorphisms in, e.g., the gene for the metabolizing enzyme cytochrome P450 2C9, but also due to variability in the pharmacodynamic response, e.g., due to vitamin K intake. Based on established population pharmacokinetic–pharmacodynamic models characterizing the antithrombotic effect of the warfarin exposure in relation to the risk of bleeding as measured by the prothrombin time INR [22–24], a Bayesian warfarin dose individualization tool was developed by Hamberg et al. [25]. There is a pronounced delay between the dosing of warfarin and the INR response, which is included in the population pharmacokinetic–pharmacodynamic model by a transduction model consisting of a flexible parallel compartment chain, comparable to a transit-chain compartment model, which sits in between the direct drug effect on the inhibition of the vitamin K cycle and the ultimately observed increase in INR from baseline. The developed model-based tool allows the estimation of an a priori dose based on body weight, baseline and target INR, and optionally relevant genetic polymorphisms, while an a posteriori update of the individualized dose is enabled through Bayesian forecasting and additional incoming information about the warfarin dose history and INR observations solely. The tool is a good example of how population pharmacokinetic–pharmacodynamic models can be employed and implemented in a clinical setting together with relevant biomarker measurements to enable not only starting doses, but also dose adaptation in the course of treatment based on a highly relevant pharmacodynamic biomarker.

Neutrophil-Guided Dose Individualization of Chemotherapy

A typical example where drug concentrations are maximized based on acceptable tolerability in the individual patient is chemotherapy dosing in anticancer treatment, where there is a continuous and dynamic balance between achieving maximal chemotherapeutic exposure to maximize the probability of reducing the tumor load while at the same time maintaining a tolerable toxicity profile, acceptable for the patient. Neutropenia is one of the most frequent and most severe adverse events of chemotherapy as it is life-threatening, making patients highly vulnerable with an increased risk of infections. Various semi-mechanistic pharmacodynamic and pharmacokinetic–pharmacodynamic models have been developed to characterize the time course of myelosuppression leading to neutropenia and its relationship to drug dosing and cumulative drug exposure [26]. Based on this, a dosing tool, specifically focused at etoposide, has been developed – and implemented in Microsoft Excel – to make the population pharmacodynamic model more easily available to non-modelers [27]. The tool requires previous neutrophil counts from a previous treatment course to derive and based on a Bayesian estimation procedure predicts a dose that results in a desired neutrophil nadir for the next treatment cycle.

Later various other approaches for model-informed precision dosing based on neutropenia and neutrophil counts have been presented [28–30]. One of the challenges to choose which model and which model-informed precision dosing tool fits best the clinical application and context is, as described earlier, model averaging or model selection [20].

sVEGFR-3 for Tyrosine Kinase Inhibitor Sunitinib Dose Individualization

Tyrosine kinase inhibitors have been a major game-changer for the safety and effectiveness of treatment of a wide variety of malignancies. They are more patient-friendly as they can be taken orally and were designed as more targeted therapies compared to conventional chemotherapy. Nevertheless, many of the tyrosine kinase inhibitors have shown to exhibit large between-patient variability in both pharmacokinetics and pharmacodynamics in terms of both safety and effectiveness endpoints. There is thus a large need for further dose individualization in order to optimize treatment outcome and patient tolerability. Most dose individualization of tyrosine kinase inhibitors has been based on therapeutic drug monitoring of drug concentrations given the large between-patient variability in drug exposure and dose–exposure–effect relationships, e.g., focusing on the area under the concentration–time curve or the trough concentration at steady-state, various therapeutic drug monitoring targets have been suggested for both adults and children [31, 32]. Other dose individualization approaches for tyrosine kinase inhibitors have been focused on pharmacodynamic markers related to the targeted effect or toxicity such as soluble biomarkers, blood pressure, or neutrophil counts [33]. One of these biomarkers that have been evaluated and proposed for dose individualization is sVEGFR-3 for sunitinib, where semi-mechanistic population pharmacokinetic–

pharmacodynamic models have been developed to capture between-patient variability and longitudinal time course of the biomarker [34]. Centanni and Friberg presented a pharmacometric framework to evaluate the effect of model-based dosing individualization based on sVEGFR-3 not only on outcome endpoints but also in terms of cost-effectiveness and compared it performance to more conventional dose individualization strategies such as based on therapeutic drug monitoring using sunitinib drug concentrations or adjustment based on clinical toxicity measurements [35]. The model-based simulations showed that a sVEGFR-3-based dosing led to the longest median overall survival compared to fixed, therapeutic drug monitoring-based or neutrophil counts-based (2.16 vs 1.71, 1.80 and 1.90 years, respectively). On top of that, it was also predicted to be highly cost-effective compared to the other dose individualization approaches, with a cost per additional quality-adjusted life year of €36,784 versus €173,150 and €104,438 for therapeutic drug monitoring-based and neutrophil counts-based, respectively. This framework provides a good example of how model-based dose individualization based on pharmacodynamic biomarkers linked to the main clinical endpoint of overall survival can provide an improved prediction of effects of dose adjustments particularly for drugs and drug classes where there is large variability in exposure-response relationships or generally large between-patient variability in biomarker response. A prospective clinical trial should validate these findings in a "real-world" population and setting, based on which the framework and dose individualization algorithms could be further adapted to the clinical needs and context.

5.2.3 Optimizing Pediatric Dosing

Dose optimization between patient subpopulations is most often focused on achieving a similar level of drug response between the various subpopulations. Pediatric patients form a sub-population which is consistently being neglected during drug development [36], most often because of ethical concern, logistical challenges, and lack of financial interest. If pediatric pharmacokinetic data are available, these data are often highly heterogeneous and sparse in nature, which makes interpretation difficult. Particular focus in model-informed drug development is therefore paid to the extrapolation of dosing regimens to children based on adult pharmacokinetic and pharmacodynamic data. In all diseases for which the exposure-response relationship is expected to be similar in adults and children, the general aim is to derive a pediatric dosing regimen that provides an equivalent level of drug exposure that was found effective in adults [37]. Pediatric dose optimization or extrapolation in that context is primarily focused on adjusting the adult dose regimen by accounting for effects of body size and maturation of physiological systems involved in the distribution and metabolism of drugs [38]. If a specific pediatric formulation is used, or the adult formulation is manipulated to enable dosing in children not able to swallow whole tablets, potential effect of the administration form could also be considered.

Based on the general concept of allometry in metabolism, which was first coined by Kleiber in 1938 [39] and investigated the relationship between an organism's body size and metabolic processes, the theory of allometric scaling has been widely accepted in the pharmacokinetic field. This relationship between body size and drug clearance, for small molecules, is described by a non-linear power function with an exponent of 0.75, which particularly in older children above the age of 2 years is able to predict both clearance and variability in clearance based on adult pharmacokinetic data [40, 41]. The relationship between volume of distribution and body size is linear with a power exponent of 1. The most practical and most easy to measure parameter reflecting the quantification of body size is total body weight, which is most often used for this type of extrapolations. An additional factor to consider when optimizing dose regimens in children is the developmental changes in metabolism which mainly take place within the first 2 years after birth. These maturation effects particularly affect drug-metabolizing enzyme expression and glomerular filtration and are most often a function of increasing metabolic function with increasing age.

The allometry of pharmacokinetics implies that clearance is relatively larger in children compared to adults when normalized to body weight, which means that children (over 2 years of age at least) will generally require a higher mg/kg dose than adults to reach the same level of drug exposure [42]. Whether this is needed is of course dependent on the therapeutic window or range of drug concentrations which is required to be attained for a safe and effective usage of the drug. In addition, there might be a need to adapt for scaling of the pharmacodynamic response from adults to children in diseases where the effect of the drug might be subject to age maturation as well, such as immunological effects. In children below 2 years of age, the extrapolation is not as straightforward and is largely depending on what is known about the specific maturation function of the enzyme and renal functions involved in the specific metabolism of that drug.

A model-based approach is the most suitable approach to incorporate all these biologically supported body size and age effects on the pharmacokinetics, and to decide on optimal dosing weight bands based on the available dose strengths. Various examples are available where a model-based informed dose regimen has been introduced in place of the adult mg/kg dosage. Such dosages have often been developed and evaluated based on pharmacokinetic simulations of virtual pediatric patient populations relevant for the pediatric population of interest. Two case examples will be used to further illustrate this: (1) the update of pediatric dosing guidelines of bedaquiline for the treatment of rifampicin-resistant tuberculosis, and (2) the optimized dose regimen of miltefosine for the treatment of children with the neglected tropical disease visceral leishmaniasis.

5.2.3.1 Updating Pediatric Dosing Guidelines for Tuberculosis in Children

Every year about one million children worldwide fall ill with tuberculosis, almost half of those are 4 years or younger [43]. Tuberculosis is an infectious disease caused by *Mycobacterium tuberculosis,* most commonly affecting the lungs. Effective

combination treatments including up to four drugs are available, but mycobacterial strains resistant to the most important first-line drugs are becoming increasingly common. Fortunately, a few novel drugs have been approved for treatment in adults in the last decade and these are now becoming available for children as well. However, pediatric data from clinical trials investigating the novel anti-tuberculosis compounds are very limited. Modeling and simulations played a key role when the World Health Organization (WHO) recently (2021) updated their guidance on treatment of multi-drug resistant tuberculosis in children and published weight- and age-based dosing tables as part of an Operational Handbook [44]. This section describes how the WHO recommendations for dosing of bedaquiline in children were determined, as an illustrative example. The process is described in detail in the public report from the associated WHO expert consultation [45].

Bedaquiline was approved for treatment of rifampicin-resistant tuberculosis by the U.S. FDA in 2012. It has a novel mechanism of action, shortens the time to culture conversion (i.e., when mycobacteria no longer can be detected in sputum samples collected from the patient), and improves long-term treatment outcomes [46]. A decade later, the pediatric trials to determine optimal bedaquiline dosing in children are still not finalized and the dosing recommendations from stringent regulatory authorities only cover children 5 years and older. The reasons for the slow progress with the pediatric trials are multiple and have to do with the difficulty to include young children with the relevant diagnosis, lack of qualified trial sites in the part of the world where the disease is common, the use of inefficient age-de-escalation study designs, and sub-optimal planning. In the meantime, bedaquiline has become a cornerstone in combination therapy of rifampicin-resistant tuberculosis in adults and is categorized as a group A drug according to WHO, which means that it should always be included if possible. After a review of the limited clinical data available, a WHO guideline development group recommended that bedaquiline can be used in children of all ages (down to infants) and this was publicized through a so-called WHO rapid communication (conditional recommendation, very low certainty of evidence) [47]. After that, a technical consultation was conducted to determine how to practically conduct the dosing.

The scope to the dosing scheme was defined as children of all ages down to term-born infants of 3 kg or more. Another prerequisite was that the dosing schedule should follow the pattern of the approve regimen in adults, with includes a 2-week loading phase with daily administration (400 mg) and a 22-week-long continuation phase with three times weekly (TIW) dosing (200 mg). A 100 mg tablet and a 20 mg scored dispersible tablet (bioequivalence demonstrated indirectly) are the available formulations. Key features of bedaquiline pharmacokinetics to note include the long terminal half-life (>5 months), strong positive effect of food on bioavailability, and high protein binding (>99.9%) [48]. Bedaquiline is metabolized by CYP3A4 to the less active M2 metabolite. Weekly average bedaquiline concentrations have been linked to efficacy (rate of decline in bacterial load) and M2 concentrations have been linked to the most important side effect of bedaquiline treatment, QT prolongation [49, 50].

A simulation framework was developed with the aim to select pediatric doses predicted to achieve exposures as close as possible to exposures achieved in adults on the approved dosing regimens. This is in line with the FDA general clinical pharmacology considerations for pediatric anti-infective drugs, where for anti-infectives it is often reasonable to assume that adults and children share a sufficiently similar disease course and response to intervention [37]. The simulation framework included the following components:

- *Weight Banding Approach*

     To align with other components in the multi-drug regimen, the weight banding implemented in the previous version of the WHO Operational handbook was primarily followed, with a few small adjustments. The approach included 9 categories with 8 cut-off points between 5 and 50 kg. Given the expected strong influence of age on clearance, doses for the lower weight range were evaluated in age group categories (0 to <3 months, 3 to <6 months, and ≥6 months).

- *Virtual Pediatric Population*

     The population included 40,000 children aged between 0 and 18 years with body weight 3 kg or higher (50–50 girls and boys). The weight-per-age distribution was based on WHO growth standards (0–10 years) enriched with data from the US National Health and Nutrition Examination Survey (NHANES) database (10–18 years). To be representative of children with tuberculosis disease which are generally smaller than healthy children of the same age, the age–weight distribution was adjusted using an earlier reported approach [51].

- *Target Exposures*

     The main target was set as the weekly median steady-state exposures in adults who received WHO-recommended bedaquiline dosing. Exposures of the main metabolite (M2) during the loading phase were also considered, based on the assumption that too high exposures might cause toxicity.

- *Population Pharmacokinetic Model*

     A population pharmacokinetic model developed on data from adults was used for the exposure simulations [52]. This model describes the pharmacokinetics of bedaquiline using three disposition compartments for bedaquiline, and two for the M2 metabolite. Semi-physiological models were used to characterize changes in weight and albumin over time. Weight and albumin were correlated; they typically increased after the start of treatment and significantly affected bedaquiline and M2 plasma disposition. Allometric scaling based on body weight with the theoretical components (0.75 for clearance and 1 for volumes) accounted for size effects. The age effect was included with published CYP3A4 maturation functions [53, 54]. Two different options were used given that the available information from children on bedaquiline was too limited to determine which of them fitted best. Bioavailability was assumed to be unaffected by age. The model was applied to a limited dataset from children and found to describe the data adequately.

Table 5.2 Pharmacometric model-based weight-banded dosing for bedaquiline in pediatric patients with rifampicin-resistant tuberculosis

Weight range	Age category	Dosing of bedaquiline[a]
3 to <5 kg	0 to <3 months	30 mg QD/10 mg TIW
	≥3 months	60 mg QD/20 mg TIW
5 to <7 kg	0 to <3 months	30 mg QD/10 mg TIW
	≥3 months	60 mg QD/20 mg TIW
7 to <10 kg	0 to <3 months	30 mg QD/10 mg TIW
	3 to <6 months	60 mg QD/20 mg TIW
	≥6 months	80 mg QD/40 mg TIW
10 to <16 kg	3 to <6 months	60 mg QD/20 mg TIW
	≥6 months	120 mg QD/60 mg TIW
16 to <30 kg		200 mg QD/100 mg TIW
≥30 kg		400 mg QD/200 mg TIW

QD once a day, *tuberculosis* tuberculosis, *TIW* thrice weekly (Monday/Wednesday/Friday)
[a]Dosing is provided for the intensive phase (2 weeks) followed by dosing for the continuation phase (22 weeks)

Different practically feasible dosing options were outlined and evaluated in the simulation framework. Expected exposures were presented with boxplots also including the target exposure and a reference range for low and high exposures seen in phase 2 trials in adults. The simulation results were presented to an independent expert panel with representation from all continents including medical and pharmacological expertise, pediatricians, civil society, and national tuberculosis program representatives. The panel collectively assessed the model-derived dosing options in a dynamic process, weighting the risks linked to over-versus under-exposure, and finally selected the doses to bring forward in the WHO Operational Handbook (Table 5.2). The modeling and simulation work was instrumental in the process to generate dosing recommendations in a populations where limited direct data are available, making the most out of drug-specific information from adults and established knowledge about developmental physiology. The appropriateness of the dosing schedule should be evaluated in clinical studies, but the immediate inclusion in the WHO Operational Handbook demonstrated the confidence in careful model-based extrapolation to facilitate access to life-saving bedaquiline treatment for children of all ages affected by rifampicin-resistant tuberculosis.

5.2.3.2 Optimized Dose Regimens for Children with the Neglected Tropical Disease Visceral Leishmaniasis

Visceral leishmaniasis is globally one of the most neglected tropical diseases and the second largest killer among parasitic disease, only after malaria. After a successful elimination campaign on the Indian subcontinent, the main burden of this fatal disease caused by the *Leishmania* parasite is currently in Eastern Africa, where about 50–60% of the patients are pediatric. Historically clinical trials to evaluate new drugs for leishmaniasis have largely been focused on adult patients. One of the key drugs to treat leishmaniasis is oral miltefosine, which is a repurposed drug originally

developed for the treatment of cancer and is the only oral drug currently available for leishmaniasis. During the initial clinical development of this drug in India, only limited attention was given to the clinical pharmacokinetics of this drug: for instance, only very sparse descriptive pharmacokinetic data were reported in the registration documents that were initially filed in India (2002) and Germany (2004) [55].

Early studies on miltefosine in visceral leishmaniasis in India already indicated a lower end-of-treatment/steady-state concentration in children compared to adults [56], while given a similar 2.5 mg/kg/day regimen for 28 days. However, this was not given much attention due to an adequate efficacy in both children and adults in that region. Later the pediatric underexposure was confirmed in a Nepalese cohort study, where again children had around 30% lower steady-state concentrations compared to adults [57]. The relevance of this finding in Nepal was corroborated by the observation that a longer follow-up time of patients of 12 months revealed a much larger failure rate of the treatment in terms of relapse of disease. Most of the patients experiencing treatment failure were children [58], who were underexposed to the drug in comparison with adults. A pharmacokinetic–pharmacodynamic model identified an exposure-response relationship and revealed that the time that the miltefosine concentration was above the in vitro susceptibility EC_{90} ($t > EC_{90}$) was related to the probability of experiencing a relapse of infection [59]. A similar finding was done in Eastern Africa, where it was demonstrated that children below the age of 12 years were exposed to significantly and clinically relevant lower concentrations of miltefosine compared to adult patients with a higher body weight, with again on average a difference of 36% in end-of-treatment steady-state concentrations [60].

The relevance of achieving sufficient miltefosine exposure has been demonstrated through various established exposure-response relationships, in an attempt to characterize and explain the increased treatment failure rate of this drug in Eastern Africa compared to the Indian subcontinent. Not only was experiencing a relapse within 12 months associated with a lower drug exposure, but in Eastern Africa it was also demonstrated that the time until relapse of infection was associated with the miltefosine $t > EC_{90}$, affecting the relapse hazard in a pharmacometric time-to-event model [61]. This lack of efficacy of the conventional 2.5 mg/kg/day miltefosine regimen really prevented the use of the only oral drug available for the treatment of leishmaniasis in Eastern Africa, given that >50% of the visceral leishmaniasis patients in that region are pediatric [60].

Various observations from controlled and observational studies from both the Indian subcontinent and Eastern Africa confirmed that children accumulate the drug to a lesser degree than adults when administered 2.5 mg/kg/day. This pediatric underexposure with the conventional mg/kg dosing is consistent with the clinical observations from various regions of endemicity that children are more at risk of failing miltefosine treatment and later relapse of infection [58, 59, 63]. Based on a pooled population pharmacokinetic analysis combining pharmacokinetic data from both Indian adult, Indian pediatric and European adult visceral leishmaniasis patients with a wide distribution of body weights (range 9–113 kg), clearance of miltefosine

was most accurately estimated when scaled allometrically with a power exponent of 0.75, based on fat-free mass of the patient [64]. Model-based simulations confirmed once again the pediatric underexposure with a mg/kg/day dose. An allometric dose was developed based on the most significant body size descriptor fat-free mass, which was derived from the body weight, height, and sex of a patient (Fig. 5.1) [64]. This so-called allometric miltefosine dosing regimen was predicted to result in equivalent exposure in Indian and Eastern African children compared to adults.

A pediatric Phase II trial with this allometric miltefosine regimen administered for 28 days was conducted in Kenya on 30 pediatric visceral leishmaniasis patients ($\leq$12 years of age) to assess pharmacokinetic equivalence, efficacy, and safety of this regimen. Efficacy with this allometric regimen increased to 90% compared to 59% with the conventional miltefosine regimen. Exposure in terms of pharmacokinetic target $t > EC_{90}$ attainment and AUC_{d0-28} was improved and specifically less variable compared to the mg/kg dose, while the increased absolute daily dose was found to be tolerable with no particular increase in toxicity [62, 65]. Based on these promising results, the model-based allometric miltefosine dosing regimen enabled the first ever shortened partly-oral combination treatment regimen for visceral leishmaniasis without the highly toxic antimonial sodium stibogluconate. This 14-day pediatric-adapted allometric miltefosine + paromomycin regimen showed again comparable drug exposure, pharmacokinetic target attainment, and efficacy between pediatric and adult patients and was found to be non-inferior to the current 17-day WHO-recommended paromomycin + sodium stibogluconate treatment [66]. This new 14-day allometric miltefosine + paromomycin regimen is currently being rolled out and access is being promoted by implementation in the treatment guidelines for visceral leishmaniasis in the Eastern African region. Similar shortened combination treatments based on the pediatric allometric miltefosine dosing regimen are currently being evaluated clinically in other clinical presentations of leishmaniasis such as post-kala-azar dermal leishmaniasis [67].

5.3 Use of Pharmacokinetic–Pharmacodynamic Models in Design of Clinical Studies

Two key aspects of a clinical trial including pharmacokinetics or longitudinal biomarker data collection are how many patients to include and when to sample. Pharmacokinetic–pharmacodynamic modeling can be used to guide design of clinical studies through power evaluation and clinical trial simulation. A prerequisite is that a population model describing the components of interest, directly or indirectly through extrapolation or assumptions, is available. Optimizing study design is important to maximize the chance to answer the posed research questions while minimizing the burden for participants and costs. Relevant approaches and tools are outlined in this section.
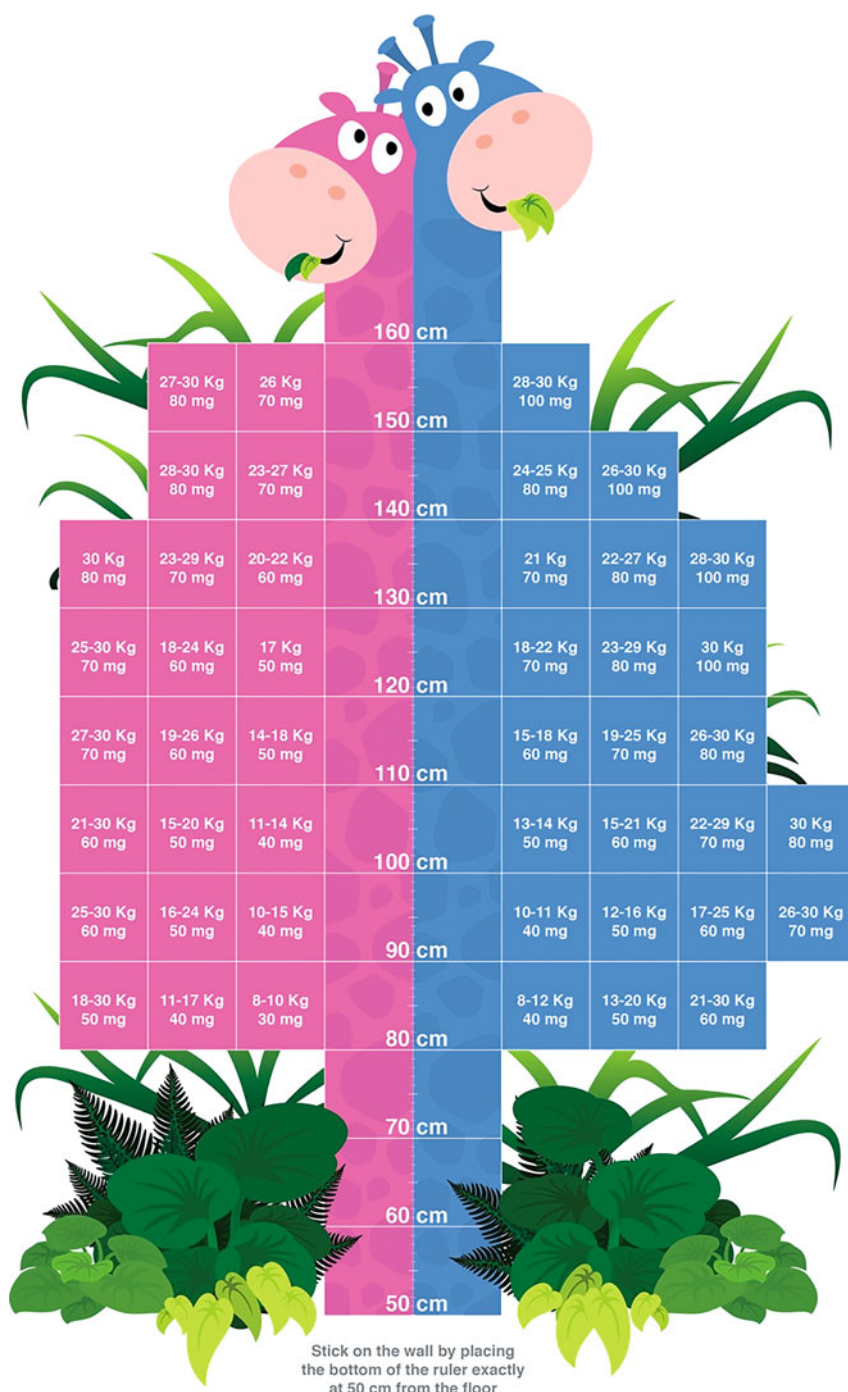
Fig. 5.1 Dosing table height chart for the pediatric allometric miltefosine regimen, based on fat-free mass of the pediatric visceral leishmaniasis patient, as used in clinical practice during the pediatric Phase II trial on allometric miltefosine in Kenya [62]

5.3.1 Stochastic Simulation and Estimation

The Stochastic Simulation and Estimation (SSE) approach is sometimes also called a parametric bootstrap. It is a tool that can investigate parameter identifiability and precision as well as power to detect a certain effect, answering question like "How long after dose administration do we need to sample to estimate clearance accurately?" or "How many subjects do we need to have at least 80% power to detect a covariate effect of X size on parameter Y?" An SSE consists of the following steps:

1. Make a data frame describing an initial sampling schedule
2. Add a virtual population of the initial sampling size, including covariates if relevant for the used simulation model
3. Simulate X number of clinical trials based on the population model and the data frame
4. Estimate the model parameters in each of the X simulated trials
5. If evaluating power: Estimate an alternative reduced model not including the effect of interest in each of the X simulated trials
6. Summarize the results, e.g., parameter precision and in the case of power estimation, the difference in objective function value (OFV) for the original and reduced alternative model. The power is the proportion of trials where the difference in OFV is larger than the relevant cut-off value for the desired statistical significance level.

How many trials should be simulated and estimated? This depends on the certainty needed in the results and the available computational resources. Commonly used numbers are between 100 and 1000. The results from the SSE only directly inform about the tested scenario, but parametric power estimation can be used to extrapolate to a full power curve [68]. To evaluate parameter precision and identifiability under other sampling schedules, the process needs to be repeated.

5.3.2 Monte-Carlo Mapped Power

The Monte-Carlo Mapped Power (MCMP) approach is a way to estimate power at different sample sizes [69]. It cannot evaluate other aspects like parameter precision. An MCMP consists of the following steps:

1. Make a data frame describing a selected sampling schedule
2. Make a large virtual population, including covariates if relevant for the used simulation model
3. Simulate results for the whole virtual population one time
4. Estimate on the whole virtual population one time with the original model and one time with the reduced model not including the effect of interest
5. Calculate the individual differences in OFV (ΔiOFV)

6. Randomly sample X ΔiOFV from the large dataset and sum up. Repeat 1000 times
7. Power for X individual is the proportion of the 1000 replicates where the difference in OFV is larger than the relevant cut-off value for desired statistical significance level
8. Repeat for X + 1, X + 2. . . individuals to get the full power curve

How large should the initial dataset to sample from be? It is relative to the sample size needed for desired power and a rule of thumb is at least 50 times larger than the sample size selected. Fulfillment of this condition should be checked in the end of the procedure. Both SSE and MCMP procedures can be automated though implementations in programs such as Perl-speaks-NONMEM (PsN) [70].

In the SSE and MCMP approaches, the user is required to provide an initial design of the study and a sampling schedule to start evaluations from. An alternative is optimal design methodology where an optimal sampling schedule is the output of the procedure. Optimal here means that model parameters are as precise as possible. The standard errors of parameter estimates are one measure of precision, and Optimal Design methodology utilizes the so-called Fisher Information Matrix to find a design that minimizes the standard errors. Optimal design procedure can be conducted in specialized software such as PopED or PFIM [71, 72]. Recently, the much-used software for population modeling NONMEM added functionality to perform simple design evaluation including optimization of sampling timepoints through the $DESIGN option [73].

5.3.3 Aiding the Study Design of Clinical Studies Focusing on Dose–Exposure–Response

An example of a pharmacometric-based model approach and the use of SSE in evaluating the study design of clinical trials was recently presented, investigating a parallel design versus cross-over design to assess the effect of two different dosing regimens on a pharmacodynamic toxicity outcome [74]. Irinotecan and its metabolite SN-38 are metabolized by the UGT1A1 enzyme, where genetic variants of this enzyme may confer reduced enzyme activity and lead to a phenotype that could be characterized as "poor metabolizer." The impact of a 30% initial dose reduction for these poor metabolizers based on the pharmacogenetic UGT1A1 profile on the irinotecan-induced hematologic toxicity versus non-reduced initial dose was assessed. The clinical trial simulation combined population pharmacokinetic models for irinotecan and its metabolite SN-38, in combination with a semi-mechanistic model of drug-induced myelosuppression to describe the time course of neutrophils and the incidence of grade 4 neutropenia. Through clinical trial simulations two study designs were compared, with a 21-day parallel design versus a 63-day cross-over design, based on virtual clinical trial populations including a proportion of poor metabolizers. Five-hundred clinical trial simulations were performed and were analyzed using two distinct data analysis methods (Fig. 5.2):
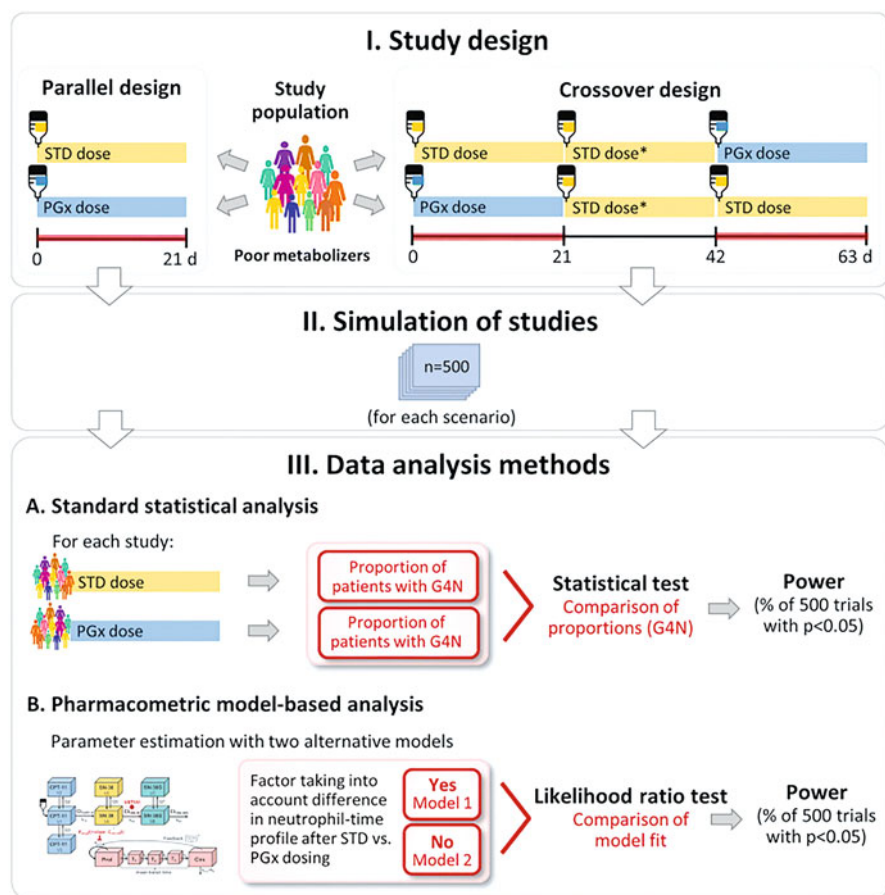
Fig. 5.2 Workflow of the pharmacometric model-based study design evaluation to assess the effect of the standard (STD) versus pharmacogenomic (PGx) dose of irinotecan on the pharmacodynamic endpoint of grade 4 neutropenia (G4N). (Reproduced from Minichmayr et al. Pharm Res. 2021 [74] under a Creative Commons Attribution 4.0 International License)

1. A conventional statistical analysis based on the comparison of fractions of patients experiencing grade 4 neutropenia for the reduced versus standard dose regimen.
2. A pharmacometric model-based analysis, where a base pharmacokinetic–pharmacodynamic model was compared to an alternative model with an additional estimated dose-dependent difference in the neutrophil-time profiles.

Consistently, the pharmacometric model-based analysis method showed a higher efficiency of identifying a difference in grade 4 neutropenia, resulting in a lower number of study participants in the trial to identify this difference. To achieve >80% power, with $\alpha = 0.05$, a study size of 220/100 patients per treatment arm/sequence was needed when using the conventional statistical approach, while only 100/15 patients were needed when using the model-based analysis approach for the parallel/

cross-over clinical study design, respectively. At the same time, the pharmacometric-based clinical trial simulations allowed the investigation of alternative scenarios and the impact of certain model assumptions and study design features, through sensitivity analyses. This not only helps rationalizing the design of the clinical trial, but also aids to avoid unfeasible trials. For instance, it was shown that the parallel versus cross-over study design had a major impact on the detectability of differences in occurrence of grade 4 neutropenia events. Additionally, the magnitude of the pharmacogenetic effect, i.e., the extent of reduction in metabolite clearance in poor metabolizers, was identified to have a high impact on the power of the study.

Other clinical trial simulations have shown similar advantages of analyzing the endpoints using a model-based analysis of clinical trial data compared to more conventional statistical analysis of the comparison of treatment arms or sequences. Consistently, model-based analyses have shown to reach a higher statistical power, resulting in a ≤ 8.5 times lower required sample size to identify an effect for a wide variety of study designs and therapeutic fields, such as stroke, diabetes, cancer, and hyperhidrosis [75–78]. This is an inherent effect of the higher information density in the model-based analysis due to consideration of all available longitudinal data and information contained in these data throughout the observation period in the clinical trial instead of an, often binary or categorical, outcome at a certain pre-specified time point or even a summary statistic of this longitudinal data.

References

1. Sheiner LB, Beal S, Rosenberg B, Marathe VV (1979) Forecasting individual pharmacokinetics. Clin Pharmacol Ther 26:294–305. https://doi.org/10.1002/cpt1979263294
2. Sheiner LB, Beal SL (1983) Evaluation of methods for estimating population pharmacokinetic parameters. III. Monoexponential model: routine clinical pharmacokinetic data. J Pharmacokinet Biopharm 11:303–319. https://doi.org/10.1007/BF01061870
3. Sheiner LB, Beal SL (1980) Evaluation of methods for estimating population pharmacokinetic parameters. I. Michaelis–Menten model: routine clinical pharmacokinetic data. J Pharmacokinet Biopharm 8:553–571. https://doi.org/10.1007/BF01060053
4. Sheiner LB, Rosenberg B, Marathe VV (1977) Estimation of population characteristics of pharmacokinetic parameters from routine clinical data. J Pharmacokinet Biopharm 5:445–479. https://doi.org/10.1007/BF01061728
5. McArthur GA, Chapman PB, Robert C, Larkin J, Haanen JB, Dummer R, Ribas A, Hogg D, Hamid O, Ascierto PA, Garbe C, Testori A, Maio M, Lorigan P, Lebbé C, Jouary T, Schadendorf D, O'Day SJ, Kirkwood JM, Eggermont AM, Dréno B, Sosman JA, Flaherty KT, Yin M, Caro I, Cheng S, Trunzer K, Hauschild A (2014) Safety and efficacy of vemurafenib in BRAF(V600E) and BRAF(V600K) mutation-positive melanoma (BRIM-3): extended follow-up of a phase 3, randomised, open-label study. Lancet Oncol 15:323–332. https://doi.org/10.1016/S1470-2045(14)70012-9
6. Henricks LM, Opdam FL, Beijnen JH, Cats A, Schellens JHM (2017) DPYD genotype-guided dose individualization to improve patient safety of fluoropyrimidine therapy: call for a drug label update. Ann Oncol 28:2915–2922. https://doi.org/10.1093/annonc/mdx411
7. Holford N, Ma G, Metz D (2022) TDM is dead. Long live TCI! Br J Clin Pharmacol 88:1406–1413. https://doi.org/10.1111/bcp.14434

8. Sheiner LB (1969) Computer-aided long-term anticoagulation therapy. Comput Biomed Res 2: 507–518. https://doi.org/10.1016/0010-4809(69)90030-5

9. Sheiner LB, Rosenberg B, Melmon KL (1972) Modelling of individual pharmacokinetics for computer-aided drug dosage. Comput Biomed Res 5:411–459. https://doi.org/10.1016/0010-4809(72)90051-1

10. Jelliffe RW, Buell J, Kalaba R (1972) Reduction of digitalis toxicity by computer-assisted glycoside dosage regimens. Ann Intern Med 77:891–906. https://doi.org/10.7326/0003-4819-77-6-891

11. Darwich AS, Ogungbenro K, Vinks AA, Powell JR, Reny J-L, Marsousi N, Daali Y, Fairman D, Cook J, Lesko LJ, McCune JS, Knibbe CAJ, de Wildt SN, Leeder JS, Neely M, Zuppa AF, Vicini P, Aarons L, Johnson TN, Boiani J, Rostami-Hodjegan A (2017) Why has model-informed precision dosing not yet become common clinical reality? Lessons from the past and a roadmap for the future. Clin Pharmacol Ther 101:646–656. https://doi.org/10.1002/cpt.659

12. Wright DFB, Martin JH, Cremers S (2019) Spotlight commentary: model-informed precision dosing must demonstrate improved patient outcomes. Br J Clin Pharmacol 85:2238–2240. https://doi.org/10.1111/bcp.14050

13. Neely MN, Kato L, Youn G, Kraler L, Bayard D, van Guilder M, Schumitzky A, Yamada W, Jones B, Minejima E (2018) Prospective trial on the use of trough concentration versus area under the curve to determine therapeutic vancomycin dosing. Antimicrob Agents Chemother 62:e02042–e02017. https://doi.org/10.1128/AAC.02042-17

14. Fuchs A, Csajka C, Thoma Y, Buclin T, Widmer N (2013) Benchmarking therapeutic drug monitoring software: a review of available computer tools. Clin Pharmacokinet 52:9–22. https://doi.org/10.1007/s40262-012-0020-y

15. Kantasiripitak W, Van Daele R, Gijsen M, Ferrante M, Spriet I, Dreesen E (2020) Software tools for model-informed precision dosing: how well do they satisfy the needs? Front Pharmacol 11:620. https://doi.org/10.3389/fphar.2020.00620

16. Keizer RJ, ter Heine R, Frymoyer A, Lesko LJ, Mangat R, Goswami S (2018) Model-informed precision dosing at the bedside: scientific challenges and opportunities. CPT Pharmacometrics Syst Pharmacol 7:785–787. https://doi.org/10.1002/psp4.12353

17. Cheng Y, Wang C-Y, Li Z-R, Pan Y, Liu M-B, Jiao Z (2021) Can population pharmacokinetics of antibiotics be extrapolated? Implications of external evaluations. Clin Pharmacokinet 60:53–68. https://doi.org/10.1007/s40262-020-00937-4

18. Broeker A, Nardecchia M, Klinker KP, Derendorf H, Day RO, Marriott DJ, Carland JE, Stocker SL, Wicha SG (2019) Towards precision dosing of vancomycin: a systematic evaluation of pharmacometric models for Bayesian forecasting. Clin Microbiol Infect 25:1286.e1–1286.e7. https://doi.org/10.1016/j.cmi.2019.02.029

19. Hughes JH, Tong DMH, Lucas SS, Faldasz JD, Goswami S, Keizer RJ (2021) Continuous learning in model-informed precision dosing: a case study in pediatric dosing of vancomycin. Clin Pharmacol Ther 109:233–242. https://doi.org/10.1002/cpt.2088

20. Uster DW, Stocker SL, Carland JE, Brett J, Marriott DJE, Day RO, Wicha SG (2021) A model averaging/selection approach improves the predictive performance of model-informed precision dosing: vancomycin as a case study. Clin Pharmacol Ther 109:175–183. https://doi.org/10.1002/cpt.2065

21. Abrantes JA, Jönsson S, Karlsson MO, Nielsen EI (2019) Handling interoccasion variability in model-based dose individualization using therapeutic drug monitoring data. Br J Clin Pharmacol 85:1326–1336. https://doi.org/10.1111/bcp.13901

22. Hamberg A-K, Wadelius M, Lindh JD, Dahl ML, Padrini R, Deloukas P, Rane A, Jonsson EN (2010) A pharmacometric model describing the relationship between warfarin dose and INR response with respect to variations in CYP2C9, VKORC1, and age. Clin Pharmacol Ther 87:727–734. https://doi.org/10.1038/clpt.2010.37

23. Hamberg A-K, Dahl M-L, Barban M, Scordo MG, Wadelius M, Pengo V, Padrini R, Jonsson EN (2007) A PK-PD model for predicting the impact of age, CYP2C9, and VKORC1 genotype

on individualization of warfarin therapy. Clin Pharmacol Ther 81:529–538. https://doi.org/10.1038/sj.clpt.6100084

24. Hamberg A-K, Friberg LE, Hanséus K, Ekman-Joelsson B-M, Sunnegårdh J, Jonzon A, Lundell B, Jonsson EN, Wadelius M (2013) Warfarin dose prediction in children using pharmacometric bridging – comparison with published pharmacogenetic dosing algorithms. Eur J Clin Pharmacol 69:1275–1283. https://doi.org/10.1007/s00228-012-1466-4

25. Hamberg A-K, Hellman J, Dahlberg J, Jonsson EN, Wadelius M (2015) A Bayesian decision support tool for efficient dose individualization of warfarin in adults and children. BMC Med Inform Decis Mak 15:7. https://doi.org/10.1186/s12911-014-0128-0

26. Friberg LE, Henningsson A, Maas H, Nguyen L, Karlsson MO (2002) Model of chemotherapy-induced myelosuppression with parameter consistency across drugs. J Clin Oncol 20:4713–4721. https://doi.org/10.1200/JCO.2002.02.140

27. Wallin JE, Friberg LE, Karlsson MO (2009) A tool for neutrophil guided dose adaptation in chemotherapy. Comput Methods Prog Biomed 93:283–291. https://doi.org/10.1016/j.cmpb.2008.10.011

28. Netterberg I, Nielsen EI, Friberg LE, Karlsson MO (2017) Model-based prediction of myelosuppression and recovery based on frequent neutrophil monitoring. Cancer Chemother Pharmacol 80:343–353. https://doi.org/10.1007/s00280-017-3366-x

29. Maier C, Hartung N, de Wiljes J, Kloft C, Huisinga W (2020) Bayesian data assimilation to support informed decision making in individualized chemotherapy. CPT Pharmacometrics Syst Pharmacol 9:153–164. https://doi.org/10.1002/psp4.12492

30. Maier C, Hartung N, Kloft C, Huisinga W, de Wiljes J (2021) Reinforcement learning and Bayesian data assimilation for model-informed precision dosing in oncology. CPT Pharmacometrics Syst Pharmacol 10:241–254. https://doi.org/10.1002/psp4.12588

31. Verheijen RB, Yu H, Schellens JHM, Beijnen JH, Steeghs N, Huitema ADR (2017) Practical recommendations for therapeutic drug monitoring of kinase inhibitors in oncology. Clin Pharmacol Ther 102:765–776. https://doi.org/10.1002/cpt.787

32. Janssen JM, Dorlo TPC, Steeghs N, Beijnen JH, Hanff LM, van Eijkelenburg NKA, van der Lugt J, Zwaan CM, Huitema ADR (2020) Pharmacokinetic targets for therapeutic drug monitoring of small molecule kinase inhibitors in pediatric oncology. Clin Pharmacol Ther 108:494–505. https://doi.org/10.1002/cpt.1808

33. Hansson EK, Ma G, Amantea MA, French J, Milligan PA, Friberg LE, Karlsson MO (2013) PKPD modeling of predictors for adverse effects and overall survival in Sunitinib-treated patients with GIST. CPT Pharmacometrics Syst Pharmacol 2:e85. https://doi.org/10.1038/psp.2013.62

34. Hansson EK, Amantea MA, Westwood P, Milligan PA, Houk BE, French J, Karlsson MO, Friberg LE (2013) PKPD modeling of VEGF, sVEGFR-2, sVEGFR-3, and sKIT as predictors of tumor dynamics and overall survival following Sunitinib treatment in GIST. CPT Pharmacometrics Syst Pharmacol 2:e84. https://doi.org/10.1038/psp.2013.61

35. Centanni M, Friberg LE (2020) Model-based biomarker selection for dose individualization of tyrosine-kinase inhibitors. Front Pharmacol 11:316. https://doi.org/10.3389/fphar.2020.00316

36. Verrest L, Dorlo TPC (2017) Lack of clinical pharmacokinetic studies to optimize the treatment of neglected tropical diseases: a systematic review. Clin Pharmacokinet 56:583–606. https://doi.org/10.1007/s40262-016-0467-3

37. Food and Drug Administration (FDA) (2022) General clinical pharmacology considerations for pediatric studies of drugs, including biological products. In: U.S. Food and Drug Administration. https://www.fda.gov/regulatory-information/search-fda-guidance-documents/general-clinical-pharmacology-considerations-pediatric-studies-drugs-including-biological-products. Accessed 14 Dec 2022

38. Cella M, Knibbe C, Danhof M, Della Pasqua O (2010) What is the right dose for children? Br J Clin Pharmacol 70:597–603. https://doi.org/10.1111/j.1365-2125.2009.03591.x

39. Kleiber M (1947) Body size and metabolic rate. Physiol Rev 27:511–541. https://doi.org/10.1152/physrev.1947.27.4.511

40. Edginton AN, Shah B, Sevestre M, Momper JD (2013) The integration of Allometry and virtual populations to predict clearance and clearance variability in pediatric populations over the age of 6 years. Clin Pharmacokinet 52:693–703. https://doi.org/10.1007/s40262-013-0065-6

41. Anderson BJ, Holford NHG (2008) Mechanism-based concepts of size and maturity in pharmacokinetics. Annu Rev Pharmacol Toxicol 48:303–332. https://doi.org/10.1146/annurev.pharmtox.48.113006.094708

42. Denti P, Wasmann RE, Francis J, McIlleron H, Sugandhi N, Cressey TR, Mirochnick M, Capparelli EV, Penazzato M, WHO Pediatric Antiretroviral Working Group (2022) One dose does not fit all: revising the WHO paediatric dosing tool to include the non-linear effect of body size and maturation. Lancet Child Adolesc Health 6:9–10. https://doi.org/10.1016/S2352-4642(21)00302-3

43. Yerramsetti S, Cohen T, Atun R, Menzies NA (2022) Global estimates of paediatric tuberculosis incidence in 2013-19: a mathematical modelling analysis. Lancet Glob Health 10:e207–e215. https://doi.org/10.1016/S2214-109X(21)00462-9

44. World Health Organization (WHO) WHO operational handbook on tuberculosis: module 5: management of tuberculosis in children and adolescents. https://www.who.int/publications-detail-redirect/9789240046832. Accessed 14 Dec 2022

45. World Health Organization (WHO) Report of a WHO expert consultation on dosing to enable implementation of treatment recommendations in the WHO consolidated guidelines on the management of TB in children and adolescents. https://www.who.int/publications-detail-redirect/9789240055193. Accessed 14 Dec 2022

46. Diacon AH, Pym A, Grobusch MP, de los Rios JM, Gotuzzo E, Vasilyeva I, Leimane V, Andries K, Bakare N, De Marez T, Haxaire-Theeuwes M, Lounis N, Meyvisch P, De Paepe E, van Heeswijk RPG, Dannemann B, TMC207-C208 Study Group (2014) Multidrug-resistant tuberculosis and culture conversion with bedaquiline. N Engl J Med 371:723–732. https://doi.org/10.1056/NEJMoa1313865

47. World Health Organization (WHO) Rapid communication on updated guidance on the management of tuberculosis in children and adolescents. https://www.who.int/publications-detail-redirect/9789240033450. Accessed 14 Dec 2022

48. van Heeswijk RPG, Dannemann B, Hoetelmans RMW (2014) Bedaquiline: a review of human pharmacokinetics and drug-drug interactions. J Antimicrob Chemother 69:2310–2318. https://doi.org/10.1093/jac/dku171

49. Svensson EM, Karlsson MO (2017) Modelling of mycobacterial load reveals bedaquiline's exposure-response relationship in patients with drug-resistant TB. J Antimicrob Chemother 72:3398–3405. https://doi.org/10.1093/jac/dkx317

50. Tanneau L, Svensson EM, Rossenu S, Karlsson MO (2021) Exposure-safety analysis of QTc interval and transaminase levels following bedaquiline administration in patients with drug-resistant tuberculosis. CPT Pharmacometrics Syst Pharmacol 10:1538–1549. https://doi.org/10.1002/psp4.12722

51. Svensson EM, Yngman G, Denti P, McIlleron H, Kjellsson MC, Karlsson MO (2018) Evidence-based Design of Fixed-Dose Combinations: principles and application to pediatric anti-tuberculosis therapy. Clin Pharmacokinet 57:591–599. https://doi.org/10.1007/s40262-017-0577-6

52. Svensson EM, Dosne A-G, Karlsson MO (2016) Population pharmacokinetics of Bedaquiline and metabolite M2 in patients with drug-resistant tuberculosis: the effect of time-varying weight and albumin. CPT Pharmacometrics Syst Pharmacol 5:682–691. https://doi.org/10.1002/psp4.12147

53. Johnson TN, Rostami-Hodjegan A, Tucker GT (2006) Prediction of the clearance of eleven drugs and associated variability in neonates, infants and children. Clin Pharmacokinet 45:931–956. https://doi.org/10.2165/00003088-200645090-00005

54. Salem F, Johnson TN, Abduljalil K, Tucker GT, Rostami-Hodjegan A (2014) A re-evaluation and validation of ontogeny functions for cytochrome P450 1A2 and 3A4 based on in vivo data. Clin Pharmacokinet 53:625–636. https://doi.org/10.1007/s40262-014-0140-7

55. Dorlo TPC, Balasegaram M, Beijnen JH, de Vries PJ (2012) Miltefosine: a review of its pharmacology and therapeutic efficacy in the treatment of leishmaniasis. J Antimicrob Chemother 67:2576–2597. https://doi.org/10.1093/jac/dks275

56. Sundar S, Jha TK, Sindermann H, Junge K, Bachmann P, Berman J (2003) Oral miltefosine treatment in children with mild to moderate Indian visceral leishmaniasis. Pediatr Infect Dis J 22:434–438. https://doi.org/10.1097/01.inf.0000066877.72624.cb

57. Rijal S, Ostyn B, Uranw S, Rai K, Bhattarai NR, Dorlo TPC, Beijnen JH, Vanaerschot M, Decuypere S, Dhakal SS, Das ML, Karki P, Singh R, Boelaert M, Dujardin J-C (2013) Increasing failure of miltefosine in the treatment of Kala-azar in Nepal and the potential role of parasite drug resistance, reinfection, or noncompliance. Clin Infect Dis 56:1530–1538. https://doi.org/10.1093/cid/cit102

58. Ostyn B, Hasker E, Dorlo TPC, Rijal S, Sundar S, Dujardin J-C, Boelaert M (2014) Failure of miltefosine treatment for visceral leishmaniasis in children and men in South-East Asia. PLoS One 9:e100220. https://doi.org/10.1371/journal.pone.0100220

59. Dorlo TPC, Rijal S, Ostyn B, de Vries PJ, Singh R, Bhattarai N, Uranw S, Dujardin J-C, Boelaert M, Beijnen JH, Huitema ADR (2014) Failure of miltefosine in visceral leishmaniasis is associated with low drug exposure. J Infect Dis 210:146–153. https://doi.org/10.1093/infdis/jiu039

60. Wasunna M, Njenga S, Balasegaram M, Alexander N, Omollo R, Edwards T, Dorlo TPC, Musa B, Ali MHS, Elamin MY, Kirigi G, Juma R, Kip AE, Schoone GJ, Hailu A, Olobo J, Ellis S, Kimutai R, Wells S, Khalil EAG, Strub Wourgaft N, Alves F, Musa A (2016) Efficacy and safety of AmBisome in combination with sodium stibogluconate or miltefosine and miltefosine monotherapy for African Visceral Leishmaniasis: phase II randomized trial. PLoS Negl Trop Dis 10:e0004880. https://doi.org/10.1371/journal.pntd.0004880

61. Dorlo TPC, Kip AE, Younis BM, Ellis SJ, Alves F, Beijnen JH, Njenga S, Kirigi G, Hailu A, Olobo J, Musa AM, Balasegaram M, Wasunna M, Karlsson MO, Khalil EAG (2017) Visceral leishmaniasis relapse hazard is linked to reduced miltefosine exposure in patients from Eastern Africa: a population pharmacokinetic/pharmacodynamic study. J Antimicrob Chemother 72:3131–3140. https://doi.org/10.1093/jac/dkx283

62. Mbui J, Olobo J, Omollo R, Solomos A, Kip AE, Kirigi G, Sagaki P, Kimutai R, Were L, Omollo T, Egondi TW, Wasunna M, Alvar J, Dorlo TPC, Alves F (2019) Pharmacokinetics, safety, and efficacy of an Allometric Miltefosine regimen for the treatment of visceral Leishmaniasis in eastern African children: an open-label, phase II clinical trial. Clin Infect Dis 68:1530–1538. https://doi.org/10.1093/cid/ciy747

63. Bhattacharya SK, Sinha PK, Sundar S, Thakur CP, Jha TK, Pandey K, Das VR, Kumar N, Lal C, Verma N, Singh VP, Ranjan A, Verma RB, Anders G, Sindermann H, Ganguly NK (2007) Phase 4 trial of miltefosine for the treatment of Indian visceral leishmaniasis. J Infect Dis 196:591–598. https://doi.org/10.1086/519690

64. Dorlo TPC, Huitema ADR, Beijnen JH, de Vries PJ (2012) Optimal dosing of miltefosine in children and adults with visceral leishmaniasis. Antimicrob Agents Chemother 56:3864–3872. https://doi.org/10.1128/AAC.00292-12

65. Palić S, Kip AE, Beijnen JH, Mbui J, Musa A, Solomos A, Wasunna M, Olobo J, Alves F, Dorlo TPC (2020) Characterizing the non-linear pharmacokinetics of miltefosine in paediatric visceral leishmaniasis patients from Eastern Africa. J Antimicrob Chemother 75:3260–3268. https://doi.org/10.1093/jac/dkaa314

66. Musa AM, Mbui J, Mohammed R, Olobo J, Ritmeijer K, Alcoba G, Muthoni Ouattara G, Egondi T, Nakanwagi P, Omollo T, Wasunna M, Verrest L, Dorlo TPC, Musa Younis B, Nour A, Taha Ahmed Elmukashfi E, Ismail Omer Haroun A, Khalil EAG, Njenga S, Fikre H, Mekonnen T, Mersha D, Sisay K, Sagaki P, Alvar J, Solomos A, Alves F (2022) Paromomycin and Miltefosine combination as an alternative to treat patients with visceral Leishmaniasis in eastern Africa: a randomized, controlled, multicountry trial. Clin Infect Dis:ciac643. https://doi.org/10.1093/cid/ciac643

67. Drugs for Neglected Diseases (2020) An open label, randomized, parallel arm clinical trial of two regimens to assess the safety and efficacy for treatment of Post Kala-azar Dermal Leishmaniasis (PKDL) Patients in Sudan. clinicaltrials.gov

68. Ueckert S, Karlsson MO, Hooker AC (2016) Accelerating Monte Carlo power studies through parametric power estimation. J Pharmacokinet Pharmacodyn 43:223–234. https://doi.org/10.1007/s10928-016-9468-y

69. Vong C, Bergstrand M, Nyberg J, Karlsson MO (2012) Rapid sample size calculations for a defined likelihood ratio test-based power in mixed-effects models. AAPS J 14:176–186. https://doi.org/10.1208/s12248-012-9327-8

70. Lindbom L, Pihlgren P, Jonsson EN (2005) PsN-Toolkit – a collection of computer intensive statistical methods for non-linear mixed effect modeling using NONMEM. Comput Methods Prog Biomed 79:241–257. https://doi.org/10.1016/j.cmpb.2005.04.005

71. Nyberg J, Ueckert S, Strömberg EA, Hennig S, Karlsson MO, Hooker AC (2012) PopED: an extended, parallelized, nonlinear mixed effects models optimal design tool. Comput Methods Prog Biomed 108:789–805. https://doi.org/10.1016/j.cmpb.2012.05.005

72. Dumont C, Lestini G, Le Nagard H, Mentré F, Comets E, Nguyen TT, PFIM Group (2018) PFIM 4.0, an extended R program for design evaluation and optimization in nonlinear mixed-effect models. Comput Methods Prog Biomed 156:217–229. https://doi.org/10.1016/j.cmpb.2018.01.008

73. Bauer RJ, Hooker AC, Mentre F (2021) Tutorial for $DESIGN in NONMEM: clinical trial evaluation and optimization. CPT Pharmacometrics Syst Pharmacol 10:1452–1465. https://doi.org/10.1002/psp4.12713

74. Minichmayr IK, Karlsson MO, Jönsson S (2021) Pharmacometrics-based considerations for the design of a Pharmacogenomic clinical trial assessing irinotecan safety. Pharm Res 38:593–605. https://doi.org/10.1007/s11095-021-03024-w

75. Karlsson KE, Vong C, Bergstrand M, Jonsson EN, Karlsson MO (2013) Comparisons of analysis methods for proof-of-concept trials. CPT Pharmacometrics Syst Pharmacol 2:e23. https://doi.org/10.1038/psp.2012.24

76. Mehrotra S, Schmith VD, Dumitrescu TP, Gobburu J (2015) Pharmacometrics-guided drug development of antihyperhidrosis agents. J Clin Pharmacol 55:1256–1267. https://doi.org/10.1002/jcph.536

77. Langenhorst JB, Dorlo TPC, van Kesteren C, van Maarseveen EM, Nierkens S, de Witte MA, Boelens JJ, Huitema ADR (2020) Clinical trial simulation to optimize trial design for fludarabine dosing strategies in allogeneic hematopoietic cell transplantation. CPT Pharmacometrics Syst Pharmacol 9:272–281. https://doi.org/10.1002/psp4.12486

78. Karlsson KE, Grahnén A, Karlsson MO, Jonsson EN (2007) Randomized exposure-controlled trials; impact of randomization and analysis strategies. Br J Clin Pharmacol 64:266–277. https://doi.org/10.1111/j.1365-2125.2007.02887.x

Chapter 6
On the Verge of Impossibility: Accounting for Variability Arising from Permutations of Comorbidities that Affect the Fate of Drugs in the Human Body

Amin Rostami-Hodjegan and Brahim Achour

Abstract Contending with variability in drug exposure and effect in disease populations requires patient characterization for changes in drug metabolism and transport pathways and predictive modelling platforms within the framework of systems pharmacology. In this chapter, we explore current and emerging patient characterization approaches, the role of physiologically based pharmacokinetic modelling in stratified versus individualized predictions, the possibility of exploring the impact of permutations of comorbidities, and application of these elements in model-informed precision dosing.

6.1   Introduction

> "*Variability is the law of life*, and as no two faces are the same, so no two bodies are alike, and no individuals react alike and behave alike under the abnormal conditions which we know as disease" – Sir William Osler (1849–1919), Professor of Medicine, Oxford, England

Current drug development mainly focuses on 'typical' representation of patients and many of the subtypes involving other comorbidities are studied at later stages after regulatory approval. The latter does not provide any evidence for potential

---

A. Rostami-Hodjegan (✉)
The University of Manchester, Centre for Applied Pharmacokinetic Research, Manchester, UK
e-mail: amin.rostami@manchester.ac.uk

B. Achour
Department of Biomedical and Pharmaceutical Sciences, University of Rhode Island, Kingston, RI, USA
e-mail: achour@uri.edu

requirements of dosage adjustment that might be necessary for effective and safe medication of patients with certain comorbidities or combinations of these. Hence, in recent years, drug regulatory agencies, as well as professional associations related to drug development and pharmacotherapy, advocated widening the recruitment criteria during clinical studies to provide information on the fate of drugs beyond what is known in a 'typical patient'. Two recent Guidance for the Industry documents issued by the US Food and Drug Administration (FDA) concerning "Enhancing the Diversity of Clinical Trial Populations — Eligibility Criteria, Enrollment Practices, and Trial Designs" [41] and "Diversity Plans to Improve Enrollment of Participants from Underrepresented Racial and Ethnic Populations in Clinical Trials" [42] are typical examples of such attempts. Although widening recruitment improves gathering of information, and subsequent data analysis can highlight some of the significant changes using sparse samples and non-linear mixed-effect models (so-called population pharmacokinetics or POP-PK), these are not a panacea for the huge lack of data in special populations that may suffer from more than one or two comorbidities. Requesting conduct of clinical studies for every given permutation of concurrent comorbidities places such an act on the verge of impossibility for any drug development entity. However, we cannot leave patients in such special groups without sound and scientific decisions on the best dosage regimen for a given drug and permit off-label use to become the norm for these patients.

The solution may lie within the so-called mechanistic models framing the fate of drugs. These are known as physiologically based pharmacokinetic (PBPK) models and they can accommodate and propagate the physiological and pathological changes in bodily systems to consequences for any given drug if the interplay of parameters with the drug is adequately characterized using in vitro systems. Even in the case of known comorbidities, such as organ impairment (mainly renal or hepatic), which are assessed much more often than other conditions regarding their impact on the fate of drugs, Jadhav et al. [49] reported in 2015 that over 50% of drugs released onto market did not have any information on the impact of severe impairment. These authors as well as others went on to say that PBPK models can fill the void in such conditions. The situation with the void of information on subpopulations has not improved since the report by Jadhav et al. in 2015 as evidenced by our internal unpublished data that demonstrate the case for renal impairment patients (Fig. 6.1). In this chapter, we explore the role of PBPK, in conjunction with existing and emerging patient characterization approaches, in addressing this lack of dosing information for special populations.
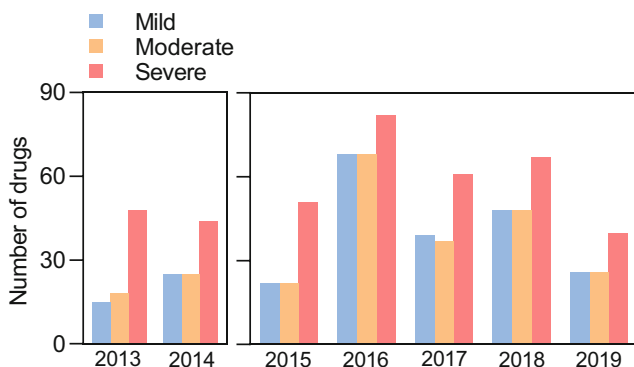
Fig. 6.1 The number of FDA-approved drugs without explicit dosing recommendation for patients with renal impairment at the point of entry to the market. The plot shows data (for 2013 and 2014) from Jadhav et al. [49] and unpublished in-house data (for 2015–2019)
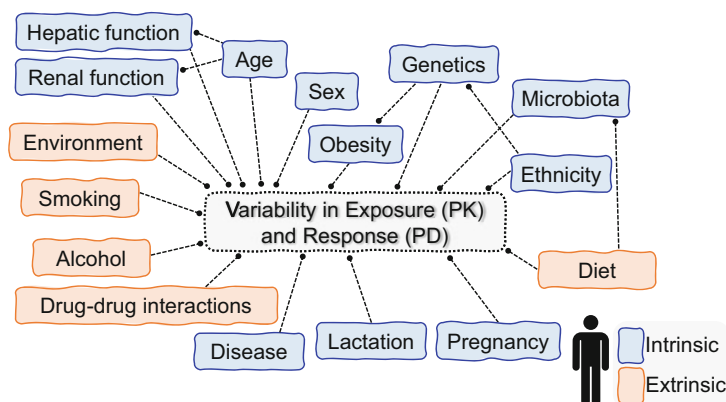
Fig. 6.2 Factors intrinsic and extrinsic to the patient which affect variability in drug exposure and response. Factors are inter-dependent making accounting for their effect challenging. The use of modelling allows prediction of the effect of different permutations of such factors. Abbreviations: *PD* pharmacodynamics, *PK* pharmacokinetics

6.2 Accounting for Sources of Interindividual Variability in Pharmacokinetics

Numerous internal and external factors, with complex interplay, affect between-patient variability in drug kinetics (Fig. 6.2); these have an impact on patient physiology, biology, and expression of proteins involved in drug disposition. Other factors unrelated to patient biology, such as compliance, can also add to the apparent PK variability [68]. Quantitative assessment of variability in the fate of drugs in the body due to these factors follows mathematical formalism of pharmacokinetics. This can be in the form of simple equations that describe temporal

changes of drug concentration after dosing. Finding the covariates that define interindividual differences in the various model parameters is an a posteriori activity within these models (e.g. using POP-PK methods for sparse samples that employ non-linear mixed-effect methods). However, predicting such individual variations in concentration–time profiles in advance of conducting clinical studies requires more mechanistic models in the form of physiologically based pharmacokinetics (PBPK) [19].

Adequate drug exposure, as defined by the area under the curve of the concentration-time profile (AUC) or either maximum or minimum exposure, respectively defined by the highest concentration (C_{max}) or trough concentration (C_{trough}), is an essential element of reaching therapeutic response. Together, absorption, distribution, metabolism, and excretion (ADME) of drugs determine the features of the concentration-time profile following drug administration. Data generated from in vitro studies are used to determine and understand ADME variations in different individuals by integration of data with PBPK models [80, 81]. However, the multi-scale nature of these mechanistic models [96] necessitates large efforts and wide expertise to create and verify the model elements, putting PBPK under the framework of systems pharmacology/biology [51] that requires drug-independent systems data, as enlisted below [52].

- Physiological, anatomical, biological, and biochemical data for each individual (some are defined based on demography, such as ethnicity, sex, age, and environment of the population that an individual belongs to when the actual individual values are not known).
- Trial design parameters, such as the conditions under which the drug is taken (e.g. fed versus fasted state) or any concomitant drugs interfering with the functions of the systems that handle the drug (e.g. perturbing enzyme expression or function).

The above are combined with drug data (physicochemical properties, e.g. LogP and pKa, drug intrinsic clearance by certain enzymes, affinity to certain transporters) to help not only understand but also predict the behaviour of the drug in certain individuals or a subgroup of patients using a realistic compartmental structure defined as a set of differential equations. Critical considerations are listed below.

- The factors affecting the variability of the absorption and bioavailability of orally administered drugs are described previously [53]. It is important to note that cytochrome P450 (CYP) 3A and multidrug resistance P-glycoprotein (P-gp), which have wide interindividual variability, are present at high levels in the villi tips of enterocytes in the small intestine [6] and they can cause variations in the bioavailability of drugs, as shown for tacrolimus controlled-release formulation in the case of Afro-Americans versus their Caucasian counterparts [60, 91]. Variations in these proteins as well as other CYP and non-CYP enzymes and transporters in the small intestine are demonstrated in disease states, such as Crohn's disease [9] and can play a significant role in altering the fate of drugs in such patients [10].

- Early screening tools can assess the relative importance of the routes of metabolism by various metabolic pathways. Hence, it is now possible to employ information on in vivo intrinsic clearance as well as transporter-mediated uptake to postulate about variability associated with hepatic clearance in human populations [80]. This is facilitated with knowledge of scaling factors [1, 2, 13, 67].
- Aspects defining variations in renal excretion are also formulated under systems pharmacology [83, 84] and capture the role of urine flow and pH alongside the physical chemistry, lipophilicity, and ionization of the compound that define plasma protein and erythrocyte binding and add knowledge of drug affinity to efflux transporters [85] and abundance of such transporters in human kidney [7].
- Variability in volume of distribution does not have an impact on overall exposure (as measured by AUC_0). However, it defines the shape of the temporal changes of the concentration-time profiles (C_{max} and C_{trough}); hence, defining/predicting its variability is important. The physical volume of tissues and their blood flows are components of PBPK models that capture population variability related to these parameters. Nonetheless, there are other aspects of the volume of distribution which are more relevant to protein binding in the systemic circulation as well as tissues. Many of these can be measured in vitro and used for in vitro–in vivo extrapolation (IVIVE) purposes through PBPK models [16, 72, 75].

6.3 The Growing Role of Physiologically Based Pharmacokinetics (PBPK)

In a recent survey, El-Khateeb et al. [37] demonstrated that the first two decades of the twenty-first century have witnessed a more than 40-fold increase in the applications of PBPK (based on the number of publications in the literature). This was in contrast to the general discipline of pharmacokinetics which had a relatively modest increase of around fourfold, in line with an increase in the bulk of scientific publications by threefold. The fastest growing area of PBPK applications according to the survey was focused on addressing alterations to kinetics (or lack thereof) in special populations. Indeed, this was one of the areas that regulatory scientists advocated for the use of PBPK over a decade ago [101] by harnessing the natural compatibility between PBPK and assessment of internal/external factors affecting the kinetics of drugs in various patients.

So, what are the attributes of PBPK that make it so popular with determining the impact of patient variability? The essence of PBPK modelling was described by Rostami-Hodjegan [77] in relation to separation of the system parameters from those of drugs and formulations (Fig. 6.3). Therapeutic effects of a minority of drugs can be monitored relatively easily using established biomarkers (e.g. international normalized ratio, INR, for anticoagulants, blood pressure for antihypertensive agents, and blood glucose for antidiabetic agents) for dose adjustment. However, for most
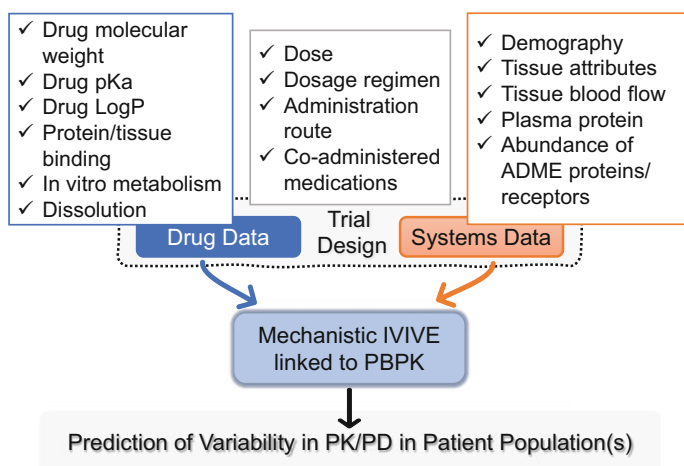
Fig. 6.3 Separation of parameters related to the drug from parameters related to the population in PBPK models. This approach enables testing different permutations of factors, allowing assessment of changes in PK (or PD) in the target population a priori to conducting clinical studies. Abbreviations: ADME, absorption, distribution, metabolism and excretion; IVIVE, in vitro–in vivo extrapolation; PBPK, physiologically based pharmacokinetics; PD, pharmacodynamics; PK, pharmacokinetics

drugs, such effects are not readily measurable or finding out the outcome takes a long time (e.g. patient survival). On the other hand, accounting for drug exposure differences can minimize a large part of the variation in patient outcomes that is related to kinetics. One of the major sources of variability in kinetics is related to interindividual differences in metabolic and transporter-mediated clearance. Clearance and first pass gut and liver metabolism together define internal exposure of the bioavailable dose after entering the gut wall. Many drugs have an optimal therapeutic window for exposure. Whereas for renal clearance, creatinine can be used as a general marker for glomerular filtration as well as active secretion of the drugs into the urine, hepatic clearance does not have a single universal marker that can be applied to all drugs. Characterization of metabolism becomes very important in various groups of patients when we consider that >70% of 698 orally administered marketed drugs have high levels of metabolism as part of their clearance [15]. As shown by Rostami-Hodjegan and Tucker [80], PBPK models can readily incorporate the known variations in drug metabolism and propagate them to projected clearance values using IVIVE techniques. Availability of liver [93, 99], intestinal [9, 33], brain [5, 17, 87], kidney [7, 57], skin [29], and lung [40] tissue for conducting quantitative analysis of proteins related to drug ADME has contributed to advancing a priori understanding of likely differences in kinetics in special populations before conducting any clinical studies. Table 6.1 summarizes prominent examples of such applications. With this approach, and if the baseline in healthy adults (or other control cohorts) is established, it is possible to simulate kinetics in special populations, such as foetal exposure to medications taken by pregnant mothers, or

Table 6.1 Prominent examples of recent applications of tissue proteomics in the investigation of disease impact on human drug metabolism and transport pathways

Disease/Condition	Tissue	Targets quantified	Drugs in PK simulations	Proteomic methods	Applications	References
Liver disease						
Cirrhosis (CP scores A–C)	Liver	14 CYPs, 9 UGTs, 8 non-CYP non-UGT enzymes, 19 transporters	Repaglinide, dabigatran etexilate, zidovudine	Targeted proteomics	Effect of disease; dose adjustment	El-Khateeb et al. [38]
Cirrhosis	Liver	7 CYPs, 4 UGTs, 6 non-CYP non-UGT enzymes	Zidovudine[a], morphine[a]; lamotrigine[b]	Targeted proteomics	Effect of disease; dose adjustment	Prasad et al. [74], Ladumor et al. [62]
Cirrhosis	Liver	12 transporters	Repaglinide[c]; rosuvastatin[d]	Targeted proteomics	Effect of disease; dose adjustment	Wang et al. [98], Kumar et al. [58]
Hepatitis C-induced, alcoholic, autoimmune, and cholestatic liver diseases	Liver	14 transporters	–	Targeted proteomics	Effect of disease	Drozdzik et al. [34]
Hepatitis C-induced, alcoholic, autoimmune, and cholestatic liver diseases	Liver	10 CYPs, 4 UGTs	–	Targeted proteomics	Effect of disease	Drozdzik et al. [35]
Liver disease (metastatic liver cancer, cirrhosis)	Liver (cancer set: tumorous and histologically normal tissue)	13 CYPs, 10 UGTs, 8 non-CYP non-UGT enzymes, 18 transporters	–	Targeted and global proteomics	Effect of disease	Vasilogianni et al. [93]
Metastatic liver cancer	Liver (tumorous and histologically normal tissue)	14 CYPs, 8 UGTs, 25 transporters	50 substrates (Simcyp library)	Targeted proteomics	Effect of disease; dose adjustment	Vasilogianni et al. [94]
		9 CYPs, 4 UGTs	–		Effect of disease	

(continued)

Table 6.1 (continued)

Disease/Condition	Tissue	Targets quantified	Drugs in PK simulations	Proteomic methods	Applications	References
Metastatic liver cancer	Liver (histologically normal tissue)			Targeted proteomics		Kurzawski et al. [59]
Primary liver cancer	Liver	10 transporters	–	Targeted proteomics	Effect of disease	Billington et al. [17]
Hepatitis C-induced liver disease	Liver	15 transporters	–	Targeted proteomics	Effect of disease	Drozdzik et al. [36]
NAFLD/NASH with type 2 diabetes mellitus	Liver	CYP3A4	Midazolam	Global proteomics	Effect of comorbidity on CYP3A substrates	Jamwal et al. [54]
Wilson's disease	Liver	10 CYPs, 4 UGTs, 16 transporters	–	Targeted proteomics	Effect of disease	Szelag-Pieniek et al. [90]
Kidney disease						
Kidney cancer	Kidney cortex (histologically normal)	9 enzymes, 22 transporters	–	Targeted and global proteomics	Quantitative expression in disease; local kinetics in kidney	Al-Majdoub et al. [7]
Kidney cancer	Kidney cortex (histologically normal)	20 transporters	–	Targeted proteomics	Effect of disease on renal tissue expression	Oswald et al. [69]
Kidney cancer	Kidney cortex (histologically normal)	12 transporters	Metformin[e]	Targeted proteomics	Regional expression of transporters; IVIVE of renal secretory clearance	Prasad et al. [73], Kumar et al. [57]

Intestinal disease

Crohn's disease	Ileum, colon	13 CYPs, 5 UGTs, 28 non-CYP non-UGT enzymes, 58 transports	Verapamil[f], digoxin[f], rosuvastatin[f]	Global proteomics	Effect of (inflamed and non-inflamed) disease; changes in oral bioavailability	Alrubia et al. [9], Alrubia et al. [10]
Ulcerative colitis	Colon	14 transporters	–	Targeted proteomics	Effect of disease and inflammation on enzymes[i] and transporters	Erdmann et al. [39]

Neuropathology

Dementia (Alzheimer's disease, dementia with Lewy bodies)	Brain cortex (frontal lobe)	53 transporters	–	Targeted and global proteomics	Effect of disease on blood-brain barrier (BBB) transporters	Al-Majdoub et al. [5]
Alzheimer's disease	Hippocampus, parietal lobe, cerebellum	4 transporters and 1 receptor (LRP1)	–	Targeted proteomics	Effects of disease on BBB transporters in different regions of the brain	Storelli et al. [89]
Glioblastoma	Brain cortex	6 transporters	Fexofenadine	Targeted proteomics	Effect of disease on brain drug exposure	Bao et al. [14]
Epilepsy	Brain cortex	5 transporters	–	Targeted proteomics	Effects of epilepsy on transporter abundance and vasculature in the brain	Brukner et al. [22]
Epilepsy	Brain cortex	7 enzymes and 19 transporters	–	Targeted proteomics	Effect of disease on BBB transporters	Shawahna et al. [87]

(continued)

Table 6.1 (continued)

Disease/Condition	Tissue	Targets quantified	Drugs in PK simulations	Proteomic methods	Applications	References
Obesity						
	Liver	OATP1B1, OATP1B3, OATP2B1, NTCP	Rosuvastatin	Global proteomics	Prediction of individual drug exposure	Wegler et al. [99]
	Jejunum	CYP3A4, UGT2B7, P-gp, MRP2, MRP3	Morphine	Targeted proteomics	Oral kinetics in obesity	Lloret-Linares et al. [64]
	Jejunum	13 CYPs, 9 UGTs, 29 transporters	–	Targeted proteomics	Effect of disease on enzymes and transporters	Miyauchi et al. [66]
	Liver, jejunum	CYP3A4	Midazolam	Global proteomics	Dose individualization using 4-β-hydroxycholesterol in obesity	Kvitne et al. [61]
	Liver, jejunum	32 CYPs, 14 UGTs, 58 non-CYP non-UGT enzymes, 199 transporters	–	Global proteomics	Effect of obesity on expression profiles in liver and intestine	Wegler et al. [100]
Pregnancy						
Drug effects on foetus	Placenta	7 transporters	Nelfinavir[g], efavirenz[g], imatinib[g], dexamethasone[h], betamethasone[h], darunavir[h], lopinavir[h]	Targeted proteomics	Prediction of foetal drug exposure	Anoshchenko et al. [11], Peng et al. [70], Anoshchenko et al. [12]

Paediatric disease

| Biliary atresia | Liver | 21 ABC transporters | – | Global proteomics | Effect of biliary atresia on hepatobiliary transporter expression | Al-Majdoub et al. [8] |

ABC ATP-binding cassette, *CP score* Child-Pugh score, *CYP* cytochrome P450, *UGT* UDP-glucuronosyltransferase, *P-gp* P-glycoprotein, *MRP* multidrug resistance protein, *OATP* organic anion transporting polypeptide, *NTCP* sodium-taurocholate co-transporting polypeptide, *LRP1* LDL receptor-related protein 1, *IVIVE* in vitro–in vivo extrapolation, *PK* pharmacokinetics, *NAFLD* non-alcoholic fatty liver disease, *NASH* non-alcoholic steatohepatitis

[a]Simulations reported in Prasad et al. [74]
[b]Simulations reported in Ladumor et al. [62]
[c]Simulations reported in Wang et al. [98]
[d]Simulations reported in Kumar et al. [58]
[e]Simulations reported in Kumar et al. [57]
[f]Simulations reported in Alrubia et al. [10]
[g]Simulations reported in Peng et al. [70]
[h]Simulations reported in Anoshchenko et al. [12]
[i]Quantification of enzymes (5 CYPs, 4 UGTs) and inflammation markers was done using transcriptomic methods

in disease groups, such as patients with hepatic impairment [67]. While availability of human samples for these applications is certainly increasing, access is still restricted by ethical and logistic obstacles, with samples largely limited to post-mortem or surgical surplus tissue.

The principles of PBPK can also be extended to propagation of interindividual variability to drug pharmacodynamics (PD) within the framework of quantitative systems pharmacology [25]. PBPK-PD models are mainly used to predict drug effects in special populations (e.g. predicting dental analgesic effect of ibuprofen in children [30]) and PD effects of drug-drug interactions (DDI) (e.g. the impact of coadministration of domperidone and ketoconazole on QT prolongation in the electrocardiogram of patients [65]). Application of quantitative proteomics to monitoring changes in drug receptors and other PD targets, such as the insulin receptor (INSR) in the human blood–brain barrier [92] and receptor tyrosine kinases in human metastatic liver cancer from colon [95], is expected to facilitate modelling of drug concentration–effect relationships in special/disease populations.

6.4   Predicting Pharmacokinetics in Subgroups of Patients Versus Predictions in an Individual

Despite advances made in the prediction of changes that occur in pharmacokinetics in subgroups of patients, predicting the fate of drugs in a specific individual who may not be the average patient in his or her subgroup requires characterization of changes that happen in ADME proteins in that particular individual as opposed to the average person in the relevant subgroup. Figure 6.4 summarizes current and emerging characterization methods.

Genotyping can identify the bracket of the pharmacogenetic subgroup for an individual patient, which is then linked to a specific activity score, such as the case of CYP2D6 genotype [44]. The Clinical Pharmacogenetics Implementation Consortium (CPIC) [23] has published several guideline reports demonstrating the value of such tests in managing optimal dosing for many drugs, e.g. tacrolimus (CYP3A5 genotype), clopidogrel (CYP2C19 genotype), and efavirenz (CYP2B6 genotype) [18, 32, 86]. CPIC guidelines typically offer recommendation of dose adjustment, the use of therapeutic drug monitoring or consideration of alternative therapeutic agents for each genotype group. However, there are wide population variations in the activity of proteins encoded by the same gene, and indeed, some ADME proteins with large population variability in abundance and activity do not have known genotypes that correlate with changes in activity. Hence, endogenous biomarkers and exogenous probes have been used to characterize patients regarding sets of important ADME pathways (e.g. cocktails of drug substrates). Established probe cocktails include the Geneva cocktail (6 enzymes and 1 transporter [20]), the Cooperstown 5 + 1 cocktail (5 enzymes [24]), the Karolinska cocktail (5 enzymes [26]), and the Pittsburgh cocktail (5 enzymes [43]). The issue with these biomarkers
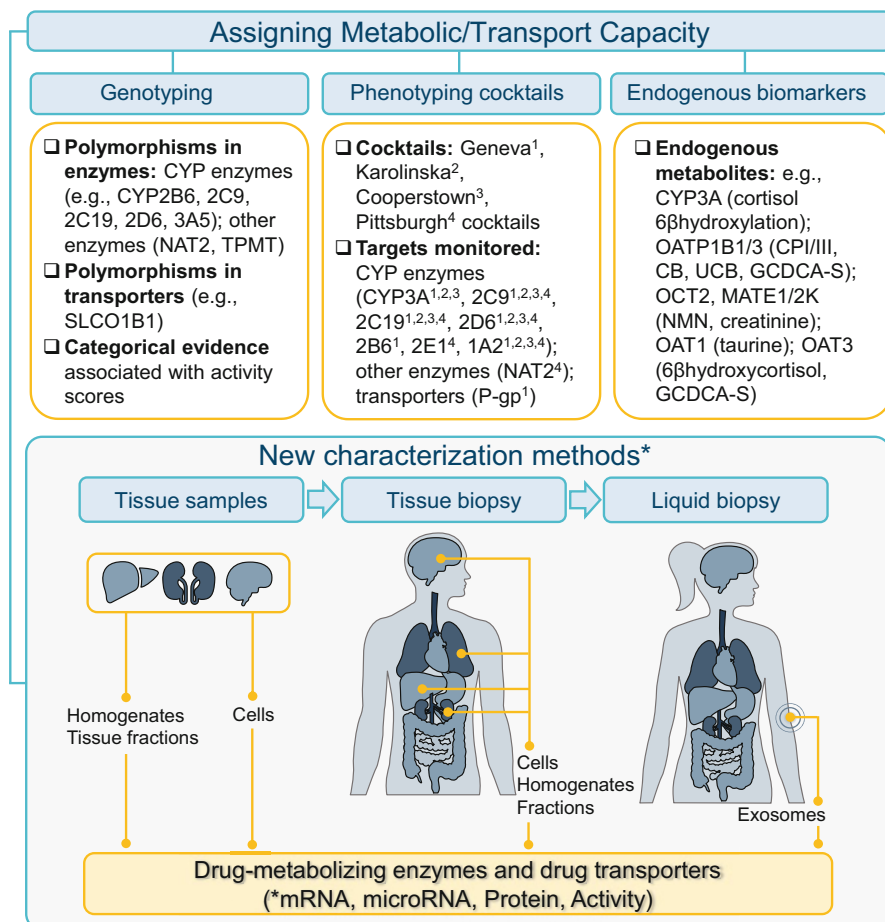
Fig. 6.4 Methods used for the characterization of drug-metabolizing and transporting pathways. Traditionally used methods include genotyping of polymorphic enzymes/transporters, characterization with specific probes (in cocktails administered orally) or the use of endogenous biomarkers for enzyme and transporter activity. More recent methods assess the expression/activity of enzymes and transporters in human samples (either from surgical surplus or post-mortem), in tissue biopsies (from individual patients), or in liquid biopsies (tissue-shedded exosomes). The measurements require modelling platforms for prediction of drug exposure and response. Abbreviations: *CB* conjugated bilirubin, *CPI/III* coproporphyrin I and III, *CYP* cytochrome P450, *GCDCA-S* glycochenodeoxycholate-3-O-sulphate, *MATE1/2 K* multidrug and toxin extrusion protein 1 and 2 K, *NAT2* N-acetyltransferase 2, *NMN* N1-methylnicotinamide, *OATP1B1/3* organic anion transporting polypeptide 1B1 (gene name SLCO1B1) and 1B3, *OAT1/3* organic anion transporter 1 and 3, *OCT2* organic cation transporter 2, *P-gp* P-glycoprotein, *TPMT* thiopurine methyltransferase, *UCB* unconjugated bilirubin. Under phenotyping cocktails, superscript numbers indicate the pathways each cocktail can monitor

is their limited scope which does not cover all relevant pathways of metabolism and transport for the range of clinically used drugs and the specificity of several substrates shows considerable overlap. Whereas tissue proteomics is able to address the quantitative nature of ADME/PD proteins for large sets of targets (a few thousand proteins in the same experiment), obtaining tissue from donors is fraught with ethical and logistic challenges. Hence, the recently introduced possibility of using liquid biopsy offers a more practical alternative for characterization of patients as an input compatible with PBPK models.

Liquid biopsies are biofluids sampled from a patient for diagnostic, companion diagnostic or therapeutic applications. Exosomes shedded by tissue into a biofluid offer a snapshot of the cellular biomolecular pool of macromolecules, which reflect the functional state of their tissue of origin (Fig. 6.5). The vesicles (30–150 nm in size) enclose DNA, (non-coding, messenger and micro) RNA, and (transmembrane and non-membrane) proteins, offering protection from degradation, and therefore longer half-lives of cargo molecules in systemic circulation [21]. 'Omics' analysis generates quantitative data for the cargo of extracted exosomes and the levels are linked to the abundance/activity of corresponding proteins in the liver or other organs. Several FDA-approved diagnostic oncology tests rely on liquid biopsy profiling with RNA or DNA sequencing to generate qualitative expression and mutation profiles of batteries of disease markers (e.g. the receptor tyrosine kinases, EGFR and ERBB2) [63]. Integration of quantitative transcriptomic and proteomic analyses into such assays is the next step in the development trajectory of current screening tests towards precision diagnostics and therapeutics. In addition to monitoring ADME proteins (PK variability), liquid biopsy can be used to define between-patient variability in receptors and other therapeutic targets (PD variability). Achour et al. [3, 4] demonstrated the possibility to monitor variability in the expression of over 500 ADME genes (171 enzymes, 362 transporters and the neonatal Fc receptor, FcRn) and over 80 FDA-approved drug targets after appropriate normalization for between-patient differences in the rate of shedding (defined based on expression of a set of tissue-specific stably expressed markers). Although not very well understood, exosome shedding is, in essence, a physiological process that is altered under pathological conditions, adding another parameter that modelling PK variability needs to contend with. Determination of such parameter becomes critical when the patient cohort includes a heterogeneous mix of diseases. The use of tissue-specific cell surface markers can help with purification, by immunoenrichment, of specific extracellular vesicles originating from the tissue of interest, e.g. asialoglycoprotein receptor 1, ASGR1, in the case of liver exosomes [76].

With sufficient validation and rapidly declining costs, the use of liquid biopsy will facilitate implementation of model-informed precision dosing owing to the inherent advantages of the technique; it is minimally invasive, quantitative (connecting exosomal profiles to tissue expression), and compatible with modelling platforms, such as Virtual Twins [31, 71]. Virtual Twins should incorporate detailed individual data, such as demographics, genotype, PK/PD expression grades (e.g. from liquid biopsy), and clinical scores (e.g. eGFR for renal function) into a generic PBPK
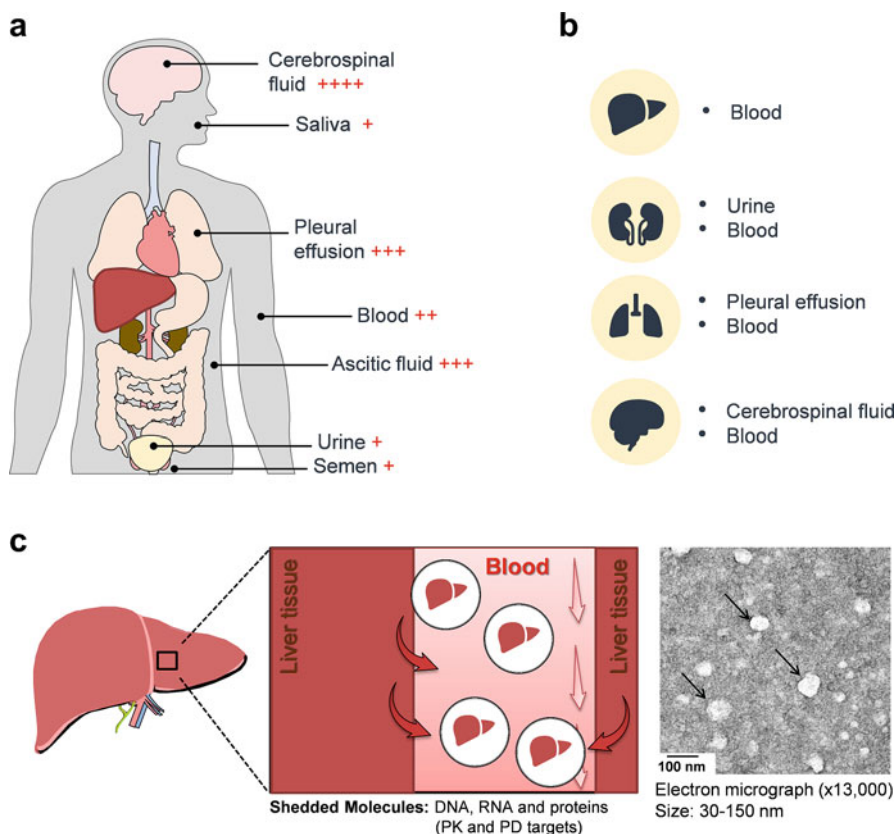
Fig. 6.5 Liquid biopsies, their nature, and attributes. (**a**) The anatomical origin and level of invasiveness of commonly sampled liquid biopsies (+, least invasive; ++++, most invasive, but all are less invasive than tissue biopsies). (**b**) Biofluids used to probe ADME/PD protein expression in liver, kidney, lung, and brain tissue as some of the main systems studied in PK/PD research. (**c**) Blood is the most widely used liquid biopsy with diagnostic, companion diagnostic and therapeutic applications. Tissue (liver) is perfused in blood and continuously sheds microvesicles (exosomes) into the systemic circulation. Molecules shedded include proteins and RNA (of PK and PD targets). The electron micrograph shows exosomes extracted from plasma (size range: 30–150 nm). Abbreviations: *ADME* absorption, distribution, metabolism and excretion, *PD* pharmacodynamics, *PK* pharmacokinetics

model of the cohort that the individual patient belongs to (Fig. 6.6). The use of liquid biopsy data with such modelling platforms opens the possibility of a priori selection of the optimal initial dose in a treatment regimen for an individual patient and allows identification of patients most likely to experience adverse events or lack of efficacy (for closer therapeutic monitoring). Achour et al. [4] demonstrated correlation with activity in a cohort of patients with cardiovascular disease monitored with the Geneva cocktail (for CYP1A2, CYP2B6, CYP2C9, CYP3A and P-gp), in support of findings by Rowland et al. [82] for CYP3A4 in a set of healthy volunteers before
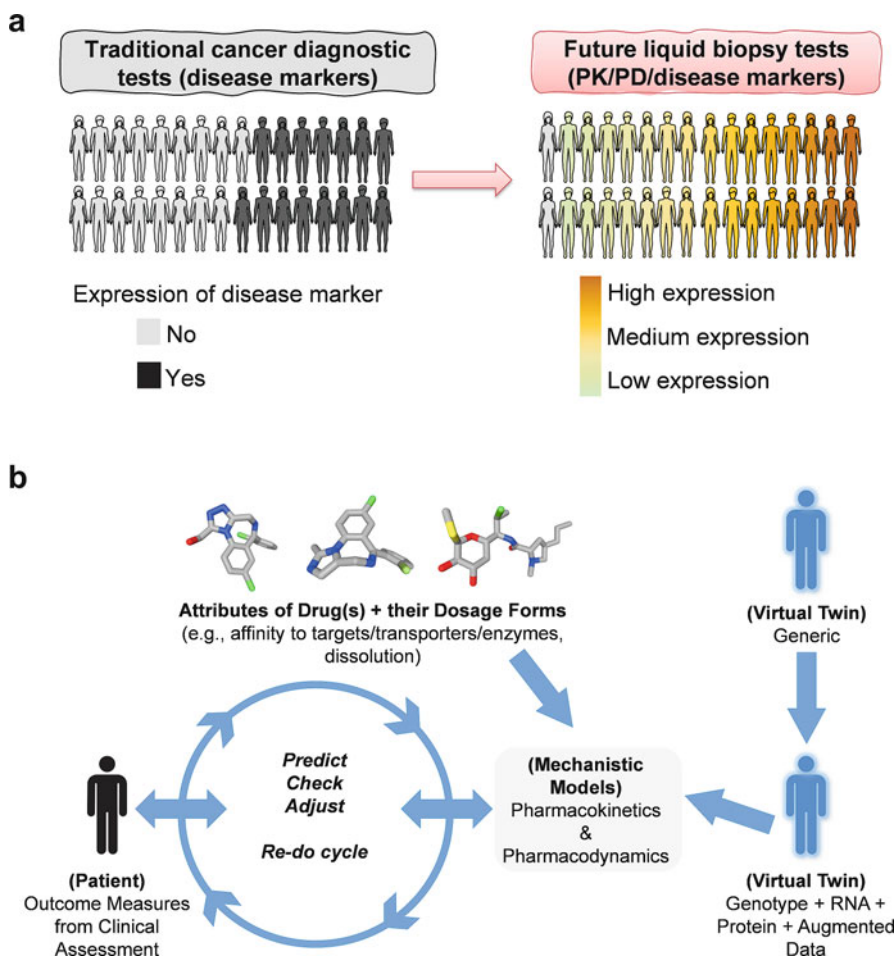
Fig. 6.6 The use of a liquid biopsy with modelling platforms for precision therapeutics. (**a**) Liquid biopsy can be used as a test for grading patients based on quantitative measurement of PK/PD targets while traditional tests (in oncology diagnostics) rely on qualitative evidence of the presence/absence of disease markers and the mutation profiles of such markers. (**b**) Quantitative data for PK and PD targets from liquid biopsy can be used to generate Virtual Twin models for individualized therapeutics. Abbreviations: *PD* pharmacodynamics, *PK* pharmacokinetics

and after induction. Early applications have focused on precision dosing and investigation of DDI potential [3, 76].

Despite its potential applications, liquid biopsy requires specialist expertise in isolation and purification of exosomes from biofluids, extraction of RNA and protein, and multi-omic analysis (genomics, RNAseq and proteomics). For this reason, the bulk of recent work has focused on assessment of enzymes and transporters in readily accessible systems, such as plasma exosomes [3, 27, 45, 56, 82],

while measurements of ADME targets in more challenging biofluids, such as urine [28] and cerebrospinal fluid, are lacking.

6.5 Modelling the Impact of Permutations of Various Comorbidities

The added value of PBPK becomes paramount when we consider combinations of factors that influence the fate of the drug, which are very difficult, if not impossible, to study in advance of the drug becoming available on the market. We take the example of DDIs as the case here. In 1999, Krayenbühl et al. [55] proposed that interpretation of interaction studies should focus not only on mean DDI effect but also observed and theoretically conceivable extremes. This initiated some efforts within the PBPK community to conduct virtual clinical studies involving large groups of virtual patients where various scenarios could be tested (the platform later became known as the Simcyp Population Based PBPK Platform) [52]. One of the essential elements of the system is its ability to run "what if" scenarios such as those shown in Fig. 6.7. "What if" scenarios take into account factors that affect the outcome of the interaction, e.g. genetics, renal/hepatic impairment, age, or combinations of these elements [79]. It took almost another decade before such facilities were put to practical use by some scientists. In 2012, researchers at the Office of Clinical Pharmacology (OCP) at the US FDA published a PBPK study that verified a previously reported case study [88] on DDI in renal impairment for telithromycin [97]. They went on then to prospectively project on the level of DDI for rivaroxaban
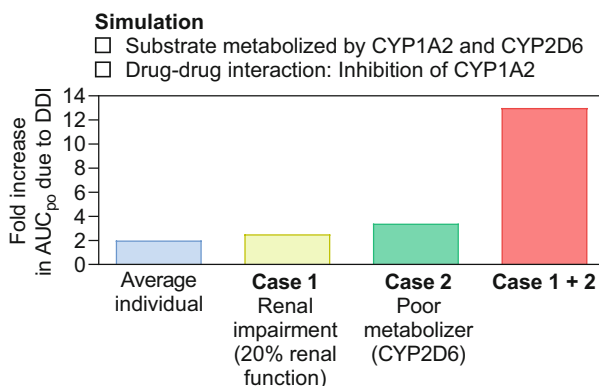
Fig. 6.7 "What if" scenarios simulated with PBPK modelling for a DDI between a substrate (metabolized by CYP1A2 and CYP2D6) and an inhibitor of CYP1A2. Scenarios examined the magnitude of interaction in renal impairment, CYP2D6 poor metabolizer genotype and a combination of the two. Abbreviations: AUC_{po} area under the plasma concentration-time profile after oral administration, *DDI* drug-drug interaction. (The concept of the figure is adopted from Rostami-Hodjegan and Tucker [79])

in renal impairment where no clinical data were available [46]. The study informed the label for the drug and was a guide to prescribers dealing with these rare occasions. Almost 10 years later, real-world data (RWD) analysis on retrospective information for rivaroxaban and associated side effects clearly demonstrated twofold higher incidence of bleeding in renally impaired patients who were receiving inhibitors of metabolic/transporter clearance (Grillo et al. [47]). The analysis was based on extracts from electronic health records (EHR) from HIPAA-compliant anonymized individual-patient-level data for 117 US institutions in the Cerner-Oracle RWD dataset for a 5-year period (2017–2021). One can postulate that such adverse effects could have been more frequent if the label did not contain the information on the combined impact of renal impairment and DDI. The example above is not unique and there are now many other cases where PBPK information has informed the drug label in the absence of clinical data. Table 6.2 shows a list of examples collated in an internal database by Certara. Similar but less comprehensive lists are published elsewhere [48, 50].

6.6   Conclusions and Future Use of PBPK for Model-Informed Precision Dosing

While the debate on the nature of PBPK models (Open Source Code versus Closed Source Code) continues [78], the use of closed-source systems has certainly accelerated applications in drug development. Achieving a similar success in model-informed precision dosing faces many hurdles and not just the lack of a user-friendly interface for PBPK. These are discussed by Darwich et al. [31] in the lines of creating virtual twins of patients [71]. However, the first critical step of such efforts is the faithful characterization of patients' phenotypes beyond genetic-based categorization. It appears that liquid biopsy, in conjunction of omics analyses, may just provide such capacity, if the technical aspects of such game-changing initiatives are addressed [4].

Table 6.2 A representative list of approved drugs where PBPK simulations informed the drug label. The list is an internal database of more than 300 label claims for over 90 novel drugs based on the Simcyp Simulator (2009–2022). (Source: Certara Ltd.)

Oncology	**Agios**	Tibsovo (ivosidenib)	**Genentech**	Polivy (polatuzumab vedotin-piiq)	**Novartis**	Kisqali (ribociclib succinate)
	Amgen	Blincyto (blinatumomab)	**Genentech**	Rozlytrek (entrectinib)	**Novartis**	Rydapt (midostaurin)
	Amgen	Lumakras (sotorasib)	**Genentech**	Cotellic (cobimetinib)	**Novartis**	Tabrecta (capmatinib)
	Ariad	Alunbrig (brigatinib)	**Genentech**	Alecensa (alectinib)	**Novartis**	Scemlix (asciminib)
	Ariad	Iclusig (ponatinib)	**Incyte**	Pemazyre (pemigatinib)	**Novartis**	Vijoice (alpelisib)
	AstraZeneca	Lynparza (olaparib)	**Janssen**	Balversa (erdafitinib)	**Pfizer**	Bosulif (bosutinib)
	AstraZeneca	Tagrisso (osimertinib)	**Janssen**	Erleada (apalutamide)	**Pfizer**	Lorbrena (lorlatinib)
	AstraZeneca	Calquence (acalabrutinib)	**Lilly**	Verzenio (abemaciclib)	**Pharmacyclics**	Imbruvica (ibrutinib)
	Beigene	Brukinsa (zanubrutinib)	**Lilly**	Retevmo (selpercatinib)	**Sanofi**	Jevtana (cabazitaxel)
	BluePrint Medicines	Ayvakit (avapritinib)	**Loxo Oncology**	Vitrakvi (larotrectinib)	**Seattle Genetics**	Tukysa (tukatanib)
	Celgene	Inrebic (fedratinib hydrochloride)	**Novartis**	Jakavi (ruxolitinib)	**Spectrum**	Beleodaq (belinostat)
	Daiichi Sankyo	Turalio (pexidartinib)	**Novartis**	Odomzo (sonidegib)	**Takeda**	Exkivity (mobocertinib)
	Eisai	Lenvima (lenvatinib)	**Novartis**	Farydak (panobinostat)	**Verastem**	Copiktra (duvelisib)
	EMD Serono	Tepmetko (tepotinib hydrochloride)	**Novartis**	Zykadia (certinib)		
Rare Disease	**Auriana**	Lupkynis (voclosporin)	**Intercept**	Oclavia (obeticholic acid)	**Sanofi Genzyme**	Cerdelga (eliglustat tartrate)
	Akarx	Doptelet (avatrombopag maleate)	**Kadman**		**Vertex**	Symdeko (tezacaftor/ivacaftor)

(continued)

Table 6.2 (continued)

	AstraZeneca	Koselugo (selumetinib)		Rezurock (belumosudil mesylate)	Vertex	Trikafta (elexacaftor/ivacaftor/tezacaftor)
	Genentech	Enspryng (satralizumab)	Merck	Welireg (belzutifan)	Mitsubishi Tanabe	Dysval (valbenazyne)
	Genentech	Evrysdi (risdiplam)	Mirum	Livarti (maralixbat)		
	Global Blood Therapeutics	Oxbryta (voxelotor)	Novartis	Isturida (osilodrostat)		
			PTC Therapeutics	Emflaza (deflazacort)		
Central Nervous System	AbbVie	Qulipta (atogepant)	GW Research	Epidiolex (cannabidiol)	Lilly	Rayvow (lasmiditan succinate)
	Alkermes	Aristada (aripiprazole)	Idorsia	Quviviq (daridorexant)	Novartis	Mayzent (siponimod fumaric acid)
	Alkermes	Lybalvi (olanzapine/samidorphan)	Janssen	Ponvory (ponesimid)	UCB	Briviact (brivaracetam)
	Eisai	Dayvigo (lemborexant)	Kyowa Kirin	Nourianz (istradefylline)	AbbVie	Rinvoq (upadacitinib)
Infectious Disease	Gilead	Remdesivir (veklury)	Merck	Prevymis (letermovir)	Tibotec	Edurant (rilpivirine)
	Viiv	Cabenuva kit (cabotegravir/rilivirine)	Merck	Pifeltro (doravirine)	Novartis	Egaten (triclabendazole)
	Janssen	Olysio (simeprevir)	Nabriva	Zenita (lefamulin acetate)		
Gastroenterology	AstraZeneca	Movantik (naloxegol)	Shionogi	Symproic (naldemedine)	Shire	Motegrity (prucalopride)
	Helsinn	Akynzeo (fosnetupitant/palonosetron)	Phathom	Voquezna Triple Pak		
Cardiovascular	Actelion	Opsumit (macitentan)	Johnson & Johnson	Xarelto (rivaroxaban)	Pfizer	Revatio (sildenafil)

	BMS	Canzyos (mavacamten)	Novartis	Entresto (sacubitril/valsartan)	Bayer/Merck	Verquvo (vericiguat)
Other	Agios	Pyrukynd (mitapivat)	Lilly	Olumiant (baricitinib)	Merck	Steglatro (ertugliflozin)
	Galderma	Aklief (trifarotene)	AbbVie	Orilissa (elagolix)	Takeda	Livtenicity (maribivar)
	Lilly	Mounjaro (tirzepadide)	Janssen	Invokana (canagliflozin)	Peloton/Merck	Welireg (ertugliflozin)

Data are presented in the order: pharmaceutical company (in bold), commercial name, and generic name of the drug (in parentheses). The last group denoted 'other' therapeutic classes includes metabolic disease, anaemia, post-transplant treatment, diabetes mellitus, inflammation, and dermatology

References

1. Achour B, Barber J, Rostami-Hodjegan A (2014) Expression of hepatic drug-metabolizing cytochrome p450 enzymes and their intercorrelations: a meta-analysis. Drug Metab Dispos 42: 1349–1356

2. Achour B, Rostami-Hodjegan A, Barber J (2014) Protein expression of various hepatic uridine 5′-diphosphate glucuronosyltransferase (UGT) enzymes and their inter-correlations: a meta-analysis. Biopharm Drug Dispos 35:353–361

3. Achour B, Al-Majdoub ZM, Grybos-Gajnak A et al (2021) Liquid biopsy enables quantification of the abundance and interindividual variability of hepatic enzymes and transporters. Clin Pharmacol Ther 109:222–232

4. Achour B, Gosselin P, Terrier J et al (2022) Liquid biopsy for patient characterization in cardiovascular disease: verification against markers of cytochrome P450 and P-glycoprotein activities. Clin Pharmacol Ther 111:1268–1277

5. Al-Majdoub ZM, Al Feteisi H, Achour B et al (2019) Proteomic quantification of human blood-brain barrier SLC and ABC transporters in healthy individuals and dementia patients. Mol Pharm 16:1220–1233

6. Al-Majdoub ZM, Couto N, Achour B et al (2021) Quantification of proteins involved in intestinal epithelial handling of xenobiotics. Clin Pharmacol Ther 109:1136–1146

7. Al-Majdoub ZM, Scotcher D, Achour B et al (2021) Quantitative proteomic map of enzymes and transporters in the human kidney: stepping closer to mechanistic kidney models to define local kinetics. Clin Pharmacol Ther 110:1389–1400

8. Al-Majdoub ZM, Achour B, Couto N et al (2021) Mass spectrometry-based abundance atlas of ABC transporters in human liver, gut, kidney, brain and skin. FEBS Lett 594:4134–4150

9. Alrubia S, Al-Majdoub ZM, Achour B et al (2022) Quantitative assessment of the impact of Crohn's disease on protein abundance of human intestinal drug-metabolising enzymes and transporters. J Pharm Sci 111:2917–2929

10. Alrubia S et al (2022) Altered bioavailability and pharmacokinetics in Crohn's disease: capturing systems parameters for PBPK to assist with predicting the fate of orally administered drugs. Clin Pharmacokinet 61:1365–1392

11. Anoshchenko O, Prasad B, Neradugomma NK et al (2020) Gestational age-dependent abundance of human placental transporters as determined by quantitative targeted proteomics. Drug Metab Dispos 48:735–741

12. Anoshchenko O, Storelli F, Unadkat JD (2021) Successful prediction of human fetal exposure to P-glycoprotein substrate drugs using the proteomics-informed relative expression factor approach and PBPK modeling and simulation. Drug Metab Dispos 49:919–928

13. Badée J, Achour B, Rostami-Hodjegan A et al (2015) Meta-analysis of expression of hepatic organic anion–transporting polypeptide (OATP) transporters in cellular systems relative to human liver tissue. Drug Metab Dispos 43:424–432

14. Bao X, Wu J, Xie Y et al (2020) Protein expression and functional relevance of efflux and uptake drug transporters at the blood-brain barrier of human brain and glioblastoma. Clin Pharmacol Ther 107:1116–1127

15. Benet LZ, Broccatelli F, Oprea TI (2011) BDDCS applied to over 900 drugs. AAPS J 13:519–547

16. Berezhkovskiy LM (2004) Volume of distribution at steady state for a linear pharmacokinetic system with peripheral elimination. J Pharm Sci 93(6):1628–1640

17. Billington S, Ray AS, Salphati L et al (2018) Transporter expression in noncancerous and cancerous liver tissue from donors with hepatocellular carcinoma and chronic hepatitis c infection quantified by LC-MS/MS proteomics. Drug Metab Dispos 46:189–196

18. Birdwell KA, Decker B, Barbarino JM et al (2015) Clinical pharmacogenetics implementation consortium (CPIC) guidelines for CYP3A5 genotype and tacrolimus dosing. Clin Pharmacol Ther 98:19–24

19. Bois FY, Jamei M, Clewell H (2010) PBPK modelling of inter-individual variability in the pharmacokinetics of environmental chemicals. Toxicology 278(3):256–267

20. Bosilkovska M, Samer CF, Déglon J et al (2014) Geneva cocktail for cytochrome P450 and P-glycoprotein activity assessment using dried blood spots. Clin Pharmacol Ther 96:349–359

21. Boukouris S, Mathivanan S (2015) Exosomes in bodily fluids are a highly stable resource of disease biomarkers. Proteomics Clin Appl 9:358–367

22. Brukner AM, Billington S, Benifla M et al (2021) Abundance of P-glycoprotein and breast cancer resistance protein measured by targeted proteomics in human epileptogenic brain tissue. Mol Pharm 18:2263–2273

23. Caudle KE, Klein TE, Hoffman JM et al (2014) Incorporation of pharmacogenomics into routine clinical practice: the Clinical Pharmacogenetics Implementation Consortium (CPIC) guideline development process. Curr Drug Metab 15:209–217

24. Chainuvati S, Nafziger AN, Leeder JS et al (2003) Combined phenotypic assessment of cytochrome P450 1A2, 2C9, 2C19, 2D6, and 3A, N-acetyltransferase-2, and xanthine oxidase activities with the "Cooperstown 5+1 cocktail". Clin Pharmacol Ther 74:437–447

25. Chetty M, Rose RH, Abduljalil K et al (2014) Applications of linking PBPK and PD models to predict the impact of genotypic variability, formulation differences, differences in target binding capacity and target site drug concentrations on drug responses and variability. Front Pharmacol 5:258

26. Christensen M, Andersson K, Dalén P et al (2003) The Karolinska cocktail for phenotyping of five human cytochrome P450 enzymes. Clin Pharmacol Ther 73:517–528

27. Conde-Vancells J, Rodriguez-Suarez E, Embade N et al (2008) Characterization and comprehensive proteome profiling of exosomes secreted by hepatocytes. J Proteome Res 7:5157–5166

28. Console L, Scalise M, Tonazzi A et al (2018) Characterization of exosomal SLC22A5 (OCTN2) carnitine transporter. Sci Rep 8:3758–3767

29. Couto N, Newton JRA, Russo C et al (2021) Label-free quantitative proteomics and substrate based mass spectrometry imaging of xenobiotic metabolizing enzymes in ex vivo human skin and a human living skin equivalent model. Drug Metab Dispos 49:39–52

30. Cristofoletti R, Dressman JB (2016) Bridging the gap between in vitro dissolution and the time course of ibuprofen-mediating pain relief. J Pharm Sci 105:3658–3667

31. Darwich AS, Polasek TM, Aronson JK et al (2021) Model-informed precision dosing: background, requirements, validation, implementation, and forward trajectory of individualizing drug therapy. Annu Rev Pharmacol Toxicol 61:225–245

32. Desta Z, Gammal RS, Gong L et al (2019) Clinical pharmacogenetics implementation consortium (CPIC) guideline for CYP2B6 and efavirenz-containing antiretroviral therapy. Clin Pharmacol Ther 106:726–733

33. Drozdzik M, Gröer C, Penski J et al (2014) Protein abundance of clinically relevant multidrug transporters along the entire length of the human intestine. Mol Pharm 11:3547–3555

34. Drozdzik M, Szelag-Pieniek S, Post M et al (2020) Protein abundance of hepatic drug transporters in patients with different forms of liver damage. Clin Pharmacol Ther 107:1138–1148

35. Drozdzik M, Lapczuk-Romanska J, Wenzel C et al (2021) Gene expression and protein abundance of hepatic drug metabolizing enzymes in liver pathology. Pharmaceutics 13:1334

36. Drozdzik M, Lapczuk-Romanska J, Wenzel C et al (2022) Protein abundance of drug transporters in human hepatitis C livers. Internat J Mol Sci 23:7947

37. El-Khateeb E, Burkhill S, Murby S et al (2021) Physiological-based pharmacokinetic modeling trends in pharmaceutical drug development over the last 20-years; in-depth analysis of applications, organizations, and platforms. Biopharm Drug Dispos 42:107–117

38. El-Khateeb E, Achour B, Al-Majdoub ZM et al (2021) Non-uniformity of changes in drug-metabolizing enzymes and transporters in liver cirrhosis: implications for drug dosage adjustment. Mol Pharm 18:3563–3577

39. Erdmann P, Bruckmueller H, Martin P et al (2019) Dysregulation of mucosal membrane transporters and drug-metabolizing enzymes in ulcerative colitis. J Pharm Sci 108:1035–1046

40. Fallon JK, Houvig N, Booth-Genthe CL et al (2018) Quantification of membrane transporter proteins in human lung and immortalized cell lines using targeted quantitative proteomic analysis by isotope dilution nanoLC–MS/MS. J Pharm Biomed Anal 154:150–157

41. FDA (2020) Enhancing the diversity of clinical trial populations—eligibility criteria, enrollment practices, and trial designs, guidance for industry. Available from: https://www.fda.gov/regulatory-information/search-fda-guidance-documents/enhancing-diversity-clinical-trial-populations-eligibility-criteria-enrollment-practices-and-trial

42. FDA (2022) Diversity plans to improve enrollment of participants from underrepresented racial and ethnic populations in clinical trials; Draft Guidance for Industry. Available from: https://www.fda.gov/regulatory-information/search-fda-guidance-documents/diversity-plans-improve-enrollment-participants-underrepresented-racial-and-ethnic-populations

43. Frye RF, Matzke GR, Adedoyin A et al (1997) Validation of the five-drug "Pittsburgh cocktail" approach for assessment of selective regulation of drug-metabolizing enzymes. Clin Pharmacol Ther 62:365–376

44. Gaedigk A, Simon SD, Pearce RE et al (2008) The CYP2D6 activity score: translating genotype information into a qualitative measure of phenotype. Clin Pharmacol Ther 83:234–242

45. Gotanda K, Hirota T, Saito J et al (2016) Circulating intestine-derived exosomal miR-328 in plasma, a possible biomarker for estimating BCRP function in the human intestines. Sci Rep 6:32299–32307

46. Grillo JA, Zhao P, Bullock J et al (2012) Utility of a physiologically-based pharmacokinetic (PBPK) modeling approach to quantitatively predict a complex drug-drug-disease interaction scenario for rivaroxaban during the drug review process: implications for clinical practice. Biopharm Drug Dispos 33:99–110

47. Grillo J, Zhao P, McNair D (Unpublished) Analysis of Cerner-Oracle RWD dataset for 2017–2021

48. Huang S-M, Abernethy DR, Wang Y et al (2013) The utility of modeling and simulation in drug development and regulatory review. J Pharm Sci 102:2912–2923

49. Jadhav PR, Cook J, Sinha V et al (2015) A proposal for scientific framework enabling specific population drug dosing recommendations. J Clin Pharmacol 55:1073–1078

50. Jamei M (2016) Recent advances in development and application of physiologically-based pharmacokinetic (PBPK) models: a transition from academic curiosity to regulatory acceptance. Curr Pharmacol Rep 2:161–169

51. Jamei M, Dickinson GL, Rostami-Hodjegan A et al (2009) A framework for assessing inter-individual variability in pharmacokinetics using virtual human populations and integrating general knowledge of physical chemistry, biology, anatomy, physiology and genetics: a tale of 'bottom-up' vs 'top-down' recognition of covariates. Drug Metab Pharmacokinet 24:53–75

52. Jamei M, Marciniak S, Feng K et al (2009) The Simcyp® population-based ADME simulator. Expert Opin Drug Metab Toxicol 5:211–223

53. Jamei M, Turner D, Yang J et al (2009) Population-based mechanistic prediction of oral drug absorption. AAPS J 11:225–237

54. Jamwal R, de la Monte SM, Ogasawara K et al (2018) Nonalcoholic fatty liver disease and diabetes are associated with decreased cyp3a4 protein expression and activity in human liver. Mol Pharm 15:2621–2632

55. Krayenbühl JC, Vozeh S, Kondo-Oestreicher M et al (1999) Drug-drug interactions of new active substances: mibefradil example. Eur J Clin Pharmacol 55:559–565

56. Kumar S, Sinha N, Gerth KA et al (2017) Specific packaging and circulation of cytochromes P450, especially 2E1 isozyme, in human plasma exosomes and their implications in cellular communications. Biochem Biophys Res Commun 491:675–680

57. Kumar V, Yin J, Billington S et al (2018) The importance of incorporating OCT2 plasma membrane expression and membrane potential in IVIVE of metformin renal secretory clearance. Drug Metab Dispos 46:1441–1445

58. Kumar V, Yin M, Ishida K et al (2021) Prediction of transporter-mediated rosuvastatin hepatic uptake clearance and drug interaction in humans using proteomics-informed REF approach. Drug Metab Dispos 49:159–168

59. Kurzawski M, Szelag-Pieniek S, Łapczuk-Romańska J et al (2022) The reference liver-CYP450 and UGT enzymes in healthy donor and metastatic livers: the impact of genotype. Pharmacol Rep 74:204–215

60. Kuypers DRJ (2018) Tacrolimus formulations and African American kidney transplant recipients: when do details matter? Am J Kidney Dis 71:302–305

61. Kvitne KE, Hole K, Krogstad V et al (2022) Correlations between 4β-hydroxycholesterol and hepatic and intestinal CYP3A4: protein expression, microsomal ex vivo activity, and in vivo activity in patients with a wide body weight range. Eur J Clin Pharmacol 78:1289–1299

62. Ladumor MK, Thakur A, Sharma S et al (2019) A repository of protein abundance data of drug metabolizing enzymes and transporters for applications in physiologically based pharmacokinetic (PBPK) modelling and simulation. Sci Rep 9:9709

63. Lanman RB, Mortimer SA, Zill OA et al (2015) Analytical and clinical validation of a digital sequencing panel for quantitative, highly accurate evaluation of cell-free circulating tumor DNA. PLoS One 10:e0140712

64. Lloret-Linares C, Miyauchi E, Luo H et al (2016) Oral morphine pharmacokinetic in obesity: the role of P-glycoprotein, MRP2, MRP3, UGT2B7, and CYP3A4 jejunal contents and obesity-associated biomarkers. Mol Pharm 13:766–773

65. Mishra H, Polak S, Jamei M et al (2014) Interaction between domperidone and ketoconazole: toward prediction of consequent QTC prolongation using purely in vitro information. CPT Pharmacometrics Syst Pharmacol 3:e130

66. Miyauchi E, Tachikawa M, Declèves X et al (2016) Quantitative atlas of cytochrome P450, UDP-glucuronosyltransferase, and transporter proteins in jejunum of morbidly obese subjects. Mol Pharm 13:2631–2640

67. Neuhoff S, Harwood M, Rostami-Hodjegan A et al (2021) Application of proteomic data in the translation of in vitro observations to associated clinical outcomes. Drug Discov Today Technol 39:13–22

68. Ogna VF, Bassi I, Menetrey I et al (2017) Comparative long-term effect of three anti-P2Y12 drugs after percutaneous angioplasty: an observational study based on electronic drug adherence monitoring. Front Pharmacol 8:738

69. Oswald S, Müller J, Neugebauer U et al (2019) Protein abundance of clinically relevant drug transporters in the human kidneys. Int J Mol Sci 20:5303

70. Peng J, Ladumor MK, Unadkat JD (2022) Estimation of fetal-to-maternal unbound steady-state plasma concentration ratio of p-glycoprotein and/or breast cancer resistance protein substrate drugs using a maternal-fetal physiologically based pharmacokinetic model. Drug Metab Dispos 50:613–623

71. Polasek TM, Rostami-Hodjegan A (2020) Virtual twins: understanding the data required for model-informed precision dosing. Clin Pharmacol Ther 107:742–745

72. Poulin P, Theil FP (2002) Prediction of pharmacokinetics prior to in vivo studies. 1. Mechanism-based prediction of volume of distribution. J Pharm Sci 91:129–156

73. Prasad B, Johnson K, Billington S et al (2016) Abundance of drug transporters in the human kidney cortex as quantified by quantitative targeted proteomics. Drug Metab Dispos 44:1920–1924

74. Prasad B, Bhatt DK, Johnson K et al (2018) Abundance of phase 1 and 2 drug-metabolizing enzymes in alcoholic and hepatitis C cirrhotic livers: a quantitative targeted proteomics study. Drug Metab Dispos 46:943–952

75. Rodgers T, Rowland M (2007) Mechanistic approaches to volume of distribution predictions: understanding the processes. Pharm Res 24:918–933

76. Rodrigues AD, van Dyk M, Sorich MJ et al (2021) Exploring the use of serum-derived small extracellular vesicles as liquid biopsy to study the induction of hepatic cytochromes P450 and organic anion transporting polypeptides. Clin Pharmacol Ther 110:248–258

77. Rostami-Hodjegan A (2012) Physiologically based pharmacokinetics joined with in vitro-in vivo extrapolation of ADME: a marriage under the arch of systems pharmacology. Clin Pharmacol Ther 92:50–61

78. Rostami-Hodjegan A, Bois FY (2021) Opening a debate on open-source modeling tools: pouring fuel on fire versus extinguishing the flare of a healthy debate. CPT Pharmacometrics Syst Pharmacol 10:420–427

79. Rostami-Hodjegan A, Tucker GT (2004) 'In silico' simulations to assess the 'in vivo' consequences of 'in vitro' metabolic drug-drug interactions. Drug Discov Today Technol 1:441–448

80. Rostami-Hodjegan A, Tucker GT (2007) Simulation and prediction of in vivo drug metabolism in human populations from in vitro data. Nat Rev Drug Discov 6:140–148

81. Rowland M, Peck C, Tucker G (2011) Physiologically-based pharmacokinetics in drug development and regulatory science. Annu Rev Pharmacol Toxicol 51:45–73

82. Rowland A, Ruanglertboon W, van Dyk M et al (2019) Plasma extracellular nanovesicle (exosome)-derived biomarkers for drug metabolism pathways: a novel approach to characterize variability in drug exposure. Br J Clin Pharmacol 85:216–226

83. Scotcher D, Jones C, Posada M et al (2016) Key to opening kidney for in vitro–in vivo extrapolation entrance in health and disease: part I: in vitro systems and physiological data. AAPS J 18:1067–1081

84. Scotcher D, Jones C, Posada M et al (2016) Key to opening kidney for in vitro-in vivo extrapolation entrance in health and disease: part II: mechanistic models and in vitro-in vivo extrapolation. AAPS J 18:1082–1094

85. Scotcher D, Jones CR, Galetin A et al (2017) Delineating the role of various factors in renal disposition of digoxin through application of physiologically based kidney model to renal impairment populations. J Pharmacol Exper Ther 360:484–495

86. Scott SA, Sangkuhl K, Gardner EE et al (2011) Clinical pharmacogenetics implementation consortium guidelines for cytochrome P450-2C19 (CYP2C19) genotype and clopidogrel therapy. Clin Pharmacol Ther 90:328–332

87. Shawahna R, Uchida Y, Declèves X et al (2011) Transcriptomic and quantitative proteomic analysis of transporters and drug metabolizing enzymes in freshly isolated human brain microvessels. Mol Pharm 8:1332–1341

88. Shi J, Chapel S, Montay G et al (2005) Effect of ketoconazole on the pharmacokinetics and safety of telithromycin and clarithromycin in older subjects with renal impairment. Int J Clin Pharmacol Ther 43:123–133

89. Storelli F, Billington S, Kumar AR et al (2021) Abundance of P-glycoprotein and other drug transporters at the human blood-brain barrier in Alzheimer's disease: a quantitative targeted proteomic study. Clin Pharmacol Ther 109:667–675

90. Szeląg-Pieniek S, Oswald S, Post M et al (2021) Hepatic drug-metabolizing enzymes and drug transporters in Wilson's disease patients with liver failure. Pharmacol Rep 73:1427–1438

91. Trofe-Clark J, Brennan DC, West-Thielke P et al (2018) Results of ASERTAA, a randomized prospective crossover pharmacogenetic study of immediate-release versus extended-release tacrolimus in African American kidney transplant recipients. Am J Kidney Dis 71(3):315–326

92. Uchida Y, Ohtsuki S, Katsukura Y et al (2011) Quantitative targeted absolute proteomics of human blood–brain barrier transporters and receptors. J Neurochem 117:333–345

93. Vasilogianni A-M, El-Khateeb E, Al-Majdoub ZM et al (2022) Proteomic quantification of perturbation to pharmacokinetic target proteins in liver disease. J Proteomics 263:104601

94. Vasilogianni A-M, Al-Majdoub ZM, Achour B et al (2022) Quantitative proteomics of hepatic drug-metabolizing enzymes and transporters in patients with colorectal cancer metastasis. Clin Pharmacol Ther 112:699–710

95. Vasilogianni A-M, Al-Majdoub ZM, Achour B et al (2022) Proteomics of colorectal cancer liver metastasis: a quantitative focus on drug elimination and pharmacodynamics effects. Br J Clin Pharmacol 88:1811–1823

96. Vicini P (2010) Multiscale modeling in drug discovery and development: future opportunities and present challenges. Clin Pharmacol Ther 88(1):126–129
97. Vieira MLT, Zhao P, Berglund EG et al (2012) Predicting drug interaction potential with a physiologically based pharmacokinetic model: a case study of telithromycin, a time-dependent CYP3A inhibitor. Clin Pharmacol Ther 91:700–708
98. Wang L, Collins C, Kelly EJ et al (2016) Transporter expression in liver tissue from subjects with alcoholic or hepatitis C cirrhosis quantified by targeted quantitative proteomics. Drug Metab Dispos 44:1752–1758
99. Wegler C, Garcia LP, Klinting S et al (2021) Proteomics-informed prediction of rosuvastatin plasma profiles in patients with a wide range of body weight. Clin Pharmacol Ther 109:762–771
100. Wegler C, Wiśniewski JR, Robertson I et al (2022) Drug disposition protein quantification in matched human jejunum and liver from donors with obesity. Clin Pharmacol Ther 111:1142–1154
101. Zhao P, Rowland M, Huang S-M (2012) Best practice in the use of physiologically based pharmacokinetic modeling and simulation to address clinical pharmacology regulatory questions. Clin Pharmacol Ther 92:17–20

Chapter 7
Impact of Clinical Pharmacology on the Modernization of Drug Development and Regulation

Liang Zhao and Carl C. Peck

Abstract This chapter provides a brief history of the influence of clinical pharmacology on modernizing drug regulation and development. The intertwined emergence of bioequivalence and clinical pharmacology in regulatory science, the evolving role of clinical pharmacology in drug development, and the application of quantitative pharmaco-statistical models (pharmacometrics) for decision-making are traced throughout the last half-century. The prospects for incorporation of real-world data, artificial intelligence, and machine-learning techniques in drug development and regulatory assessment are considered. Finally, the impact of clinical pharmacology in drug regulation via guidance, statutory recognition, regulatory initiatives for model-informed drug development (MIDD), and model-integrated evidence (MIE) that strongly encourage employment of quantitative clinical pharmacology, altogether provide perspectives for the future.

Keywords Clinical pharmacology · Drug regulation · Regulatory science · Model-informed drug development · Bioequivalence

7.1 Introduction

Clinical pharmacology concerns how drugs influence human pathophysiology and how the body deals with them. It is a translational science which aims to provide a rationale, scientistic, and mechanistic causal approach for optimizing the benefit–risk profile in individual patients and application to therapeutic monitoring and management strategies [1]. Prior to the 1970s, drug development and regulation

L. Zhao (✉)
Division of Quantitative Methods and Modeling, Office of Reseach and Standards, Office of Generic Drugs, Center for Drug Evaluation and Research, FDA, Silver Spring, MD, USA
e-mail: liang.zhao@fda.hhs.gov

C. C. Peck (✉)
Bioengineering and Therapeutic Sciences, University of California at San Francisco (UCSF) and NDA Partners (a ProPharma Company), San Luis Obispo, CA, USA

practices were largely empirical and ad hoc. In the meantime, the science of clinical pharmacology has played a critical role in modernizing the development and regulation of drugs, and their use in the practice of medicine. The fundamental sciences supporting clinical pharmacology focus on the interaction between drugs and human physiology and involve chemistry, biochemistry, toxicology, drug metabolism, pharmacokinetics (PK), pharmacodynamics (PD), quantitative modeling, pharmacogenomics, clinical pharmacology practice, drug interactions, and clinical drug trials. In the regulatory realm, clinical pharmacology focuses on influences of intrinsic and extrinsic factors on inter-patient and intra-subject variability in drug exposure, and clinical responses including those that impact dose adjustments in various populations, drug–drug interactions (DDIs), optimization of dosing regimens, designs of clinical study, and precision medicine, etc. [1]. In this chapter, the authors give an account of the chronical influence of clinical pharmacology in the modernization of drug development and regulation.

7.2   A Historical Account of the Clinical Pharmacology Emergence in Drug Regulation

7.2.1   The Evolving Landscape for Drug Regulation for Licensing Drug Products in FDA

At the beginning of the twentieth century, no federal regulations were in place to protect the public by regulating the composition and sale of food and drugs produced in the United States. An important step in FDA's history was the formation by Harvey W. Wiley, M.D., in 1902 of a Drug Laboratory in the USDA Bureau of Chemistry, which began researching adulteration and misbranding of foods and drugs on the domestic market. In 1906, President Theodore Roosevelt signed the Pure Food and Drugs Act prohibiting interstate commerce of misbranded and adulterated foods, drinks, and drugs. The label of a food or drug could not be false or misleading and was required to list the presence and amount of 11 dangerous ingredients (e.g., alcohol, heroin, and cocaine). Specifically, "adulterated" drugs were those in which the "standard of strength, quality, or purity" of the active ingredient was not clearly stated on the label or listed in the United States Pharmacopeia or the National Formulary. Wiley's USDA Bureau of Chemistry, which became the Food and Drug Administration in 1938, was responsible for examining food and drugs for such "adulteration" or "misbranding" [2–6].

Motivated by the Elixir Sulfanilamide tragedy in 1937, when a formulation of sulfanilamide drug made sweet with propylene glycol (antifreeze) was responsible for the deaths of more than 100 people across the country [3], the Food, Drug, and Cosmetic Act (FD & C Act) was signed into law in 1938. The Act vastly expanded federal regulatory powers of the FDA by requiring pre-market review of the safety of all new drugs and mandated that a new drug application (NDA) would automatically

become effective within 60 days from its submission unless FDA actively refused to approve the application. FDA's affirmative approval of an NDA was not a requirement until codified in the 1962 Drug Amendment [7]. The FD & C Act also eliminated the Sherley Amendment requirement to prove intent to defraud in drug misbranding cases, and the Act set safe tolerances for unavoidable poisonous substances, authorized factory inspections, expanded enforcement powers, and standards of identity, quality, and fill-of-container for foods, and extended federal regulatory authority to cosmetics and therapeutic devices [2–6].

Prior to 1938, few regulatory barriers existed to the marketing of drugs, including the generic versions of brand name products [7, 8]. FDA interpreted the 1938 FD & C Act to mean that drugs marketed prior to the 1938 law those drugs did not require FDA approval, and as such, those drugs were grandfathered. Following the 1938 amendment, however, a new drug could only be marketed after its NDA as approved by FDA or the drug was generally recognized as safe (GRAS) [7, 8]. Both new and generic drugs were required to submit animal and in vitro toxicity data but given the lack of resources to review the submitted applications, FDA began an informal practice of issuing "Not New Drug" letters to the generic manufacturers. Such practice was discontinued in 1968 and all "Not New Drug" letters were formally revoked by FDA. Between 1938 and 1962, FDA considered drugs that were identical, similar, or related to drugs with effective applications to be covered by those approvals and allowed those drugs to be marketed without independent approval [7, 8].

Motivated by the worldwide disaster linked to thalidomide for rare, severe birth defects [4], in 1962, Congress approved the Kefauver-Harris Drug Amendment [9], which added evidence of effectiveness as a condition for approval of a drug and required a retrospective evaluation of the effectiveness of all drugs approved as safe between 1938 and 1962 [7, 8]. In addition to the effectiveness requirement, the amendments also set standards for good manufacturing practices and required adverse event reporting. In 1966, FDA contracted with the National Academy of Science (NAS)/National Research Council (NRC) to evaluate the effectiveness of 3400 drugs approved on the basis of safety alone between 1938 and 1962 by reviewing medical literature. Subsequently, FDA established the Drug Efficacy Study Implementation (DESI) program in 1968 to implement the NAS recommendations [10, 11]. When data were not sufficient to determine efficacy, the company was allowed time to generate such data. Determination of bioavailability (BA) was also required for each case. By 1984, the DESI had issued final regulatory actions on 3443 products; of which 64.6% were found to be effective ($n = 2225$), 30.5% not effective ($n = 1051$), and 4.8% pending more research ($n = 167$). Of note, more than 1000 drugs were removed from the market as deemed ineffective [10, 11]. While the DESI process is largely complete, a few drugs remain subject to further review to date [11].

Having terminated the issuance of "Not New Drug" letters, academic concerns were raised that different formulations of marketed generic drugs might not be equivalent [7, 8]. Thus, and in view of the 1962 amendment requiring evidence of effectiveness as a condition for approval, the FDA established a new form of NDA,

the Abbreviated New Drug Application (ANDA) system. Prior to the ANDA system, FDA had interpreted the 1962 amendment to mean that all generic drug formulations marketed between 1938 and 1962 had to file NDAs and establish equivalency to the approved brand name product [8]. The ANDA application required sponsors only to prove sameness of active ingredients and "bioequivalence" of the generic product to that of the innovative marketed product. As well, FDA would not require toxicological or clinical studies if the information was already available in the innovators' NDA [8].

Congress passed the Hatch-Waxman Amendments to the FD & C Act in 1984 [12]. The amendments aimed to create an abbreviated pathway for generic drug approval with even more simplified requirements and to provide for patent extensions, thus addressing concerns of the innovator drug industry about losing the effective period of patent protection due to the lengthy and costly development and NDA approval process. The amendments also introduced market exclusivity incentives for both research and challenging patents. The Hatch-Waxman Act created two new abbreviated statutory pathways: (i) ANDAs submitted under section 505(j); and (ii) NDAs submitted under section 505(b)(2) [12]. Overall, the Hatch-Waxman Act aimed to enable competitive marketing of safe and effective generics as quickly as possible after expiration of the underlying patent and while protecting rights of brand-name manufacturers [7].

In the 1980s, the FDA drug review process was often criticized for being too slow, while, based on FDA's estimates, a 1-month delay in a new drug's approval could cost its sponsor $ten million. At the same time, FDA had not received sufficient appropriations from Congress to hire the additional staff necessary to end the backlog of drugs pending market approval. In 1988, the Food and Drug Administration Act was officially established FDA as an agency of the Department of Health and Human Services with a Commissioner of Food and Drugs and broadly spelled out the responsibilities for research, enforcement, education, and information [13].

In 1992, Congress passed the Prescription Drug User Fee Act (PDUFA) [14], mandating that drug and biologics manufacturers pay user fees for product applications and supplements, and other services so the FDA could hire more reviewers to assess application and speed up drug review times, without compromising standards. In exchange for the additional resources, the FDA was required to meet certain performance benchmarks for review times. As a result of the PDUFA implementation, user fees have been instrumental in expediting the drug approval process [15]. PDUFA must be reauthorized every 5 years and was renewed in 1997 (PDUFA II), 2002 (PDUFA III), 2007 (PDUFA IV), 2012 (PDUFA V), 2017 (PDUFA VI), and 2022 (PDUFA VII) [15].

In November 21, 1997, the Food and Drug Administration Modernization Act (FDAMA) was enacted, which amended the FD & C Act relating to the regulation of food, drugs, devices, and biological products [16]. With the passage of FDAMA, Congress enhanced FDA's mission in ways that recognized the Agency would be operating in the twenty-first century, characterized by increasing technological, trade, and public health complexities [16]. PDUFA II was renewed under

FDAMA. FDAMA also supported accelerated approval, single-trial approval, and awarded an extra period (6 months) of marketing exclusivity to manufacturers that carried out studies in children. This legislation affirmed the CDER's public health protection role, calling for the FDA to continue promoting the public health by efficiently reviewing drugs and to join with representatives of other countries to harmonize regulatory requirements [16].

Analogous to PDUFA, Congress first enacted the Generic Drug User Fee Act (GDUFA) in 2012, with the aim of expanding FDA resources for speeding and increasing access to safe and effective generic drugs to the public, while reducing costs to industry [17, 18]. Under GDUFA, FDA user fees had to be paid by all firms that manufacture human generic drug products, and active ingredients for human generic drug products that are distributed in U.S. commerce. GDUFA fees are directly related to the Agency's ability to perform critical program functions to reduce costs and review timelines [18]. GDUFA also must be reauthorized every 5 years and was renewed in 2017 (GDUFA II) and 2022 (GDUFA III) [18, 19] (assuming that GDUFDAIII and PDUFA VII will be officially renewed by the publication date of this chapter). Of note, clinical pharmacology as a discipline has contributed significantly to the success of both PDUFA and GDUFA.

7.2.2   The Intertwined Emergence of Bioequivalence (BE) and Clinical Pharmacology in Regulatory Science

7.2.2.1   The Emerging Need and Evolving Selection of Criteria for BE Assessment

Methods for estimating bioequivalence (BE) were demonstrated to the FDA as early as 1969 by Professor John Wagner, who compared areas under the serum concentration versus time curves (AUC) of generic and brand name drugs [8]. However, at that time, such studies were deemed not necessary by FDA, since the agency did not believe a problem existed and thus Wagner's approach was ignored. The "Bioavailability Problem" was considered a "Content Uniformity Problem" by the Offices of Pharmaceutical Research and Compliance in the Bureau of Medicine and the Commissioner's [8, 20]. The FDA was reorganized in 1974, with the establishment of an "Office of Drug Monographs" in the newly established Bureau of Drugs (former Bureau of Medicine) [8]. This Office was formed with the purpose of publishing the formulation information on various drug products that could be used to manufacture generic products for which bioequivalence would be ensured given identical formulations, both chemically and functionally. For functionality, the dissolution test [8] appeared to be promising. As such, there would be no need for in vivo bioequivalence (BE) studies [8]. In vivo/in vitro correlations were expected to support dissolution specifications for lot-to-lot BE assurance, after content uniformity to the innovator's product had been determined [8]. However, this approach was challenged when the same generic company marketed two different lots of digoxin differing in systemic bioavailability (BA) by over 100% [20].

After the enaction of the 1984 amendment, demonstration of in vivo BE was required for all generic drug approvals [8]. Studies on blood levels and/or urinary excretion were required by law to be carried out when feasible [8, 21]. Alternative pharmacodynamic studies could be used to demonstrate BA/BE, if the above-mentioned studies were considered not possible due to non-systemically available drugs. However, full clinical studies of safety and effectiveness would be required if neither blood level/urinary excretion studies nor pharmacodynamic studies were feasible. Pharmacodynamic measurements could be hard to interpret, so only a few pharmacodynamic endpoints have gained regulatory acceptance, such as the cutaneous vasoconstrictor assay for topical glucocorticoids [8, 22–25] and forced-expiratory-volume-in-1 s (FEV1) based metrics for orally inhaled asthma and chronic obstructive pulmonary disease (COPD) products [26]. For locally acting dermatological products, efforts to develop a pharmacokinetics-based BE approach using a skin-stripping method proved unsuccessful [8]. After a difficult but fascinating journey, the FDA Division of Biopharmaceutics was ultimately divided into several review divisions under the Office of Clinical Pharmacology [8].

7.2.2.2 The Co-emergence of Quantitative Clinical Pharmacology (QCP) and Modern BE Assessment and Uptake by the FDA

In the 1970s, the first quantitative clinical pharmacology (QCP) breakthrough occurred when FDA became aware that varying absorption rates, bioavailability, and systemic exposures were observed within manufactured lots and between among marketed oral drug products containing the same active ingredient [27], as mentioned above with digoxin [20]. Thus, without comparative systemic bioavailability testing, the interchangeability of generic and brand name drugs was called into question, particularly for those drugs with a narrow therapeutic range [27]. As a result, a regulation was issued in 1977 mandating drug manufacturers to apply rigorous statistical procedures to assure BE and to document BA of all new drugs [21, 27].

The huge policy leap of requiring demonstration of in vivo BE using pharmacokinetic methods for ANDA approval can be credited to clinical pharmacology. To understand the historical context of the public health impact of equivalence determinations, it is important to recognize that the early advances in pharmacokinetics were driven mostly by discussion about sameness, which was the topic of an ongoing debate between academia, industry, and regulators since the 1960s [28, 29]. Under the ANDA system, which requires FDA approval before a generic drug product could be legally marketed, neither toxicological nor clinical effectiveness studies were required, provided that FDA already had such information in the innovators' new drug application [8]. The requirement for BE and its evaluation process represented a powerful advance, based upon pharmacokinetic principles of clinical pharmacology. In fact, not only are all systemically bioavailable generic drug approvals critically based on BE, such evaluations are routinely used to bridge different formulations during development of new drugs [27]. Essentially, testing BE

is the most universally used "surrogate" endpoint accepted by FDA. BE enables market approval of a generic drug to rely on a showing of BE with a small PK study in normal volunteers—in essence, substituting for an entire clinical development program with the BE PK study [27].

7.2.2.3 Uptake of QCP in New Drug Development and Regulation

During the 1970s, PK and drug metabolism concepts, and integration of PK and PD [27] rapidly evolved [30–32]. As a result, patient differences in age, body size, sex, renal and hepatic disease, and stage of disease gathered increased attention to account for individualization of drug dosage [27]. In the early 1980s, the FDA showed interest in the population PK (popPK) methods and PK/PD model estimation approaches that by Sheiner and colleagues introduced in the 1970s [33, 34], to support computer-assisted dosage individualization approaches and clinical therapeutic drug monitoring algorithms. This development provided the basis for FDA's "PK screen," a term first coined in a paper on studying drugs for special populations such as the elderly [35], as a potential means of explaining unexpected outcomes and identification of PK outliers potentially at risk of adverse reactions in a phase 3 trial [27, 35–38].

Physiologically based PK (PBPK) modeling, pioneered by Malcolm Rowland et al. [39–45], has steadily gaining traction and both the pharmaceutical industry and regulatory science practitioners have used this approach to further drug development and approval [27]. PBPK is a computer modeling approach using animal and human body models that are both anatomically and physiologically correct, to inform computer simulations of expected PK and drug–drug interactions in humans. PBPK modeling represents a mechanistic approach to study and predict the PK of drugs based not only on physiologic and anatomic characteristics, but also on the physical and chemical properties of a given drug (e.g., incorporation of pre-clinical in vitro data on drug physicochemical properties, metabolizing enzymes, transporters and permeability properties, etc.) [27, 36, 46, 47].

The first uses of PBPK were reported in the 1970s within the context of academic pharmacology research [44]. In the 1990s, the first regulatory application of PBPK was documented by FDA in its review and approval of tretinoin, the active ingredient of a teratogenic topical wrinkle cream [48]. FDA requested PBPK modeling and simulations to assess the risk of fetal exposure, on which basis, fetal exposure was concluded by FDA to be de minimis. The data from clinical studies and the nonclinical pharmacokinetic data in the NDA were employed in the PBPK model to estimate maternal and fetal plasma concentrations of tretinoin and its metabolites in a theoretical maximum exposure situation (i.e., after excessive topical application of tretinoin to the skin of upper body of a pregnant human and assuming maximal absorption of 10% of the applied product). Relying on the PBPK model, the FDA reviewers concluded that exposure to the fetus of tretinoin and potentially toxic metabolites under such conditions were several orders of magnitude below that from endogenous sources, rendering the exposure to be essentially a non-teratogenic dose of retinoic acid [27, 49].

7.3 The Evolving Role of Clinical Pharmacology in Drug Development

7.3.1 Clinical Pharmacology in the Twentieth Century

A quantitative, theoretical pathophysiological foundation of drug action was not inherent in the development and regulation of new drugs prior to 1970s [27]. Rowland, Benet and colleagues pioneered the current understanding of drug clearance concepts and drove the development of crucial tools for drug development and regulatory scientists, such as PBPK modeling and standard approaches for characterizing drug metabolism. Drug regulatory science has been fundamentally impacted by such key advances via the central understanding that pharmacodynamic effects (including disease biomarkers and clinical outcomes) are driven by quantitative variations in drug concentrations, rather than assigned dosage alone [27].

Drug development relies on clinical pharmacology including both in vitro and in vivo studies to evaluate the pharmacokinetic and pharmacodynamic characteristics of the drug, such as absorption, distribution, metabolism, and excretion (ADME), and desired drug activity and adverse effects, respectively [1]. As shown in Fig. 7.1, such studies evaluate how drug exposure and response are impacted by intrinsic (e.g., age, gender, race/ethnicity, genomics, physiology) and extrinsic factors (e.g., food effect, smoking, and DDIs) [1].
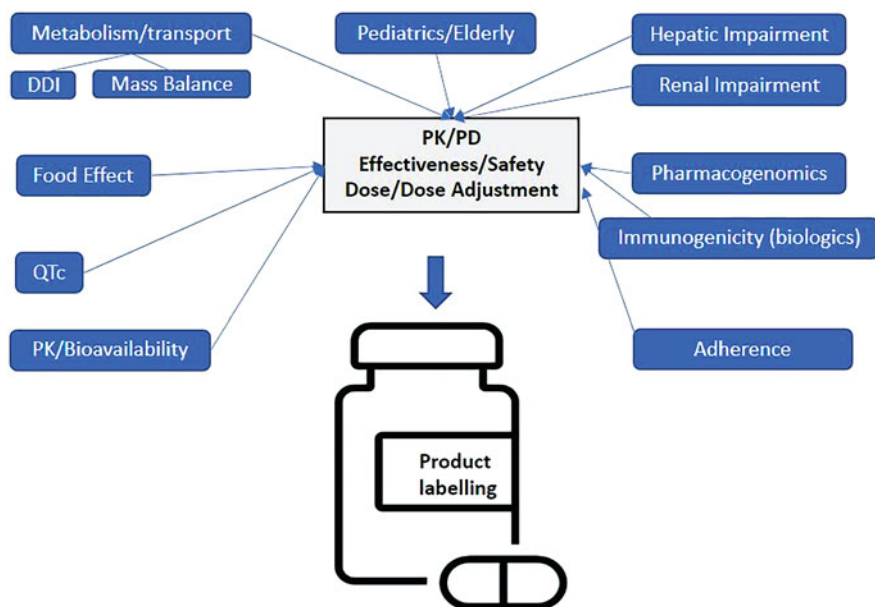

Fig. 7.1 Scope of clinical pharmacology in the twentieth century

7.3.2 Clinical Pharmacology in the Twenty-First Century

Incorporation of advanced quantitative clinical pharmacology procedures is being incorporated into regulatory science procedures, as articulated by the Model-Informed Drug Development (MIDD) initiative, and expanded in the real-world data (RWD) program [1]. The MIDD Pilot program has quickly matured to facilitate decision-making in drug development by employing a wide range of quantitative models. These advances in clinical pharmacology have helped to achieve better drug efficacy and safety by making the drug development process more rational and efficient and improving access to patient-tailored new drug treatments [1].

Clinical pharmacology-related questions in NDAs and BLAs pivot around dose selection, dosing regimen optimization, dose adjustment in specific populations, pediatric dose selections, benefit–risk assessment in whole and sub-populations [1, 50]. Once a drug is approved, the product labeling must provide relevant clinical pharmacology information, especially factors influencing PK, PD, effectiveness, and safety, possibly requiring dose adjustment [1]. When needed, post-marketing requirements (PMRs) may include studies to investigate issues that have not been adequately addressed [1]. PMRs may be needed to provide dosing instructions for subpopulations of patients who may not yet have been studied, to prevent serious adverse events when treated with the new drug [1]. For example, the approval letter for remdesivir treatment of COVID-19—approved 76 days after submission—required a PMC study in pregnant women and a PMR study in children and patients with renal and hepatic impairment, as well as evaluation of the drug's potential to prolong the QT interval [1, 51].

7.3.3 Pharmacometrics: The Combination of Pharmacology Models and Statistics for Decision-Making

In the last three decades, pharmacometrics has been increasingly employed in drug development and regulatory reviews. Efficient drug development and regulatory decisions are facilitated by pharmacometrics, a maturing science that quantifies drug, disease, and trial information [52]. Pharmacometrics scientists are part of multidisciplinary teams working closely with clinicians and statisticians comprising quantitative clinical pharmacologists, engineers, statisticians, and data management experts [52]. Pharmacometrics is central to drug, disease, and trial models that describe, respectively, (i) individual patient characteristics and the relationship between PK and PD for both desired and undesired effects, (ii) the relationship between biomarkers and clinical outcomes, time course of disease and placebo effects, (iii) the inclusion/exclusion criteria in clinical studies, patient dis-continuation, and adherence [52].

Characteristically, pharmacometric approaches employ pharmaco-statistical drug models, for simulation of concentration–effect, dose–response, PKPD relationships. Such analyses are planned, carried out, and discussed in the context of drug development and the therapeutic and regulatory decision-making process. Most importantly, such analyses can integrate knowledge about biology, compounds, and the development program, which is their most crucial strength [52].

7.3.3.1 Model-Informed Drug Development (MIDD)

The FDA's MIDD initiative was formally announced in 2018 in the sixth iteration of Prescription Drug User Fee Act (PDUFA VI), included as part of the FDA Reauthorization Act of 2017. Overall, the MIDD program aims to guide medical product developers to efficiently employ quantitative drug modeling for the following purposes, e.g., (i) dose optimization, (ii) supportive evidence for efficacy, and (iii) clinical trial design, [1, 53, 54]. In addition to traditional compartmental and empirical PK modeling and population PKPD in MIDD, new approaches are gaining traction, such as mechanistic models, systems pharmacology models, machine-learning models, and real-world data/evidence. Application of model-based analysis is steadily increasing in NDA submissions. MIDD has been adopted by new drug industry rapidly in recent years [54, 55]. MIDD models provide a platform for characterizing patient characteristics, pharmacology, and the current understanding of a disease.

Under PDUFA VI, FDA committed to advancing many key FDA activities via increased MIDD efforts by developing MIDD-related guidance updates, holding public workshops, and establishing a standard operating procedure to review MIDD-related submissions. Since 2018, FDA has also offered an MIDD Pilot Program to facilitate the development and application of MIDD approaches, i.e., exposure-based, biological, and statistical models using preclinical and clinical data. Successful application of these MIDD approaches can advance efficiency of clinical trials, decrease attrition rate, and optimize and/or individualize dosing regimens when dedicated trials are not available [56]. Via the MIDD Pilot Program, sponsors can meet with FDA scientists to discuss modeling approaches in product development [56]. The Pilot Program is administered jointly by CDER and the Center of Biologics Evaluation and Research, with CDER's Office of Clinical Pharmacology (OCP) as the point of contact. The pilot program aims to connect multidisciplinary efforts and make a regulatory platform available to all stakeholders early in the development of a new drug.

Under the MIDD Pilot Program, FDA has conducted an average 12 meetings a year during the last 2 years (2021–2022). The submissions posed questions such as dose/dosing regimen justifications, design of clinical trials, and post-approval dosing regimen changes by employing a variety of approaches including popPK, exposure–response [29] modeling, quantitative systems biology, and PBPK modeling [1]. As of 2021, these discussions between FDA and sponsors under this pilot program have led to the MIDD-supported approval of two regulatory submissions, a supplemental

NDA, and a supplemental Biological License Application [1]. Between 2018 and 2019, there was an increase in the use of PBPK submissions for drug development in several application areas, such as evaluating potential DDIs involving metabolizing enzymes and transporters; pediatrics; assessment of drug exposure in patients with renal impairment, etc. [47, 54, 57, 58]. Additionally, different model types used in MIDD are increasingly used either in sequence or simultaneously, such as combining mechanistic modeling with machine learning (ML) for response prediction, which will create its own set of challenges and opportunities in the future [1, 54, 59].

7.3.3.2   Generic Drugs

A principal application of clinical pharmacology to generic drug use is derivation of actionable knowledge of the variability connected to generic substitution during the drug product's lifecycle [29]. Intrasubject variability can be observed when different results are observed resulting from the administration to a patient of the same identical drug product on two different occasions [29]. Several authors have described how variability can impact patient perception of generic substitution, and how differences in excipients can affect both the BA and pharmacology of generic drug products. Significant differences may be present in the clinical pharmacology between batches of the brand drug product, which—while permissible— can make evaluation of BE more challenging [29, 60]. Authorized generics, exact same drug products as the branded drug product, manufactured by the brand name company but without the brand name on their label, have been described as a natural experiment, allowing scientists to assess variability of clinical effects due to differences in drug product appearance [29, 61] as perceived by the consumer.

Model-based integration of the data obtained during a drug product lifecycle can be used to design of accurate, sensitive, and efficient BE studies that incorporate the current understanding of drug exposure mechanisms and the variability sources in both patients and healthy subjects [29]. By leveraging the existing clinical pharmacological knowledge of the brand product, PBPK and QCP models can be used to generate model-integrated evidence to inform decisions in generic drug development and approval [62]. Such tools are used extensively by FDA to make regulatory review decisions and to establish recommendations for demonstrating drug product BE to the reference listed drug, as described in the FDA product-specific guidances for industry for generic drug development [63]. FDA has been employing PBPK modeling in both policy and standards development [27, 64–67]. For example, in FDA's generics drug review section used PBPK techniques to investigate several challenging policy issues including BCS class II/III biowaiver and food effect on PK. An example of how PBPK can be used in generic drug development from an industry perspective has been published recently [68]. Using a model to gain knowledge about the population PK of a drug can result in a model-based BE study that is more efficient than a larger, more expensive, and less sensitive comparative clinical end-point BE study [29, 69]. Of note, new clinical study designs and statistical analyses for efficient conduct of comparative clinical endpoint BE for

generic drug development are also emerging [70], such as patient enrichment strategies, stratified randomization by baseline or demographic characteristics, replication, adaptive designs, clinical data aggregation and analysis in real time, and product-specific clinically justified equivalence criteria.

Evaluation of generic drug sameness and BE for substitution in patients present several scientific challenges, which in turn propagate within a complex regulatory and economic environment. For example, the FDA's generic drug program receives circa 1000 new ANDA submissions each year and responds to over 3000 written development questions prior to application submission (i.e., controlled correspondence) [29]. More than 1600 product-specific guidances have been created by FDA to assist generic drug developers to meet FDA standards for specific brand products. Each of these actions has a scientific foundation and potential regulatory, and economic impact on both brand and generic product developers, and impact on patient access to generic products. By applying scientifically sound, efficient, sensitive, and accurate BE studies, regulatory clinical pharmacologists, working in FDA, have lasting impacts on public health by ultimately ensuring ensure timely access to generic drugs and correct decisions on generic drug substitution. Clinical pharmacologists can expand and refine the application of these tools of sameness, equivalence, and substitution so that their utility can be further expanded to not only the generic drug space but also other aspects of drug and biologic product development [29].

7.3.3.3 Real-World Data

Real-word data (RWD) are the data relating to the health status of patients and/or the delivery of health care which are regularly collected from several different sources. Different sources RWD include electronic health records (EHRs), claims and billing activities, product and disease registries, patient-generated data including in home-use settings, other sources (e.g., mobile devices). Analysis of RWD can yield clinical evidence on the use and potential benefits or risks of a medical product, which is referred to as real-world evidence (RWE). RWE was also defined by Congress as data derived from sources other than traditional clinical trials. Different study designs or analyses can generate RWE, such as randomized trials, pragmatic trials, and observational studies [1, 71].

RWD have been used to generate RWE and provide insights into different pharmacotherapeutic issues including identification of adverse event and comparison of effectiveness. While there are challenges and opportunities associated with employment of RWD, evidence from RWD has been used to address clinical pharmacology issues and promote therapeutic individualization [72, 73]. In particular, RWD have been used for optimization of dose and dosing regimen, evaluation of benefit/risk in specific populations, and optimization of treatment for intrinsic and extrinsic factors, filling the gap between traditional clinical trials and real-world clinical practice, and development of endpoints and biomarkers [72, 73].

The digital ecosystem for healthcare is rapidly evolving. Electronic health record systems have been widely adopted in the recent past, and patients also generate large amounts of personal health data on a constant basis in their mobile devices, wearables, and other biosensors. While already on the rise in the last decade, the COVID-19 pandemic has accelerated the use of wearable digital health technology and telemedicine [1]. Such a large trove of health data can potentially be used to answer previously unanswerable questions and improve the design and conduct of clinical trials and studies.

Given the rapidly evolving healthcare setting and the challenges such as COVID-19, clinical pharmacologists have both the chance and responsibility to use RWE from RWD at their full potential to promote public health [1]. Even though FDA has traditionally used RWD and RWE for safety surveillance, as also emphasized in PDUFA VI and VII [74, 75], additional focus on their use to support regulatory decisions was introduced by the twenty-first Century Cures Act in 2016 (e.g., for new indications for approved drugs) [1, 76]. Specifically, the Cures Act mandated FDA to develop a framework which was issued in 2018 with the aim to evaluate the use of RWD/RWE in regulatory decisions and included considerations whether (i) RWD is fit for use, (ii) the trial or study design RWE is generated from provides adequate scientific evidence to answer the regulatory question, and (iii) the conduct of the study meets FDA regulatory requirements [71, 77].

Clinical pharmacology knowledge can be employed bridge knowledge gaps between clinical trials and real-world clinical practice [1, 72]. Using RWD, the benefit–risk profile of a drug can be better understood in patients that are either underrepresented or absent in the clinical trials conducted during drug development (e.g., infants and children, pregnant women, older adults, patients with organ dysfunction or receiving concomitant medications, or individuals with different drug metabolism) [1], leading to the development of appropriate treatment monitoring and management strategies. RWD/RWE can also be applied to the selection of the optimal treatment and dosing regimens for different patient populations, simplification of clinical trials and drug development by guiding the eligibility criteria of the clinical trials, and disease modeling and the development of biomarkers and clinical endpoints [1].

However, there are limitations to the use of RWE from RWD in drug development and regulation, and additional regulatory research is necessary to determine where and how RWD can be most helpful and to develop best practices [78]. RWE can be hindered by the suboptimal quality, incompleteness, and unstructured formats of data, which would make the analyses time-consuming. A lack of randomization in the data may also lead to analyses subject to confounding and bias. Finally, the multiple systems hosting patient information may be non-interoperable due to incompatible formats and standards, which may compromise data aggregation and subsequent analyses [1].

To illustrate the use of RWD/RWE, randomized clinical trial data and a cohort derived from RWD were recently used in a collaborative study between FDA, a RWD company, and a health system, to investigate the incidence of on-treatment pneumonitis in patients with non-small-cell lung cancer (NSCLC) treated with chemotherapy or immune checkpoint inhibitors (ICI). The clinical trial data

comprised a comparison of ICI treatment (with/without chemotherapy) to a chemotherapy alone control arm using pooled data from approximately 6500 patients from 8 randomized trials. The RWD sample included about 1200 patients from the health system. Both clinical trial and RWD cohorts showed a higher incidence of treatment-associated pneumonitis among ICI-treated NSCLC patients compared to those receiving chemotherapy alone. Both clinical trials and RWD also showed a consistent increase of treatment-associated pneumonitis in patient with a prior medical history of pneumonitis as compared to patients without it [1, 79].

Another recent example of the use to RWD is a 2022 study comparing serum thyrotropin (TSH) levels between patients who continued taking the same generic levothyroxine product and those who switched, using a large data set from a national administrative claims database linked to laboratory test results. No clinically significant changes in TSH level were observed as a result of switching among different generic levothyroxine products. Such findings conflict with what recommended in the current guideline [80].

7.3.4 Role of Academia in the Science of Drug Development and Regulation

Advances in clinical pharmacology as a discipline have been greatly advanced and driven by collaborations between academic experts and drug development and regulatory scientists. Pharmaceutical medical science aims to employ clinical pharmacology learnings on how drugs work and vary in patients' response, what their limitations are, and how to optimally use them in practice. [81, 82]. The successful evaluation of potential new medicines relies on of clinical pharmacology expertise, based on effective integration of diverse skills. It is therefore key to nurture such skills, including experimental and clinical research methods, PK and PK/PD modeling and simulation, and translational knowledge, through innovative partnerships between industry and academia which will benefit both partners [81, 82]. For example, the discipline of population-based modeling originated from academia. Non-linear mixed-effects modeling techniques and the NONMEM software package for population pharmacokinetic modeling were developed by Stuart L. Beal and Lewis B. Sheiner in the late 1970s at the University of California San Francisco and have served as foundations of pharmacometrics ever since [83].

A vibrant academic clinical pharmacology community has contributed a large body of concepts and techniques for drug researchers, while also being instrumental in the training of researcher–clinical pharmacologist [82]. For example, believing that industry and academia could collaborate in a more integrated and productive way, GlaxoSmithKline developed the Academic Discovery Performance Unit (AcDPU) as a new business model to manage the early development of a few drugs [84]. AcDPUs combine academia's in-depth scientific and clinical expertise with industry's expertise in drug discovery and development. Such collaborations can facilitate the design and execution of a preclinical and clinical plan, up to the

proof-of-concept stage—generating enough evidence about the safety and efficacy of a promising new drug to warrant the investment in larger Phase II clinical trials [84]. However, as previous interactions between pharmaceutical industries and academia have resulted in conflict-of-interest challenges, a commitment to joint objectives between the two partners is necessary to help address conflicting priorities and different approaches to publication, for example [84].

To further facilitate fruitful collaborations, industry could commit to publish results of all studies, both positive and negative, and explore new models of shared risk, shared reward, IP pools, etc. Collaborations could also be enhanced by allowing access to tool compounds and industry labs and projects for training of clinical pharmacologists at different career stages. With due attention to preventing conflicts of interest, careful creation of shared and revolving door appointments (i.e., movement of high-level employees from public-sector jobs to private-sector jobs and vice versa) could also benefit a thriving collaboration across different stakeholders. At the same time, academia should not perceive industry exclusively as a source of financial support only but recognize industry partners as equal scientific and clinical partners. Clinicians should be encouraged to take part in research and engage with industry as training partners. Academics should fully use the collective excellence across academic institutions and accept a level of risk in return for longer term reward [85].

FDA collaborates with academic institutions via Centers of Excellence in Regulatory Science and Innovation (CERSIs), aimed at advancing regulatory science through innovative research, training, and scientific exchanges. Through these collaborations, FDA's scientific staff has access to regulatory science-related training, workshops, and seminars. For example, current research and advancements in regulatory science are presented via FDA's CERSI Lecture Series addressing the safety and efficacy of medical products at a pre-clinical stage and emerging technologies [86].

The American Course on Drug Development and Regulatory Sciences (ACDRS), established by the University of California San Francisco (UCSF) in 2007, is an advanced level postgraduate training program for professionals in the fields of pharmaceutical, medical devices, regulatory authorities, government, and academia. The ACDRS Course covers all facets of pharmaceutical sciences relating to the development of medicine and medical product https://pharm.ucsf.edu/acdrs. In collaboration with Beijing University, UCSF collaborated in the 2009 launch of the Chinese Course on Drug Development and Regulatory Science (CCDRS), aimed at improving the quality and acceptance of pharmaceuticals and pharmaceutical products exported from China [87]. Dr. Carl Peck and colleagues have played a pivotal role in launching these courses.

In Europe, the European Center of Pharmaceutical Medicine (ECPM) is the main university institute for medicines and drug development, after "sowing the seeds for training in pharmaceutical medicine" in 1989 by FDA scientists Drs. Carl Peck and Robert O'Neill as recognized by the ECPM community. The ECPM's education/training and research departments aim to form highly skilled drug development specialists (https://ecpm.unibas.ch/).

7.4   Training in FDA

FDA has long been engaged in staff training and regulatory research. The forerunner agency to the FDA, the Drug Laboratory in the USDA Bureau of Chemistry headed by Harvey Wiley, trained its staff and set standards based upon research of poisons in food substances and identification of ingredients of drugs. Skelly [8] documents the FDA's research on BA and BE that led to BE requirements of bioequivalence and generic drug pharmaceutical quality standards. In 1987, the FDA Bureau of Drugs and Biologics was renamed to recognize FDA "research" functions in the respective center names (e.g., Center for Drug Evaluation and Research (CDER) and Center for Biologics Evaluation and Research (CBER)).

In 1988, the Office of Professional Development and Staff College was established in CDER for the purpose intramural postgraduate training of FDA reviewers in regulatory clinical pharmacology, biostatistics, and other disciplines required to competently review regulatory submissions [88]. This new Office aimed to train and professionally develop a team of regulatory clinical pharmacologists and enrich CDER's scientific environment [88]. Establishing an intramural training program was envisioned to advance both the regulatory science and clinical pharmacology fields by (i) training newly recruited professionals and bringing them up to a high skill level in critical CDER program areas as quickly as possible; (ii) enhancing the competency of current scientists by creating opportunities for CDER staff to acquire and maintain essential knowledge; (iii) using different formal fellowship programs to develop regulatory science specialists, (iv) communicate and cooperate with the drug development and general medical communities by disseminating information about regulatory science; and (v) improving the drug development process based on outcome of research projects.

Professional development in FDA is achieved via participation in intramural courses, online training modules, studying of guidances, experience and practice of drug regulatory science, and reviewer-initiated regulatory research projects [88]. While fundamental to the development of highly skilled staff, the above-mentioned activities are complementary to a mentor-mentee relationship [88]. Numerous training courses in a wide range of scientific and reviewer procedures have been offered to FDA staff. In 2018, the CDER's Division of Learning and Organizational Development (DLOD) was established to be responsible (DLOD) for the development of scientific, regulatory, core competency, and leadership skills in support of CDER's mission. DLOD provides several different learning opportunities, educational activities, and professional development through a variety of instructional methods to best prepare CDER staff to meet the organization's mission. While DLOD's offerings are for FDA staff's use only, many other public training opportunities are available. Today, FDA offers many courses and opportunities for FDA staff, consumers, and industry personnel [89].

The Critical Path Initiative (CPI) was launched in March 2004. It represents the Agency's plan to update and improve via scientific innovation the development, evaluation, and manufacture process of FDA-regulated medical products. At launch,

FDA released the landmark report "Innovation/Stagnation: Challenge and Opportunity on the Critical Path to New Medical Products," describing a slowdown in innovative medical treatments therapies submitted to the FDA for approval, even after scientific discoveries with the potential to prevent and cure diseases such as diabetes, cancer, and Alzheimer's. That report raised the urgent concern about the difficulties and unpredictability associated with the development of medical products. It called for urgent collective action to modernize the Critical Path, i.e., the medical product development process, by using scientific, technical, and information technology to evaluate and predict the safety, effectiveness, and manufacturability of medical products, thus making product development more predictable and less costly [90]. For example, the FDA's Sentinel Initiative was launched in 2008, a long-term program designed to build and implement a national electronic system for monitoring the safety of FDA-approved drugs and other medical products. A list of Critical Path reports is archived at http://wayback.archive-it.org/7993/201801250 75636/https://www.fda.gov/ScienceResearch/SpecialTopics/CriticalPathInitiative/ CriticalPathOpportunitiesReports/default.htm.

7.4.1 Tools for Drug Development and Evaluation that Leverage Advances in Basic, Biomedical, and Clinical Science

The twenty-first Century Cures act added a new section to the FD & C Act "Qualification of Drug Development Tools" (DDTs) [76]. DDTs comprise methods, materials, or measures able to potentially aid drug development [1, 91] and can include biomarkers, clinical outcome assessments (COAs), and certain animal models. To support DDT development and qualification, FDA has established qualification programs with a multi-step process [1, 92, 93]. Qualification concludes that the DDT can reliably provide specific interpretation and application in drug development and regulatory review within the stated context of use. Once qualified, DDTs can be used in any drug development program for the qualified context of use and generally included in IND, NDA, or BLA submissions without FDA having to reconsider and reconfirm its suitability [1, 92, 93].

Clinical pharmacologists in the FDA are an essential part of the program as they are responsible for reviewing submissions to the DDT qualification program and conducting active regulatory research to help develop DDTs [1, 93]. For example, for cardiac condition treatment like high cholesterol in the development of biosimilars, the Division of Applied Regulatory Science in the Office of Clinical Pharmacology (OCP) sponsored a clinical study for PD biomarker identification [1, 94]. OCP is also collaborating with different stakeholders (i.e., foreign counterparts, non-profits, academia, and drug developers) on the vitro Proarrhythmia Assay (CiPA), to potentially estimate the risk for a drug to cause cardiac arrhythmia torsades de pointes [1, 95]. Human genomic testing as a tool for precision medicine

has been steadily moved forward through research including use of in vitro assays. For example, FDA qualified a cystic fibrosis mutation test to detect the presence of CFTR [1, 96]. The FDA is also researching emerging technologies and facilitating scientific discussion and advancement by also organizing workshops on innovative topics co-sponsored with the Centers of Excellence in Regulatory Science and Innovation, and Center of Research for Complex Generics [1, 86, 97].

FDA has leveraged its access to patient and study-level clinical data during drug application to develop a series of disease progression models [52]. Disease progression models are necessary to understand the progression of disease and are valuable in retrospective cohort analyses. Such models rely on longitudinal observation of patients and the temporal profiles of cognitive scores to predict the patient's status at baseline [98]. There are three broad categories of disease progression models: empirical, semi-mechanistic, and systems biology. Empirical and system biology models represent the two extremes, with the former if exclusively data driven, and the latter physiologically based. Semi-mechanistic models can be described as the midpoint between empirical and systems biology models [98]. Empirical models serve as mathematical frameworks to interpolate between observed data and do not describe underlying biological processes. Systems biology models utilize as much molecular detail as possible to mathematically represent biological, pathophysiological, and pharmacological processes in the course of the disease [98]. Based on the problem at hand, a specific model type would be more appropriate than others. For example, empirical models are better suited to answer questions with a relatively narrow in scope, such as dose selection or clinical trial design and interpretation [98]. On the other hand, broader scientific questions, such as those on drug effects prediction, identification of novel target(s), or use of biomarker data for risk projection, are better answered by semi-mechanistic and systems models, given their more mechanistic nature [98–100].

Additionally, disease models are often developed for the characterization of slowly progressing chronic diseases, and as such, they require disease severity data collected over protracted time periods. Pooling of data from several clinical studies is often necessary to provide sufficient observations to model a disease progression. Consequently, disease modeling has greatly benefited by model-based meta-analysis by pooling results of multiple previously conducted studies [98].

7.4.2　Generic Drug Development and Research

The GDUFA-funded Science and Research program aims to establish standards for drug equivalence and provide the American public with safe, effective, and high-quality generic drug products, by supporting the advance of state-of-the-art methodologies and tools [101]. In 2021, OGD funded generic drug science and research programs with about $20 million in the forms of grants and contracts. Several research outcomes were highlighted by FDA, such as those focusing on the use of (i) in vitro and in vivo studies to better assess the role of excipients in abuse-deterrent

opioid drug products, (ii) AI methods to improve data analytics, and (iii) differences in animal and human anatomy and physiology to improve the extrapolation of animal data to humans [101]. Facilitating the development of complex generic drugs was also on the OGD research agenda by focusing on the development of an efficient in vitro BE approach (which led to the approval of two generic ophthalmologic drugs) [101].

A complex generic is a generic that could have a complex active ingredient, complex formulation, complex route of delivery, or complex drug device combinations. They are harder to develop and for which few or no generics are available as a result. In the absence of market competition among generic alternatives, patients needing such medicines may not be able to afford them as they can be so expensive. Therefore, a program like the GDUFA Science and Research program is particularly important for complex products [101].

Understanding of these complex products is improved as a result of GDUFA-funded research and its outcomes, which often contribute to the development of advanced methods for product quality and performance characterization. Such methods may play a critical role in how FDA assesses the quality and BE of complex generic products. These methods may also be the scientific basis for novel and more efficient pathways for the development of complex generics [101]. As a result, these methods can be included in new and revised product-specific guidances (PSGs), as well as general guidances for industry, which are published on a regular basis to communicate BE and quality recommendations to the generic industry [63]. Furthermore, FDA uses GDUFA research outcomes to determine the likely suitability of proposed BE approaches in submitted in pre-ANDA product development meetings, and the most current scientific insights and regulatory expectations, thus helping prospective ANDA applicants with scientific and technical advice. FDA facilitated 87 product development and pre-submission pre-ANDA meetings in Fiscal Year 2021. The GDUFA research outcomes also helped FDA assess ANDA referencing complex products, thus ultimately improving patient access to complex generics for which development was presumed unfeasible even just a few years ago [101].

As part of FDA's commitment to expand its collaboration and communication with industry, the Center for Research on Complex Generics (CRCG) was established in FY 2021, to overcome challenges impacting patient access to high quality, safe, and effective generic products by bringing generic industry stakeholders and FDA together [101]. The CRCG ultimately aims to successfully develop complex generics by helping the generic industry stakeholders efficiently and effectively use GDUFA Science and Research outcomes (i.e., scientific insights, technical methods, study designs, data analyses, and others) [101].

Every fiscal year, FDA and industry stakeholders develop scientific priorities [102]. Many of the 15 scientific priorities developed for FY 2021 [102] are clinical pharmacology and modeling related and include the establishment, implementation, improvement, integration, and/or expansion of:

- Predictive in silico, in vitro, and animal models to evaluate immunogenicity risk of formulation or impurity differences in generic products
- Improvement of drug absorption PBPK models via complex routes of delivery (e.g., nasal, inhalation, dermal, ophthalmic) so they can be used to support alternative BE approaches,
- In vitro methods with PK and other methods as alternative to the use of comparative clinical endpoint BE studies for nasal and inhaled drug products,
- Quantitative pharmacology and BE trial simulation to optimize design of BE studies for generic drug products and establish a foundation for model-based BE study designs,
- Predictive dissolution, PBPK, PK/PD models, and ML to evaluate in vitro BE options for orally administered drug products and support global harmonization of the most efficient BE recommendations,
- Scientific understanding of the role of excipients in generic drug products to support the expansion of the Biopharmaceutics Classification System (BCS) Class 3 biowaivers to drug products with differences in formulations larger than currently recommended in FDA guidance.

As mentioned above, many of the GDUFA research outcomes critically benefited complex generic drug approvals, which could be otherwise difficult to be approved. As a case example, application PBPK modeling on topical dermatological products was instrumental in the approval of first generic Diclofenac topic gel [103]. Conducting comparative clinical endpoint studies for dermatological drug products can be expensive and certain formulation differences may not be detected considering the studies may not be sufficiently sensitive. Minimized or no human testing can be supported by using quantitative methods and modeling, such as PBPK modeling. PBPK models used for regulatory decision-making should be sufficiently verified and validated (V & V) for their intended purpose [103]. The generic diclofenac sodium topical gel was approved by FDA based on a totality of evidence, including qualitative and quantitative sameness and physical and structural similarity to the reference product, an in vivo BE study with PK endpoints, and, notably, a virtual BE (VBE) assessment using dermal PBPK modeling and simulation in place of a comparative clinical endpoint study in patients [103]. Describing the relationship among systemic (plasma) and local (skin and synovial fluid) diclofenac exposure with the modeling approach allowed BE of the generic and reference products at the presumed site of action to be demonstrated. Based on the validation-for-purpose principle, the V & V process involved assessing the goodness of fit for observed data of diclofenac concentrations in skin tissues and plasma, and the overall performance of the modeling platform for predicting local and systemic exposures for relevant products following the same route of delivery. This instance illustrates how PBPK modeling and simulation can be used for regulatory decision-making and offers scientific considerations on good practices for the validation and verification of models and the determination of BE for dermatological drugs [103].

7.4.3 Coupling Real-World Data on Generic Drugs with Clinical Pharmacology

In the field of generic drug, RWD analysis using post-market data represents a great opportunity to compare the real-world performance of generic and brand name products to address concerns inherent in medical practice for certain therapeutic areas. For example, the current guideline recommendation in medical practice warns clinicians about potential changes in TSH levels associated with switching among levothyroxine products sourced from different manufacturers. Recently, FDA-sponsored research retrospectively looked at the clinical dynamics related to the therapeutic use of levothyroxine, a drug that not only has a narrow therapeutic window, but that also is one of the most widely prescribed drugs in the United States. The research, published in JAMA Internal Medicine [80], capitalizes on the use of health records to anonymously identify hypothyroid patients who have switched in their use of manufactured thyroxine products while being monitored for thyroid function over time. The focus on levothyroxine allowed the researchers to execute a real-world clinical review (within limitations dictated by available claims data) of an FDA-approved therapeutic available from several alternative manufacturers [80]. Additionally, the investigators' analysis extended to a consideration of whether social or institutional concerns, rather than potential evidence-based issues related to generic product performance, may ultimately place limitations on the uptake and prescribing practices of approved generic drug products. Results of this comparative effectiveness research study suggest that switching among different generic levothyroxine products was not associated with clinically significant changes in TSH level. These findings would counter the current guideline recommendation [80].

To safeguard the continual safety and effectiveness of generic drugs, also given the high rate of generic drug usage in the US, effective post-marketing surveillance of generic drugs is fundamental [104]. Generic post-marketing surveillance and new drug surveillance share the identical aim of monitoring drug use, clinical effectiveness, and safety issues after a drug is marketed and reaches a larger and broader population [104]. Nevertheless, surveillance of generic drugs presents additional and specific issues [104]. Evaluation of substitutability can supplement BE testing and determine if patient characteristics interact with formulation differences between products.

7.4.4 Research on Artificial Intelligence (AI) and Machine Learning (ML) Models

The rapid development of AI and ML may revolutionize drug development, manufacture, and regulatory approval. It is therefore necessary to have a shared understanding and standardization of AI and its subset models and machine learning (ML), as well as the associated best practices and regulatory expectations. ML

models can be developed by training algorithms through analysis of data and prior experience, without explicit mechanistic bases [105, 106]. For drug development, AI/ML applications in the broad context of drug development include drug target identification/selection/prioritization, drug candidate screening and design, the development of in vivo predictive models based on preclinical information, dose/dosing regimen optimization, selection of trial participants, patient recruitment, adherence monitoring, patient retention, clinical trial data collection/management/analysis, and clinical endpoint assessment. For post-marketing surveillance, AI/ML have been used for case processing and case submission. For pharmaceutical manufacturing, AI/ML have been used in optimization of process design, advanced process control, smart monitoring and maintenance, and trend monitoring.

7.5 The Evolving Role of Clinical Pharmacology in Drug Regulation and Guidance

Clinical pharmacology can be classified as non-quantitative or quantitative [27]. Non-quantitative clinical pharmacology focuses on the classification of drug actions and its variability and as such includes several different concepts (i.e., biological, biochemical, genetic, demographic, environmental, and immunological), and factors (i.e., formulation and manufacturing). These characteristics represent the underlying sources of variability in drug absorption, metabolism, and elimination, and drug effects. Broadly, non-quantitative clinical pharmacology focuses on where the drug goes and what the body does to the drug (e.g., PK) and what the drug does to the body (e.g., PD) [27]. Drug disposition in healthy individuals and patients allows to track a drug and its metabolite(s) during the time the drug is passing through the body. In contrast, pharmacodynamics studies the effects of the drug and its metabolites on cells, tissues, and the body at a whole [27].

Quantitative clinical pharmacology involves modeling drug disposition, providing measurable, numerical meaning to the mass, volume, concentration, and time dimensions, and calculable metrics for PD effects and clinical responses [27]. Quantified pathophysiological–pharmacological relationships can be modeled using PK/PD or exposure-response models. The addition of stochastic elements to models allows the pharmacostatistical estimation of model parameters (using datasets derived from experiments and trials), and the PK/PD simulation in individuals, populations, and clinical trials [27]. Overall, "pharmacometrics" comprises methods and approaches for PK, PD, population estimations, and simulations. The term, which initially had a more limited definition [107], was used in the current meaning by Rowland and Benet [32].

Starting in the 1990s, FDA started applying advanced QCP approaches that included PK-guided clinical trial designs [27, 108], and encouraging wide usage of popPK and PD [27]. Development of QCP-based clinical trial simulation techniques represented a far-reaching enhancement of such approaches [27, 109, 110]. The approximate timeline for QCP-related guidances and policies is depicted
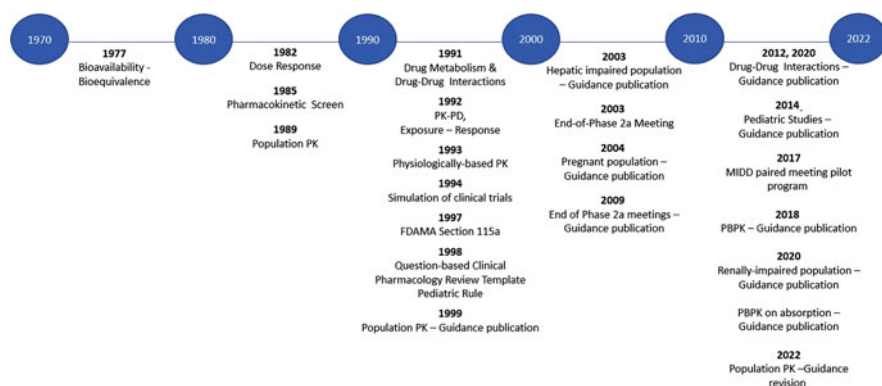
Fig. 7.2 Approximate timeline of major events for incorporating quantitative clinical pharmacology concepts into FDA practice, guidance, and policies. (Partially adapted from Reference [27])

in Fig. 7.2. In 1992, a national meeting focusing on applications in drug development and regulation was held building on the advances in PK, PD, and population PKPD of the previous decades [27, 111]. During that time, FDA also focused its attention to safety consequences of drug metabolism based DDIs following sudden deaths in patients using a common non-sedating antihistamine terfenadine (Seldane), in combination with ketoconazole, an antifungal agent [27]. It was determined that ketoconazole caused a CYP3A4-mediated clearance reduction of terfenadine, resulting in an increase of cardiotoxic systemic plasma concentrations of terfenadine. This resulted in increased regulatory requirements regarding data on the drug's metabolism, possibly interfering drugs, and the association of electrocardiographic QT-interval prolongation and fatal arrhythmia [27, 112]. The research findings of Malcolm Rowland and others provided necessary advice to drug developers and has been represented the critical foundations on which guidances regarding vitro and in vivo drug metabolism and DDI studies were based on [27].

FDA further emphasized PK-centric regulatory research, guidance, and review [27]. Particularly, important developments were the creation of (i) the Clinical Pharmacology Subcommittee of the Advisory Committee on Pharmaceutical Science and Clinical Pharmacology, (ii) the Division of Pharmacometrics, (iii) the Clinical Pharmacology Question-based Review template, identifying key QCP elements required for the review of the clinical pharmacology section of a filed NDA, and (iv) the meeting procedure for End-of-Phase 2a, allowing cooperation between industry and regulatory scientists to apply QCP interpretation and planning of ongoing INDs [27].

A guideline with general recommendations for BA and BE data was published at time of the 1977 bioavailability regulation [21]. FDA subsequently released updated guidances containing detailed study design and statistical data analysis procedures for BA and BE studies [27]. FDA started encouraging for dose–response information to be included in NDAs in the early 1980s. Such a recommendation was heightened in in 1994 when the International Council for Harmonisation of Technical

Requirements for Pharmaceuticals for Human Use (ICH) released a Dose-Response guidance stating that "Agencies should also be open to the use of various statistical and pharmacometric techniques such as Bayesian and population methods, modeling, and pharmacokinetic-pharmacodynamic approaches" [113]. The guidance on derivation and analysis of exposure–response (PKPD) data further recommended and described advanced QCP pharmacometrics approaches [114].

All official FDA guidances are available at https://www.fda.gov/regulatory-information/search-fda-guidance-documents. Users can filter results by specific keywords, product, issue date, FDA organizational unit, type of document, subject, draft or final status, and comment period. As of April 14th, 2022, OCP has issued a total of 29 guidances. The Office of Generic Drugs has issued 12 guidances, including such as "Bioequivalence Studies With Pharmacokinetic Endpoints for Drugs Submitted Under an Abbreviated New Drug Application" and "Topical Dermatologic Corticosteroids: in Vivo Bioequivalence." Overall, there are a total of 43 guidances associated with clinical pharmacology on broad drug development topics (Table 7.1). Each published guidance is the product of years of regulatory research and represents the Agency's current thinking on a particular subject. For example, the recently published guidance for industry: Bioavailability Studies Submitted in NDAs or INDs – General Considerations is consolidated from three decades of scientific thinking as well as regulatory practices and reflects an achievement from all stakeholders including FDA, industry, academia, and other regulatory agencies [115]. In addition, the final recommendations account for the comments received during the public comment period when the draft guidance documents were published.

The successful and efficient development of new drugs to protect and promote public health critically relies on the availability of clear, practical, and current guidances and policies to inform drug development and regulatory evaluation [116]. As a result, several stakeholders (e.g., drug developers, Congress, FDA leadership, and patient advocacy groups) have highlighted the need for timely revision and issuance of new FDA guidance documents and policies. Considering the broad field of clinical pharmacology, an integrated collaborative approach across different stakeholders is required to satisfy this need. The Guidance and Policy Team (GPT) was formed by OCP to act in a collaborative and transparent manner to lead the development and implementation of current and evidence-based guidance and policies governing clinical pharmacology in drug development [116].

Guidance documents represent what the FDA is currently thinking regarding a particular topic. Guidances are not enforceable as they are neither regulations or laws. Guidance documents describe FDA's interpretation of FDA's policy on a regulatory issue. They "usually discuss more specific products or issues that relate to the design, production, labeling, promotion, manufacturing, and testing of regulated products. Guidance documents may also relate to the processing, content, and evaluation or approval of submissions as well as to inspection and enforcement" [117]. Comments can be made on FDA draft guidance documents at www.regulations.gov/. Electronic or written comments on the draft guidance should be made before the close date, to ensure that the Agency considers your comment before it begins working on the final version of the guidance. Policy refers to an

Table 7.1 Current list (as of July 2022) of the 43 FDA total Guidances associated with clinical pharmacology on broad drug development topics, obtained from https://www.fda.gov/regulatory-information/search-fda-guidance-documents. The asterisk indicates guidances for which comments are still open as of April 2022

Summary	Issue Date	FDA Organization[a]	Guidance Status	Docket Number
The use of published literature in support of new animal drug approvals	20-Apr-2022	CVM	Draft*	FDA-2021-D-1155
Bioavailability studies submitted in NDAs or INDs – General considerations	15-Apr-2022	CDER	Final	FDA-2018-D-4367
Clinical pharmacology considerations for antibody-drug conjugates guidance for industry: Draft guidance for industry	7-Feb-2022	CDER CBER	Draft*	FDA-2021-D-1051
Population pharmacokinetics: guidance for industry	3-Feb-2022	CDER CBER	Final	FDA-2019-D-2398
Pharmacokinetic-based criteria for supporting alternative dosing regimens of programmed cell death Receptor-1 (PD-1) or programmed cell death-ligand 1 (PD-L1) blocking antibodies for treatment of patients with cancer: draft guidance for industry	25-Aug-2021	OCE CDER	Draft	FDA-2021-D-0691
Bioequivalence studies with Pharmacokinetic endpoints for drugs submitted under an abbreviated new drug application	20-Aug-2021	CDER	Draft	FDA-2013-D-1464
Demonstrating bioequivalence for soluble powder Oral dosage form products and type A medicated articles containing active pharmaceutical ingredients considered to be soluble in aqueous media	21-May-2021	CVM	Final	FDA-2019-D-3764
Evaluation of gastric pH-dependent drug interactions with acid-reducing agents: study design, data analysis, and clinical implications guidance for industry: draft guidance for industry	30-Nov-2020	CDER	Draft	FDA-2020-D-1794
Clinical drug interaction studies with combined Oral contraceptives guidance for industry: draft guidance for industry	20-Nov-2020	CDER	Draft	FDA-2020-D-1848
The use of physiologically based Pharmacokinetic analyses — biopharmaceutics applications for oral drug product development, manufacturing changes, and controls. Guidance for industry	30-Sep-2020	CDER	Draft	FDA-2020-D-1517
Pharmacokinetics in patients with impaired renal function — study design, data analysis, and impact on dosing and labeling	3-Sep-2020	CDER	Draft	FDA-2010-D-0133
		CBER CDER	Draft	

(continued)

Table 7.1 (continued)

Summary	Issue Date	FDA Organization[a]	Guidance Status	Docket Number
Drug-drug interaction assessment for therapeutic proteins guidance for industry: draft guidance for industry	7-Aug-2020			FDA-2020-D-1480
Clinical drug Interaction studies — cytochrome P450 enzyme- and transporter-mediated drug Interactions guidance for industry	23-Jan-2020	CDER	Final	FDA-2017-D-5961
In vitro drug Interaction studies — cytochrome P450 enzyme- and transporter-mediated drug Interactions guidance for industry	23-Jan-2020	CDER	Final	FDA-2017-D-5961
Drugs for treatment of partial onset seizures: full extrapolation of efficacy from adults to pediatric patients 2 years of age and older guidance for industry	6-Sep-2019	CDER	Final	FDA-2018-D-0178
Osteoporosis: nonclinical evaluation of drugs intended for treatment guidance for industry: guidance for industry	15-Aug-2019	CDER	Final	FDA-2016-D-1273
General clinical pharmacology considerations for neonatal studies for drugs and biological products guidance for industry	1-Aug-2019	CDER	Draft	FDA-2019-D-3132
Maximal usage trials for topically applied active ingredients being considered for inclusion in an over-the -counter monograph: study elements and considerations	10-May-2019	CDER	Final	FDA-2018-D-1456
Clinical lactation studies: considerations for study design	9-May-2019	CDER	Draft	FDA-2018-D-4525.
Assessing the effects of food on drugs in INDs and NDAs – clinical pharmacology considerations	26-Feb-2019	CDER	Draft	FDA-2018-D-4368
Testicular toxicity: evaluation during drug development	25-Oct-2018	CDER	Final	FDA-2015-D-2306
Developing targeted therapies in low-frequency molecular subsets of a disease	16-Oct-2018	CBER CDER	Final	FDA-2017-D-6617
Physiologically based Pharmacokinetic analyses — format and content guidance for industry	4-Sep-2018	CDER	Final	FDA-2016-D-3969
General principles for evaluating the abuse deterrence of generic solid oral opioid drug products guidance for industry	21-Nov-2017	CDER	Final	FDA-2016-D-0785
Clinical pharmacology data to support a demonstration of biosimilarity to a reference product	29-Dec-2016	CBER CDER	Final	FDA-2014-D-0234

Table 7.1 (continued)

Summary	Issue Date	FDA Organization[a]	Guidance Status	Docket Number
Bioequivalence: blood level Bioequivalence study	16-Dec-2016	CVM	Final	FDA-2014-D-1352
General clinical pharmacology considerations for pediatric studies for drugs and biological products	9-Dec-2014	CDER	Draft	FDA-2013-D-1275
Clinical pharmacogenomics: premarket evaluation in early-phase clinical studies and recommendations for labeling	28-Jan-2013	CDER CDRH CBER	Final	FDA-2011-D-0082
Safety reporting requirements for INDs (investigational new drug applications) and BA/BE (bioavailability/bioequivalence) studies: guidance for industry and investigators	20-Dec-2012	CDER CBER	Final	FDA-2010-D-0482
Safety reporting requirements for INDs and BA/BE studies: guidance for industry and investigators	20-Dec-2012	CDER CBER	Final	FDA-2010-D-0482
Individual product bioequivalence recommendations for specific products	10-Jun-2010	CDER	Final	FDA-2007-D-0433
Guidance for industry – end-of-phase 2A meetings	18-Sep-2009	CDER	Final	FDA-2008-D-0514
Bioequivalence guidance	8-Nov-2006	CVM	Final	FDA-1994-D-0317
Pharmacokinetics in pregnancy — study design, data analysis, and impact on dosing and labeling	1-Nov-2004	CDER CBER	Draft	FDA-2004-D-0459
Pharmacokinetics in patients with impaired hepatic function: study design, data analysis, and impact on dosing and labeling	30-May-2003	CDER CBER	Final	FDA-1999-D-0063
Exposure-response relationships — study design, data analysis, and regulatory applications	5-May-2003	CDER CBER	Final	FDA-2002-D-0177
Statistical information from the June 1999 draft guidance and statistical information for in vitro bioequivalence data posted on August 18, 1999	11-Apr-2003	CDER	Draft	na
Bioavailability and Bioequivalence studies for nasal aerosols and nasal sprays for local action	3-Apr-2003	CDER	Draft	FDA-1999-D-0050
Statistical approaches to establishing bioequivalence	1-Feb-2001	CDER	Final	01D-0027

(continued)

Table 7.1 (continued)

Summary	Issue Date	FDA Organization[a]	Guidance Status	Docket Number
Content and format of INDs for phase 1 studies of drugs, including well-characterized, therapeutic, biotechnology-derived products. Questions and answers: guidance for industry Q & A	1-Oct-2000	CDER CBER	Final	None found
Content and format of investigational new drug applications (INDs) for phase 1 studies of drugs, including well-characterized, therapeutic, biotechnology-derived products: Guidance for industry	1-Nov-1995	CDER CBER	Final	FDA-1995-D-0251
Topical dermatologic corticosteroids: in vivo bioequivalence	2-Jun-1995	CDER	Final	FDA-2021-D-0384
Format and content of the human pharmacokinetics and Bioavailability section of an application	1-Feb-1987	CDER	Final	AA3: E45

[a]*CVM* Center for Veterinary Medicine, *CDER* Center for Drug Evaluation and Research, *CBER* Center for Biologics Evaluation and Research, *OCE* Oncology Center of Excellence, *CDRH* Center for Biologics Evaluation and Research

internal document describing the regulatory thinking on a particular topic with the goal of accuracy and consistency to the review of drug applications. The public cannot comment on policies, given their nature of being internal to the agency [116]. However, attention can be brought to specific areas for policy development by emailing CDER at the proper channel. Federal Register Notice is the Federal government's official publication to inform the public on many Agency actions. Formal comments on rules, proposed rules, and notices should be submitted via Regulations.gov, to the agency dockets on Regulations.gov, or to other places identified under the "Addresses" heading in Federal Register documents. For example, the public commented on four Federal Register notices on different topics such as pH-dependent and therapeutic protein drug interactions, E-R relationships, and oligonucleotide therapeutics [116]. Technical specifications are sometimes used by FDA to communicate expectations for changing clinical and non-clinical study data, for example to outline a general framework for organizing study data (including templates). Comments can be submitted to Docket No FDA-2018-D-1216 or by contacting the relevant FDA center as described [118]. CDER's Manual of Policies and Procedures (MAPPs) are federal directives and documentation of internal policies and procedures. MAPPs are required by law and made available to the public to make CDER a more transparent organization [116].

7.5.1 Statutory Recognition and Regulatory Initiatives on Quantitative Clinical Pharmacology (QCP)

In the 1997 FDA Modernization Act (FDAMA), Congress recognized that "science and practice of drug development and clinical evaluation have evolved significantly in the past 35 years, and this evolution has implications for the amount and type of data needed to support effectiveness in certain cases" [16, 27, 119]. This amendment to the FD & C Act marked statutory recognition of the value of QCP procedures in two sections, one on Pediatric Studies (Section 111) and one on Clinical Investigations (Section 115A). Under Section 111, incentives were established for drug developers to apply for pediatric labeling approval by FDA in part "based upon the known pharmacokinetics of the drug, as opposed to requiring pediatric clinical trials for efficacy" [27, 119]. Under Section 115a, FDA was confirmed to have the authority to accept effectiveness evidence resulting from a single-phase III trial, with the support of "confirmatory evidence," described as "scientifically sound data from any investigation in the NDA that provides substantiation as to the safety and effectiveness of the new drug. . .consisting of earlier clinical trials, pharmacokinetic data, or other appropriate scientific studies" [27, 120].

In May 1998, FDA issued the guidance "Providing Clinical Evidence of Effectiveness for Human Drug and Biological Products" elucidating QCP-based evidentiary requirements to prove drug effectiveness. For instance, the guidance states that a new dose, regimen, or dosage form can be deemed effective based on PK data alone, in cases where blood levels and exposure are not very different. It may be also possible to conclude effectiveness of a new dose, regimen, or dosage form on PK data without an additional clinical efficacy trial even if blood levels are quite different. This is possible if there is a well-understood relationship between blood concentration and response, including an understanding of the time course of that relationship. In this situation, the controlled trial results from one dose, regimen, or dosage form can be translated to a new dose, regimen, or dosage form, based on the use of PK data, together with the well-defined PK/PD relationship [27, 121]. The guidance was updated in December 2019, to complement and expand on the 1998 guidance mentioned above [122]. Several opportunities and applications of FDAMA Section 115a have been described [27, 123].

Overall, traditional drug development and regulatory practice have been profoundly impacted by advances in QCP on drug regulation, and on drug development practices, moving from an inefficient, empirical non-scientific approach into an efficient model-based, quantitative scientific discipline [27]. FDA's Critical Path Initiative highlighted QCP as expressed in model-based regulatory research and clinical trial simulations [90]. When applying the "learn & confirm" paradigm of efficient science management in drug development and regulation, QCP offers a pharmacostatistical framework for application of modern mechanistic causality theory for drug intervention in disease states, which can provide compelling effectiveness evidence [27, 124, 125]. Regulatory scientists have utilized QCP for pharmacometric-intensive regulatory reviews, guidance, labeling, and approval decisions. Several authors have documented FDA's record of the hundreds of applications of QCP in NDA reviews [27, 55, 126–129].

7.6   Perspectives for the Future

An increasing demand for improved and individualized, patient-centric approaches to drug safety and efficacy is expected in the next few years, and the field of pharmacology has been well positioned to respond by focusing on personalized or precision medicine [1, 130]. A prerequisite for such a development will be a robust communication platform and exchange between clinical and experimental pharmacologists, toxicologists, clinicians, and researchers in biomedical sciences. Interdisciplinarity and cross-skilling will be the most important means to shape pharmacology to address current shortcomings and ensure public health for future generations.

Clinical pharmacology has been particularly important in pioneering and shaping precision medicine mostly via pharmacogenomics and therapeutic drug monitoring [130, 131]. The individual efficacy and safety of drugs have been improved by insights on PK parameters (e.g., organ functions, drug transporters, or genetic variations in CYP enzymes, or HLA gene variants) [47, 130–132]. A more informed and individualized drug treatment can also be achieved by identifying novel drug target or clinical subtypes of disease with reverse translational research approaches [130, 133, 134]. Additionally, biobanks and databanks, high-throughput methods, and computational tools may become increasingly available, and the amount of available data may prove invaluable in supporting precision medicine and reverse translational research [130, 133, 135–138]. In the future, large amounts of RWD will continue to be generated considering the ever-increasing use of electronic data in healthcare. Therapeutic individualization of approved drugs and development of new drugs could be critically supported by integrating and linking currently siloed data sources. RWE obtained from prospective, randomized, pragmatic studies using EHRs and other RWD could help address clinical pharmacology issues, such as comparing dosing regimens in the post-approval setting [72].

Considering our intense information/digital age, we foresee an increasingly important role of RWD and RWE in informing clinical pharmacology assessment of new and approved drugs, by adding to the totality of evidence and further aiding regulatory decision-making. A significant body of new scientific evidence and increased complexity will likely be available for clinical and experimental pharmacologists, which will offer novel opportunities for develop individualized drug treatment [72].

To allow AI/ML models to have a bigger impact in product development life cycles, the effort to qualify them in regulatory decision-makings could involve method development and model validation. This is partially due to the fact that AI/ML models can often lack a clear definition on the scope of use, transparency, and mechanistic interpretation due to their inherent nature of relying on data and empirical learning. As a result, biased results and erroneous predictions can be obtained when applied out of scope and context and this in turn can raise ethics, privacy, and civil liberty issues. Therefore, future efforts should focus on the identification of the scope of use, development of novel algorithm under different

contexts, and mitigation and legalization of ethical issues. To allow for regulatory impacts and model relevance, NIST guidelines on key characteristics of AI trustworthiness should be closely followed, including accuracy, explainability, interpretability, reliability, privacy, robustness, safety, security, and mitigation of unintended and/or harmful bias.

References

1. Liu Q, Ahadpour M, Rocca M, Huang SM (2021) Clinical pharmacology regulatory sciences in drug development and precision medicine: current status and emerging trends. AAPS J 23(3):54
2. U.S. F.D.A (2018) Milestones in U.S. Food and Drug Law. Available from: https://www.fda.gov/about-fda/fda-history/milestones-us-food-and-drug-law. Last Accessed
3. U.S. F.D.A (2018) Part II: 1938, Food, Drug, Cosmetic Act. Available from: https://www.fda.gov/about-fda/changes-science-law-and-regulatory-authorities/part-ii-1938-food-drug-cosmetic-act. Last Accessed 26 May 2022
4. U.S. F.D.A (2018) Part III: drugs and foods under the 1938 Act and its amendments. Available from: https://www.fda.gov/about-fda/changes-science-law-and-regulatory-authorities/part-iii-drugs-and-foods-under-1938-act-and-its-amendments. Last Accessed 26 May 2022
5. U.S. F.D.A (2018) Part IV: regulating cosmetics, devices, and veterinary medicine after 1938. Available from: https://www.fda.gov/about-fda/changes-science-law-and-regulatory-authorities/part-iv-regulating-cosmetics-devices-and-veterinary-medicine-after-1938. Last Accessed 26 May 2022
6. U.S. F.D.A (2018) Part V: consumer protection in the late-20th century. Available from: https://www.fda.gov/about-fda/changes-science-law-and-regulatory-authorities/part-v-consumer-protection-late-20th-century. Last Accessed 26 May 2022
7. Adams DG, Cooper RM, Hahn MJ (2015) Food and drug law and regulation, 3rd edn, p 995
8. Skelly JP (2010) A history of biopharmaceutics in the Food and Drug Administration 1968–1993. AAPS J 12(1):44–50
9. US Congress. Drug Amendments of 1962. Public Law 87–781. 1962 USA. Available from: https://www.govinfo.gov/content/pkg/STATUTE-76/pdf/STATUTE-76-Pg780.pdf. Last Accessed 26 May 2022
10. National Academy of Sciences (2022) Organized collections – the drug efficacy study of the National Research Council's Division of Medical Sciences, 1966–1969. Available from: http://www.nasonline.org/about-nas/history/archives/collections/des-1966-1969-1.html. Last Accessed 26 May 2022
11. U.S. F.D.A (2022) Drug Efficacy Study Implementation (DESI). Available from: https://www.fda.gov/drugs/enforcement-activities-fda/drug-efficacy-study-implementation-desi. Last Accessed 26 May 2022
12. US Congress. S.2748 – drug price competition and patent term restoration Act of 1984 (Hatch-Waxman Act). 1984 USA. Available from: https://www.congress.gov/bill/98th-congress/senate-bill/2748. Last Accessed 26 May 2022
13. US Congress. H.R.1226 – Food and Drug Administration Act of 1987. 1987 USA. Available from: https://www.congress.gov/bill/100th-congress/house-bill/1226/text. Last Accessed 26 May 2022

14. US Congress. H.R.5952 – Prescription Drug User Fee Act of 1992. 1992 USA. Available from: https://www.congress.gov/bill/102nd-congress/house-bill/5952. Last Accessed 26 May 2022

15. U.S. F.D.A (2022) Prescription drug user fee amendments. Available from: https://www.fda.gov/industry/fda-user-fee-programs/prescription-drug-user-fee-amendments. Last Accessed

16. US Congress. S.830 – Food and Drug Administration Modernization Act of 1997 (FDAMA). Public Law No: 105–115. 1997 USA. Available from: https://www.congress.gov/bill/105th-congress/senate-bill/830. Last Accessed 26 May 2022

17. US Congress. S.3187 – Food and Drug Administration Safety and Innovation Act. Public Law No: 112–144 2012 USA. Available from: https://www.congress.gov/bill/112th-congress/senate-bill/3187. Last Accessed 26 May 2022

18. U.S. F.D.A (2022) Generic drug user fee amendments. Available from: https://www.fda.gov/industry/fda-user-fee-programs/generic-drug-user-fee-amendments. Last Accessed 26 May 2022

19. US Congress. H.R.2430 – Fda Reauthorization Act of 2017 (FDARA). Public Law No: 115–52. 2017 USA. Available from: https://www.congress.gov/bill/115th-congress/house-bill/2430/text. Last Accessed 26 May 2022

20. Vitti TG, Banes D, Byers TE (1971) Bioavailability of digoxin. N Engl J Med 285(25):1433–1434

21. Federal Register. Basis for demonstrating in-vivo bioavailability or Bioequivalence requirements. 21 Code of Federal Regulations. 1977 USA. Available from: https://www.ecfr.gov/current/title-21/chapter-I/subchapter-D/part-320/subpart-B/section-320.23. Last Accessed 26 May 2022

22. McKenzie AW, Stoughton RB (1962) Method for comparing percutaneous absorption of steroids. Arch Dermatol 86(5)

23. Shah VP, Peck CC, Skelly JP (1989) 'Vasoconstriction' – Skin Blanching –Assay for Glucocorticoids –a Critique. Arch Dermatol 125(11):1558–1561

24. Skelly JP (1991) Topical corticosteroid-induced skin blanching measurement: eye or instrument?-reply. Arch Dermatol 127(7)

25. Stoughton RB (1987) Are generic formulations equivalent to trade name topical glucocorticoids? Arch Dermatol 123(10):1312–1314

26. Lu D, Lee SL, Lionberger RA, Choi S, Adams W, Caramenico HN, Chowdhury BA, Conner DP, Katial R, Limb S, Peters JR, Yu L, Seymour S, Li BV (2015) International guidelines for bioequivalence of locally acting orally inhaled drug products: similarities and differences. AAPS J 17(3):546–557

27. Peck CC (2010) Quantitative clinical pharmacology is transforming drug regulation. J Pharmacokinet Pharmacodyn 37(6):617–628

28. Greene JA (2019) When is a medicine good enough?: science, similarity, and the history of generic drugs. Clin Pharmacol Ther 105(2):290–291

29. Lionberger R, Uhl K (2019) Generic drugs: expanding possibilities for clinical pharmacology. Clin Pharmacol Ther 105(2):278–281

30. Pang KS, Rowland M (1977) Hepatic clearance of drugs. I. Theoretical considerations of a "well-stirred" model and a "parallel tube" model. Influence of hepatic blood flow, plasma and blood cell binding, and the hepatocellular enzymatic activity on hepatic drug Clearance. J Pharmacokinet Biopharm 5(6):625–653

31. Roberts MS, Rowland M (1986) A dispersion model of hepatic elimination: 1. Formulation of the model and bolus considerations. J Pharmacokinet Biopharm 14(3):227–260

32. Rowland M, Benet LZ, Graham GG (1973) Clearance concepts in pharmacokinetics. J Pharmacokinet Biopharm 1(2):123–136

33. Sheiner LB, Rosenberg B, Marathe VV (1977) Estimation of population characteristics of pharmacokinetic parameters from routine clinical data. J Pharmacokinet Biopharm 5(5):445–479

34. Sheiner LB, Steimer JL (2000) Pharmacokinetic/Pharmacodynamic modeling in drug development. Annu Rev Pharmacol Toxicol 40:67–95

35. Temple R (1985) Food and Drug Administration's guidelines for clinical testing of drugs in the elderly. Drug Inf J 19(4):483–486

36. Rowland M, Noe CR, Smith DA, Tucker GT, Crommelin DJ, Peck CC, Rocci ML Jr, Besancon L, Shah VP (2012) Impact of the pharmaceutical sciences on health care: a reflection over the past 50 years. J Pharm Sci 101(11):4075–4099

37. Sheiner LB, Benet LZ (1985) Premarketing observational studies of population pharmacokinetics of new drugs. Clin Pharmacol Ther 38(5):481–487

38. U.S. F.D.A. – Center for Drug Evaluation and Research (1989) Study of Drugs likely to be used in the elderly. Date Available from: https://www.fda.gov/media/71114/download. Last Accessed 26 May 2022

39. Blakey GE, Nestorov IA, Arundel PA, Aarons LJ, Rowland M (1997) Quantitative structure-pharmacokinetics relationships: I. development of a whole-body physiologically based model to characterize changes in pharmacokinetics across a homologous series of barbiturates in the rat. J Pharmacokinet Biopharm 25(3):277–312

40. Rodgers T, Rowland M (2007) Mechanistic approaches to volume of distribution predictions: understanding the processes. Pharm Res 24(5):918–933

41. Rodgers T, Leahy D, Rowland M (2005) Physiologically based pharmacokinetic modeling 1: predicting the tissue distribution of moderate-to-Strong bases. J Pharm Sci 94(6):1259–1276

42. Benowitz N, Forsyth FP, Melmon KL, Rowland M (1974) Lidocaine disposition kinetics in monkey and man. I. Prediction by a perfusion model. Clin Pharmacol Ther 16(1):87–98

43. Bischoff KB, Dedrick RL (1968) Thiopental pharmacokinetics. J Pharm Sci 57(8):1346–1351

44. Bischoff KB, Dedrick RL, Zaharko DS, Longstreth JA (1971) Methotrexate pharmacokinetics. J Pharm Sci 60(8):1128–1133

45. Huang SM, Rowland M (2012) The role of physiologically based pharmacokinetic modeling in regulatory review. Clin Pharmacol Ther 91(3):542–549

46. Rostami-Hodjegan A, Tucker GT (2007) Simulation and prediction of in vivo drug metabolism in human populations from in vitro data. Nat Rev Drug Discov 6(2):140–148

47. International Transporter Consortium, Giacomini KM, Huang SM, Tweedie DJ, Benet LZ, Brouwer KL, Chu X, Dahlin A, Evers R, Fischer V, Hillgren KM, Hoffmaster KA, Ishikawa T, Keppler D, Kim RB, Lee CA, Niemi M, Polli JW, Sugiyama Y, Swaan PW, Ware JA, Wright SH, Yee SW, Zamek-Gliszczynski MJ, Zhang L (2010) Membrane transporters in drug development. Nat Rev Drug Discov 9(3):215–236

48. Clewell HJ, Andersen ME, Wills RJ, Latriano L (1997) A physiologically based pharmacokinetic model for retinoic acid and its metabolites. J Am Acad Dermatol 36(3):S77–S85

49. U.S. F.D.A. – Center for Drug Evaluation and Research (1999) Clinical Pharmacology and Biopharmaceutics Review: NDA 21–108 0.02% Tretinoin Emollient Cream (RENOVA®). Date Available from: http://www.accessdata.fda.gov/drugsatfda_docs/nda/2000/21-108_Renova_BioPharmr.pdf. Last Accessed 26 May 2022

50. U.S. F.D.A. – Center for Drug Evaluation and Research (2016) Manual of policies and procedures: good review practices: clinical pharmacology review of New Molecular Entity (NME) New Drug Applications (NDAs) and Original Biologics License Applications (BLAs). Date Available from: https://www.fda.gov/media/71709/download. Last Accessed 26 May 2022

51. U.S. F.D.A. – Center for Drug Evaluation and Research (2020) NDA approval letter: VEKLURY (Remdesivir) for injection. Date Available from: https://www.accessdata.fda.gov/drugsatfda_docs/appletter/2020/214787Orig1s000ltr.pdf. Last Accessed 26 May 2022

52. U.S. F.D.A (2021) Division of pharmacometrics. Available from: https://www.fda.gov/about-fda/center-drug-evaluation-and-research-cder/division-pharmacometrics. Last Accessed 31 May 2022

53. Madabushi R, Wang Y, Zineh I (2019) A holistic and integrative approach for advancing model-informed drug development. CPT Pharmacometrics Syst Pharmacol 8(1):9–11

54. Wang Y, Zhu H, Madabushi R, Liu Q, Huang SM, Zineh I (2019) Model-informed drug development: current us regulatory practice and future considerations. Clin Pharmacol Ther 105(4):899–911

55. Bhattaram VA, Booth BP, Ramchandani RP, Beasley BN, Wang Y, Tandon V, Duan JZ, Baweja RK, Marroum PJ, Uppoor RS, Rahman NA, Sahajwalla CG, Powell JR, Mehta MU, Gobburu JV (2005) Impact of Pharmacometrics on drug approval and labeling decisions: a survey of 42 new drug applications. AAPS J 7(3):E503–E512

56. U.S. F.D.A (2022) Model-informed drug development pilot program. Available from: https://www.fda.gov/drugs/development-resources/model-informed-drug-development-pilot-program. Last Accessed 31 May 2022

57. Zhang X, Yang Y, Grimstein M, Fan J, Grillo JA, Huang SM, Zhu H, Wang Y (2020) Application of Pbpk modeling and simulation for regulatory decision making and its impact on US prescribing information: an update on the 2018-2019 submissions to the US FDA's Office of Clinical Pharmacology. J Clin Pharmacol 60(Suppl 1):S160–S178

58. Grimstein M, Yang Y, Zhang X, Grillo J, Huang SM, Zineh I, Wang Y (2019) Physiologically based pharmacokinetic modeling in regulatory science: an update from the U.S. Food and Drug Administration's Office of Clinical Pharmacology. J Pharm Sci 108(1):21–25

59. Mentre F, Friberg LE, Duffull S, French J, Lauffenburger DA, Li L, Mager DE, Sinha V, Sobie E, Zhao P (2020) Pharmacometrics and systems pharmacology 2030. Clin Pharmacol Ther 107(1):76–78

60. Benet LZ, Jayachandran P, Carroll KJ, Burmeister Getz E (2019) Batch-to-batch and within-subject variability: what do we know and how do these variabilities affect clinical pharmacology and bioequivalence? Clin Pharmacol Ther 105(2):326–328

61. Gagne JJ, Sarpatwari A, Desai RJ (2019) Role of authorized generics in Postapproval surveillance of generic drug products. Clin Pharmacol Ther 105(2):313–315

62. Zhao L, Kim MJ, Zhang L, Lionberger R (2019) Generating model integrated evidence for generic drug development and assessment. Clin Pharmacol Ther 105(2):338–349

63. U.S. F.D.A (2021) Product-specific guidances for Generic Drug Development. Available from: https://www.fda.gov/drugs/guidances-drugs/product-specific-guidances-generic-drug-development. Last Accessed 26 May 2022

64. Oo C, Chen YC (2009) The need for multiple doses of 400 mg ketoconazole as a precipitant inhibitor of a Cyp3a substrate in an in vivo drug-drug interaction study. J Clin Pharmacol 49(3):368–369

65. Huang W, Lee SL, Yu LX (2009) Mechanistic approaches to predicting oral drug absorption. AAPS J 11(2):217–224

66. Rowland M, Peck C, Tucker G (2011) Physiologically-based pharmacokinetics in drug development and regulatory science. Annu Rev Pharmacol Toxicol 51:45–73

67. Zhao P, Ragueneau-Majlessi I, Zhang L, Strong JM, Reynolds KS, Levy RH, Thummel KE, Huang SM (2009) Quantitative evaluation of pharmacokinetic inhibition of Cyp3a substrates by ketoconazole: a simulation study. J Clin Pharmacol 49(3):351–359

68. Mitra A (2019) Maximizing the role of physiologically based Oral absorption modeling in generic drug development. Clin Pharmacol Ther 105(2):307–309

69. Seng Yue C, Ozdin D, Selber-Hnatiw S, Ducharme MP (2019) Opportunities and challenges related to the implementation of model-based bioequivalence criteria. Clin Pharmacol Ther 105(2):350–362

70. DiLiberti CE, Bon C, D'Angelo P, Gallicano K, Potvin D (2019) Suggestions for streamlining and optimizing clinical end-point bioequivalence studies for US abbreviated new drug application submissions. Clin Pharmacol Ther 105(2):310–312

71. U.S. F.D.A (2022) Real-world evidence. Available from: https://www.fda.gov/science-research/science-and-research-special-topics/real-world-evidence. Last Accessed 31 May 2022

72. Liu Q, Ramamoorthy A, Huang SM (2019) Real-world data and clinical pharmacology: a regulatory science perspective. Clin Pharmacol Ther 106(1):67–71

73. Ramamoorthy A, Huang SM (2019) What does it take to transform real-world data into real-world evidence? Clin Pharmacol Ther 106(1):10–18

74. U.S. F.D.A (2018) PDUFA VI Commitment Letter. Date Available from: https://www.fda.gov/media/99140/download. Last Accessed 26 May 2022

75. U.S. F.D.A (2021) PDUFA VII Commitment Letter. Date Available from: https://www.fda.gov/media/151712/download. Last Accessed 29 June 2022

76. US Congress. H.R.34 – 21st Century Cures Act. Public Law 114–255. 2016 USA. Available from: https://www.congress.gov/bill/114th-congress/house-bill/34/. Last Accessed 26 May 2022

77. U.S. F.D.A (2018) Framework for FDA's Real-World Evidence Program. Available from: https://www.fda.gov/media/120060/download. Last Accessed 26 May 2022

78. Beaulieu-Jones BK, Finlayson SG, Yuan W, Altman RB, Kohane IS, Prasad V, Yu KH (2020) Examining the use of real-world evidence in the regulatory process. Clin Pharmacol Ther 107(4):843–852

79. Liu Q (2020) Nsclc: pneumonitis, immunotherapy, and chemotherapy (Abstract Ct086). In AACR virtual annual meeting. June 22–24, 2020 Location Virtual. Available from: https://ascopost.com/videos/aacr-virtual-annual-meeting-2020-i/qi-liu-on-pneumonitis-immunotherapy-and-chemotherapy-in-nsclc/. Last Accessed 26 May 2022

80. Brito JP, Deng Y, Ross JS, Choi NH, Graham DJ, Qiang Y, Rantou E, Wang Z, Zhao L, Shah ND, Lipska KJ (2022) Association between generic-to-generic levothyroxine switching and thyrotropin levels among US adults. JAMA Intern Med 182(4):418–425

81. Richards D (2012) Developing and delivering clinical pharmacology in pharmaceutical companies. Br J Clin Pharmacol 73(6):870–873

82. Dollery CT (2006) Clinical pharmacology – the first 75 years and a view of the future. Br J Clin Pharmacol 61(6):650–665

83. Mentre F (2014) Lewis Sheiner ISoP/UCSF lecturer award: from drug use to statistical models and vice versa. CPT Pharmacometrics Syst Pharmacol 3:e154

84. Williams P (2010) Clinical pharmacology – career snapshots. Nat Rev Drug Discov 9(4):339–339

85. Scandura A, Iammarino S (2021) Academic engagement with industry: the role of research quality and experience. J Technol Transf

86. U.S. F.D.A (2021) Centers of Excellence in Regulatory Science and Innovation (CERSIs). Available from: https://www.fda.gov/science-research/advancing-regulatory-science/centers-excellence-regulatory-science-and-innovation-cersis. Last Accessed

87. Norris J (2009) UCSF helps launch Chinese Course on Drug Development. Available from: https://pharmacy.ucsf.edu/news/2009/02/ucsf-helps-launch-chinese-course-drug-development. Last Accessed 19 July 2022

88. Nelson RC, Peck CC (1992) Clinical pharmacology training at the Food & Drug Administration. J Clin Pharmacol 32(5):400–406

89. U.S. F.D.A (2022) Training and continuing education. Last Accessed 29 June 2022

90. U.S. F.D.A (2018) Critical path initiative. Available from: https://www.fda.gov/science-research/science-and-research-special-topics/critical-path-initiative. Last Accessed 26 May 2022

91. U.S. F.D.A (2019) Drug Development Tools | DDTs. Available from: https://www.fda.gov/drugs/development-approval-process-drugs/drug-development-tools-ddts. Last Accessed 26 May 2022

92. U.S. F.D.A (2019) Drug Development Tool (DDT) Qualification Process. Available from: https://www.fda.gov/drugs/drug-development-tool-ddt-qualification-programs/drug-development-tool-ddt-qualification-process. Last Accessed 26 May 2022

93. U.S. F.D.A (2022) Drug development tool (DDT) qualification programs. Available from: https://www.fda.gov/drugs/development-approval-process-drugs/drug-development-tool-ddt-qualification-programs. Last Accessed

94. LLC, S.C.R (2019) Pharmacodynamic biomarkers to support biosimilar development: PCSK9 inhibitors. U.S. Food and Drug Administration (FDA)

95. U.S. F.D.A (2020) Impact story: improved assessment of cardiotoxic risk in drug candidates: the comprehensive in vitro proarrhythmia assay. Available from: https://www.fda.gov/drugs/regulatory-science-action/impact-story-improved-assessment-cardiotoxic-risk-drug-candidates-comprehensive-vitro-proarrhythmia. Last Accessed 26 May 2022

96. U.S. FDA (2017) US Package Insert of KALYDECO® (Ivacaftor). Date Available from: https://www.accessdata.fda.gov/drugsatfda_docs/label/2017/203188s019lbl.pdf. Last Accessed 26 May 2022

97. U.S. F.D.A (2022) The Center for Research on complex generics. Available from: https://www.fda.gov/drugs/guidance-compliance-regulatory-information/center-research-complex-generics. Last Accessed

98. Cook SF, Bies RR (2016) Disease progression modeling: key concepts and recent developments. Curr Pharmacol Rep 2(5):221–230

99. Gobburu JV, Lesko LJ (2009) Quantitative disease, drug, and trial models. Annu Rev Pharmacol Toxicol 49:291–301

100. Visser SA, de Alwis DP, Kerbusch T, Stone JA, Allerheiligen SR (2014) Implementation of quantitative and systems pharmacology in large pharma. CPT Pharmacometrics Syst Pharmacol 3:e142

101. U.S. F.D.A (2022) FY 2021 GDUFA science and research report. Available from: https://www.fda.gov/drugs/generic-drugs/fy-2021-gdufa-science-and-research-report. Last Accessed

102. U.S. F.D.A (2022) Generic Drug Research Priorities & Projects. Available from: https://www.fda.gov/drugs/generic-drugs/generic-drug-research-priorities-projects. Last Accessed

103. Tsakalozou E, Babiskin A, Zhao L (2021) Physiologically-based pharmacokinetic modeling to support bioequivalence and approval of generic products: a case for diclofenac sodium topical gel, 1. CPT Pharmacometrics Syst Pharmacol 10(5):399–411

104. U.S. F.D.A (2017) FY2015 regulatory science research report: nanotechnology: postmarket: data analysis for generic drugs. Available from: https://www.fda.gov/industry/generic-drug-user-fee-amendments/fy2015-regulatory-science-research-report-nanotechnology-postmarket-data-analysis-generic-drugs. Last Accessed 26 May 2022

105. Gong X, Hu M, Basu M, Zhao L (2021) Heterogeneous treatment effect analysis based on machine-learning methodology. CPT Pharmacometrics Syst Pharmacol 10(11):1433–1443

106. Gong X, Hu M, Zhao L (2018) Big data toolsets to Pharmacometrics: application of machine learning for time-to-event analysis. Clin Transl Sci 11(3):305–311

107. Laurence DR, Bacharach AL (2013) Evaluation of drug activities: pharmacometrics. Elsevier

108. Sanathanan LP, Peck CC (1991) The randomized concentration-controlled trial: an evaluation of its sample size efficiency. Control Clin Trials 12(6):780–794

109. Hale M, Gillespie W, Gupta S, Tuk B, Holford N (1996) Clinical trial simulation: streamlining your drug development process. Appl Clin Trials 5:35–40

110. Holford NH, Kimko HC, Monteleone JP, Peck CC (2000) Simulation of clinical trials. Annu Rev Pharmacol Toxicol 40:209–234

111. Peck CC, Barr WH, Benet LZ, Collins J, Desjardins RE, Furst DE, Harter JG, Levy G, Ludden T, Rodman JH et al (1992) Opportunities for integration of pharmacokinetics, pharmacodynamics, and Toxicokinetics in rational drug development. Clin Pharmacol Ther 51(4):465–473

112. Peck CC (1993) Understanding consequences of concurrent therapies. J Am Med Assoc 269(12)

113. International conference on harmonisation of technical requirements for registration of pharmaceuticals for human use (1994) ICH harmonised tripartite guideline dose-response information to support drug registration E4 current step 4 version

114. U.S. F.D.A. – Center for Drug Evaluation and Research and U.S. F.D.A. – Center for Biologics Evaluation and Research (2003) Guidance- Exposure-Response Relationships — Study Design, Data Analysis, and Regulatory Applications. Date Available from: https://www.fda.gov/regulatory-information/search-fda-guidance-documents/exposure-response-relationships-study-design-data-analysis-and-regulatory-applications. Last Accessed 26 May 2022

115. U.S. F.D.A. – Center for Drug Evaluation and Research (2022) Bioavailability studies submitted in Ndas or Inds – General Considerations. Date Available from: https://www.fda.gov/media/121311/download. Last Accessed 26 May 2022

116. Madabushi R, Pfuma Fletcher E, Florian J, Milligan L, Ramamoorthy A, Yang X, Maxfield K, Sahre M, Jean D, Zhang L, Green D, Zineh I (2020) Role of guidance and policy in enhancing the impact of clinical pharmacology in drug development, regulation, and use. Clin Pharmacol Ther 108(4):710–715

117. U.S. F.D.A (2022) Guidances. Available from: https://www.fda.gov/industry/fda-basics-industry/guidances. Last Accessed 26 May 2022

118. U.S. F.D.A (2022) Study Data standards resources. Available from: https://www.fda.gov/industry/fda-data-standards-advisory-board/study-data-standards-resources. Last Accessed 26 May 2022

119. Jeffords J (1997) Senate report 105–43 – Food and Drug Administration Modernization and Accountability Act of 1997. Date Available from: https://www.congress.gov/congressional-report/105th-congress/senate-report/43/1. Last Accessed 26 May 2022

120. US Congress. House Report 105–310 – Prescription Drug User Fee Reauthorization and Drug Regulatory Modernization Act of 1997. 1997 USA. Available from: https://www.congress.gov/congressional-report/105th-congress/house-report/310. Last Accessed 5/26/2022

121. U.S. F.D.A. – Center for Drug Evaluation and Research and U.S. F.D.A. – Center for Biologics Evaluation and Research (1998) Providing Clinical evidence of effectiveness for human drug and biological products. Date Available from: https://www.fda.gov/regulatory-information/search-fda-guidance-documents/providing-clinical-evidence-effectiveness-human-drug-and-biological-products. Last Accessed 26 May 2022

122. U.S. F.D.A. – Center for Biologics Evaluation and Research and U.S. F.D.A. – Center for Drug Evaluation and Research (2019) Demonstrating substantial evidence of effectiveness for human drug and biological products – guidance for industry. Date Available from: https://www.fda.gov/regulatory-information/search-fda-guidance-documents/demonstrating-substantial-evidence-effectiveness-human-drug-and-biological-products. Last Accessed 8 July 2022

123. Peck CC, Wechsler J (2002) Report of a workshop on confirmatory evidence to support a single clinical trial as a basis for new drug approval. Drug Inf Assoc 36(3):517–534

124. Peck C (2003) Hypothesis: a single clinical trial plus causal evidence of effectiveness is sufficient for drug approval. Clin Pharmacol Ther 73(6):481–490

125. Sheiner LB (1997) Learning versus confirming in clinical drug development. Clin Pharmacol Ther 61(3):275–291

126. Bhattaram VA, Bonapace C, Chilukuri DM, Duan JZ, Garnett C, Gobburu JV, Jang SH, Kenna L, Lesko LJ, Madabushi R, Men Y, Powell JR, Qiu W, Ramchandani RP, Tornoe CW, Wang Y, Zheng JJ (2007) Impact of pharmacometric reviews on new drug approval and labeling decisions – a survey of 31 new drug applications submitted between 2005 and 2006. Clin Pharmacol Ther 81(2):213–221

127. Doblin RE (2001) Regulation of the medical use of psychedelics and marijuana. Harvard University

128. Garnett CE, Lee JY, Gobburu JVS (2011) Contribution of Modeling and Simulation in the Regulatory Review and Decision-Making: U.S. FDA Perspective. In: Kimko H, Peck C (eds) Clinical Trial Simulations. Series, vol 1. Springer, New York

129. Gobburu JV (2010) Pharmacometrics 2020. J Clin Pharmacol 50(9 Suppl):151S–157S

130. von Gunten S (2020) The future of pharmacology: towards more personalized pharmacotherapy and reverse translational research. Pharmacology 105(1–2):1–2

131. Verstegen RHJ, Ito S (2019) The future of precision medicine. Clin Pharmacol Ther 106(5):903–906
132. Zamek-Gliszczynski MJ, Taub ME, Chothe PP, Chu X, Giacomini KM, Kim RB, Ray AS, Stocker SL, Unadkat JD, Wittwer MB, Xia C, Yee SW, Zhang L, Zhang Y, C. International Transporter (2018) Transporters in drug development: 2018 ITC recommendations for transporters of emerging clinical importance. Clin Pharmacol Ther 104(5):890–899
133. Brackman DJ, Giacomini KM (2018) Reverse translational research of ABCG2 (BCRP) in human disease and drug response. Clin Pharmacol Ther 103(2):233–242
134. Gajewski TF (2015) The next hurdle in cancer immunotherapy: overcoming the non-T-cell-inflamed tumor microenvironment. Semin Oncol 42(4):663–671
135. Schneider C, Smith DF, Cummings RD, Boligan KF, Hamilton RG, Bochner BS, Miescher S, Simon HU, Pashov A, Vassilev T, von Gunten S (2015) The human IgG anti-carbohydrate repertoire exhibits a universal architecture and contains specificity for microbial attachment sites. Sci Transl Med 7(269):269ra1
136. Haas Q, Simillion C, von Gunten S (2018) A cartography of Siglecs and Sialyltransferases in gynecologic malignancies: is there a road towards a sweet future? Front Oncol 8:68
137. Jandus P, Boligan KF, Smith DF, de Graauw E, Grimbacher B, Jandus C, Abdelhafez MM, Despont A, Bovin N, Simon D, Rieben R, Simon HU, Cummings RD, von Gunten S (2019) The architecture of the IgG anti-carbohydrate repertoire in primary antibody deficiencies. Blood 134(22):1941–1950
138. Haas Q, Boligan KF, Jandus C, Schneider C, Simillion C, Stanczak MA, Haubitz M, Seyed Jafari SM, Zippelius A, Baerlocher GM, Laubli H, Hunger RE, Romero P, Simon HU, von Gunten S (2019) Siglec-9 regulates an effector memory Cd8(+) T-cell subset that congregates in the melanoma tumor microenvironment. Cancer Immunol Res 7(5):707–718

Index